CAROTENOID *IN PLANTA* DEVELOPMENT, STORAGE, AND BIOACCESSIBILITY: A COMPREHENSIVE APPROACH TO NUTRIENT ANALYSIS

A Dissertation

by

JENNIFER LEANNE JEFFERY

Submitted to the Office of Graduate Studies of
Texas A&M University
in partial fulfillment of the requirements for the degree of

DOCTOR OF PHILOSOPHY

December 2008

Major Subject: Molecular and Environmental Plant Sciences

CAROTENOID *IN PLANTA* DEVELOPMENT, STORAGE, AND BIOACCESSIBILITY: A COMPREHENSIVE APPROACH TO NUTRIENT ANALYSIS

A Dissertation

by

JENNIFER LEANNE JEFFERY

Submitted to the Office of Graduate Studies of
Texas A&M University
in partial fulfillment of the requirements for the degree of

DOCTOR OF PHILOSOPHY

Approved by:

Chair of Committee,	Stephen King
Committee Members,	Andreas Holzenburg
	Nancy Turner
	Bhimanagouda Patil
Intercollegiate Faculty Chair,	Jean Gould

December 2008

Major Subject: Molecular and Environmental Plant Sciences

ABSTRACT

Carotenoid *In Planta* Development, Storage, and Bioaccessibility:

A Comprehensive Approach to Nutrient Analysis. (December 2008)

Jennifer Leanne Jeffery, B.S., Brigham Young University

Chair of Advisory Committee: Dr. Stephen King

Plants contain a host of secondary metabolites that may be of dietary use to man. A comprehensive approach to plant-based nutrition would include investigating all aspects of a nutrient, from creation through storage and consumption. Here, experiments address each of these facets for a group of important antioxidant and pigment compounds, the carotenoids.

The carotenoid biosynthetic pathway regulatory mechanisms leading to lycopene accumulation are well defined in the model fruit, tomato. Those leading to accumulation of other carotenoids and flesh colors, however, are poorly understood. The variety of flesh colors available in watermelon fruit (red, orange, salmon yellow, and canary yellow) makes it an ideal candidate for investigating the regulation of the full pathway. Carotenoid accumulation was measured in ten watermelon varieties, representing the four flesh colors and three ploidy levels, throughout fruit maturation. It was found that the putative regulatory mechanisms controlling lycopene accumulation in red-fleshed fruit may be applied in a generalized fashion to each flesh color in respect to the major carotenoid accumulated at maturity. Additionally, triploid varieties were generally

found to have higher accumulation levels than diploids, and tetraploids were intermediate to both.

In addition to total carotenoid content, many factors are important in determining perceived benefit. Several of these factors involve components of the food matrix, cellular and subcellular species-specific characteristics of the food which act as barriers to nutrient release. Cell size, cell wall, and chromoplast (the carotenoid storage organelle) characteristics were observed in nine fruits and vegetables using light and transmission electron microscopy. Watermelon, tomato, and melon have the largest cells. Sweet potato, butternut squash, carrot, and mango have the most fibrous cell walls; mango and papaya additionally had the thickest walls. Chromoplast globular, tubular, crystalline, and membranous substructures were described for each food.

These food matrix factors may be related to differences in carotenoid bioaccessibility between food sources. An *in vitro* digestion experiment was used to determine carotenoid bioaccessibility for each of these foods. Per serving, grapefruit yielded the most lycopene while carrot gave the most α-carotene, β-carotene, lutein, and phytoene, and mango proved a good source of violaxanthin.

DEDICATION

I would like to dedicate not only this dissertation but my entire academic experience thus far to my family who taught me the personal value of education. To my grandparents, Mary and Eugene Esplin, who taught me that an education would allow me to be and remain independent despite unexpected life circumstances. To my mother, Laurel Campbell, who was in school much of my childhood renewing her teaching credentials then specializing in educational disciplines and finally earning her master's degree. Her dedication taught me that the tools and intellectual confidence that come of an education are worth the sacrifice of time and material luxuries. To my father, Ed Waters, a self-taught scientist at heart, spurred the young scientist in me, building, learning, and questioning. To my step-father, David Campbell, who has always been supportive of my education and exemplifies continual learning. To my sister, Elizabeth Fondren, who put herself through law school entirely at night while working full-time during the day. She is one of the most quick-witted, fun people I know; I am so happy to have her as a friend.

But my determination and sanity while conquering this final hurdle, the document before you, are owed entirely to my husband, Jay Jeffery. Having successfully passed this rigor one year before me, he knew how to keep me motivated, lift my burdens, and encourage my spirit. It is a wonder to me how anyone does it alone; I'm grateful he came along in time so I would never have to find out. I am excited to raise a family with him in this tradition of personally enriching education.

ACKNOWLEDGEMENTS

I would like to thank my committee chair, Dr. Stephen King, who, despite the connotations of his name, always did his best to keep my graduate experience from being a horrific one. I am grateful to my committee members, Dr. Andreas Holzenburg, Dr. Bhimanagouda Patil, and Dr. Nancy Turner, for their willingness and expediency in giving aid wherever possible. I would also like to thank Dr. Hae Jeen Bang for her contributions to parts of this research.

I am grateful for the support of the Tom Slick Fellowship Foundation which allowed me to complete my final year of study without the distraction of other responsibilities. I would finally like to thank the faculty, staff, and students of the Horticulture Department and the Vegetable and Fruit Improvement Center, my dual academic homes, for their interest in and support of all the students.

NOMENCLATURE

ANOVA	Analysis of Variance
AUC	Area Under the Curve
CC	Correlation Coefficient
DPP	Days Post Pollination
FW	Fresh Weight
HPLC	High Performance Liquid Chromatography
HSD	Honestly Significant Difference (Tukey's)
MANOVA	Multivariate Analysis of Variance
MHU	Mean Heat Units
ORAC	Oxygen Radical Absorbance Capacity
RMCD	Randomly Methylated Cyclodextrin
SD	Standard Deviation
TEM	Transmission Electron Microscopy
USDA NNDSR	United States Department of Agriculture National Nutritional Database for Standard Reference

TABLE OF CONTENTS

CHAPTER Page

CHAPTER Page

Page

LIST OF FIGURES

Page

Page

Page

Page

LIST OF TABLES

Page

CHAPTER I

INTRODUCTION: GENERAL BACKGROUND

PLANT METABOLITES

Some plant chemicals do not appear to function directly in the growth or development of the plant itself. Because of their detached role from the plant, they are commonly referred to as secondary metabolites or natural products. The line between primary (those compounds which do function in growth and development) and secondary metabolites is continually questioned as new knowledge is gained regarding the highly specialized roles of these compounds. The implication of this distinction is that primary metabolites are found in nearly all plants due to their vital functions, whereas secondary metabolites are localized to limited groups of plants which face similar environmental pressures.

Although referred to as secondary, these metabolites are now thought to function as primary driving forces in interactions with other organisms and the environment. These interactions include defense responses against microbes, fungi, herbivores, competitive plants, or adverse inorganic influences such as oxidative stress or drought. Conversely, secondary metabolites may act as elicitors to attract other organisms such as pollinators, seed dispersers, or symbiotic microbes and fungi.

This dissertation follows the style of *The Journal of Agricultural and Food Chemistry*.

Natural plant products can be categorized into three main groups based on biosynthetic origins, the terpenoids, alkaloids, and phenylpropanoids. Though most types of secondary interactions are represented in each of the classes, some are more typical of a particular class than others.

The terpenoids are the most diverse class of plant products in both form and function. Structurally, they consist of various combinations and configurations of the five-carbon product isopentenyl diphosphate (IPP) from the acetate/mevalonate pathway. Some important terpenoid examples include photosynthetic accessory and pigment molecules (carotenoids), volatile essential oils of flowers and herbs, antibiotic and antifeedant compounds (phytoalexins), and plant hormones (abscicsic acid, cytokinin, and gibberellins). Terpenoid synthesis and end-products are often sequestered into subcellular compartments (ex. chromoplasts) or specialized structures (ex. trichomes) in order to prevent interference with the plant's basic metabolism or autotoxicity.

Alkaloids are the second most varied class of plant products, which are characterized by content of at least one nitrogen atom originating from their biosynthesis from amino acids. Alkaloids are not unique to plants, but to what degree they are created de novo in animals is unknown. Some alkaloids, such as nicotine and caffeine, are toxic or bitter-tasting to insects, thus serving as deterrents. Pyrrolizidine alkaloids are toxic to animals, acting in antiherbivory roles. Additionally many ancient and modern drugs, especially painkillers and narcotics, have alkaloid origins. The use and study of opium products gave rise to

the discovery of morphine, codeine, and heroin. Most alkaloids are produced in the cytosol and sometimes stored in vacuoles. They can be either constitutively expressed or induced by tissue wounding.

Phenylpropanoids and their derived phenolic compounds, while being the least diverse of the three classes, make up 40% of the earth's circulating carbon. A good portion of this is caught up in the structural components of cell walls as lignins while others play roles in the qualitative traits of wood, petal and fruit color, or flavors. Some compounds involved in these qualitative traits are classified as lignans and also play roles in pathogen defense or as antioxidants in various plant tissues and organs. The flavanoids also serve in similar ways; the subclass of anthocyanins are important pigments acting as pollinator and seed-dispersal agents.

The evidence of these interactions led us to investigate the underlying mechanisms of action on the receiving organism as well as their native biosynthesis, regulation, and storage. To aid in the improvement of these commercially valuable traits, it is important to develop an accurate understanding of these factors for the compounds in their native states.

APPLICATIONS TO HUMAN HEALTH: CAROTENOIDS AS A CASE STUDY

In addition to the macro- (carbohydrate, fat, and protein) and micro-nutrients (vitamins and minerals) gained from consumption of these plants, natural products also

have important applications to human nutrition and health. Interestingly, research is continually drawing connections between the *in planta* roles of these compounds and their perceived benefits to human health. For example, anti-microbial and fungal agents in the plant context sometimes serve similar functions when used as medicinal components (*1*). Antioxidants that function to protect the plant from oxidative stress can serve similar functions when ingested and lead to decreased disease incidence. In these situations, natural plant products are often referred to as phytochemicals.

Carotenoids, a subclass of tetraterpenoids, provide a powerful case study in the function and utility of dietary phytochemicals. These are found mainly in fruits and vegetables with red, orange, and yellow hues; lycopene, β-carotene, and the xanthophylls lutein and zeaxanthin are the most common carotenoids responsible for these colors, respectively. Their role as dietary antioxidants seems to be related to their ubiquitous function as components of the plant photosystem within the chloroplast (*2*). Xanthophyll carotenoids, mainly lutein and violaxanthin, act as light harvesters which pass energy to the photosynthetic reaction center, facilitating photosynthesis. Carotenoids are also able to dissipate this energy, a non-photochemical process of quenching excess photosynthetic energy known as photoinhibition, when transfer to the reaction center of the photosystem could result in oxidative damage. Antioxidant activity, specifically oxidative radical quenching power, is the putative rationale for carotenoids' involvement in disease risk reduction. Carotenoids have been shown to be potent radical scavenging compounds, lycopene being the most potent (*3*).

Lycopene is often cited as being inversely correlated with the occurrence of various cancers (reviewed in *4*), acting as an anti-oxidant (*5*), in lowering rates of cardiovascular disease (*6*), and improving other various immune responses (*7*). Tomatoes are the most common source of lycopene used in these studies. Lutein and zeaxanthin, oxygenated carotenoids are recognized for their contributions to eye health (*8*, *9*) and reductions in colon cancer risk (*10*). Similar health benefits of other carotenoids have also been revealed (*11*, *12*, *13*, *14*, *15*, *16*).

Discussion of the merits of phytochemical consumption leads to the question of the applicability of nutritional supplements as potential sources. An inconclusive difference has been seen between the effects of carotenoids from whole food versus individual carotenoid supplement sources. Kim et al (*17*) found that acute liver damage inflicted by free-radicals was mitigated by administration of tomato powder but not by pure lycopene. This study clarified similar findings by Boileau et al (*18*) which had been contested (*19*) based on the dosing regimen. This discrepancy may be due, in part, to synergies which may act between any combination of phytochemical and nutritive components of the food. Shi et al (*20*) found synergistic effects in the reduction of *in vitro* liposome oxidation when lycopene was accompanied by other tomato product antioxidants, most notably vitamin E. van Weerden et al (*21*) found that synthetic lycopene reduced prostate tumor growth when combined with vitamin E. Given the division of relevant data, it seems wise to pursue both paths, whole foods and supplements, in researching disease prevention. It is clear, however, that a balanced

diet, rich in fruits and vegetables, is prudent, regardless of an individual's choice to supplement his or her diet or not.

PHYTOCHEMICAL AND NUTRIENT ACCESSIBILITY

Cellular and subcellular tissue structures play an important role in defining the qualitative features of the food matrix such as food texture and shelf life (*22*). The food matrix differs between plant species and is also heavily implicated in the variation seen in bioavailability of food nutrients and phytochemicals, especially carotenoids (*23*). Carotenoids are unique among plant nutrients and phytochemicals in their sequestration into chromoplasts, subcellular organelles. This storage technique, as well as the barrier imposed by the cell wall, may influence their accessibility through digestion, a factor known as bioaccessibility. The implications of the properties and characteristics of these structures on bioaccessibility comprise what are known as "food matrix effects," many of which will apply to the accessibility of all nutrients in the food.

Factors affecting bioavailability are discussed in several reviews (*23, 24, 25*). Only a subset of these factors, however, affects inherent carotenoid bioaccessibility[1] whereas the other factors modify bioavailability. The factors inherent to the food source are only superficially acknowledged and understood, and little attention has been given to illuminating differences in the physical structures involved.

---

[1] *Defining Bioavailability versus Bioaccessibility*

Bioavailable nutrients are the portion of those in the sample that end up in the plasma and tissues. Bioaccessibility is a measure of the fraction of the nutrient in a sample that are available to be absorbed by the body, a better measurement of the ability of the nutrient to be released from the food matrix under digestive conditions.

These factors may contribute to observations such as those of van het Hof et al (*26*) who noted a higher plasma β-carotene response in subjects fed broccoli and green peas than those fed spinach despite a ten-fold lower concentration in the former foods. de Pee et al (*27*) also found significantly greater plasma concentrations from those consuming carotene-rich fruits (mango, papaya, and pumpkin) rather than green leafy vegetables or carrots when both meals had comparable β-carotene levels.

In addition to food matrix effects, other factors affect bioaccessibility. In the case of carotenoids, the carotenoid type (e.g. lycopene versus lutein) present in a food appear to be correlated with bioaccessibility. Tyssandier et al (*28*) found, while studying carotenoid transfer from the lipid emulsion to micelles, a strong inverse correlation between incorporation and carotenoid type, specifically with regard to their hydrophobicity. This means that more polar carotenoids (most notably the xanthophylls and carotene *cis*-isomers) are more easily incorporated into micelles, while the inverse was true for lycopene, β-carotene, and other non-polar carotenoids. These observations are supported by Yeum and Russell (*29*) who hypothesized that non-polar hydrocarbons are incorporated into the interior of the micelle, whereas the oxygenated, more polar carotenoids are exposed on the exterior of the micelle, more accessible to the intestinal mucosa. This external exposure may have also led to the observation of van het Hof et al (*30*) that lutein was five times more bioavailable than β-carotene. While several studies have presented data giving a tentative ranking of carotenoid type by bioaccessibility or bioavailability, they are based only on the limited sources studied in

that model. The current study gives a broader base of specimens which may help to make such correlations.

A seemingly unrelated factor of bioavailability is fiber content. Hoffman et al (*31*) investigated the effect of various fiber types on bioavailability by supplementing meals with carotenoids and either no additional fiber or pectin, guar, or cellulose. They found pectin to have the greatest effect on reducing bioavailability of total carotenoids (38%), where guar and cellulose had smaller negative effects (22% and 18%, respectively). They also found a differential effect on the carotenoid type; lycopene and lutein bioavailability were significantly reduced by all three fiber sources, but β-carotene was not significantly affected by the presence of cellulose in the meal. Thus, carotenoid polarity does not seem to be a factor in the effect of fiber on bioavailability.

There have been several explanations proposed for these observations. Castenmiller et al (*32*) found no significant decrease in bioavailability of β-carotene between enzymatically liquefied (cell walls removed) spinach samples and the same samples with added dietary fiber (sugar beet fiber). They concluded that the significant factor, therefore, is not the presence of fiber but the food matrix itself. Riedl et al (*33*) hypothesized that fiber polysaccharides may disrupt micelle formation which is necessary for carotenoid absorption. Others argue that the effect may be due to the increased viscosity of intestinal contents, reducing contact with intestinal enterocytes (*34*, *35*).

Plants rely heavily upon their secondary metabolites to help them successfully negotiate their environment. Because of these products' powerful influence on other

organisms, they present us with a variety of potential advantages in negotiating our own health and environment. Better understanding the source, impact, and accessibility of these natural plant components will lead to improved dietary health management tools.

CHAPTER II

CAROTENOID BIOSYNTHESIS IN SEVEN VARIETIES OF DEVELOPING WATERMELON (*CITRULLUS LANATUS* (THUNB.) MATSUM. & NANAI): A DISCUSSION OF FLESH COLOR AND PLOIDY EFFECTS ON THE WATERMELON CAROTENOID BIOSYNTHETIC PATHWAY

INTRODUCTION

The focus of research on carotenoid biosynthetic pathway regulation varies somewhat in relation to the varied roles of carotenoids *in planta*. As photo-protectants, the regulation of carotenoids is relatively well understood as being primarily influenced by the degree of photo-oxidative stress experienced by the plant (reviewed in *36*). Additional environmental factors, such as drought or wound stress, have also been shown to influence the levels of carotenoid-associated proteins present in plants (*37*). In the cases of secondary storage, the regulation of the pathway is less understood and is generally viewed in terms of genetic and environmental influences. A better understanding of the mechanisms of this type of regulation is important in developing our ability to optimize nutritional benefit.

Enzymatic regulation can be species and cultivar dependent, leading to a range of carotenoid contents and the resulting colors. Many carotenoid pathway mutations are

studied in microbial systems to expedite the elucidation of the underlying genetic mechanisms of interest. *In planta* carotenoid biosynthesis, accumulation, and sequestration within fruits has been extensively studied in tomato, the model carotenoid-containing food. The "breaker" stage of tomato maturation is marked by the first signs of lycopene accumulation. Transcriptional up-regulation of precursor synthesis genes, phytoene synthase and desaturase, concomitant with complete down-regulation of lycopene β- and ε-cyclases which progress lycopene toward later downstream products, are responsible for this physiological change (*38, 39*). It is noted, however, that sequestration, and not synthesis may be important in carotenoid accumulation (*40*). Strong evidence suggests post-transcriptional regulation (*41*) and feed-back inhibition (*38, 42, 43*) also define the regulation of later stages of carotenoid development.

Several differences exist, however, between tomato and watermelon that may influence carotenoid development. First, the tomato is a climacteric fruit, meaning the fruit produces ethylene as a ripening signal (*44*). While carotenoid accumulation may be part of the ripening process in both tomato and watermelon, it is not signaled by ethylene production in watermelon, a non-climacteric fruit. Second, immature tomato fruit flesh is green, containing chlorophyll in chloroplasts whereas immature flesh is white in watermelon. Chlorophyll degradation is often associated with carotenoid accumulation (*45*), but this is not the case in watermelon. Related to this point may also be the putative relation between light signaling and carotenoid development (reviewed in *44*), presenting a clear difference between the exposed flesh of the tomato and encapsulated state of the watermelon.

Genetics of the watermelon carotenoid pathway are under continual investigation due to the multitude of flesh colors and their implications on the structure of the pathway. In brief, the putative genetic dominance ranks flesh color as follows: canary yellow flesh is dominant to red (*46*), red is dominant to orange and to salmon yellow, and orange is dominant to salmon yellow (*47*). Despite this knowledge of the complex hereditary patterns of these genes and resulting flesh color, the underlying mutations or regulatory mechanisms are poorly understood in watermelon. In many cases, it is not known whether the alleles causing the different flesh colors are variants of regulatory genes or carotenoid biosynthetic genes themselves.

A previous study in our lab has quantified gene expression for the first six genes of the watermelon carotenoid pathway (**Figure 1**) from red-fleshed watermelon by reverse transcriptase PCR in the major color variants. The cDNAs of all six genes were amplified in mature fruit in all colors at the expected molecular weight with the exception of carotenoid isomerase, which was not present in a salmon yellow genotype. These experiments indicate that differences in color are either post-transcriptionally regulated or caused by small mutations. Subsequent experiments revealed a non-synonymous single nucleotide polymorphism (SNP) in the lycopene β-cyclase gene which segregates perfectly with canary yellow and red flesh types (*48*). The source of color difference in the other color variants and, ultimately, how these differences contribute to the regulation of specific carotenoid accumulation remained unclear.

In the current study, profiles and quantities of eight carotenoid types were measured for each of the seven varieties used in the expression study above, representing

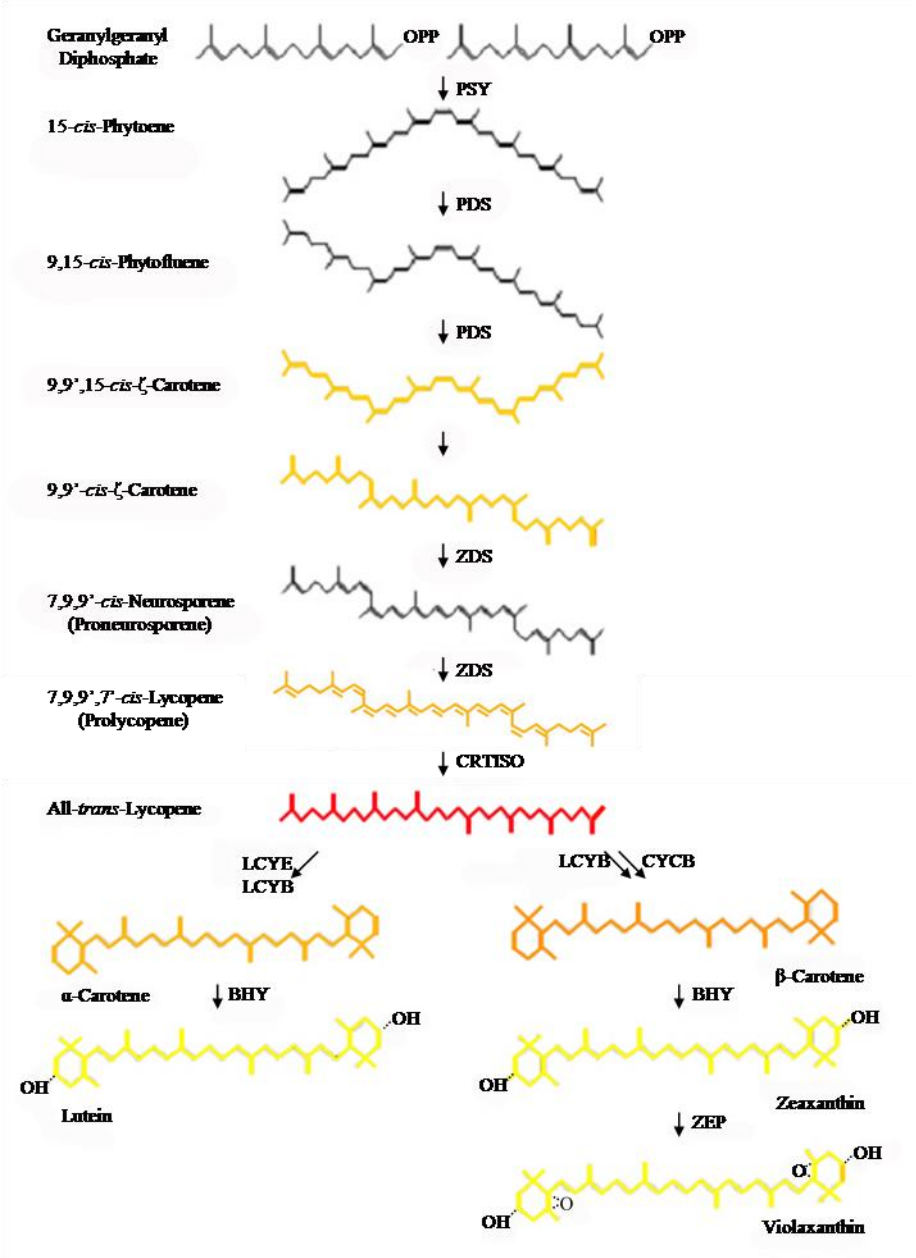

Figure 1. Putative carotenoid biosynthetic pathway in higher plants. Modified from King (*49*). Genes: Phytoene Synthase (PSY), Phytoene Desaturase (PDS), ζ-Carotene Desaturase (ZDS), Carotenoid Isomerase (CRTISO), Lycopene ε-Cyclase (LCYE), Lycopene β-Cyclase (LCYB), Lycopene Cyclase B (CYCB), β-Hydroxylase (BHY), Zeaxanthin Epoxidase (ZEP).

four color variants at two ploidy levels (a source for a triploid salmon yellow was not available) over a developmental course post pollination. Significant differences in carotenoid developmental patterns and quantitative accumulation during fruit maturation were found both between flesh colors and ploidy levels. The cumulative consideration of these evidences led to several hypotheses about pathway regulation.

MATERIALS AND METHODS

The watermelon varieties listed in **Table 1** were grown vertically in a greenhouse in coconut coir media using standard irrigation, fertilization, and pest management practices in two years. In the first year, harvest intervals were set at 10, 20, 40, and 55 days post pollination (DPP). The experimental design was expanded in the second year to include 10, 20, 30, 40, and 50 DPP harvest dates.

Table 1. Variety List (Developmental Study).

Variety Name	Flesh Color	Ploidy
Orange Flesh Tendersweet	Orange	2n
Orange Sunshine	Orange	3n
Early Moonbeam	Canary Yellow	2n
Amarillo	Canary Yellow	3n
Yellow Flesh Black Diamond	Salmon Yellow	2n
Summer Sweet 5244	Red	3n
Dixie Queen	Red	2n

Fruits were harvested and refrigerated (at 4°C) for 0-5 days until samples were taken and prepared for High Performance Liquid Chromatography (HPLC) analysis as

follows. A representative sample was homogenized using a Polytron homogenizer for 3 min at 3000 rpm. A sample amount inversely proportional to the estimated total carotenoid content of the sample was measured into an amber bottle in order to optimize extraction and carotenoid detection. Sample carotenoids were extracted according to the procedure outlined in Fish et al (*50*), an organic solvent extraction technique using ethanol, acetone, hexane, and water. All steps were carried out on ice, in partial darkness, and under nitrogen. The hexane layers were collected and dried under nitrogen flow. Dried samples were blanketed with nitrogen, capped tightly, parafilmed, and stored at -80°C until HPLC analysis.

HPLC analysis was performed with modifications to Britton (*51*). In brief, an isocratic method using a single mobile phase composed of 58.5% acetonitrile (JT Baker), 35% ethyl acetate (EMD Biosciences Inc.), 6.5% water, and 0.1% TEA (Sigma). Samples were reconstituted in 1 mL acetone. A Spherisorb 5 µm ODS-2 (Waters Corporation, Milford, MA) column was used with a flow rate of 1 mL min^{-1}. Carotenoids were observed using a Perkin-Elmer LC-250B pump, a LC-200 autosampler and photo diode array detector and peaks quantified using TurboChrome software (Perkin-Elmer, San Jose, CA).

For the first study, values are reported here as area under the curve (AUC). Carotenoid standards were available for the second study which allowed for peak identification and quantification of most major carotenoid peaks. Lycopene, β-carotene, and lutein standards were obtained from General Nutrition Centers (Pittsburg, PA, U.S.A.), phytoene from Sigma (St.Louis, MO, U.S.A.), and violaxanthin from

Carotenature (Geneva, Switzerland). Proneurosporene and prolycopene, major carotenoids in orange and salmon yellow fleshed watermelons, were approximately quantified using neurosporene and lycopene standard curves, respectively. In the second year, values were normalized to the average solvent peak area measured at 286 nm, which served as an internal standard. Analysis of variance (ANOVA) and Post Hoc tests (Tukey's HSD) were performed using SPSS 15.0 statistical software.

RESULTS

Carotenoid profiles and content varied significantly by flesh color (**Figure 2**). At approximate maturity (40 DPP), red watermelon was found to contain mostly lycopene. Orange varieties contained an average of over 50% phytoene of the total carotenoid content; half of the remainder was prolycopene. Salmon yellow had a similar profile to orange fleshed varieties, with an overall lower total carotenoid content and proportionally substantial increase in ζ-carotene. The majority of the carotenoids in canary yellow watermelons were unknown carotenoid isomers and, therefore, are not included in **Figure 2**. However, lutein and violaxanthin were importantt contributors and are represented in **Figure 3** and **Figure 4**, respectively. Triploids accumulated higher levels of their respective major carotenoids at or near ripeness in most cases.

Significant differences ($P<0.05$) in developmental patterns were found between diploid varieties for all carotenoids in the first year and in all but ζ-carotene, β-carotene, and phytoene the second (see **Figure 3**, **Figure 4**, **Figure 5**, **Figure 6**, **Figure 7**,

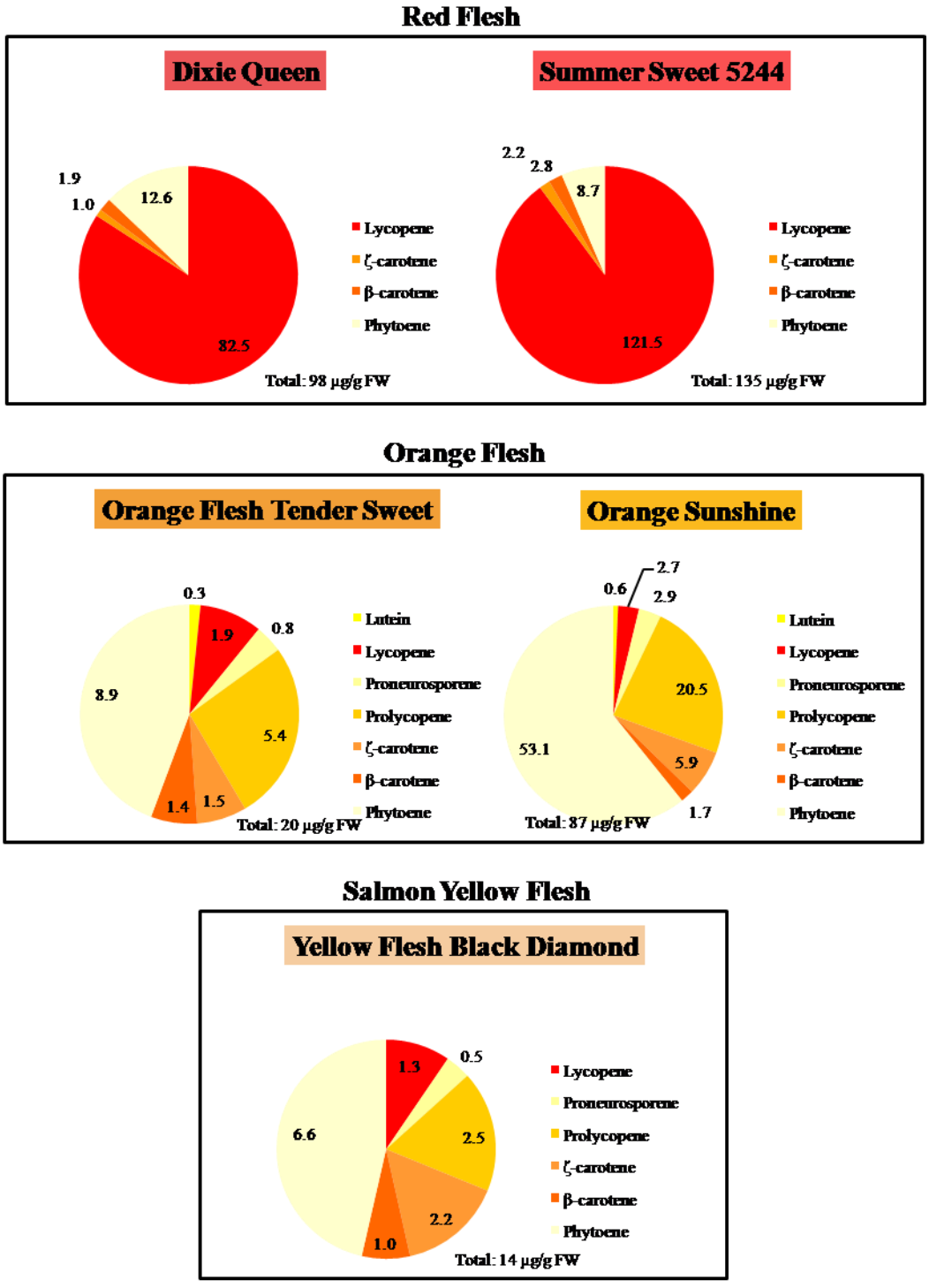

Figure 2. Carotenoid content of red, orange, and salmon yellow fleshed watermelons. Data are mean carotenoid content for each carotenoid in µg/g fresh weight (µg/g FW) at ripeness 40 DPP.

Figure 8, **Figure 9**, and **Figure 10**). Among the triploid varieties, significant differences in developmental pattern were seen in all carotenoids except lutein the first year and β-carotene the second year. It should be emphasized that such differences refer only to the developmental pattern, not amounts accumulated. They refer specifically to an interaction between flesh color and DPP for each given carotenoid (ie. carotenoid development over time) and are graphically represented by differently *shaped* curves.

These differences were expressed as distinctive patterns of accumulation in the respective major carotenoids for each flesh color. In the diploid representatives of each flesh color, major carotenoids began accumulating 20-30 DPP, peaked at maturity (approximately 40 DPP), and declined as the fruits became over ripe. An approximately 5-10 day downward shift in these maxima was seen in year 2. Red and canary yellow tripoid varieties expressed this same ($\alpha>0.05$) pattern of development among their major carotenoids. The first year the orange-fleshed triploid variety did not experience this decline after reaching ripeness but rather continued to accumulate all three of its major carotenoids after 40 DPP, beginning to taper off about 50 DPP. This variety did exhibit a notable decrease in accumulation of major carotenoids the second year.

Canary yellow varieties contained many carotenoids that eluted within the range of known xanthophylls during HPLC analysis. A greater number of these carotenoids were present in canary yellow the second year than the first. In both years, lutein and violaxanthin demonstrated unique, identifiable peaks and displayed similar development patterns to the major carotenoids in other flesh colors. A few other carotenoids were distinct, though at very low levels, in the first year and were included in that analysis.

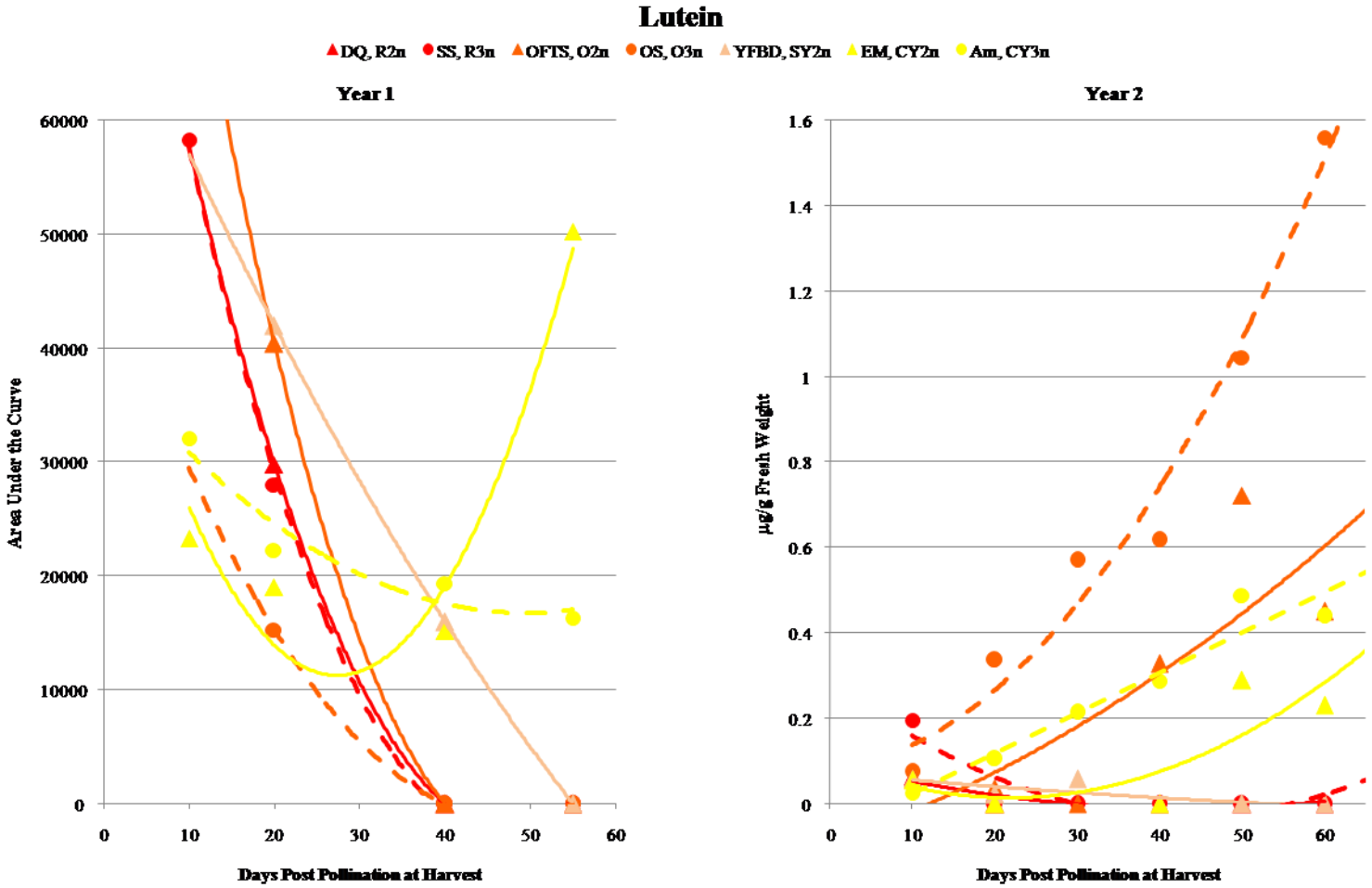

Figure 3. Developmental patterns of lutein in seven varieties of maturing watermelon. Data are means. Varieties: Dixie Queen (DQ, 2n), Summer Sweet 5244 (SS, 3n), Orange Flesh Tender Sweet (OFTS, 2n), Orange Sunshine (OS, 3n), Yellow Flesh Black Diamond (YFBD, 2n), Early Moonbeam (EM, 2n), and Amarillo (Am, 3n). Flesh colors: red (R), orange (O), salmon yellow (SY), and canary yellow (CY). Solid trendlines represent diploids. Dashed trendlines represent triploids.

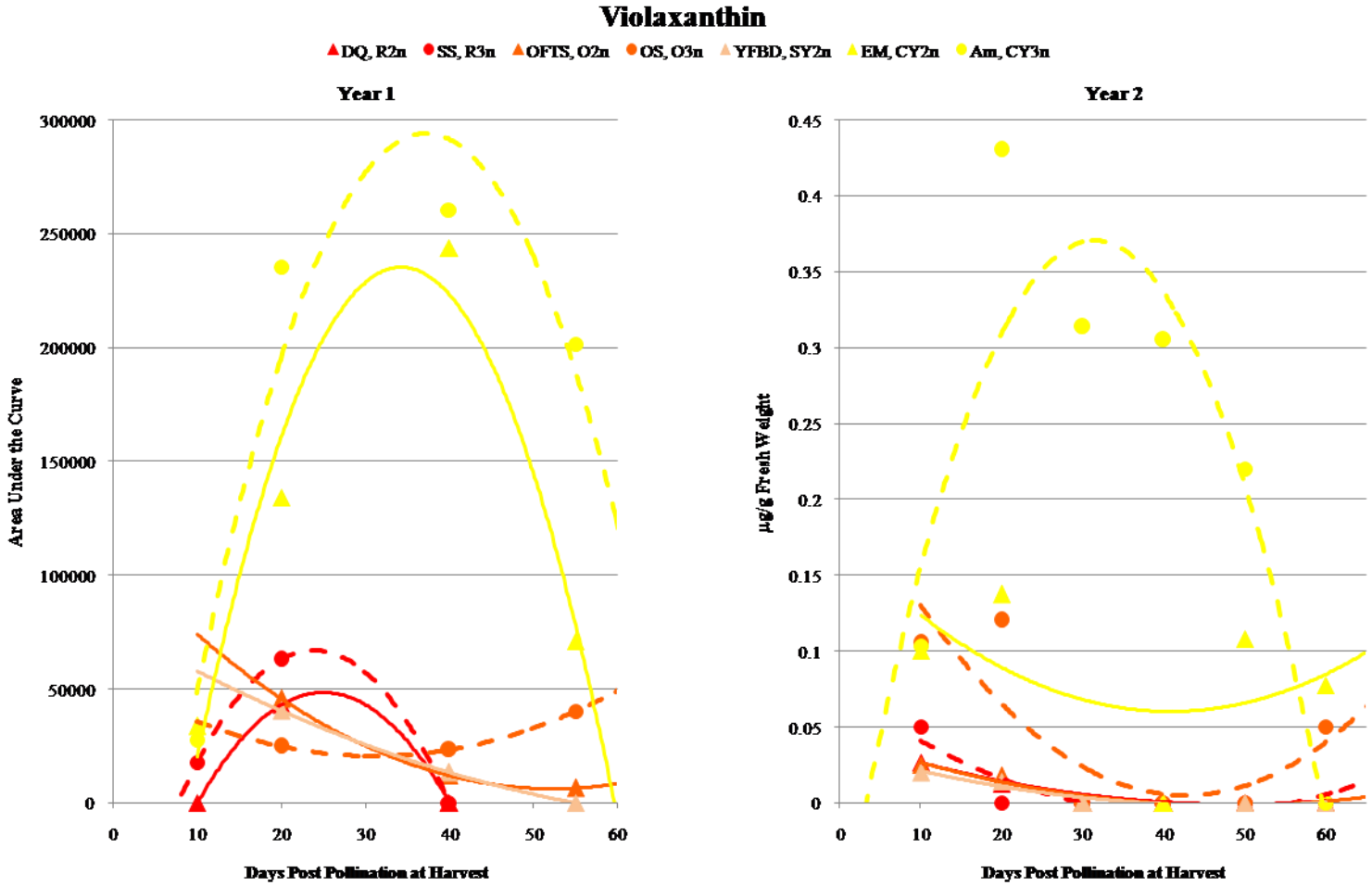

Figure 4. Developmental patterns of violaxanthin in seven varieties of maturing watermelon. Data are means. Varieties: Dixie Queen (DQ, 2n), Summer Sweet 5244 (SS, 3n), Orange Flesh Tender Sweet (OFTS, 2n), Orange Sunshine (OS, 3n), Yellow Flesh Black Diamond (YFBD, 2n), Early Moonbeam (EM, 2n), and Amarillo (Am, 3n). Flesh colors: red (R), orange (O), salmon yellow (SY), and canary yellow (CY). Solid trendlines represent diploids. Dashed trendlines represent triploids.

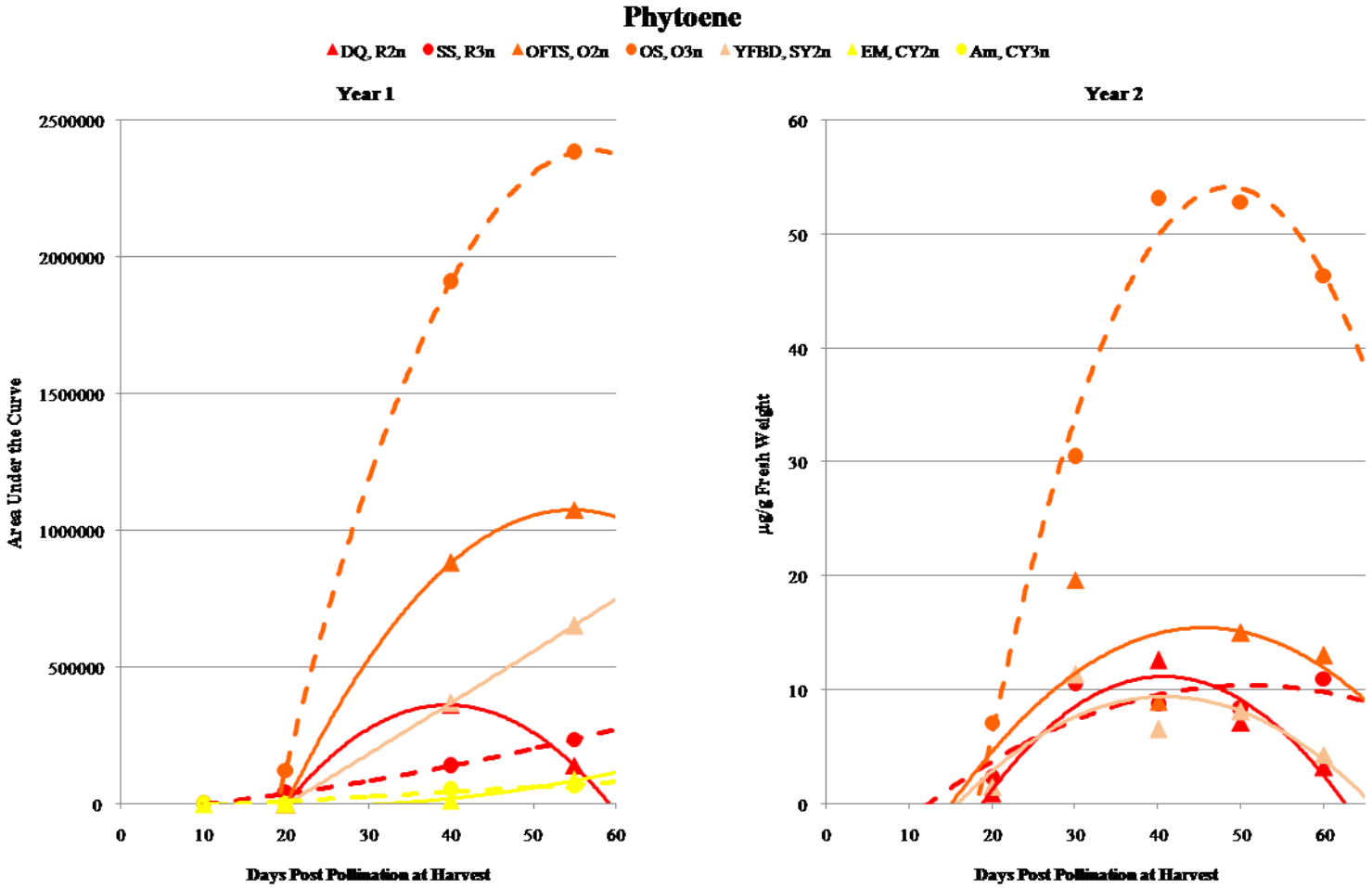

Figure 5. Developmental patterns of phytoene in seven varieties of maturing watermelon. Data are means. Varieties: Dixie Queen (DQ, 2n), Summer Sweet 5244 (SS, 3n), Orange Flesh Tender Sweet (OFTS, 2n), Orange Sunshine (OS, 3n), Yellow Flesh Black Diamond (YFBD, 2n), Early Moonbeam (EM, 2n), and Amarillo (Am, 3n). Flesh colors: red (R), orange (O), salmon yellow (SY), and canary yellow (CY). Solid trendlines represent diploids. Dashed trendlines represent triploids.

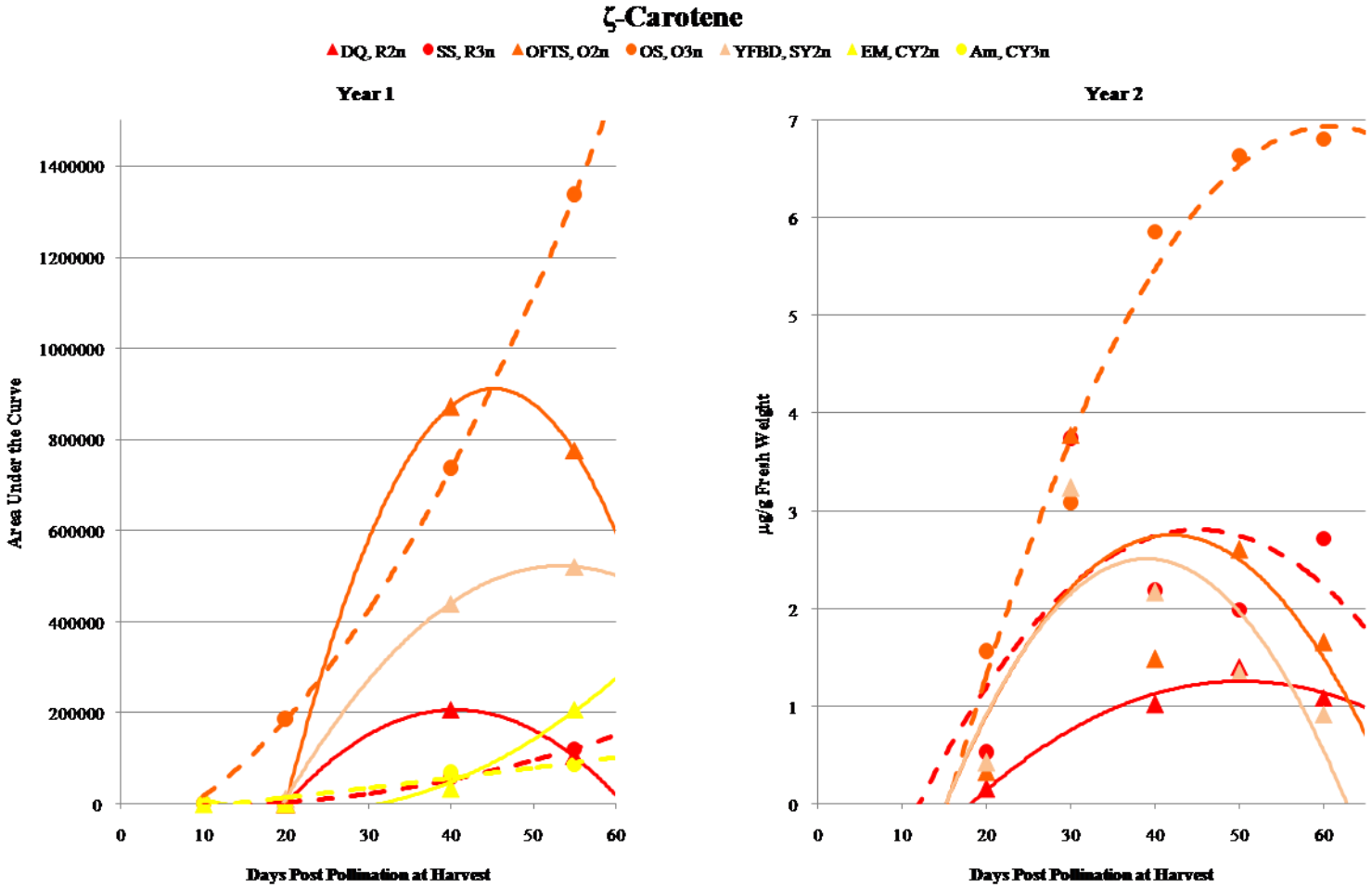

Figure 6. Developmental patterns of ζ-carotene in seven varieties of maturing watermelon. Data are means. Varieties: Dixie Queen (DQ, 2n), Summer Sweet 5244 (SS, 3n), Orange Flesh Tender Sweet (OFTS, 2n), Orange Sunshine (OS, 3n), Yellow Flesh Black Diamond (YFBD, 2n), Early Moonbeam (EM, 2n), and Amarillo (Am, 3n). Flesh colors: red (R), orange (O), salmon yellow (SY), and canary yellow (CY). Solid trendlines represent diploids. Dashed trendlines represent triploids.

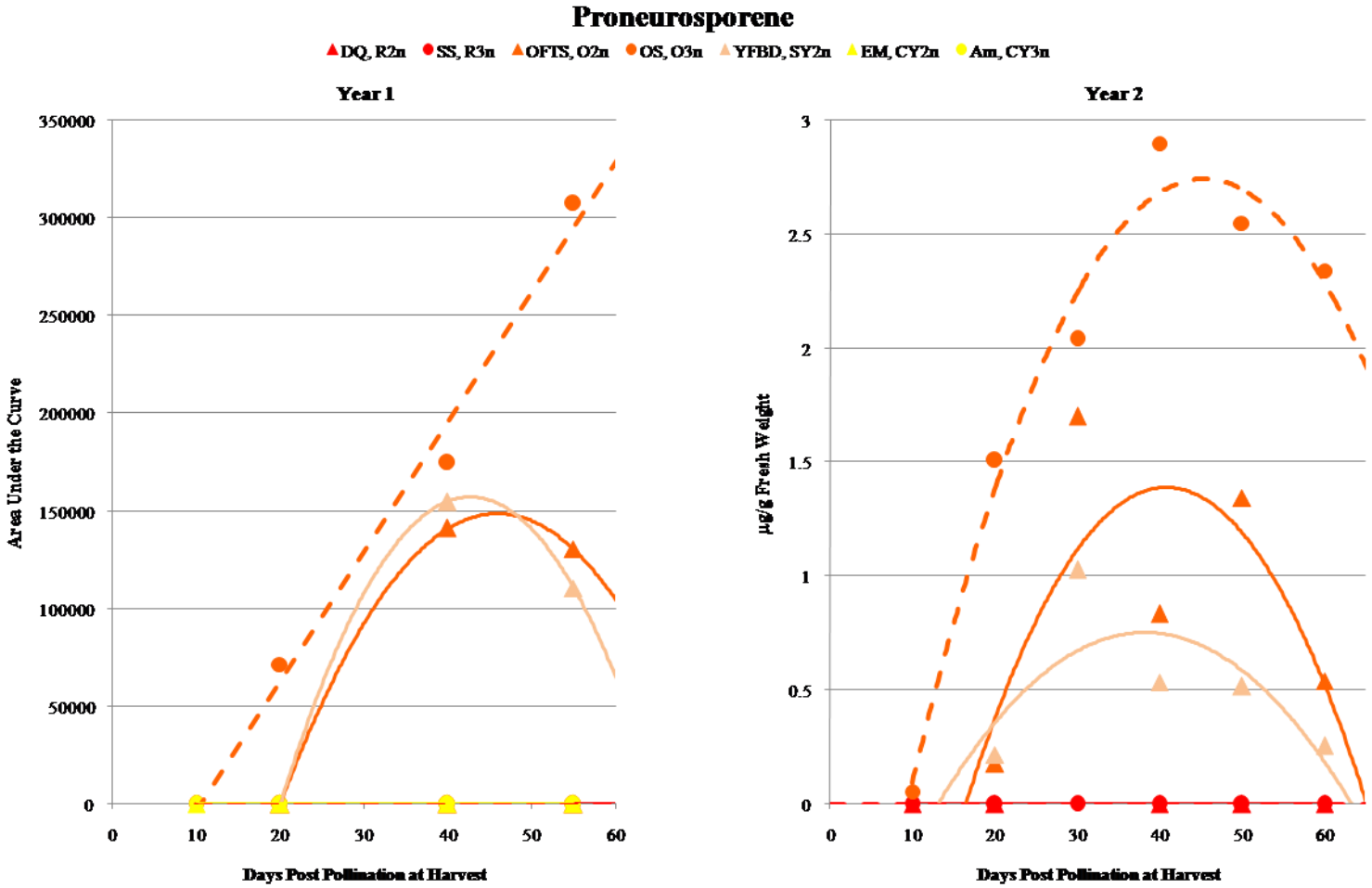

Figure 7. Developmental patterns of proneurosporene in seven varieties of maturing watermelon. Data are means. Varieties: Dixie Queen (DQ, 2n), Summer Sweet 5244 (SS, 3n), Orange Flesh Tender Sweet (OFTS, 2n), Orange Sunshine (OS, 3n), Yellow Flesh Black Diamond (YFBD, 2n), Early Moonbeam (EM, 2n), and Amarillo (Am, 3n). Flesh colors: red (R), orange (O), salmon yellow (SY), and canary yellow (CY). Solid trendlines represent diploids. Dashed trendlines represent triploids.

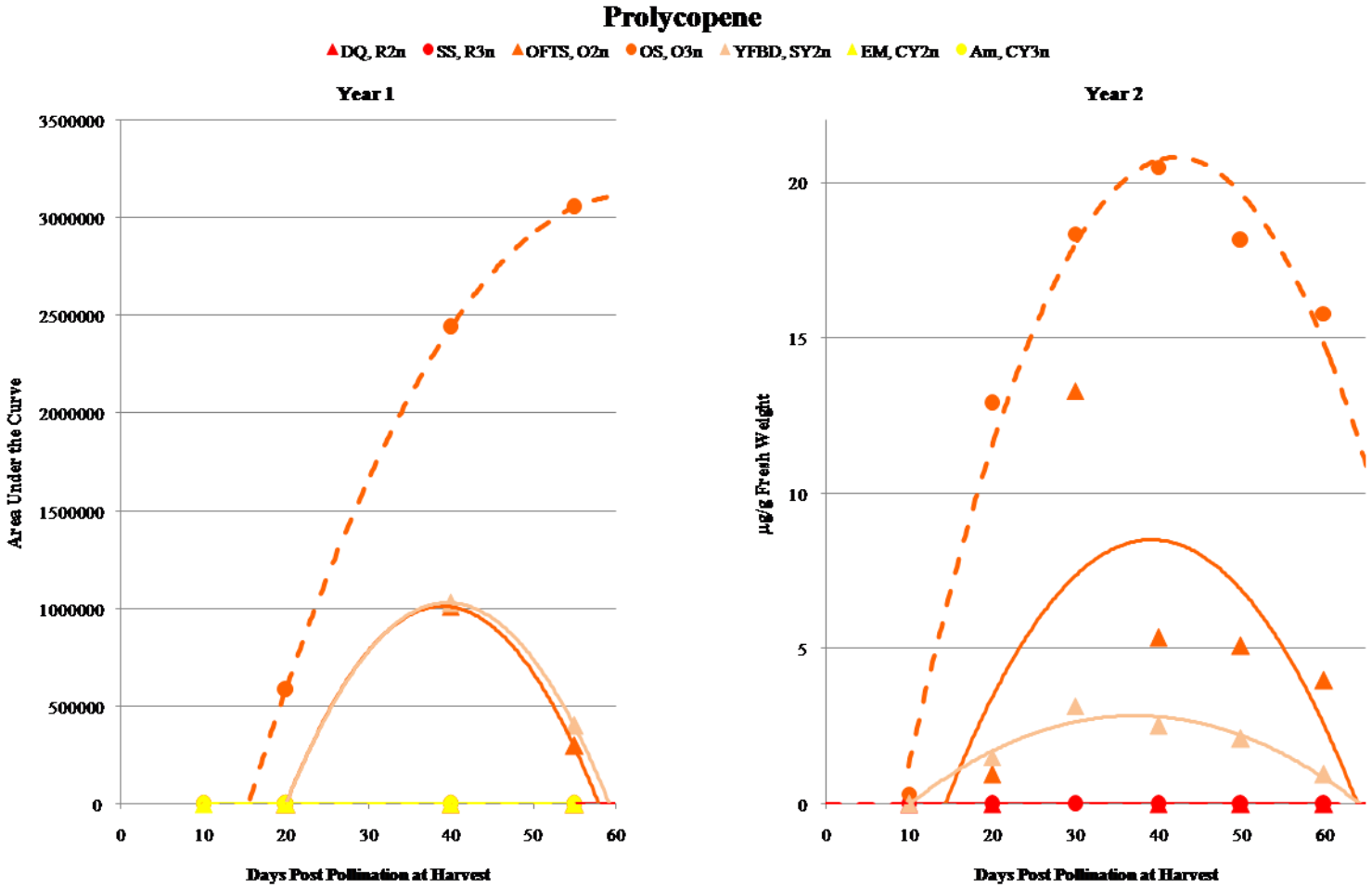

Figure 8. Developmental patterns of prolycopene in seven varieties of maturing watermelon. Data are means. Varieties: Dixie Queen (DQ, 2n), Summer Sweet 5244 (SS, 3n), Orange Flesh Tender Sweet (OFTS, 2n), Orange Sunshine (OS, 3n), Yellow Flesh Black Diamond (YFBD, 2n), Early Moonbeam (EM, 2n), and Amarillo (Am, 3n). Flesh colors: red (R), orange (O), salmon yellow (SY), and canary yellow (CY). Solid trendlines represent diploids. Dashed trendlines represent triploids.

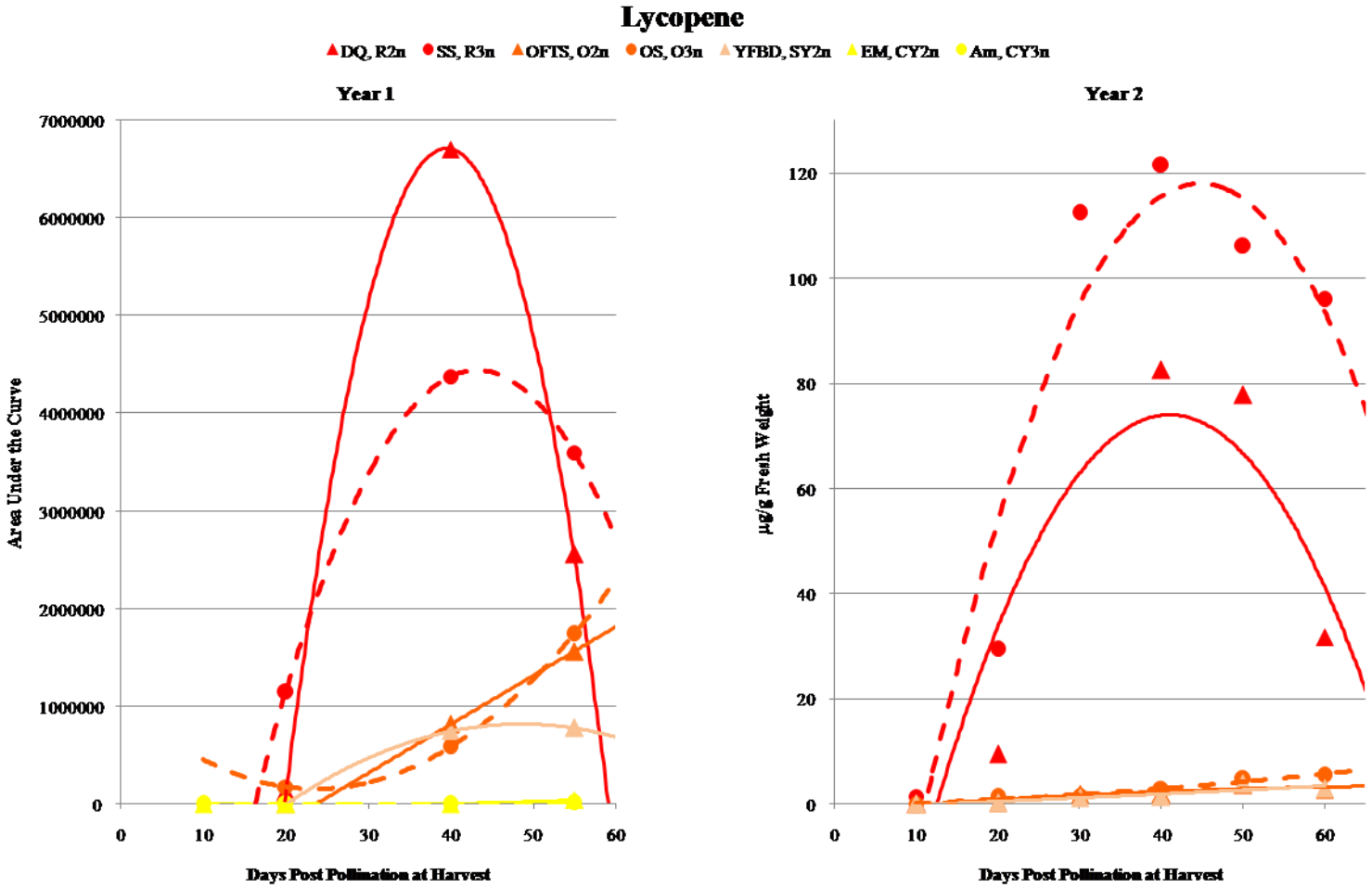

Figure 9. Developmental patterns of lycopene in seven varieties of maturing watermelon. Data are means. Varieties: Dixie Queen (DQ, 2n), Summer Sweet 5244 (SS, 3n), Orange Flesh Tender Sweet (OFTS, 2n), Orange Sunshine (OS, 3n), Yellow Flesh Black Diamond (YFBD, 2n), Early Moonbeam (EM, 2n), and Amarillo (Am, 3n). Flesh colors: red (R), orange (O), salmon yellow (SY), and canary yellow (CY). Solid trendlines represent diploids. Dashed trendlines represent triploids.

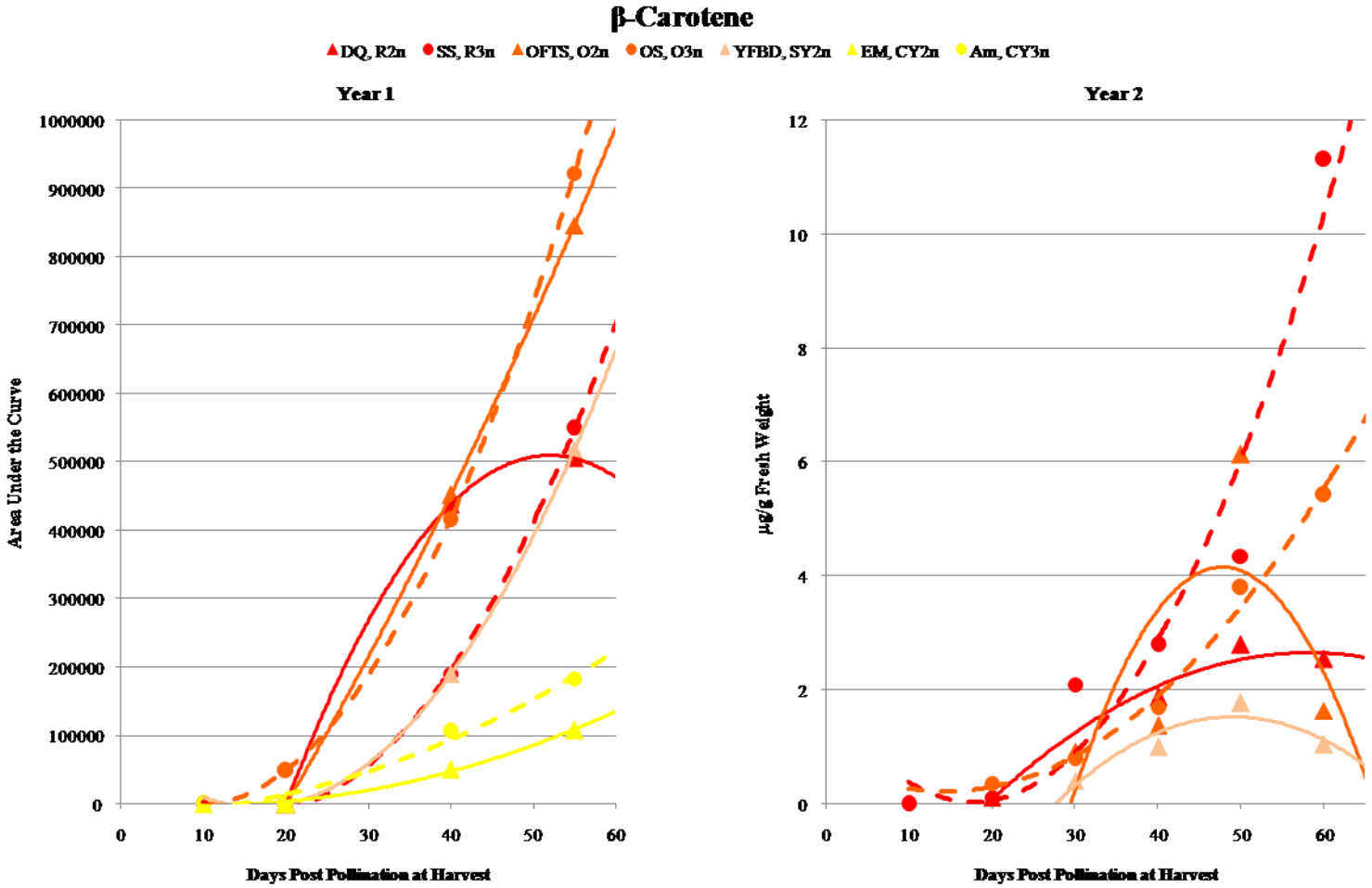

Figure 10. Developmental patterns of β-carotene in seven varieties of maturing watermelon. Data are means. Varieties: Dixie Queen (DQ, 2n), Summer Sweet 5244 (SS, 3n), Orange Flesh Tender Sweet (OFTS, 2n), Orange Sunshine (OS, 3n), Yellow Flesh Black Diamond (YFBD, 2n), Early Moonbeam (EM, 2n), and Amarillo (Am, 3n). Flesh colors: red (R), orange (O), salmon yellow (SY), and canary yellow (CY). Solid trendlines represent diploids. Dashed trendlines represent triploids.

DISCUSSION

The carotenoid profiles observed here for all colors were consistent with published reports (*52*). Also as reported elsewhere (*52*, *53*), canary yellow fleshed watermelons contained low levels of many carotenoid types, many unidentifiable with common standards. The greater influence of environmental conditions in Amarillo than in other color varieties has also been previously reported (*54*), corroborating the increased number of carotenoid peaks observed the second year of the current study. The near isolation of this phenomenon to canary yellow flesh types may be a vestigial response related to the influence of environmental conditions on photosynthetic carotenoid biosynthesis regulatory mechanisms since these varieties contained primarily xanthophylls isomers. This hypothesis is also supported by the change in lutein accumulation pattern also seen between the two years in the orange fleshed varieties.

Carotenoid accumulation patterns that could result from the transcriptional regulation discussed earlier for tomato at "breaker" stage were seen among red lycopene-accumulating varieties. These were the early accumulation of down-stream products (xanthophylls lutein and violaxanthin) and their decrease occurs approximately simultaneously with initiation of lycopene and phytoene accumulation (see **Figure 11** in conjunction with remainder of the discussion). These patterns suggest that "breaker stage" in watermelon is about 20 DPP. The alignment of the current data with these putative concepts about carotenoid regulation may lead to a more generalized hypothesis applicable to all flesh colors in the light of previous findings. The mutation in the

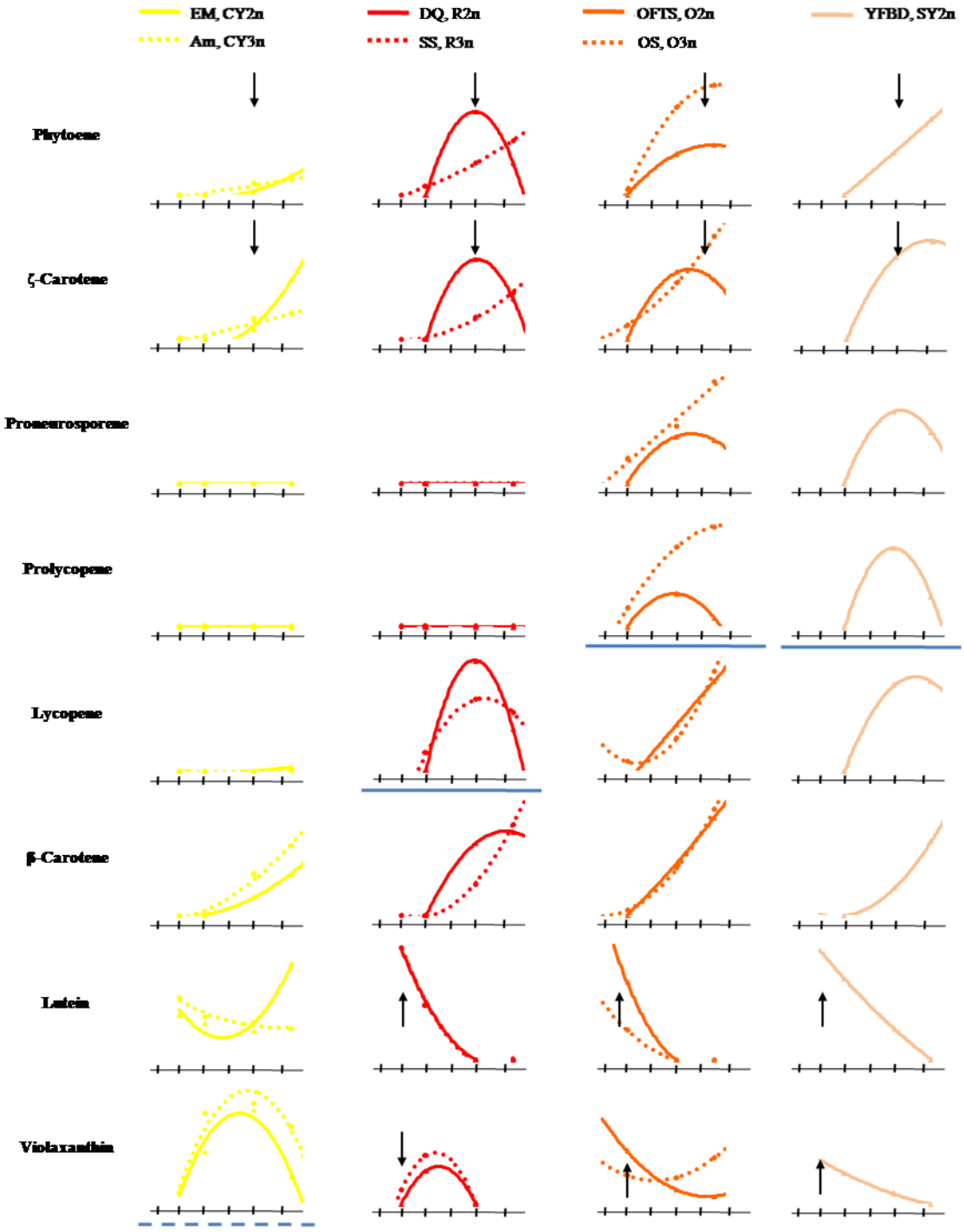

Figure 11. Graphic representation of carotenoid development in seven watermelon varieties for eight carotenoids. Biosynthetic pathway progresses from top to bottom, revealing regulatory patterns. Early accumulation of xanthophylls and late accumulation of precursors indicated by arrows. Blue lines represent possible points of genetic disruption in the pathway for each color (dashed line indicates disruption downstream of violaxanthin. Horizontal axis marked at 0, 10, 20, 30, 40, and 50 DPP. Not drawn to scale.

lycopene β-cyclase gene found to distinguish red and canary yellow flesh types and the absence of carotenoid isomerase transcription in salmon yellow may have transcriptional, post-transcriptional, or feed-back inhibition regulatory implications. Regardless of which of these is acting in this case, accumulation of products downstream of the major end-product happens in early development. This is followed at the "breaker" stage by down-regulation or mutation of the gene immediately following the major end-product with concomitant up-regulation of pathway precursors, leading to their accumulation. Near the ripeness stage, accumulation levels of the major carotenoids signal a feed-back inhibitory response which leads to the down-regulation of precursor genes, late accumulation of those precursors, and the eventual decline in the major carotenoid. To explore this hypothesis, we may focus future research energies on finding small and large mutations in the isomerase genes of orange and salmon yellow fleshed watermelons, respectively, as well as mutations downstream of violaxanthin in canary yellow genotypes in order to elucidate the genetic underpinnings of each color variant.

Additional evidence for this regulation hypothesis was observed during data analysis. Several of the unknown xanthophyll peaks which accumulated in the canary yellow varieties displayed early high levels and subsequent sharp declines in accumulation 20-30 DPP, similar to the developmental patterns of "downstream products" in other colors. These peaks may be canary yellow's downstream products which could lead to their identification as well as the identification of responsible gene mutations.

In addition to the similar behavior of diploid and triploid varieties in red and canary yellow varieties, other evidence of otherwise similar genetic backgrounds exists. Most evident is the red fleshed fruit's violaxanthin accumulation pattern as a departure from the pattern seen in orange and salmon yellow. The latter exhibit behavior characteristic of the putative regulatory mechanisms and the hypotheses regarding overall pathway regulation proposed above. While red watermelon accumulates violaxanthin early and correspondingly decreases to non-detectible levels before maturity, the accumulation behavior is clearly more reminiscent of canary yellow's patterns than those in other flesh colors. It is important to note that this pattern is not displayed for neither red nor canary yellow in the accumulation of lutein, another downstream xanthophyll. This may be an additional indicator that pertinent mutations in canary yellow lay downstream of violaxanthin, not lutein.

The general trend of higher carotenoid accumulation in triploids than diploids noted here is consistent with published reports on ripe fruit (*55*). The orange flesh varieties appeared to show the most difference in regulatory pattern between ploidy levels. This difference may have been due to a delay in potential post-transcriptional regulatory responses exhibited more readily in the other color varieties the first year. The general advancement in earliness experienced the second year may reveal support for this hypothesis in that post-ripeness declines seen in other colors were additionally seen in the orange triploid.

CONCLUSION

While total and individual carotenoid content of mature watermelons is a relatively well established parameter of flesh color and ploidy, the understanding of carotenoid development during fruit maturation gained here is a significant advancement toward elucidating underlying constitutive and regulatory implications. It was found that the putative mechanisms of carotenoid biosynthesis in tomato can be applied in a generalized format for each flesh color according to its respective major carotenoid accumulated. Optimally, all carotenoid-related genes will have real-time PCR performed to quantify gene expression in each color variant over development and these data correlated with that presented here.

It is commonly held that a fully functional pathway is the native state of the pathway. The implications of this are unclear in the cases presented here since similar regulatory patterns occur for each flesh color at different points in the pathway. The current work may lead to a better appreciation for the evolutionary basis of the various flesh colors.

CHAPTER III

GENOTYPIC EFFECTS ON WATERMELON (*CITRULLUS LANATUS* (THUNB.) MATSUM. & NANAI) CAROTENOID DEVELOPMENT IN MATURING RED-FLESH FRUIT

INTRODUCTION

An organism's genotype is defined by its genetic constitution and results in phenotypic, or visual, traits. The watermelon phenotypic traits of flesh color and presence/absence of seeds are important markers of genotypic traits, carotenoid gene alleles and ploidy, respectively. Carotenoid accumulation and development is influenced by both of these factors but to unknown degrees. Perkins-Veazie et al (*55*) reported lycopene content in 11 red watermelon varieties (genotypes). They found seedless (triploid) varieties had higher average lycopene contents than seeded (diploid) varieties. Similar results were found in the study discussed in Chapter II. A possible common explanation of this phenomena is the additional biosynthesis of carotenoids by the extra genome in triploids.

In most instances, ploidy is one of many genotypic traits which define a watermelon variety. It is difficult, therefore, to differentiate the effects of ploidy and the sum of all other genotypic effects when comparing varieties, as was done in Perkins-Veazie et al (*55*) and Chapter II herein.

The present study was designed to decipher these factors. A line of genetically identical watermelon varieties which differ only in ploidy was obtained and presented a unique opportunity for studying the effect of ploidy alone on carotenoid development. Without such evidence, it would remain unclear whether the differences seen in the studies mentioned above are due to ploidy level as is put forth or due to the sum of the remaining genetic background.

MATERIALS AND METHODS

Table 2 shows the varieties used in the study. The commercial varieties, Dixie Queen (2n) and Summer Sweet 5244 (3n), were chosen. They have different ploidy levels as well as different genetic backgrounds. Three additional genotypic lines, HNP19-2n, HNP19-3n, and HNP19-4n, were obtained which have different ploidies but otherwise identical genetic backgrounds, as discussed above. In other words, the only sources of variance in the HNP19 series are ploidy and error. Series such as this are created by performing chromosome doubling in a diploid (2n) variety to obtain a tetraploid (2n + 2n = 4n), then crossing the two to obtain a triploid (2n/2 + 4n/2 = 3n).

The remainder of the experimental design was as stated for the study presented in Chapter II.

Table 2. Red Flesh Variety List.

Variety Name	Flesh Color	Ploidy
Summer Sweet 5244	Red	3n
Dixie Queen	Red	2n
HNP19-2n	Red	2n
HNP19-3n	Red	3n
HNP19-4n	Red	4n

RESULTS

HNP19 carotenoid accumulation levels were statistically indistinguishable ($P>0.05$) among ploidy levels for all time points after 10 DPP for lycopene and lutein (**Figure 12**). As an exception, phytoene accumulation in the triploid and tetraploid did exceed that of the diploid at 40 and 50 DPP. In the commercial varieties, Summer Sweet 5244 (3n) had higher lycopene and ζ-carotene accumulation than Dixie Queen (2n) at two time points, 20 DPP and 40 DPP (see data in Chapter II).

Carotenoid development patterns were statistically similar ($P>0.05$) among diploid varieties (Dixie Queen and HNP19-2n) but not ($P<0.05$) triploids (Summer Sweet 5244 and HNP19-3n), though the same characteristic carotenoid accumulation regulation trends were seen among all varieties (**Figure 11** and **Figure 12**). When data were spilt by genetic background, Dixie Queen (2n) and Summer Sweet 5244 (3n) carotenoid development patterns were more divergent from each other than those of HNP19-2n and HNP19-3n for all carotenoids except β-carotene and phytoene for which they were less distinct. Similar to the findings for accumulation level, the pattern of

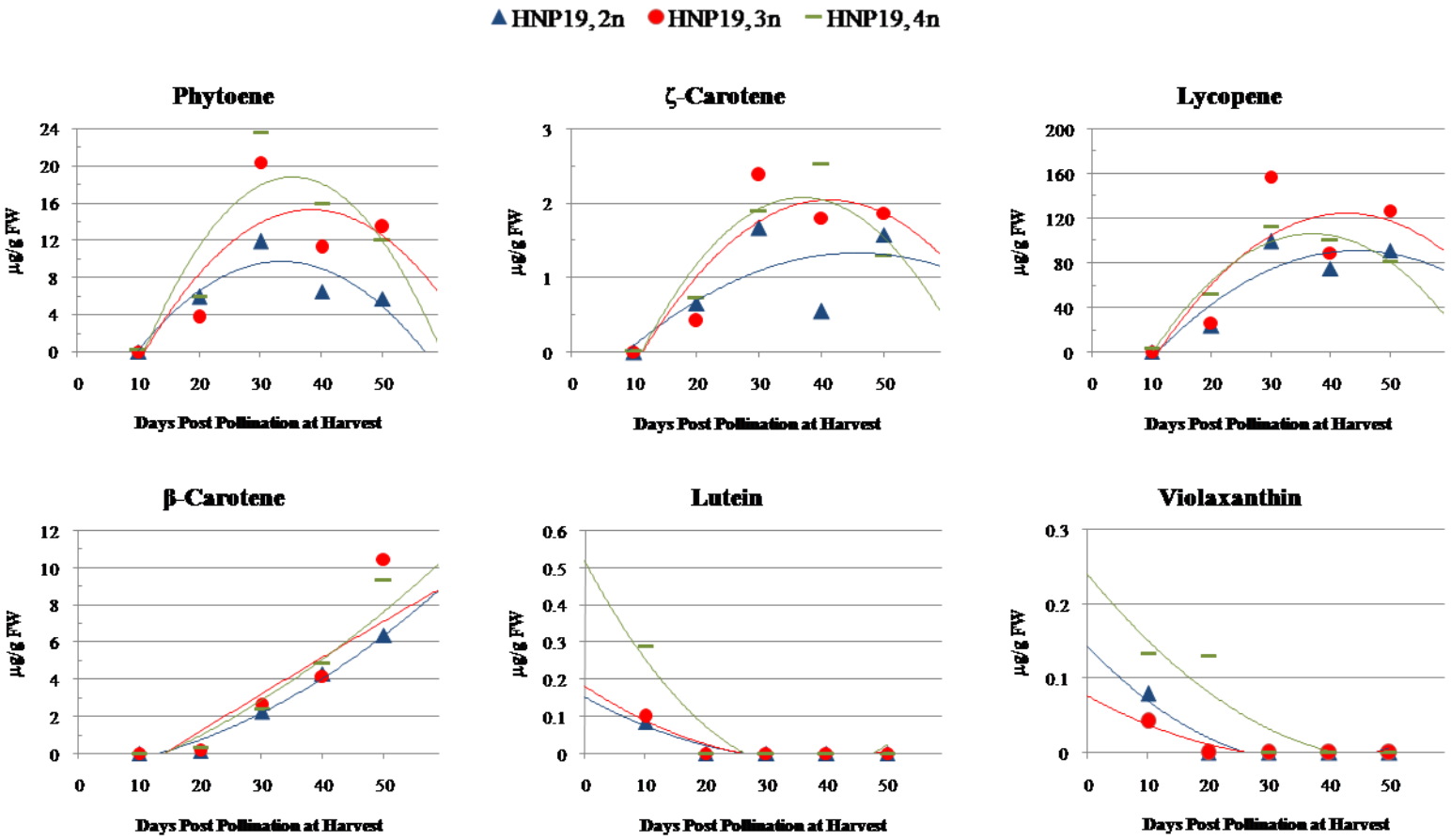

Figure 12. Developmental patterns of six carotenoids at three ploidy levels in the same genetic background. Data are means expressed as µg/g fresh weight (µg/g FW). Varieties: HNP19 (2n), HNP19 (3n), and HNP19 (4n).

carotenoid development was similar ($P>0.05$) for all HNP19 ploidy levels in all carotenoids except violaxanthin. Finally, for all varieties, diploid and triploid development patterns could only be distinguished for lutein and ζ-carotene and approached significance for lycopene.

DISCUSSION

Though it did not reach statistical significance, the HNP19 triploid mean lycopene content did exceed that of the diploid at every time point. This trend supports the hypothesis that triploids contain higher carotenoid levels than diploids. The commercial varieties upheld this concept, their behavior being its source, in a statistical manner. Commercial triploid varieties have experienced intense breeding pressure, often directed toward increased color (lycopene), due to the value of the seedless trait. This may account for the heightened response among the commercial varieties as opposed to the HPN19 series which has experienced no such breeding pressure. This evidence indicates that the common explanation of triploid and diploid behavior may oversimplify the factors involved. The relative consistency with which triploids accumulated higher levels across all colors of commercial varieties supports this hypothesis.

The putative explanation of elevated carotenoid content in triploids as a function of extra genes, called a dosing effect, would predict an even greater level of carotenoid accumulation in tetraploids (4n). Data from the HNP19 series generally did not support

this prediction, rather showing a trend placing tetraploid mean lycopene content intermediate to the diploid and triploid varieties. Dosing effects have been shown to have detrimental effects in some crops when extended beyond a certain limit (*56*). We suspect that these effects are responsible for the deflated response of the tetraploid HNP19.

The similar regulatory trends seen in all red varieties further establish the pattern as a function of flesh color. The greater difference seen between triploids may again be explained by intense breeding pressure exerted on the commercial variety. Additional insight into the influence of ploidy on developmental pattern was gained by juxtaposition of ploidy interaction statistics in the HNP19 series and those of the varieties from different genetic backgrounds. Greater difference in developmental pattern was seen between the ploidies with different genetic backgrounds than those with the same background. These observations may show that the overall genetic background is generally more responsible for the differences in carotenoid developmental patterns seen between varieties of the same color observed in Chapter II and other studies than is the ploidy level itself. The final observation that diploids and triploids could not generally be distinguished further emphasized the reduced role of ploidy in carotenoid developmental regulation.

CONCLUSION

Despite consistency in general carotenoid developmental trends, interesting genotypic and ploidy-dependent effects were observed. Evaluation of the HNP19 series allowed for a more focused look at the difference between genotypic and poidy influences. These observations may influence the meaning of results found in other studies and Chapter II herein. Further investigation with additional genetically identical lines is needed to substantiate ploidy versus genotypic effects in each color variant.

CHAPTER IV

EVALUATION OF VARIANCE IN HEAT UNIT PERCEPTION OF WATERMELON AS PART OF A FRUIT MATURATION STUDY

INTRODUCTION

Though "Days to Harvest" is an approximation of the time needed for fruit development, in many varieties temperature is an important part of fruit development, especially ripening. Perceived temperature is measured in a quantity called a heat unit. In cases where heat units are more important for fruit maturation than growing days, a cumulative number of heat units will lead to ripeness. Heat units perceived for a given day are calculated by averaging the maximum and minimum temperatures and subtracting a "basal temperature" that is specific to the crop in question. For watermelon this basal temperature is approximately 50°F (*57*), though the requirements can vary by variety. These heat units are then accumulated over the period of fruit maturation until a total is reached that is consistent with maturity for a given cultivar.

Watermelon fruit ripening is highly controlled by the number of perceived heat units. The number of days to harvest varies between cultivars and every grower will have their own preferred method of judging ripeness but, as a very general rule, watermelon will mature at approximately 40 days post pollination (DPP). This estimate, however, is based on moderate weather conditions during a normal growing season. The present study, however, was conducted in a greenhouse in the summer. Both of these

factors contributed highly to heat units in great excess of those which would be perceived under ideal circumstances.

MATERIALS AND METHODS

The primary study was designed to monitor carotenoid development in ten watermelon varieties (see **Table 3**) at multiple intervals post pollination, from shortly after pollination to well into over-ripeness. These intervals were set at 10, 20, 30, 40, 50, and 60 DPP.

Premature ripening of the fruit was observed. The influence of heat units became suspect. The present approach was undertaken to evaluate the variance in heat units perceived by the fruit at each growth stage. The data used here are estimates of the heat units based on local weather almanac recordings (recorded at an airport 1 mile away), not direct greenhouse measurements. It should be noted, however, that the greenhouse used had sub-optimal cooling which resulted in greenhouse temperatures above ambient

Table 3. Variety List (Heat Units Study).

ID#	Variety Name	Color	Ploidy
5201	Orange Flesh Tendersweet	Orange	2n
5202	Orange Sunshine	Orange	3n
5203	Early Moonbeam	Canary Yellow	2n
5204	Amarillo	Canary Yellow	3n
5205	Yellow Flesh Black Diamond	Salmon Yellow	2n
5206	Summerwseet 5244	Red	3n
5207	Dixie Queen	Red	2n
5208	HNP19-2x	Red	2n
5209	HNP19-3x	Red	3n
5210	HNP19-4x	Red	4n

during the day. Optimally, these would be the same for each variety and replicate data points. This was not the case, however, and significant differences were seen between the heat units received by each variety for each given interval in all cases. These differences are due to any factor which contributes to a non-synchronization of pollination and harvest dates within a certain tolerance level including time to first flowers and ease of fruit set. Tukey's Honestly Significant Difference (Tukey's HSD) post-hoc test was performed to determine between which varieties these differences were significant.

"Day 30" fruit were not obtainable for four of the varieties. The remaining varieties which had two or more fruit harvested 30 DPP were considered in a Tukey's HSD. Means ranked in different subsets are significantly different while those in the same subset are not. Significance levels were measured at $\alpha = .05$. Since sample size varied, a harmonic mean of the sample size was used for calculations.

Based on the evaluation of these subsets, outliers were selected which would reduce the variation in perceived heat units, thereby normalizing the data according to heat units.

RESULTS AND DISCUSSION

Table 4 shows the subsets of the means for all varieties at each time point, including all data. After the removal of outliers, the revised subsets are shown in **Table 5**. Additional or different points could be excluded based on reducing the standard

deviation (outliers within the group). The exclusion of these points may, however, be in direct conflict with the objective presented here to normalize the number of heat units perceived between groups. Such points could not, in good conscience, be removed with the sole goal of modifying the average heat units of the group. This conflict was the primary factor responsible for subsets which remained deviated from the other group (days 40 and 60 were unchanged).

Table 4. Mean Heat Units Perceived by Fruit (All Data). Missing Varieties Had No Fruit for 30 DPP. Letters Represent Tukey's HSD.

	Mean Heat Units											
Variety	10		20		30		40		50		60	
5201	365	abc	688	abc	1020	ab	1390	a	1740	a	2058	ab
5202	381	abc	738	bc	N/A		1420	b	1736	ab	2044	c
5203	374	abc	695	abc	N/A		1389	a	1736	ab	2058	ab
5204	389	abc	740	c	1030	ab	1418	b	1731	b	2050	ac
5205	351	ab	676	a	1080	b	1389	a	1737	ab	2055	ab
5206	399	c	727	abc	999	a	1417	b	1731	b	2044	c
5207	391	bc	698	abc	N/A		1399	c	1730	b	2059	b
5208	360	abc	685	ab	1061	ab	1388	a	1735	ab	2056	ab
5209	349	a	676	a	1071	ab	1389	a	1735	ab	2056	ab
5210	390	abc	694	abc	N/A		1393	a	1739	a	2057	ab

Table 5. Mean Heat Units Perceived by Fruit (Outliers Removed). Missing Varieties Had No Fruit for 30 DPP. Letters Represent Tukey's HSD.

	Mean Heat Units											
Variety	10		20		30		40		50		60	
5201	365	a	688	ab	1020	a	1390	a	1740	a	2058	ab
5202	381	a	733	ab	N/A		1420	b	1736	ab	2044	c
5203	374	a	695	ab	N/A		1389	a	1736	ab	2058	ab
5204	389	a	735	b	1030	a	1418	b	1732	ab	2050	ac
5205	354	a	676	a	1074	a	1389	a	1737	ab	2055	ab
5206	395	a	727	ab	999	a	1417	b	1732	ab	2044	c
5207	391	a	698	ab	N/A		1399	c	1730	b	2059	b
5208	360	a	685	ab	1061	a	1388	a	1735	ab	2056	ab
5209	352	a	676	a	1071	a	1389	a	1735	ab	2056	ab
5210	390	a	694	ab	N/A		1393	a	1739	a	2057	ab

CONCLUSION

By reducing the variation in perceived heat units it is hoped that we would be able to more accurately compare carotenoid accumulation data between varieties because data will represent melons grown in similar conditions. In order to test the appropriateness of excluding these data, trend lines were drawn through the data set with the outliers removed. When excluded, however, data fit to the trend line did not improve significantly. From this we may hypothesize that experimental error was not the primary source of variance in this data set. No data points were therefore excluded as outliers for statistical analysis of the main experiment described in Chapter II.

CHAPTER V

CHROMOPLAST AND CELL WALL ULTRASTRUCTURE IN NINE CAROTENOID-CONTAINING FRUITS AND VEGETABLES: "WHOLE FOOD", "MASTICATED", AND "DIGESTED" STAGES

INTRODUCTION

Despite the natural correlation between the physical food matrix and bioavailability, previous work in these two fields has remained relatively independent to date. A rare example where the interaction is discussed is a study by Rich et al (*57*) who investigated the differences in β-carotene bioavailability in spinach and carrot and noted differential reactions of each of these matrices to mechanical processing. For the most part, emphasis has been placed on assessing the effects of the food matrix by mechanically or chemically disrupting the food matrix and comparing uptake from the intact source. The concomitant study of cellular and organellar ultrastructure and whole food bioaccessibility is important, however, to give a more thorough view of how the food matrix affects eventual nutrient absorption.

Here we investigated the cellular and sub-cellular structures and components that may affect carotenoid bioaccessibility in order to focus on comparing the inherent ability of various food matrices to release nutrients. In addition to observation of these foods using light and transmission electron microscope (TEM) levels in their native state, an *in*

vitro digestion procedure was conducted on each of them and the products observed in the present study.

The implications of the work presented here rely heavily on the difference between bioaccessibility and bioavailability. Bioaccessibility is a measure of the fraction of the carotenoids in a sample that are available to be absorbed by the body while bioavailability is the portion of the sample that ends up in the plasma and tissues. Some factors, however, may overlap and affect both, such as fiber content. Since the interest of the current study was to investigate the potential of nutrient release from the food, not its uptake by the body, this distinction is important. When studies are conducted in living models (whether human or otherwise) the difference between treatments is often referred to only as bioavailability because there is no real way to distinguish them at that point. Some factors that are exclusive to bioavailability include nutrient status of the host, genetic factors, and other host-related factors (*59*).

Carotenoid Localization and Sequestration Within the Chromoplast

Rich et al (*58*) determined carotenoid localization and binding mechanism to be a significant factor in carotenoid transfer to the lipid droplet during digestion. They showed an increase in transfer to the lipid phase in raw carrots, but not in spinach after juicing, correlating to a respective degree of cellular structural component (cell wall) degradation. They argued that this evidence suggests an ease of transfer for the crystalline β-carotene in carrot as opposed to membrane-bound carotenes in spinach since they are more exposed in the more disrupted carrot matrix. A blanching step, in

both cases, further enhanced transfer to the lipid droplet. This increase was attributed to denaturation of membrane-bound carotenoproteins.

These findings are reminiscent of those by de Pee et al (*27*) who concluded that chloroplasts are less efficiently disrupted by digestion than are chromoplasts by comparing β-carotene bioavailabilities from green-leafy vegetables and carotene-rich fruits (mango, papaya, and pumpkin). However, other factors may also be playing an important role, such as chromoplast substructure. Where tomato lycopene and carrot β-carotene are sequestered into carotenoid crystals within the chromoplast, the carotenoids of the fruits used by de Pee are reportedly stored in oil globules called plastoglobuli. It is generally shown that these globules are more easily solubulized in the bile salts and, therefore, incorporated into micelles than are the crystals which have strong carotenoid-carotenoid interactions. At what stage of digestion this occurs, however, is unknown.

Good detail of chromoplast substructures is given within Camara et al's (*60*) review on chromoplast development. Given here is a brief summary of each of the chromoplast substructures.

Globular

This structural characteristic refers to the plastoglobuli which are the predominate feature of the chromoplast. Usually spherical in shape, the globules are lipid deposits in which carotenoids are dispersed. Hansmann et al (*61*) described the composition of globules in *Viola tricolor* as 90% non-polar components of which 15-25% were carotenoids, though these proportions are probably highly species or even

maturity dependent. Plastoglobuli are highly osmiophilic, and hence stain darkly in preparations using osmium tetroxide, due to their high lipid content. This is considered the most primitive, and therefore is the most ubiquitous, form of carotenoid storage (*60*). Globular carotenoids are also considered to be among the most easily solubilized during digestion since they are not encumbered by binding proteins or in a crystalline matrix (discussed below).

Tubular and Fibrillar

Though these structures are distinct, they are difficult to differentiate in micrographs and are therefore considered together. Early studies hypothesized that these elongated structures were derived from globules which were stretched and modified into tubules or fibrils and that the globules in these chromoplasts would appear "tear-drop" or "tad-pole" shaped (*62*). Though other variations built and modified this explanation to include a bundle arrangement or a less organized system (*63*), no conclusive suggestions to explain the association of globules and tubules/fibrils predominate. Fibrils are hypothesized to have a pure carotenoid interior surrounded by a lipid-protein sheath containing an approximately even ratio of lipid to protein (*64*) and a microfibrilar structure at high magnification. This microstructure is absent in tubules.

Crystalline

Carotenoid crystals are found in species containing principally lycopene and α-carotene since these are the only two carotenoids that appear to form crystals (*65*).

Though the term ‘crystal’ may be somewhat of a misnomer since carotenoid crystals have no internal crystalline structure, the term is often descriptive of their appearance. Large lycopene and α-carotene crystals may grow the length of the chromoplast, sometimes causing it to elongate. Following glutaraldehyde-osmium tetroxide fixation these crystals appear as empty, membrane-bound spaces (undulating in the case of lycopene), the carotenoids being extracted during the dehydration steps, while a glutaraldehyde-potassium permanganate fixation reveals darkly stained crystals (*66*). Conversely, small α-carotene crystals are more resistant to a glutaraldehyde-osmium tetroxide fixation. These crystals appeared to initiate from within the globules, creating less electron-dense interiors to the dark globule and elongating outward (*67*). It was unclear as to whether these crystals ever grew into the prior crystal type or were distinct in origin and end.

Membranous

Membranous chromoplasts are the least common morphotype. These chromoplasts are characterized by high concentrations of often concentric membranes continuous with the inner envelope (*68*). One definitive example is the *Or* mutant of cauliflower which accumulated β-carotene (*69*). They also usually have low plastoglobuli content (*60*). Carotenoids accumulate between closely associated membrane layers. These layers should not be confused with lamellar or thylakoid membranes, though in small areas they may resemble a similarly ordered structure.

Cell and Cell Wall Characteristics

The cell wall has been implicated as a boundary to food nutrient release until mechanically degraded (*70*, *71*). Cooked, juiced, or homogenized spinach, tomatoes, and carrots (methods of disrupting or removing cell wall structure) yielded higher bioavailability (*72*, *73*, *74* respectively). Sometimes this effect was variable for individual carotenoids, even of the same class (*32*).

The mechanical framework of a tissue has various elements, each a contributing factor in resisting the mechanical degradation of mastication. The cell wall, middle lamella, and the concurrent turgor pressure placed on these constitute these forces (*75*, *76*, *77*, *78*).

Investigating the mechanical differences between potato and carrot tissues, Zdunek and Umeda (*79*) concluded the following implications of cell wall structure:

- The fracturing of tissues composed of larger cells requires less work.
- A lower proportion of cell wall, i.e. lower density of cell walls, in the tissue leads to increased failure. This mechanism was attributed to cell volume, meaning larger cells lead to a lower proportion of cell wall volume.
- Tissue failure can occur as cell rupture, the failure point going through a cell wall, or as cell-cell debonding, where failure happens between cells. For a given food, the mode of failure transitions from rupture to cell-cell debonding as ripening progresses. This is supported by studies on fruit ripening which show degradation of the bonds between cells and of the cell wall itself as the mechanism of fruit softening (*22*). This trend, however, may have a less defined application when comparing foods. Zdunek and Umeda found that potatoes failed by cell rupture while carrots did so in a mixed manner, by rupture and cell-cell debonding.

The possible implications of cell wall thickness were not mentioned by Zdunek and Umeda (*79*), though cell wall thickness differences were not apparent from the

micrographs presented for potato and carrot. This factor may, however, have relation to their observation that the proportion of the tissue composed of cell wall affected the work to failure requirement in addition to cell volume. The principle upon which their conclusion that "the work necessary to fail the tissue increases with the density of the elements that create the mechanical skeleton", referring to the proportion of cell wall material, may also hold for the mechanical properties of the wall itself. In other words, separate from the amount of cell wall present per tissue volume, the thickness and density of the cell wall may have bearing on failure relationships.

The cell wall is composed of fibrous cellulosic microfibrils embedded in a matrix of polysaccharides, hemicellulose and pectin (*80*). Iwai et al (*81*) additionally found pectins to be a major component of the middle lamella as well as functioning in determination of cell wall thickness and porosity. **Table 6** was adapted from those found in Marlett (*82*), giving cellulose, hemi-cellulose, and pectin contents of the foods used in the present study. Mango, however, was not evaluated by Marlett and is therefore not included here, nor could the same information be found elsewhere. Marlett's values were normalized to 100g for comparison purposes. In the present study, we found various levels of fibrosity, wall thickness and density, and robustness of the middle lamella, and correlations were found to the varying levels of these components.

Table 6. Soluble and Insoluble Fiber Content of Fruits and Vegetables Observed in This Study (Excluding Mango). Data and Table Adapted From Marlett (*82*). Data Are g/100g Fresh Weight.

	Soluble Fibers			Insoluble Fibers					
	Hemi-Cellulose	Pectin	Total	Cellulose	Hemi-Cellulose	Pectin	Klason Lignin	Total	Total
Bnut Sq.	0.10	0.29	0.29	0.88	0.29	0.29	trace	1.57	1.86
Carrot	0.29	0.29	0.57	0.86	0.57	0.57	0.14	2.14	2.71
Grapefruit	0.10	0.10	0.10	0.10	0.10	0.10	trace	0.30	0.40
Melon	trace	0.13	0.13	0.38	0.13	0.13	trace	0.63	0.75
Papaya	trace	trace	0.14	0.86	0.43	0.71	trace	2.00	2.14
Sweet Pot	0.19	0.28	0.47	0.75	0.38	0.19	0.09	1.32	1.79
Tomato	trace	0.10	0.20	0.30	0.10	0.10	0.10	0.60	0.80
Watermelon	trace	trace	trace	0.13	0.13	0.13	trace	0.38	0.30

Mechanical and Chemical Forces at Work During Digestion

Understanding what we see in the micrographs at various stages of degradation of the food is aided by understanding the mechanical and chemical forces at work in the digestive process. An *in vitro* bioaccessibility model was utilized for this study to mimic the gastric and intestinal phases of digestion. For reference, the human digestive pathway of carotenoid extraction from foods is as follows: Cell adhesion and cell wall integrity is disrupted during food preparation and, to a small degree, mastication (physical disruption); degradation of these structures does not occur during chemical digestion. Upon introduction of the meal into the stomach, acid and pepsin are secreted and begin the chemical degradation of the meal. The gastric emulsion is then emptied into the duodenal intestine where the pH is raised and bile salts and lipases are secreted. The bile salts and lipases facilitate the construction of micelles, lipid monolayers with a hydrophobic core and polar surface, and carotenoid transfer to them. Micelles are the

vehicles for delivering the carotenoids to the intestinal cells since the non-polar nature of carotenoids prevent passive diffusion from intestinal fluid into the cells. The *in vitro* model used here, essentially according to a modification of Chitchumroonchokchai et al (*83*), in general, is as follows: a 'meal' consisting of the food sample of interest and a lipid source is diluted in a saline solution, the pH lowered using hydrochloric acid, and pepsin added. After a shaking incubation at physiological temperature, the pH is raised with Na_2CO_3 and bile salts and lipases added. This method will be used to compare the bioaccessibility of carotenoids from major fruit and vegetable sources.

To a degree, mastication breaks the physical barriers of the food matrix, including cell walls and cellular membranes releasing the food contents to be acted upon by the forces of digestion. Though the blending and homogenization used here are clearly extreme mimics for the chewing of foods, they are necessary for the replicability of data in further studies since irregular food particle size will yield data ranges in kind. The micrographs of "Meal" samples represent fully homogenized foods. It was hoped that differences in cell wall degradation and organelle disruption would be seen between food sources.

During gastric digestion the food matrix is further disrupted and the carotenoids partially transferred to oil droplets. Under the present protocol, this is modeled by low pH in the presence of pepsin and yogurt as a fat source. Low pH has been shown to increase transfer to the lipid phase (*84*). Pepsin begins the process of breaking proteins down into peptides, these may include proteins associated with carotenoid sequestration. This phase was not observed in this study.

The enzymes of the upper lumen, mainly pancreatin (includes amylase, lipase, and protease activities), act to hydrolyze starches into sugars, proteins into peptides, and lipids into glycerols, monoglycerides, and free fatty acids that can be incorporated into the micelles formed by the bile salts also present at this time. These "mixed micelles" are then ready to be carriers for hydrophobic components of the diet, such as carotenoids. The soluble fiber portion of the cell walls would dissolve into a gel while insoluble fibers would remain essentially intact throughout. We might expect that decipherable subjects of micrographs of the "Digesta" material would contain essentially cell wall material (insoluble fiber) and any lipid components not transferred into micelles. Micelles would, as a matter of course, remain in the supernatant during ultracentrifugation to pellet the sample for microscopy preparation and were therefore not visualized here.

In relation to the discussion and interpretation of micrographs, it should be remembered that these are two-dimensional sections of three-dimensional objects. These cross-sections create images that may be interpreted several ways as the observer consolidates available information to reconstruct a three-dimensional idea of the observed objects. One major consideration to this effect is that for organelles one must be careful in using size as a measure since any given cross-section of a sphere will yield various size two-dimensional objects. This is much less true of flattened structures like cell walls.

When work on a particular fruit or vegetable has been done elsewhere, it is referenced in the "*Results*" section of that food. In several instances where chromoplasts

have been described previously for a given food, we observed additional features not mentioned in these studies. Where reasonable, terminology was retained from these works for comparison purposes. Regardless of previous work done, in all instances, observations of the impact of digestion forces on the foods are observed for the first time here and greatly aid in the understanding of the nature of each food matrix under these conditions.

The evaluation of all such structures and mechanisms in individual food matrices is important in better understanding their implications on nutrient bioaccessibility.

MATERIALS AND METHODS

Micrographs were obtained at three stages of intactness: whole food, ground "meal", and digested product. See "Digestion" below for detailed preparation of each sample type. Samples were prepared for microscopy as follows.

Whole Foods

Fresh, ripe fruits and vegetables were commercially obtained. Samples were cut under a 5% glutaraldehyde [Electron Microscopy Sciences (EMS)], 0.1 M sesquisodium salt (PIPES) (EMS) (pH 7.0) fixative into small pieces. The pieces were rotated at room temperature in same fixative for 1-2 hours then cold microwaved (Pelco Biowave, Ted Pella, Inc.) at 250 watts (all future references to microwaving refer to cold microwave at 250 watts) for 2 min cycles of on-off-on under vacuum pressure. Samples were then

washed with 0.1M PIPES buffer solution four times with 1 min in the microwave for each wash. Post-fixation occurred in a 1% OsO_4 (EMS), 1.5% $K_3Fe(CN)_6$ (Fisher Sciences) solution in 0.1M PIPES buffer and microwaved for 2 min cycles of on-off-on. Samples were washed with water once. Dehydration occurred in 5% steps of methanol (EMS), microwaving for 1 min with each step and repeating the last step of 100% methanol twice. Epoxide infiltration began by covering samples with propylene oxide (EMS) for 15 min. Resin was formulated as follows: molar ration of 1:1 anhydride [dodecenyl succinic anhydride (DDSA)] to epoxide [equal amounts of Araldite^{502} (EMS) and Quetol (LADD Research Industries)] plus 0.2 mL/10 g resin benzyldimethylamine (BDMA) (EMS) accelerator (formulation for 10 g resin: 6.25 g DDSA, 2.73 g Araldite^{502}, 1.02 g Quetol, and 0.2 mL BDMA). Resin was successively added to propylene oxide infiltrated samples in equal volumes in three steps to accomplish approximately 95% resin. Samples were then changed three times into pure resin. All resin steps were spaced at 8 hr intervals and samples were microwaved for 1 min at the end of each step. Samples were then embedded in fresh resin and allowed to polymerize in an oven overnight.

Blocks were sectioned using an Ultracut microtome (American Optical) and diamond knife (Micro Star). For visualization of large whole-cell fields, thick sections (500 nm) were collected on glass specimen slides and stained with Toluidine Blue and viewed using Zeiss (Jena, Germany) Axiophot microscope. Images were acquired with Coolsnap cf monochrome ccd camera (Photometrics) at 10x/0.3 objective and 1.25x additional magnification (**Figure 17B** at 40x), controlled by MateVue software v. 5

(Media Cybernetics), and saved as TIFF images. Spatial calibration was performed using a stage micrometer (Graticules, Ltd, Tonbridge, England). Individual overlapping images were assembled into larger mosaics using the Photomerge function in Photoshop CS (Adobe Systems). Cell sizes were calculated by Image J v. 1.40g (NIH, USA) software using the Analyze Particles function.

Thin sections (100 nm) were also collected and picked up on 200 mesh copper grids (EMS). The grids were post-stained using uranyl acetate (JT Baker) and Reynold's lead citrate (*84*) as follows. Grids were transferred face-down to 2% aqueous uranyl acetate and microwaved for 5 sec then washed four times in freshly boiled, warm water with 2 min on a vibrator between steps. Grids were then exposed to Reynold's lead citrate in a CO_2 free environment (Petri dish with sodium hydroxide pellets) for 2 min then washed four times with water similar to previous step. Sections were viewed with a JOEL 1200 EX transmission electron microscope at 100 kV and micrographs obtained on Kodak TEM film and developed according to standard film processing techniques. Observations were made in the range of 2,500x-25,000x magnification, calibrated to between ±5% accuracy.

Ground "Meal" and Digested Samples

Meal and digested samples (for preparation of these, see "Digestion" section below) and a full-fat plain yogurt sample (as a negative control) were fixed in an approximately equal volume of Trump's fixative. Since samples were essentially fluid, they were centrifuged to pellet the pertinent material. Pelleting occurred sufficiently at

5821*g* (4000 rpm) (BC Allegra 25R) for 10 min for butternut squash meal and digest, carrot meal and digest, cantaloupe meal, and mango meal samples. These were then washed four times with Trump's buffer and repelleted under the same conditions each time to remove supernatant. All other samples did not pellet satisfactorily and were therefore ultracentrifuged at 308,444*g* (Beckman Coulter 90Ti rotor) for 30 min to form a hard pellet. This pellet formed strata. In order to maintain homogenous sampling, these samples were mixed in a small amount of buffer and then with an approximately equal volume of 4% ultrapure agarose (Invitrogen) to create a stable matrix in which to carry out the remainder of the sample preparation. The agarose-embedded samples were cut into small pieces and fixed for additional time to cross-link the agarose. The pieces were then washed four times with Trump's buffer.

Following fixation, the remainder of the sample preparation was similar to that done for the "whole food" samples except Trump's buffer was used instead of PIPES buffer and 1% p-phenylene diamine (Sigma) was added to the dehydration steps for increased staining (*86*). Samples were centrifuged at each step of the dehydration to maintain pelleting before removing the supernatant (dehydration wash).

Digestion

Edible parenchyma tissues were digested *in vitro* essentially according to a modification of the methods described in Chitchumroonchokchai et al (*83*).

In brief, fresh, ripe fruits and vegetables were "chopped" in a blender for 1 min under nitrogen gas. A quantified volume of 120 mM cold saline (NaCl) (Sigma)

solution was added and sample was further "blended" for 1 min. Samples were then measured out according to the results of the pilot study and 3 g full-fat yogurt was added. The volume was increased to 25 mL with saline and homogenized with a microhomogenizer at 40 rpm for 1 min. An aliquot of 5 mL was moved to another tube and labeled "Meal". Gastric digestion was simulated by lowering the pH to 2.0 using 1M HCl (EMD Biosciences Inc.) and adding 1600 µL of pepsin (Sigma) (10 mg/mL in 100 mM HCl). Reaction volume was brought to 32 mL with saline. Tubes were blanketed with nitrogen gas, capped, and sealed with parafilm. Samples were incubated in shaking (85rpm) water bath for 1 hr at 37 C. The gastric phase was terminated by adding 1 M $NaHCO_3$ (JT Baker) to increase the pH to 6.0 and cooling samples on ice. Intestinal digestion was initiated by adding 1600 µL pancreatin/pancreatic lipase (both from Sigma) mixture (10 mg/mL and 5mg/mL, respectively) and 2 mL of the bile mixture [7.55 mg/mL glycodeoxycholate (Sigma), 4.70 mg/mL taurodeoxycholic acid (Calbiochem), 8.06 mg/mL taurocholate (Alfa Aesar)]. The pH was then adjusted to 6.9 with 1M NaOH (EMD) and the final volume was increased to 40 mL with saline. Samples were again blanketed, sealed, and incubated for 2 hr. An aliquot was moved to another tube and labeled "Digesta".

Data Analysis

Statistics on cell size were calculated as means±SD (representing variation in cell size observed) and tested for significant difference (Tukey's HSD) to compare foods. A scoring system was also developed to quantitatively assess the character and relative

quantity of the cell wall and chromoplasts structures and identify any correlations between them. A simple correlation test (Spearman's rho) was run to determine the nature of the relationships between structures in the native food and their persistence into the meal and digest fractions. All statistics were run using SPSS 15.0 software.

RESULTS AND DISCUSSION

Butternut Squash (*Cucurbita moschata* Poir)

Whole Food

Butternut squash cells varied greatly in size and shape, from nearly circular to cubescent (**Figure 13**). Mean cell size was 2466±1448 μm^2 (n=154). Cell walls were very fibrous and uniform in width, averaging 670 nm total thickness between cells (**Figure 14A**). Two chromoplast substructure types appeared evident: tubular and globular. The tubules were similar in appearance to those described by Caiola and Canini (*87*) in *Crocus sativus* L. (Iridaceae). Transverse, longitudinal, and oblique tubule sections were all observed (**Figure 14A** and **B**). One chromoplast type had abundant plastoglobuli and electron-transparent vesicles ranging in size from very small to moderate (**Figure 14A**). Longitudinal sections of tubular chromoplasts sometimes revealed very long tubules running the entire length of the chromoplast (**Figure 14C**). A single crystalloid structure inhabited a chromoplast otherwise filled with tubules and a membranous inclusion (**Figure 14D**). This membrane and those described hereafter which take on this symmetrical and often concentrically layered appearance resemble

those reviewed by Camara et al (*60*) and described more recently by Paolillo et al (*69*) in the *Or* mutant of cauliflower. It is important to note that these membranes are lipid bilayers, the carotenoids accumulating between whole membranes and advanced accumulation leading to what are termed "crystalline" structures (*60*). Many mitochondria and a variety of vaculate structures were identified near the chromoplasts. To our knowledge, butternut squash chromoplasts have not before been described, nor the nature of its cell wall.

Meal

The meal fraction consisted of uniform osmiophilic lipid moieties (**Figure 15A**). These moieties are most likely a mix of plastoglobuli and yogurt lipid (see **Figure 15B** for yogurt negative control). Also interspersed among these moieties are non-staining structures similar in character and size to the vesicles found in the chromoplasts of the intact food (compare **Figure 14A** and **Figure 15A**). A fibrous material, possibly disrupted cell wall material, was evident (**Figure 15C**) as well as a homogenous, granular material which may consist of other disrupted cellular material (**Figure 15C** and **Figure 15D**).

Digest

The digest fraction was dominated by cell wall material (**Figure 16A** and **B**) and intact elongate (perhaps tubular) structures (**Figure 16C)**. The cell walls appear very robust and persist through successive stages of digestion. Tubules and plastoglobuli are the main carotenoid storage substructures of the chromoplast, the prior possibly persisting through digestion.

From the evidence observed here, mainly the robust nature of the cell walls and abundance of protein bound carotenoid storage substructures (tubules), we suspect butternut squash carotenoids to be moderately accessible by digestion.

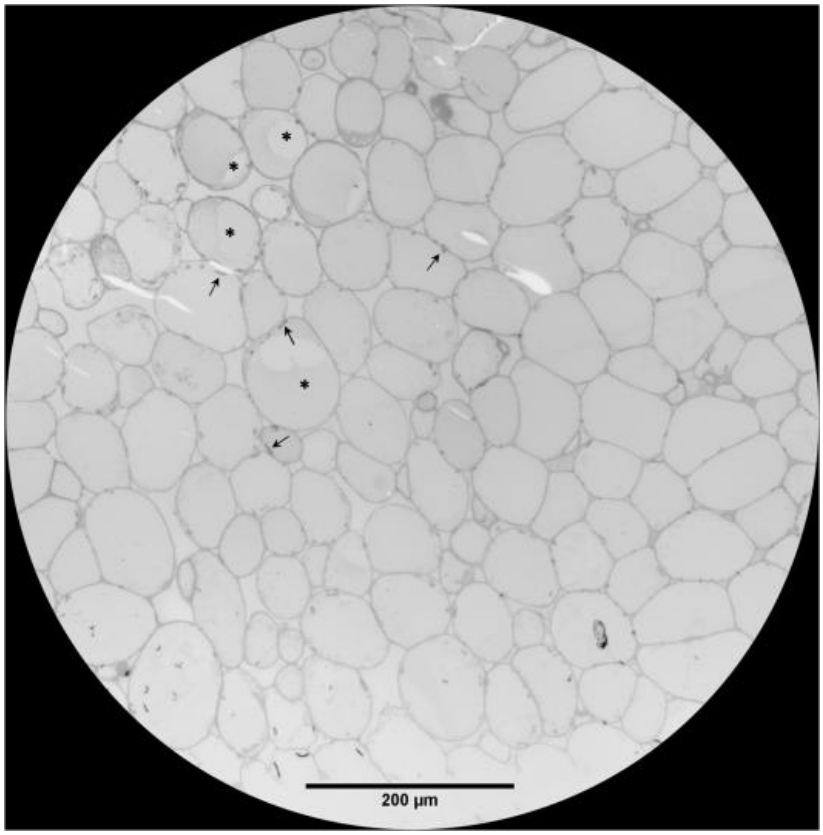

Figure 13. Light micrograph of butternut squash (*Cucurbita moschata* Poir) parenchyma cells. Chromoplasts indicated by arrows. A few cells contain mostly cytoplasm and small vacuoles (asterisks). Majority of cells mostly filled with large vacuoles.

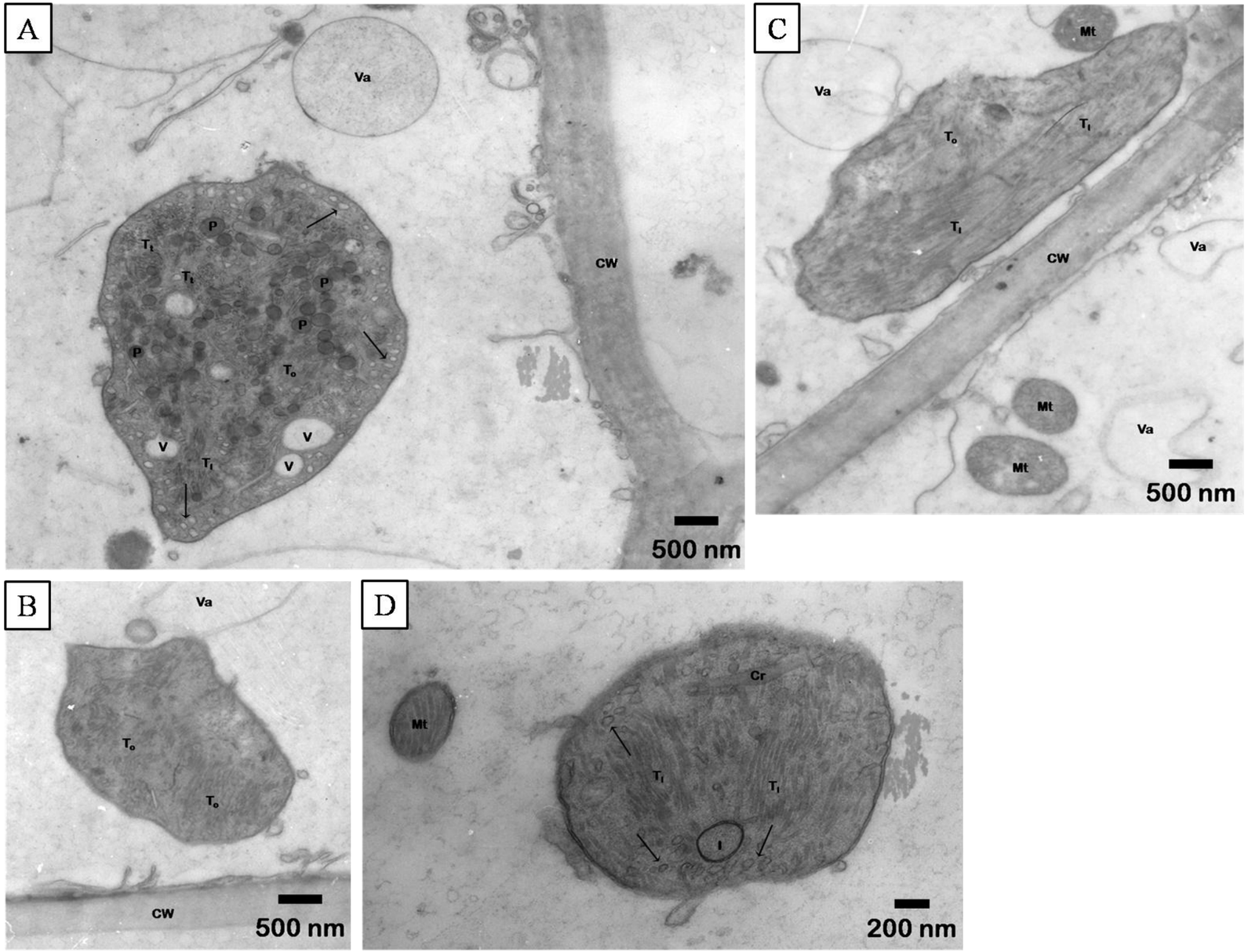

Figure 14. TEM micrographs of butternut squash chromoplasts and cell walls. **A** Globular and tubular chromoplast and cell wall. **B** Tubular chromoplast and cell wall. **C** Longitudinal tubule chromoplast and cell wall. **D** Chromoplast with tubules, carotenoid crystal, and membranous inclusion. Carotenoid crystal (Cr), cell wall (CW), membranous inclusion (I), mitochondrion (Mt), tubules in longitudinal section (T_l), tubules in oblique section (T_o), tubules in transverse section (T_t), plastoglobule (P), vesicle (V), small vesicles (arrows), vaculate structure (Va).

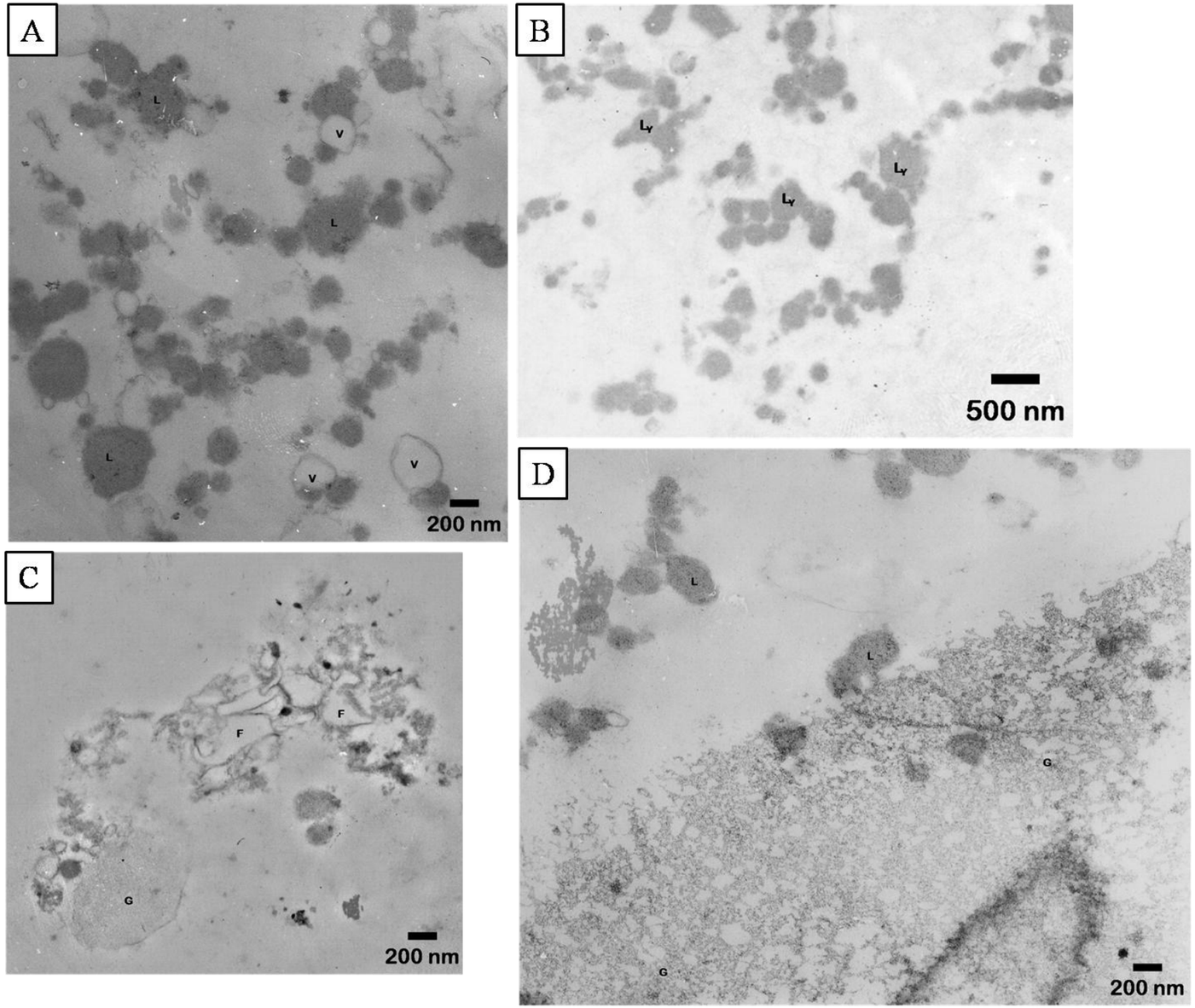

Figure 15. TEM micrographs of butternut squash and yogurt meal fractions. **A** Butternut meal lipid moieties and vesicles. **B** Yogurt meal (negative control) lipids. **C** Butternut squash meal fibrous material. **D** Butternut squash meal granular material. Fibrous material (F), granular material (G), mixed lipid moieties (L), vesicle (V), yogurt lipid moieties (L_Y).

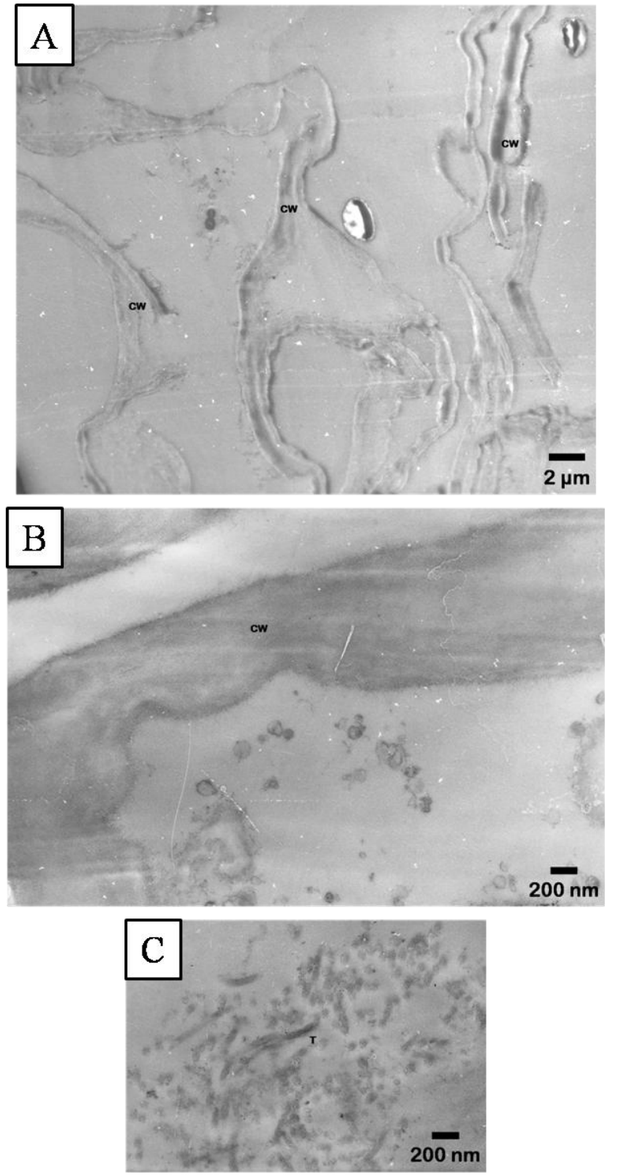

Figure 16. TEM micrographs of butternut squash digesta fraction. **A** Cell wall material. **B** Cell wall material. **C** Tubular material. Cell wall material (CW), elongate tubular material (T).

Carrot (*Daucus carota* subsp. *Sativus*)

Whole Food

Cells had irregular margins with a cubescent pattern and shape (**Figure 17A**). Mean cell size was 1818±1290 μm^2 (n=245). Chromoplasts and other organelles were evident at larger magnification (**Figure 17B**). Cell walls were very fibrous, compact, appeared to consist of layers, and measured 500-1000nm in total thickness between cells (**Figure 18A**). Distinction between the cell walls of adjoining cells was apparent. Some cell walls appear to be degrading and loosening their structure (**Figure 18B**).

In general, the chromoplasts seem to be filled with an amorphous, electron-dense material of various natures (**Figure 18A, B,** and **C**) that also appeared in the chromoplasts observed by Grote and Fromme (*88*), but was not described. Starch grains are prevalent in the chromoplasts and cytoplasm. Grote and Fromme described the prevalence of large starch grains in fresh carrot roots and their near absence after storage for 4 months. Though it is impossible to know how long the carrots we obtained from the grocery were stored, if at all, structures resembling small and large starch grains were observed in some chromoplasts and not in others. Vesicles, too spherical to be starch grains, are in a few chromoplasts (**Figure 18B** and **D**).

In rare cases, crystals took on the characteristic undulating pattern of a lycopene crystal remnant (**Figure 18C**) (*66*). Membranous inclusions were also prominent. Very large carotenoid crystal remnants appear in a few chromoplasts, sometimes rupturing the chromoplasts (**Figure 18E**).

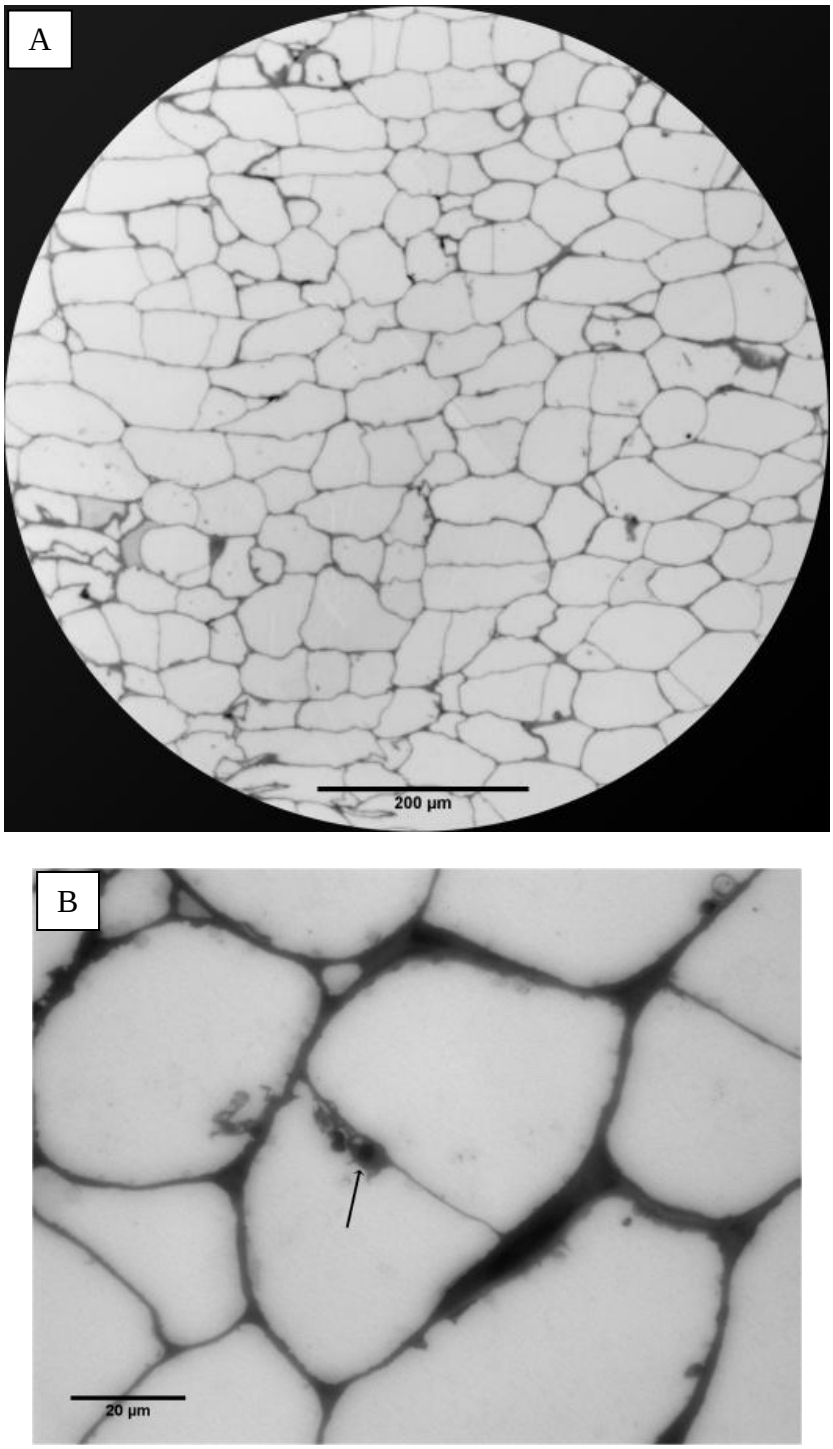

Figure 17. Light micrographs of carrot (*Daucus carota* subsp. *Sativus*) parenchyma cells. **A** Large field of whole food cells. **B** Chromoplasts in whole cell view. Chromoplasts and other organelles indicated by arrow.

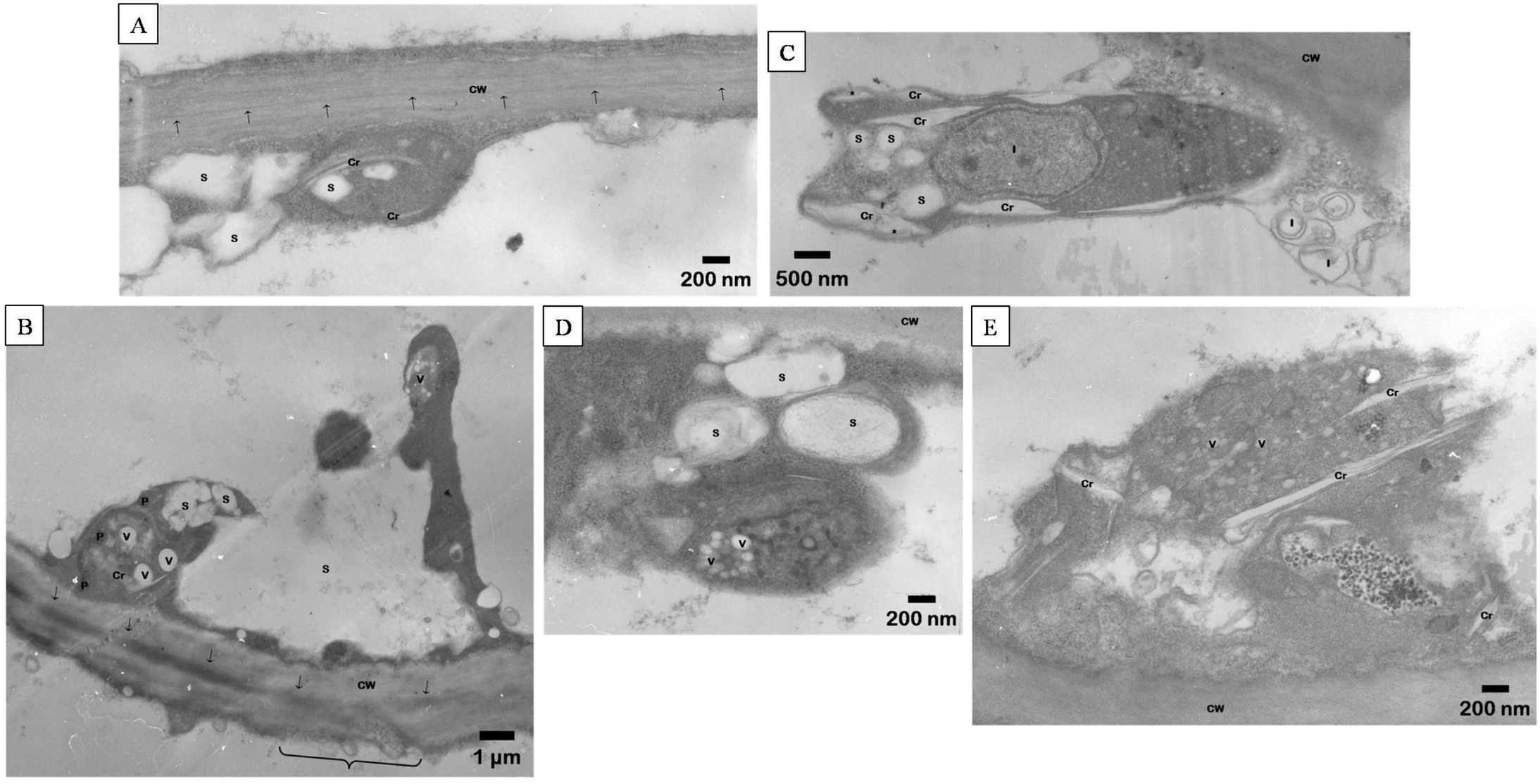

Figure 18. TEM micrographs of carrot chromoplasts and cell walls. **A** Crystalline chromoplast. **B** Two chromoplasts, large starch grain, and cell wall. **C** Crystalline chromoplast. **D** Chromoplast with vesicular inclusions and external starch grains. **E** Ruptured crystalline chromoplast. Carotenoid crystal remnant (Cr), cell wall (CW), cell wall degradation (brace), junction of cell walls (arrows), membranous inclusions (I), plastoglobule (P), starch grains (S), undulating internal structure of a lycopene crystal remnant (astrisks), vesicles (large and small) (V).

Meal

Cell wall material was still present and seemingly intact (**Figure 19A**). Two lipid types were distinguishable (**Figure 19A** and **B**). The smaller, darker globules may be derived from carotenoid plastoglobuli while the larger, lighter ones may be yogurt lipid. Though this is not greatly supported by the size of the lipid moieties seen in images of yogurt "meal" by itself (**Figure 19C**), this hypothesis is based on the lipid content of plastoglobuli being approximately 75% lipid (*31*) where the yogurt was only 3.5% (8g fat per 227g serving). The yogurt globules probably do represent a higher lipid content than this, however, since much of the water, carbohydrate, and/or protein may have dispersed into the supernatant. Still, the carrot derived lipid globules would stain more darkly. Yogurt bacteria was present (**Figure 19B**)and verified by comparison to those found in a yogurt negative control (**Figure 19C**).

Digest

Two types of materials present, though not mixed. Elongate globules with granular sub-structure were present in large fields (**Figure 20A**). A homogenous granular material was also present in large amounts (**Figure 20B**).

Though the cell walls in the intact food appear robust and fibrous, little, if any, of this material persisted into the subsequent digested fractions. Carotene crystals appear to be the major storage substructure in the chromoplast of the carrots and are thought to be among the most difficult to solubilize during digestion (*60*). And, while plastoglobuli are relatively infrequent, their lipid content is apparent in the meal fraction. The degraded cellular material in the digesta is unidentifiable with structures present in the

whole food indicating good digestion. Combined, these factors are an uncertain basis for a prediction of carotenoid accessibility from this source.

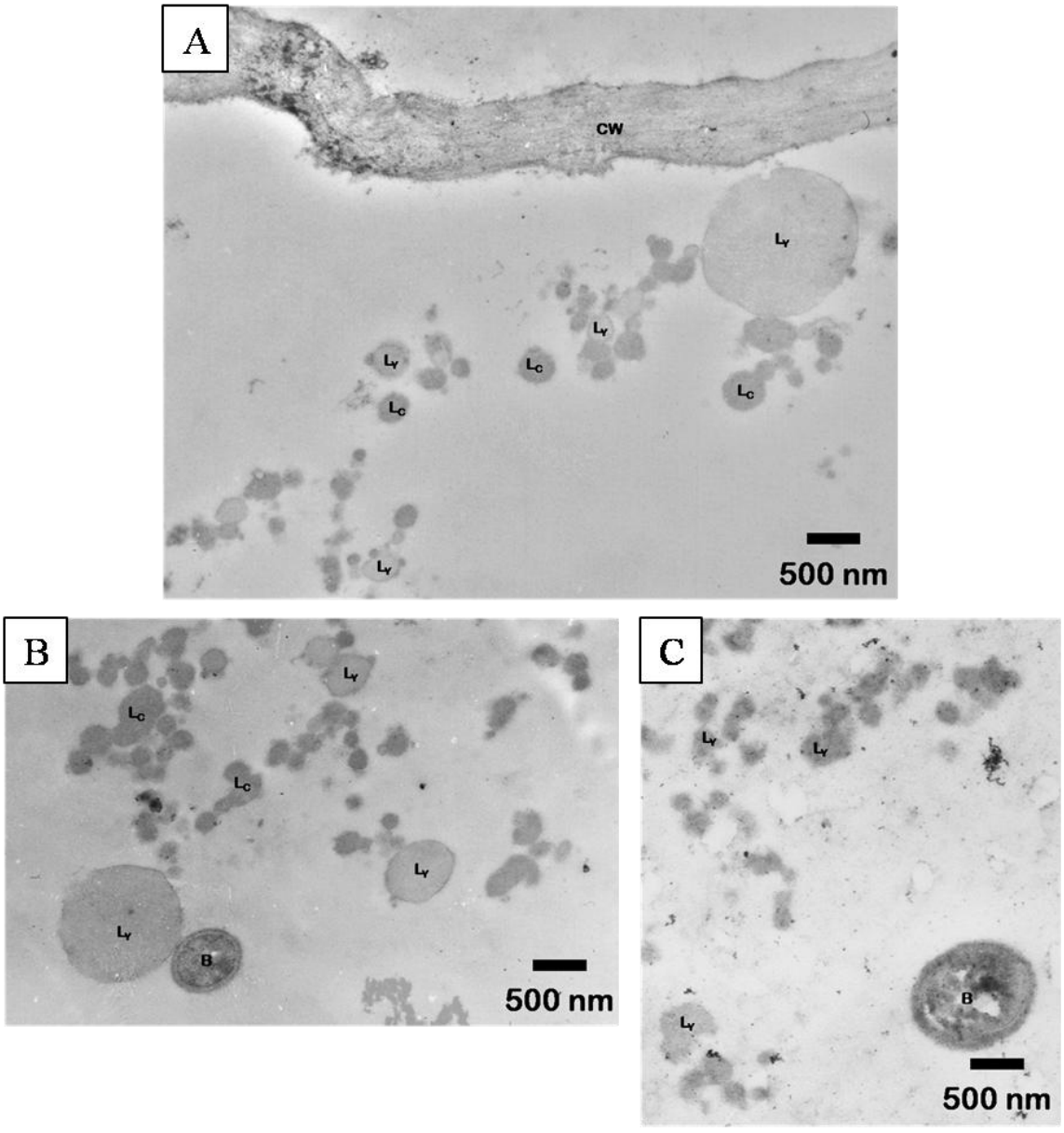

Figure 19. TEM micrographs of carrot and yogurt meal fractions. **A** Carrot cell wall remnant and lipids. **B** Carrot meal lipids and yogurt bacteria. **C** Yogurt meal (negative control) lipids and bacteria. Yogurt bacteria (B), yogurt lipid moieties (L_Y), carrot lipid (plastoglobuli) (L_C).Cell wall (CW), yogurt lipid moieties (L_Y), carrot lipid (plastoglobuli) (L_C).

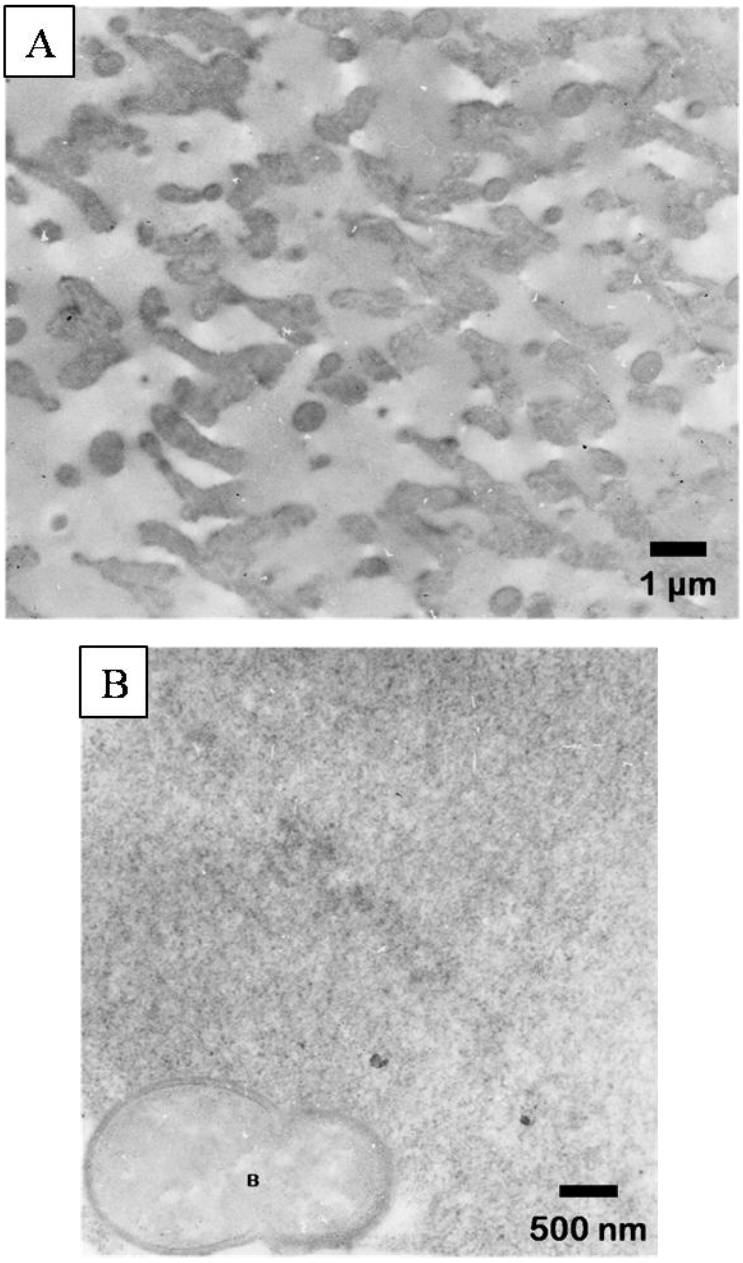

Figure 20. TEM micrographs of carrot digest fraction. **A** Lipid moieties. **B** Granular material with yogurt bacteria. Yogurt bacteria (B).

Grapefruit, Red (*Citrus paradisi* Macf.)

Whole Food

Figure 21 shows a cross-section of a juice sac. Small cubescent cells (mean area 153±98 μm^2, n=116) line the outer layer of the sac, next to a robust outer cell wall. A second layer of elongate, much larger cells lay inside this first layer (mean area 886±956 μm^2, n=75). Finally, a very loose network of very large cells with thin cell walls occupied the majority of the sac volume at the center (mean area 8719±6695 μm^2, n=71). The average cell size for all cell layers was 2684±5096 μm^2 (n=262). More detail of the outer two layers can be seen in **Figure 22** and **Figure 23A**. Cell walls were highly arboresent, varying greatly in width (200-4000 nm), even within cell layers and lightly textured, but not fibrous. Distinction between the cell walls of adjoining cells was apparent in portions of the outer layers (**Figure 23B**). Cells have large vacuoles, sometimes having vacuoles within larger vacuoles (**Figure 23A**). A fibrous material was also sometimes in the vacuoles (shown in the first layer of cells in **Figure 23A**). Cell walls were constricted at plasmodesmata and transport vesicles apparent (**Figure 23C**).

Chromoplasts were sparse and nearly exclusive to the outer cells of the juice sac. Three distinct chromoplasts were observed, though all with a background content of homogenous, electron-dense material. **Figure 23 B** shows a chromoplast that has starch-like grains within and larger without the chromoplast. The identity of these structures is uncertain since no starch content is reported for grapefruit (*89*). The most complex chromoplast contained carotenoid crystals which elongated the chromoplast and

electron-transparent vesicles (**Figure 24A**). The final chromoplast contained only the vesicles (**Figure 24B**). None of these chromoplasts resembled the one noted in passing by Shomer (*90*) during an investigation of the effects of freeze damage on grapefruit segments.

Meal

Many cell wall fragments (**Figure 25A**). Vesicles like those observed in the chromoplast also persisted into this fraction (**Figure 25B**). Uniform lipid droplets were present, yogurt and plant lipids not distinguishable (**Figure 25A** and **B**). Considering the plastoglobuli were not seen in the intact chromoplasts, we suspect that the source of the lipid seen here is most likely yogurt. Short fibrous material aggregated with some lipid droplets.

Digest

Many cell walls were still apparent after digestion (**Figure 26**). The homogenous background material was slightly fibrous and stippled in nature, very similar in appearance to the material found in the vacuoles of the intact cells (**Figure 23**).

Little attention has been given to grapefruit cell and cell wall dynamics and even less to its chromoplast's morphology. The cell walls seen at all stages of intactness suggest they are robust, though we speculate that the persistent portions of the cell walls are most likely from the outer cells where the walls were thicker than the larger inner cells with thinner walls. The chromoplasts seemed to be dominated by electron transparent vesicles, only one containing carotenoid crystals. The electron dense background material on all the chromoplasts, therefore, may be of interest when

considering little other evidence of carotenoid storage is present. Given the persistent nature of intact cell walls here along with the low presence of accessible plastoglobuli, we predict a low accessibility of grapefruit carotenoids.

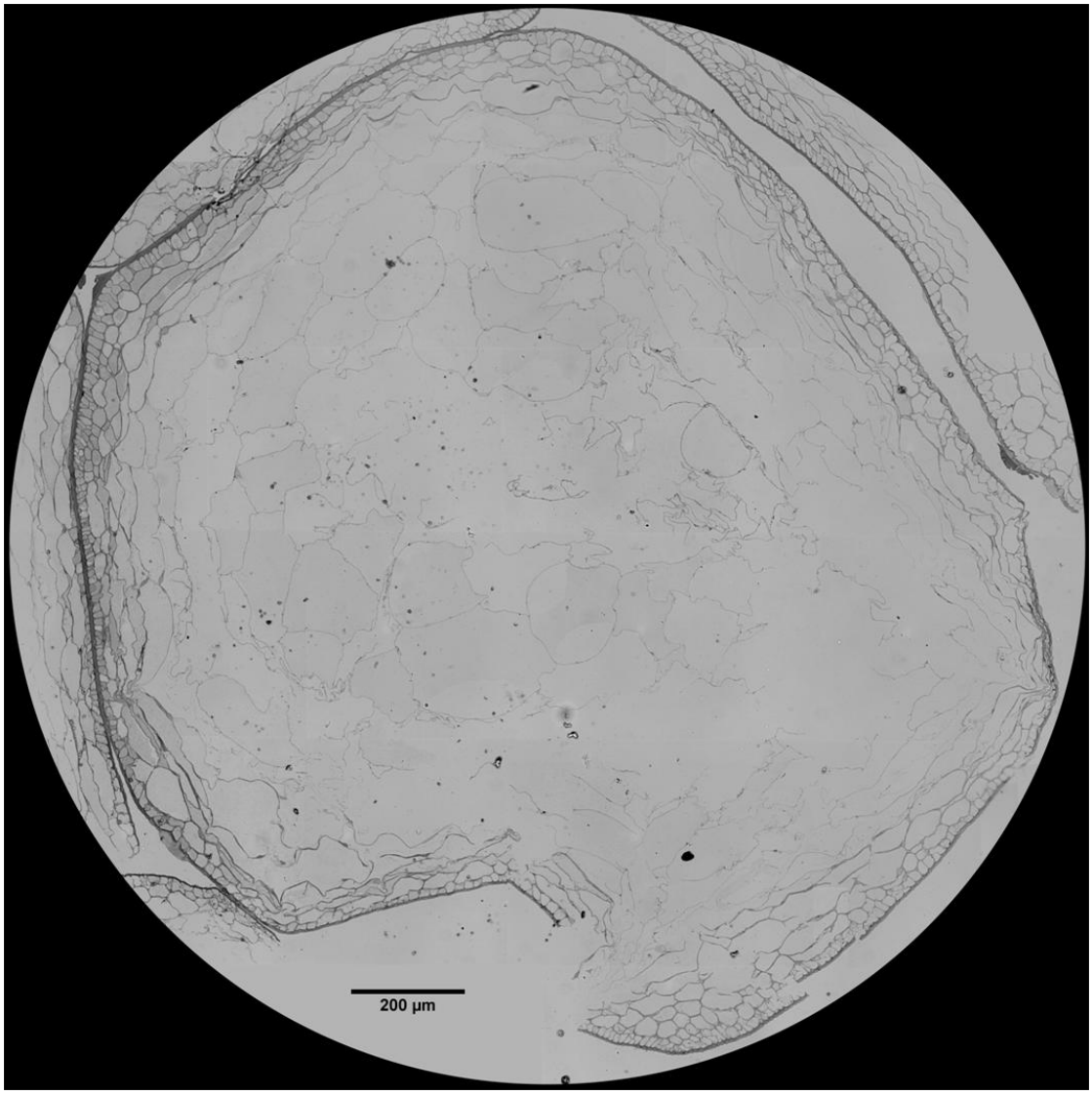

Figure 21. Light micrograph of a red grapefruit (*Citrus paradisi* Macf.) juice sac in cross-section.

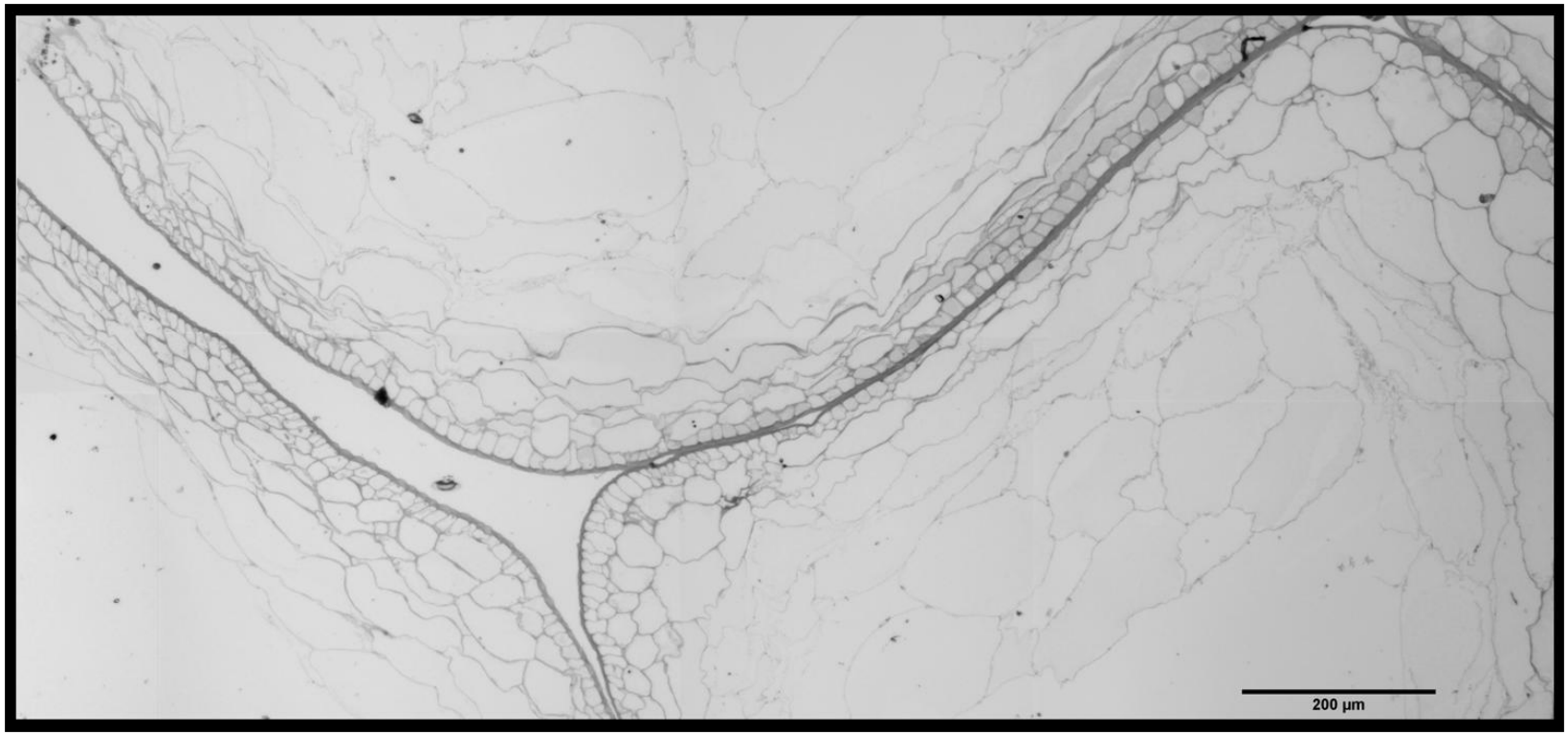

Figure 22. Light micrograph of a red grapefruit juice sac outer cells.

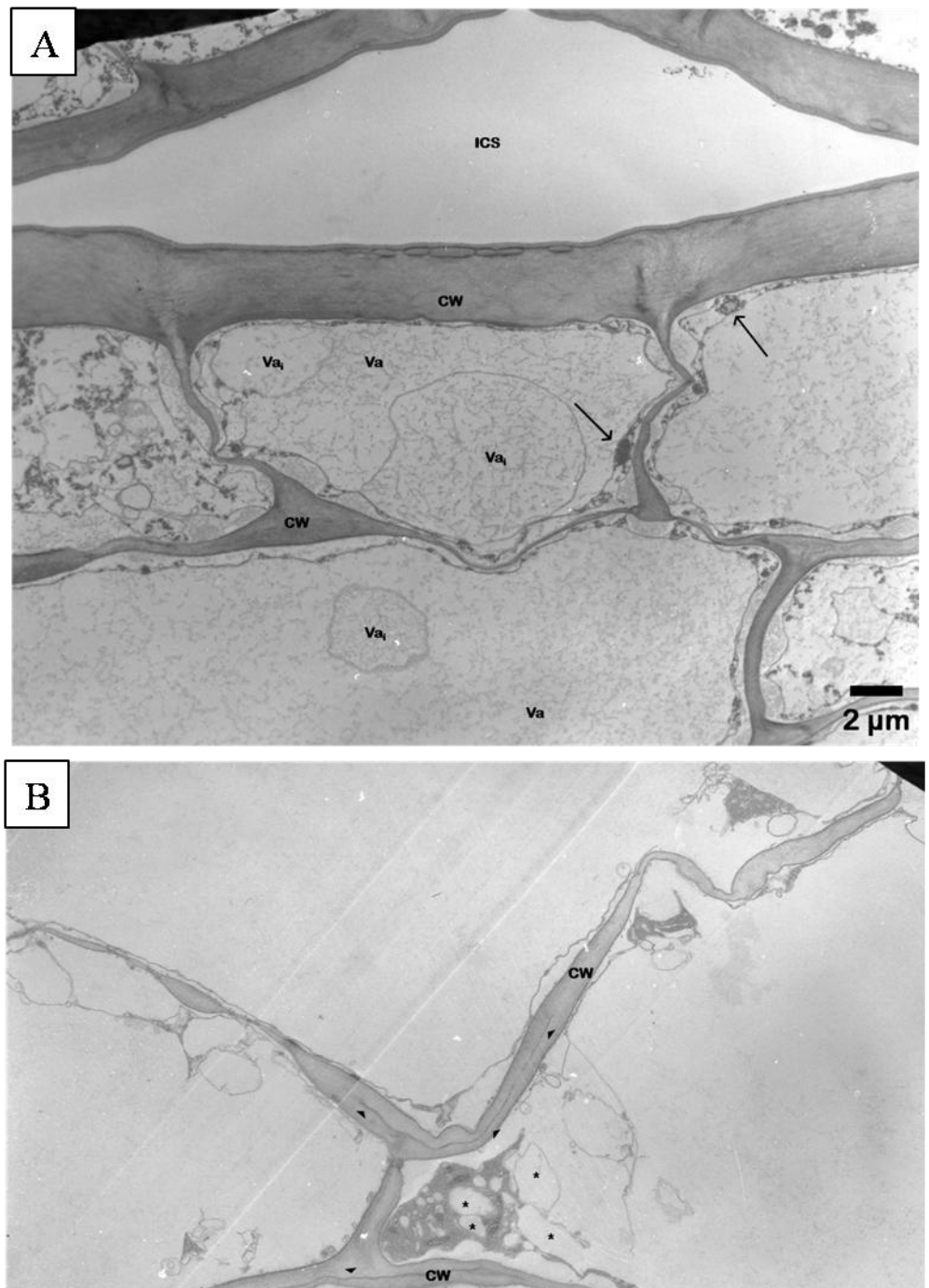

Figure 23. TEM micrographs of grapefruit cells. **A** First layer of outer cells. Note granular material in vacuoles. **B** Arborescent cell walls. Unidentified structures resembling starch grains indicated by asterisks. **C** Plasmodesmatata transversing cell wall. Cell wall (CW), chromoplasts (arrows), intercellular space (ICS), junction of cell walls (arrow heads), plasmodesmatata (braces), transport vesicles (TV), vacuole (VA), interior vacuole (VA_i).

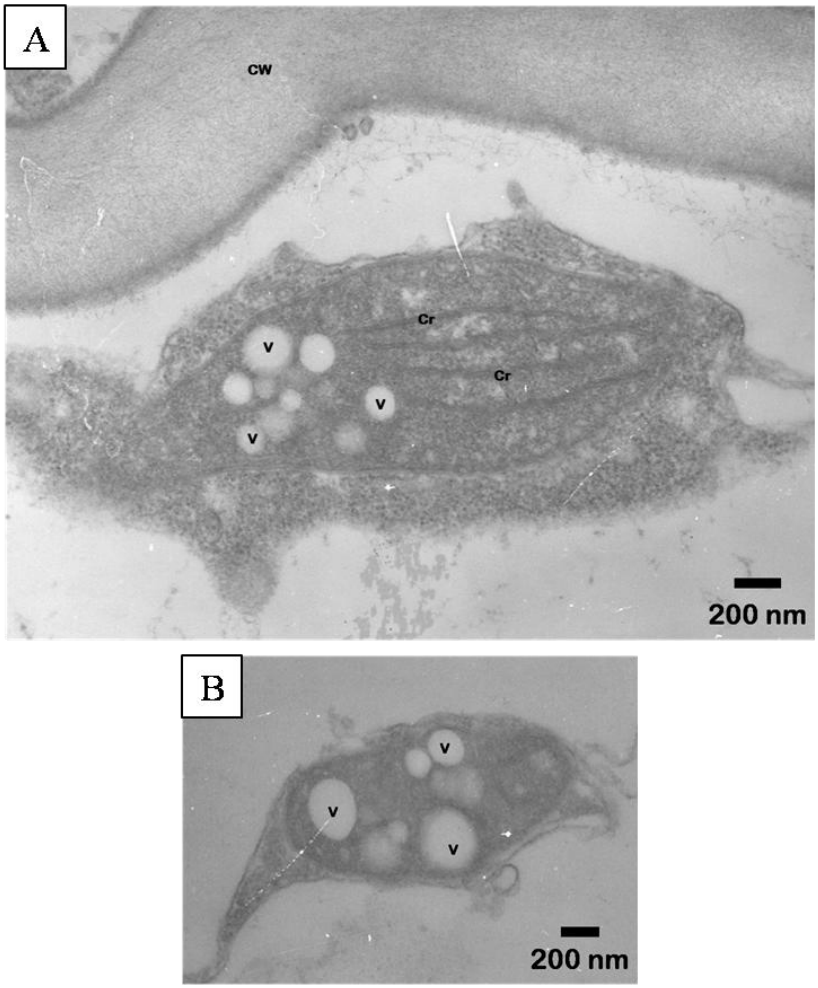

Figure 24. TEM micrographs of grapefruit chromoplasts. **A** Crystalloid chromoplasts. **B** Vesicular chromoplasts. Carotenoid crystal (Cr), cell wall (CW), vesicles (V).

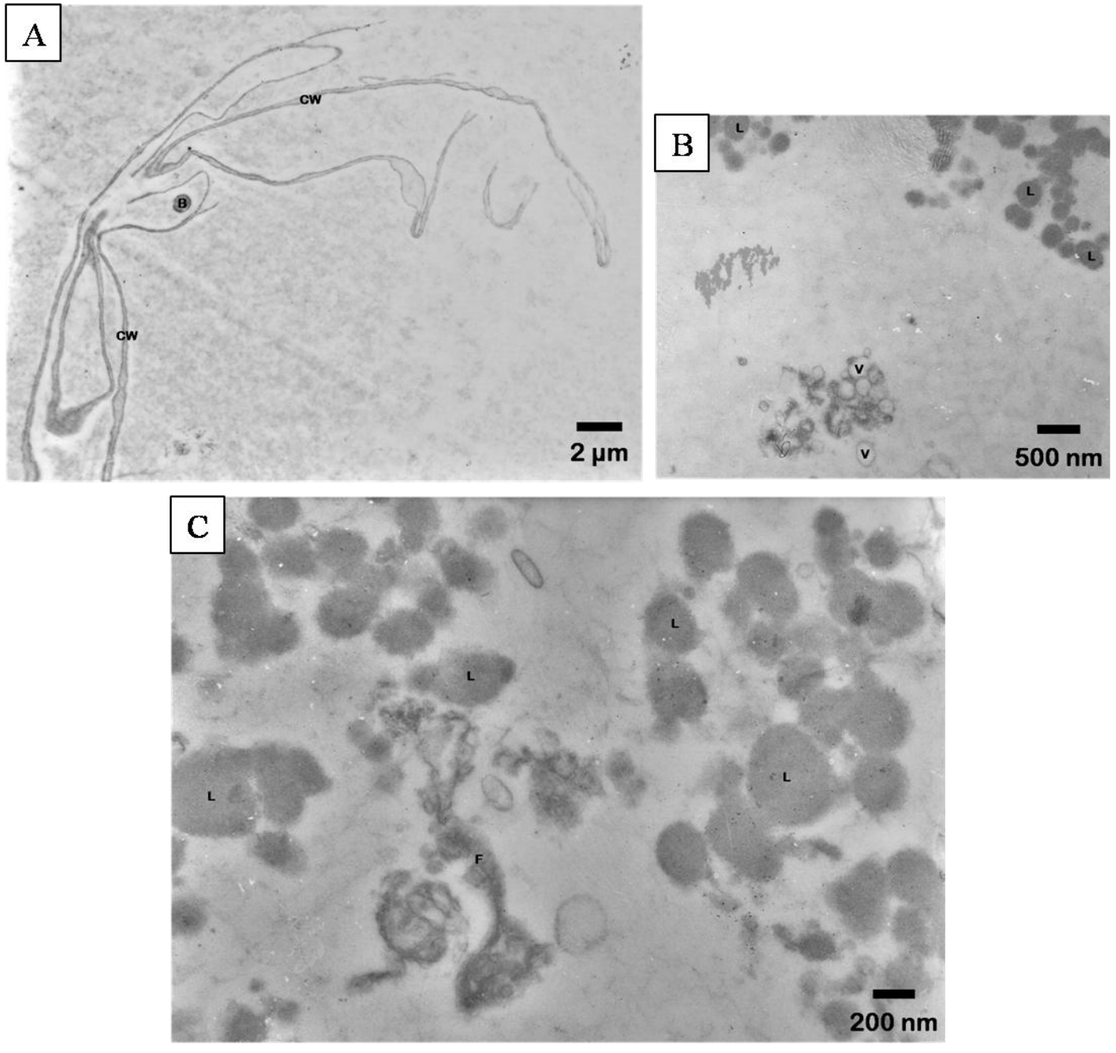

Figure 25. TEM micrographs of grapefruit meal fraction. **A** Cell wall fragment. **B** Residual vesicles and lipid. Yogurt bacteria (B), cell wall material (CW), mixed lipid moieties (L), vesicles (V).

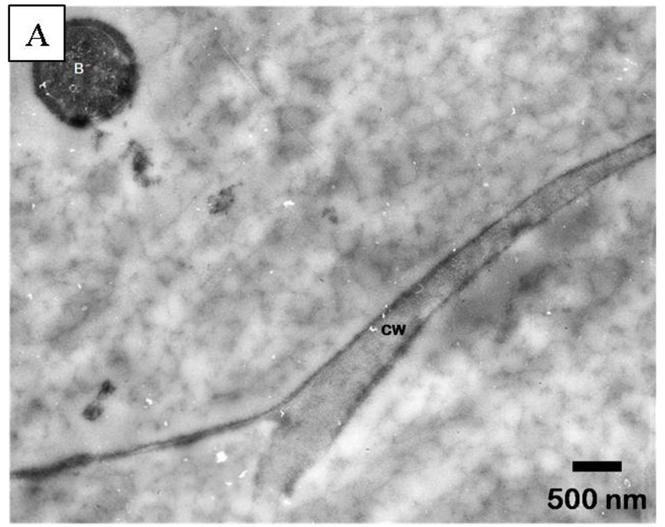

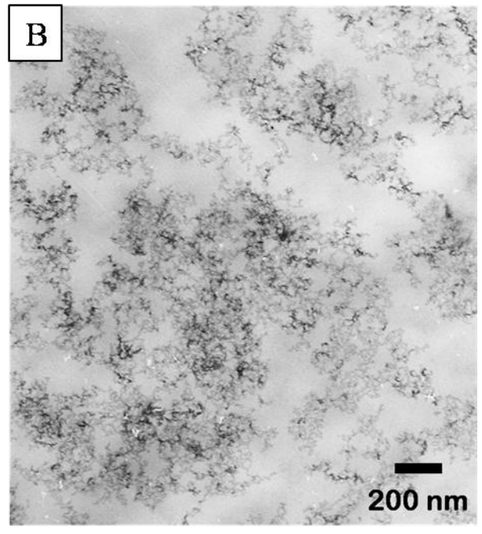

Figure 26. TEM micrographs of grapefruit digest fraction. **A** Cell wall material and yogurt bacteria. **B** Fibrous material. Yogurt bacteria (B), cell wall (CW).

Mango (*Mangifera indica* L.)

Whole Food

Mango mesocarp parenchyma cells were moderate in size (5332±3712 μm^2, n=113) (**Figure 27**). A section of xylem tissue was also observed, consisting of comparatively small cells. Extensive cell wall loosening, loss of cell-to-cell adhesion, and even cellular integrity, was apparent. This observation supports compositional data showing that cell wall components are dramatically lost during fruit ripening and softening (*91*). Cell wall thickness varied greatly from 700-5000nm (**Figure 28A**). Cell walls were very fibrous but had a loose, open structure. It appears that similar amounts of material are present in all thicknesses; however, the compression of these materials varies to yield differences in thickness.

Mangoes are relatively unique among commercially available carotenoid-containing fruits and vegetables in their content of cis-isomers (*92*). This difference has been speculated to affect carotenoid storage mechanisms and ripening chromoplast morphology accordingly investigated (*93*). The predominant feature of mango chromoplasts seen here was plastoglobuli. Many of those observed here were young or newly developing and had an ovoid shape whereas the larger globules were more spherical (**Figure 28B**), as noted by Vasquez-Caicedo et al (*93*). Also similar to Vasquez-Caicedo et al was the presence of both "networks of tubular membranes" and "prolamellar-like bodies", the fine structure of these being the distinguishing feature (ex. **Figure 28C**). The lamellar body has a more organized, honeycomb-like structure whereas the tubular network is more amorphous but still in finite singular bodies.

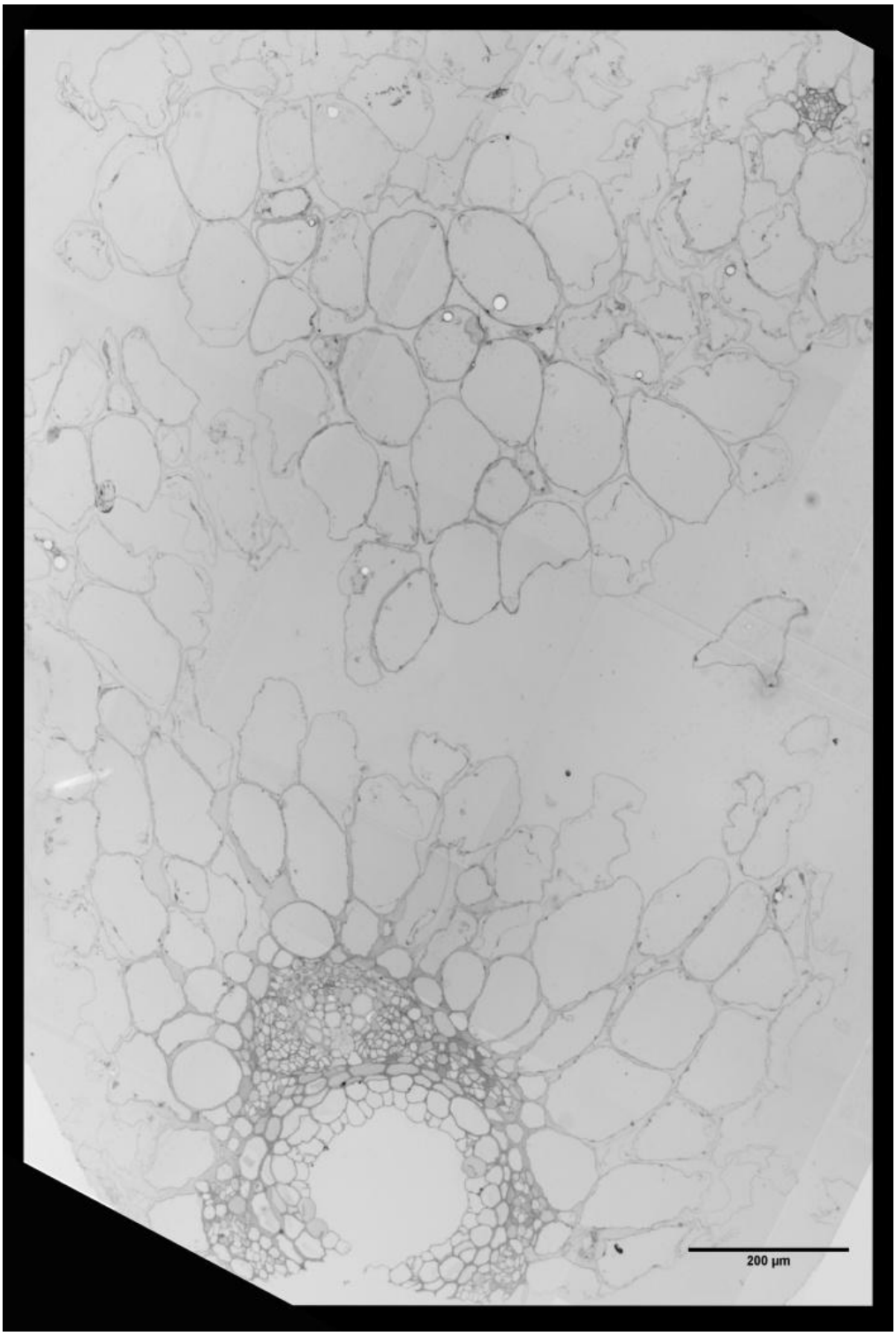

Figure 27. Light micrograph of mango (*Mangifera indica* L.) mesocarp. Section of smaller xylem cells present at the bottom of the micrograph. Cell wall loosening, loss of cell-to-cell adhesion, and even cellular integrity, is apparent.

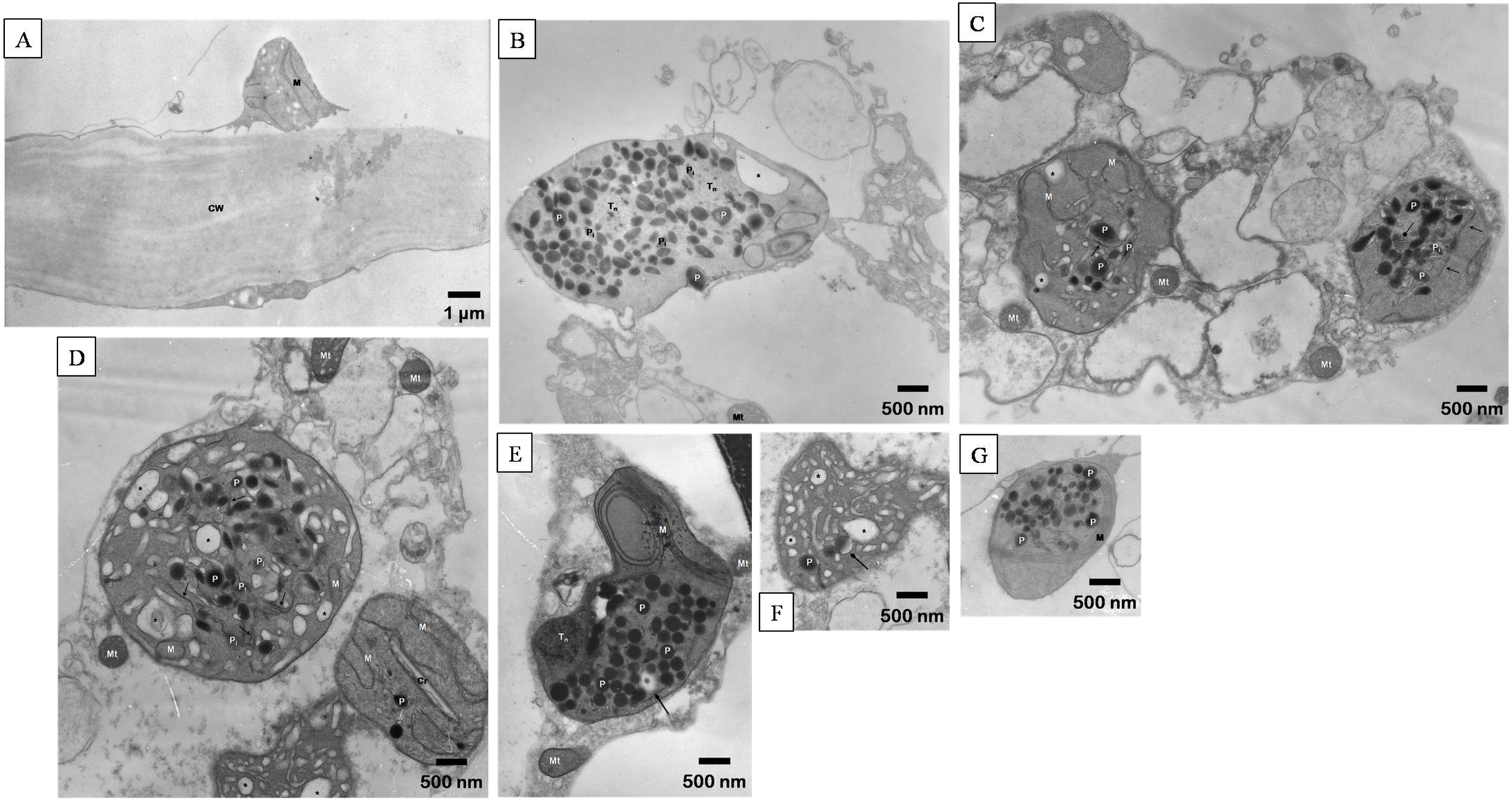

Figure 28. TEM micrographs of mango chromoplasts. **A** Cell wall with membranous chromoplasts. **B** Globular chromoplast. **C** Chromoplasts with a prolamellar body. **D** Vesicular and crystalline chromoplasts. **E** Globular and membranous chromoplast with a depleted globule. **F** Vesicular chromoplast with a depleted globule. **G** Globular and membranous chromoplasts. Cell wall (CW), large carotenoid crystal (Cr), small carotenoid crystals (arrows), carotenoid membranes (M), empty vesicle (see discussion in text) (asterisks), mitochondrion (Mt), plastoglobule (P), plastoglobule initiate (P_i), depleted globule (diamond-headed arrow), prolamellar body (round-headed arrow), small carotenoid crystals (standard arrows), tubular network (T_n).

Three features were observed here in our work that were not observed in previous work on mango. The first is the presence of seemingly membrane-bound, irregular bodies in the chromoplasts, sometimes elongate in shape (**Figure 28D** and **F**). These may be remnants of starch grains which dominate immature mango fruit cells (*93*). This is doubtful, however, since starch grains would not be membrane (nor by another lipid dense material) bound, as is seen here.

Two globules were observed for which the major part was electron dense, but otherwise electron transparent and may suggest what these structure are (**Figure 28E** and **F**). One explanation might suggest that a degree of lipid/carotenoid extraction occurred during sample preparation. Indeed, Vasquez-Caicedo et al (*93*) used acetone for dehydration where methanol was used here, which could lead to a differential extraction of lipid and/or carotenoids. We would expect, however, to see more than two instances of this partially "extracted" globules if that were the case. Regardless, none of the sub-structures observed by Vasquez -Caicedo et al (93) resemble those seen here in either shape or character. It is our opinion, therefore, that these are distinct structures, possibly membrane-bound vesicles.

A second feature unique to our observations was the presence of carotenoid crystals. Many thin, intact crystals were observed either as short crystals interspersed with plastoglobuli and the vesicles described above or larger ones (**Figure 28D**). At least one instance of a large β-carotene crystal remnant was observed. This crystal has an undulating electron-dense member adhering to the border of the crystal, usually indicative of it being a lycopene crystal remnant, but no lycopene was present in mango.

A third crystal formation observed here initiated inside the globules (**Figure 28B**). These were observed as light areas, often rod-shaped, inside an otherwise electron-dense plastoglobule. Similar observations have been made in tomato (*66*) and *Solanum capsicastrum* (*94*).

The final new sub-structure observed in the present study was abundant membranous layers, most often arranged in equally spaced, concentric layers. These were observed in several chromoplasts (**Figure 28E** and **G**). Camara et al (*60*) notes that membranous chromoplasts usually have low plastoglobuli content. This was not the case here, though the membranes are distinctly segregated from the plastoglobuli. Less organized membranes were also observed, located near the outer envelope of the chromoplast and sometimes continuous (**Figure 28C** and **D**). This type of membrane was also observed by Caiola and Canini (*87*) in *Crocus sativas* and Bonora et al (*95*) in *Arum italicum*. The individual membranes are also emphasized by exaggerated separation in this type of membrane. Bonora notes that their proximity to the outer chromoplast envelope suggests *de novo* construction from outer envelope lipid rather than thylakoid degradation products. Similar logic most likely applies to the more organized structures seen in **Figure 28E** and **G**. Bonora also confirmed the content of these membranes to be primarily carotenoids, like their more organized counterparts, in addition to the structural lipid and protein components. It may be that the less organized membranes represent the initial stages of the more organized systems.

Meal

Likely due to the fibrous nature of the cell wall and the abundance of plastoglobuli in the food, it is not surprising that cell wall material and lipid moieties predominate in this fraction (**Figure 29A**). Yogurt and mango (plastoglobuli) derived lipids were distinguishable (**Figure 29B**).

Digest

The predominant feature here is a granular substance, of various widths, that runs in long trails, implying connectivity between particles despite its appearance (**Figure 30A**). It also occasionally appears in more convoluted shapes, but the linearity is still apparent (**Figure 30B**). Highly degraded cell wall material is also present in dispersion.

The loss of cell wall adhesion and integrity, as evidenced in the whole food and the literature (*92*), lead to substantial degradation seen in the mechanically and chemically digested fractions seen here. Likewise, plastoglobuli are thought to be the most accessible form of carotenoid storage sub-structure (*60*). This combined with the perceived high solubility of plastoglobuli, would lead us to predict that the carotenoid content of mango would be highly accessible.

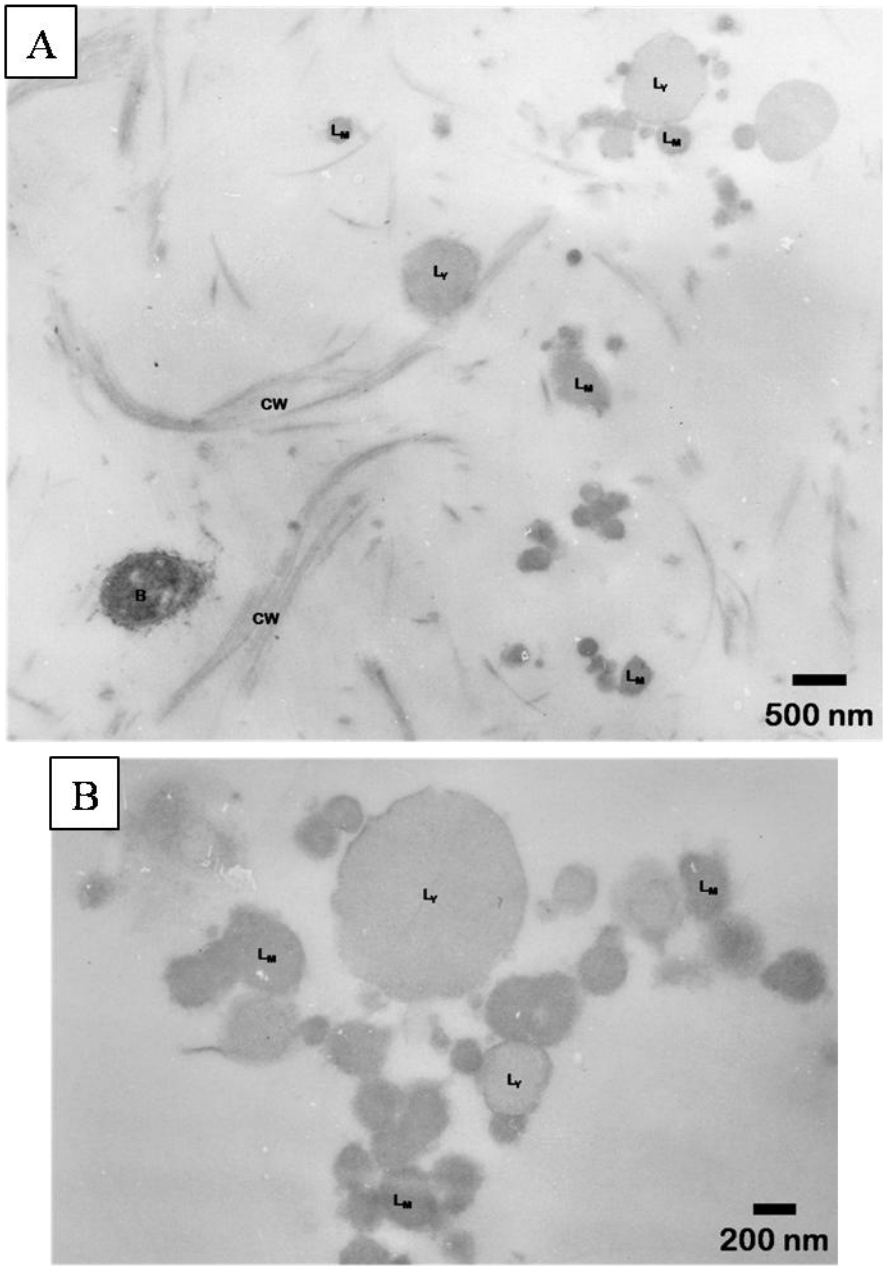

Figure 29. TEM micrographs of mango meal fraction. **A** Cell wall remnants and lipid moieties. **B** Lipid moieties. Yogurt bacteria (B), cell wall material (CW), mango lipid (L_M), yogurt lipid (L_Y).

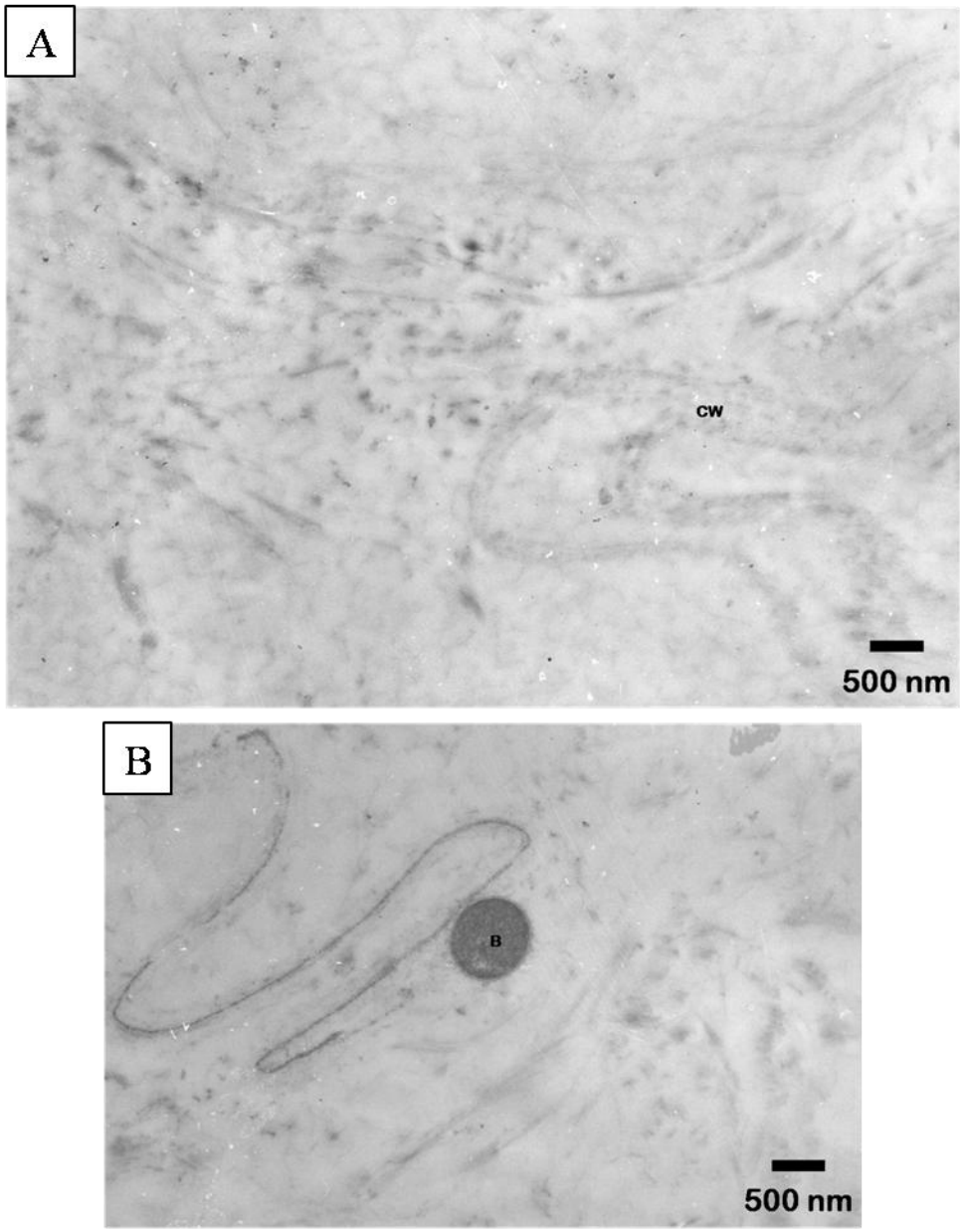

Figure 30. TEM micrographs of mango digest fraction. **A** Degraded cell wall material. **B** Linear material with yogurt bacteria. Cell wall material (CW), yogurt bacteria (B).

Melon (*Cucumis melo* L.)

Whole Food

Melon (cantaloupe) mesocarp parenchyma cells were large (11231±8651 μm^2, n=26) (**Figure 31**). Extensive cell wall loosening, loss of cell-to-cell adhesion, and even cellular integrity, is apparent. Cell walls appeared simple and slightly granular and relatively uniform in thickness (500nm) (**Figure 32A**). The cell membrane pulled away from the cell wall as a process of fruit ripening or possibly due to an osmoticum differential during sample preparation. This separation was not as severe at plamodesma since these may anchor the cells within a fixed distance.

In general, there was a notably low chromoplast to volume ratio and there were many active mitochondria. Some chromoplasts appeared to be breaking down, their plasma membrane broken in places (**Figure 32B**). This may be an indication of ripeness or over-ripeness. There were many vaculate-type structures within the chromoplasts (**Figure 32B** and **Figure 32C**), else, also empty regions (**Figure 32D** and **Figure 32E**). Note that many of these same vaculate structures exist "outside" the chromoplast. The size, density, and distribution of plastoglobuli were varied between chromoplasts but generally very small and scarce, though present in most chromoplasts observed. There also appear to be several lipid-dense moieties outside the chromoplasts (**Figure 32C**). A few crystals and crystal remnants are also noted (**Figure 32A** and **Figure 32C**). One obtuse, angular object may be a remnant of a large β-carotene crystal (**Figure 32E**).

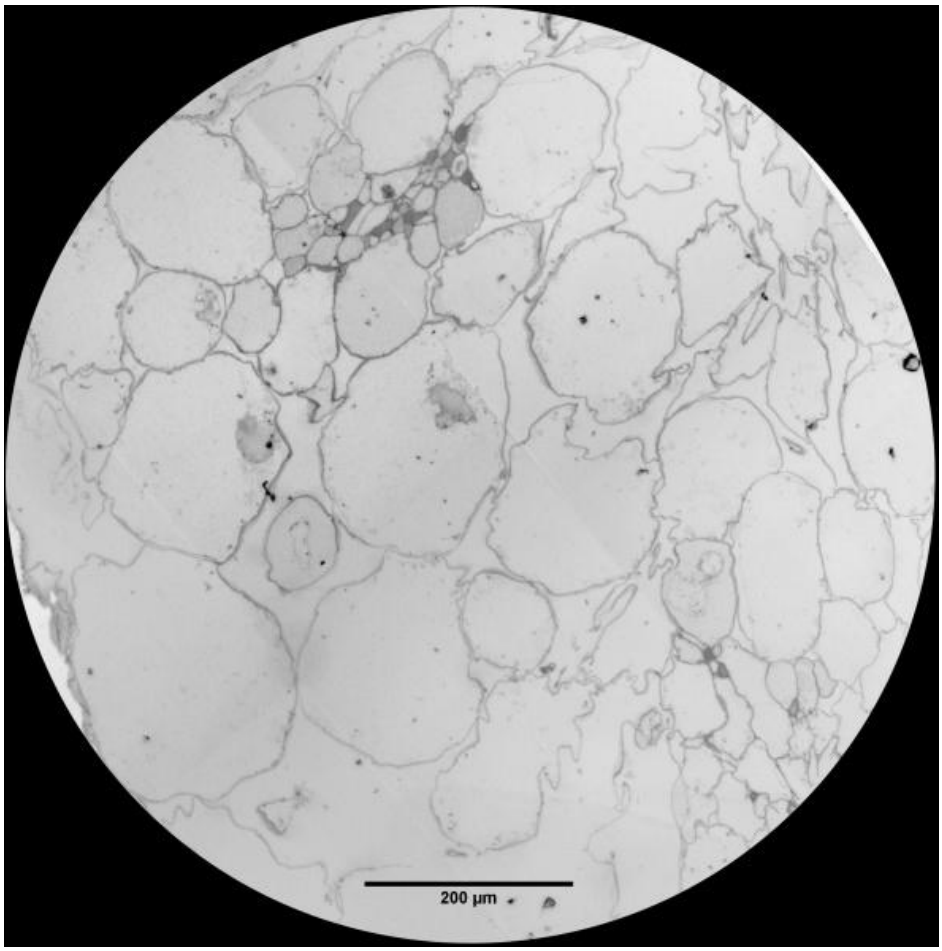

Figure 31. Light micrograph of melon (*Cucumis melo* L.) mesocarp cells. Cell wall loosening, loss of cell-to-cell adhesion, and even cellular integrity, is apparent.

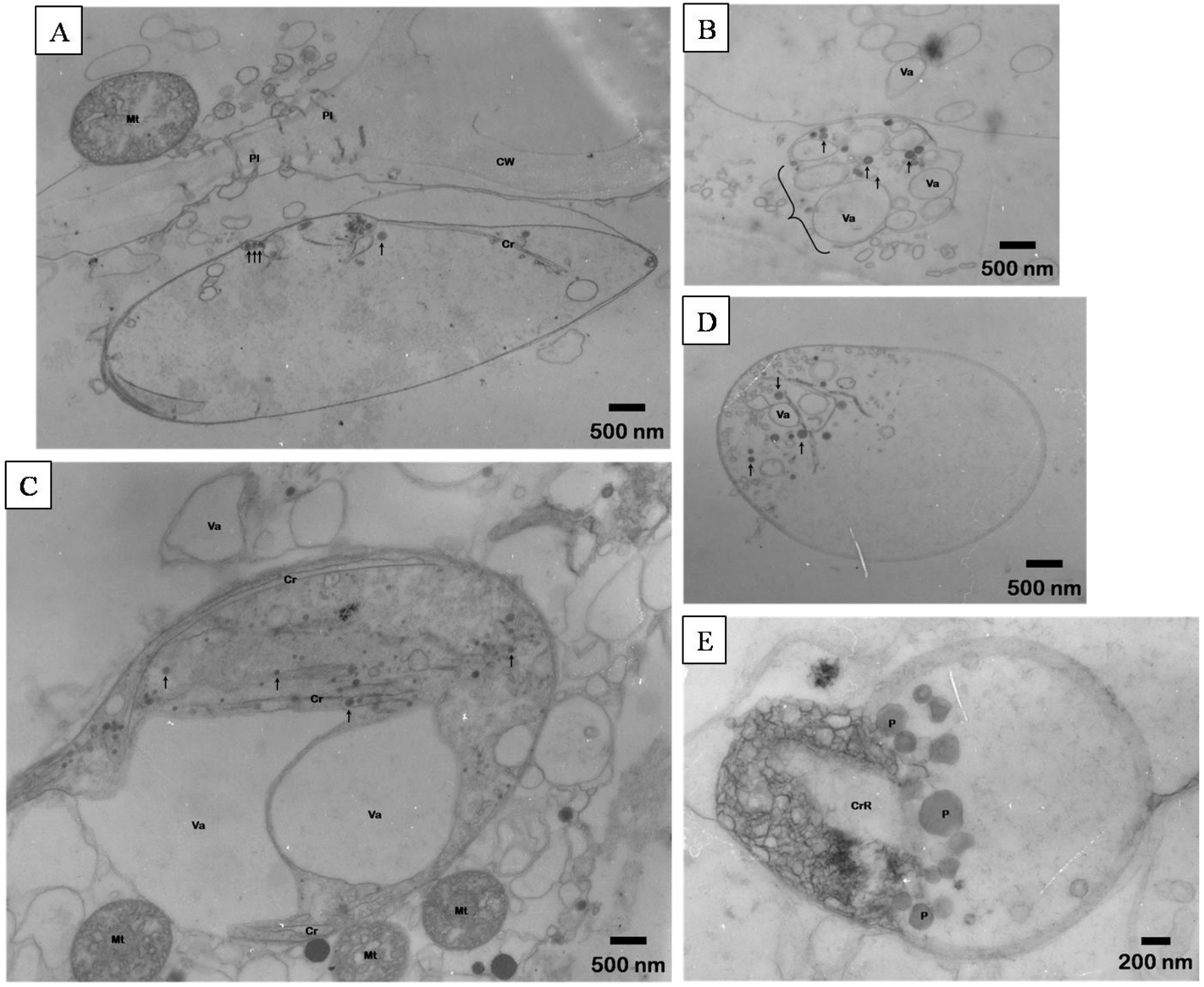

Figure 32. TEM micrographs of melon chromoplasts. **A** Chromoplast and cell wall with plasmodesmatata. **B** Degraded chromoplasts. **C** Vaculate chromoplasts. **D** Chromoplast with large electron-transparent space. **E** Chromoplast with protrusion. Carotenoid crystal (Cr), possible carotenoid crystal remnant (CrR), cell wall (CW), degrading envelope of chromoplast (bracket), mitochondrion (Mt), plasmodesmatata (Pl), plastoglobule (arrows, P), vaculate structures (Va).

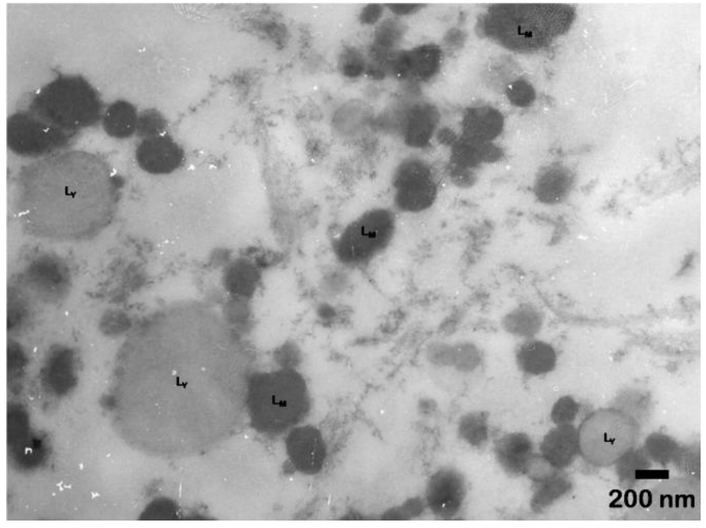

Figure 33. TEM micrograph of melon meal fraction. Yogurt lipid (L_Y), melon lipid (plastoglobuli) (L_M).

Meal

There is substantial variation in size and shape of the lipid moieties with both the yogurt and melon lipids being distinguishable (**Figure 33**). An underlying feature is also a fibrous, sometimes granular material that may be cell wall material.

Digest

Very little solid material was left in the digest fraction, mainly only small occurrences of granular material (**Figure 34A)**. One micrograph shows an ovoid structure that is an appropriate size for an organelle, though the boundary appears to be composed of the same granular material found elsewhere and not a lipid membrane (**Figure 34B**). It is also void of material other than some more of the same of which its periphery is made.

Melon appears to be well digested, most likely due to its highly degraded native state. Though the chromoplasts seem to contain little total plastoglobuli content, a moderate amount was still present in the meal fraction. On the whole, melon chromoplasts are predominated by vaculate or empty areas, explaining the relatively moderate to low carotenoid content.

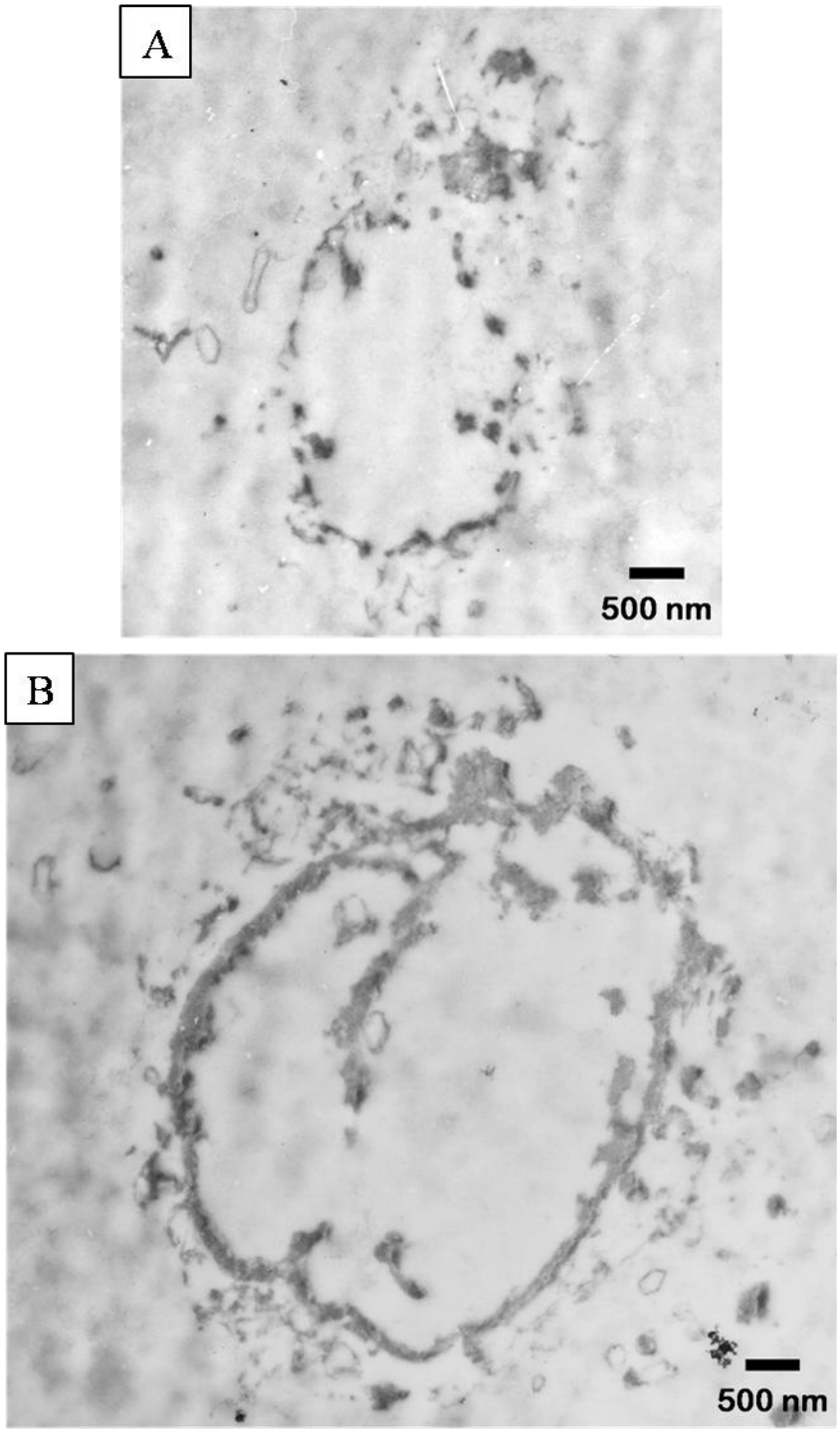

Figure 34. TEM micrographs of melon digest fraction. **A** 2 µm diameter structure. **B** Divided 4 µm diameter structure.

Papaya (*Carica papaya* L.)

Whole Food

Papaya mesocarp parenchyma cells were moderate in size (7085±4679 μm^2, n=82) (**Figure 35**). Cell wall loosening and loss of cell-to-cell adhesion was apparent. Cell walls were thick (2.5-4 μm), textured, and mildly fibrous (**Figure 36A**). The cell wall was constricted dramatically at plasmodesmatata (**Figure 36B**).

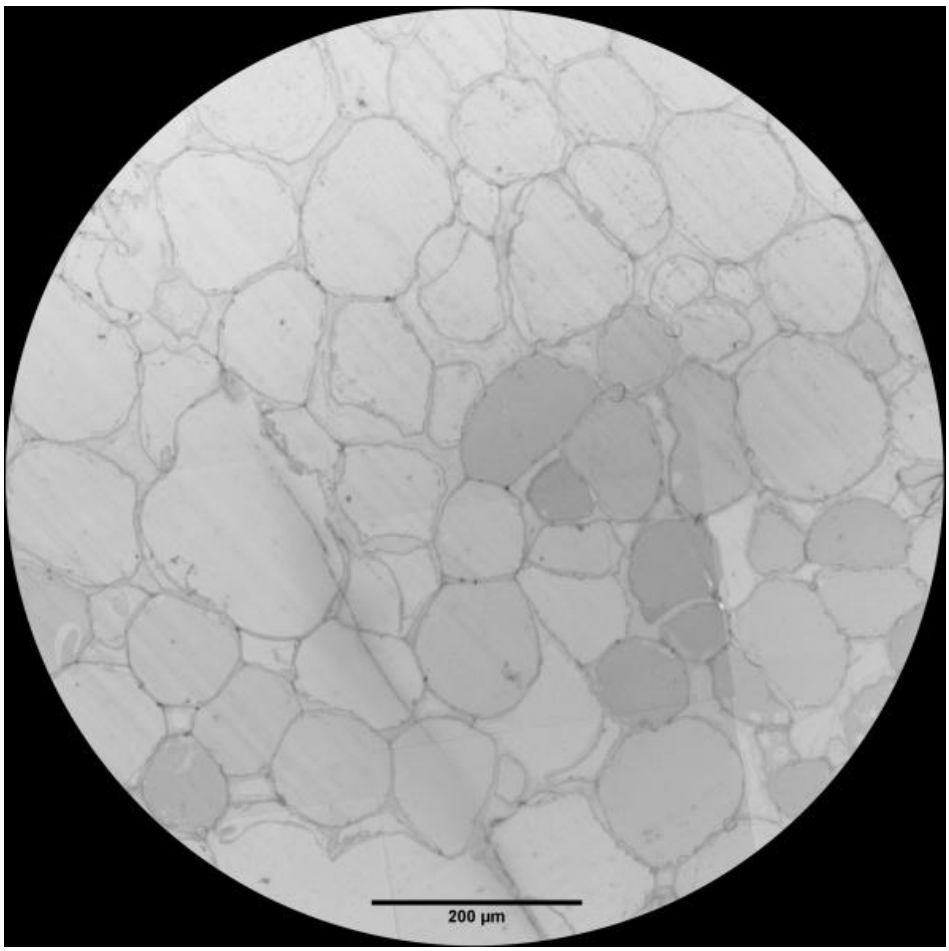

Figure 35. Light micrograph of papaya (*Carica papaya* L.) mesocarp cells. Cell wall loosening and loss of cell-to-cell adhesion is apparent.

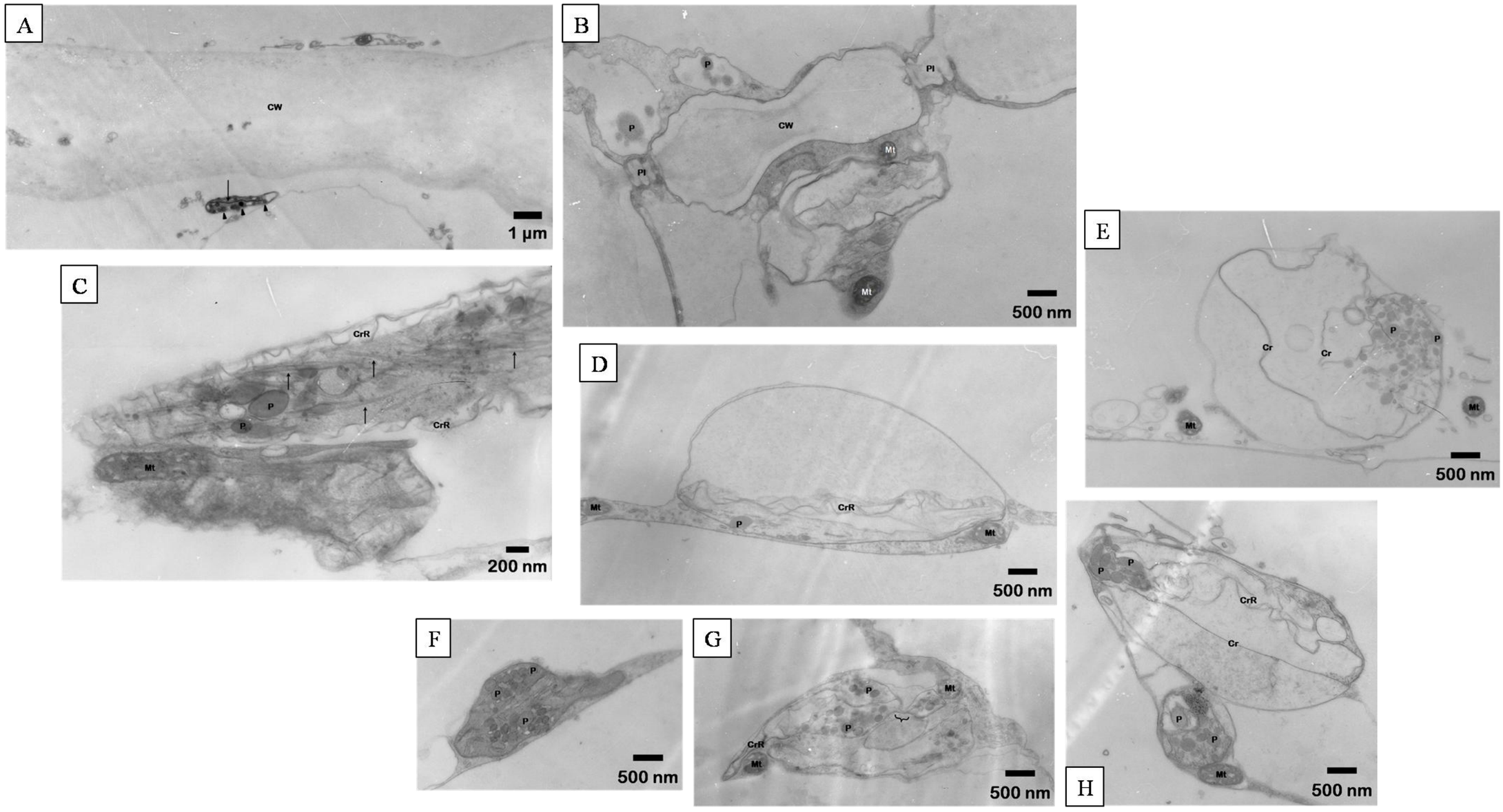

Figure 36. TEM micrographs of papaya chromoplasts and cell walls. **A** Cell wall with chromoplasts. **B** Cell wall with plasmodesmatata and globular chromoplasts. **C** Crystalline chromoplasts. **D** Electron poor chromoplasts with carotenoid crystals. **E** Crystalline and globular chromoplasts. **F** Globular chromoplasts. **G** Crystalline and globular dividing chromoplasts. **H** Crystalline chromoplast with sequestered globules. Carotenoid crystal (arrow, Cr), large lycopene crystal remnant (CrR), cell wall (CW), mitochondrion (Mt), plasmodesmata (Pl), plastoglobule (arrow heads, P), point of chromoplast division (brace).

Papaya is a good example of how long carotenoid crystals can elongate and distort the chromoplast (**Figure 36C** and **D**). Harris and Spur (*66*) describe only lycopene crystal remanants as undulating, as is the case here. Though the United States Department of Agriculture National Nutrient Database for Standard Reference (USDA NNDSR) (*89*) does not claim lycopene content in papaya, carotenoid content may vary by variety and our own analysis of papaya did reveal lycopene content (Chapter VI). Some chromoplasts exhibit spaces void of substructure and filled only with a stippled material (**Figure 36D** and **E**). Plastoglobuli are numerous, often moderately sized, and grouped in one sector of the chromoplast (**Figure 36F**, **G**, and **H**).

Meal

Abundant lipid from both papaya and yogurt was evident (**Figure 37A**). Other cellular material was also evident with some fibrous material, too small to be cell wall material, which may be persistent carotenoid crystals (**Figure 37B**).

Digest

Grainy material of various characters is the predominant feature of this fraction. The top of **Figure 38A** may be highly expanded cell wall material. In **Figure 38B**, two distinct fields can be seen, each with a different character from **Figure 38A**. Also here, shadowed areas may be disperse lipid moieties. The presence of such moieties would indicate an excess of lipid in the digestion mixture.

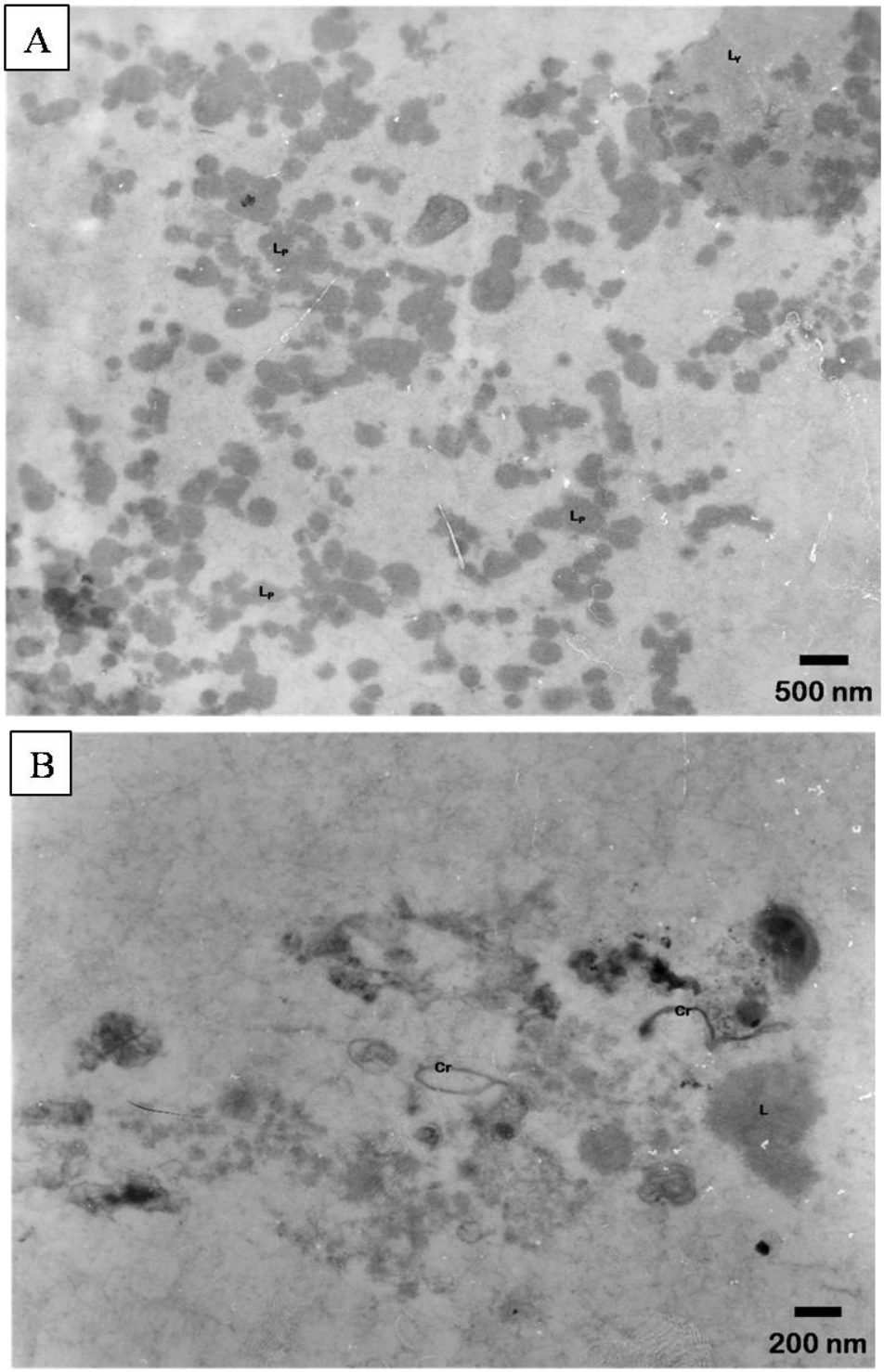

Figure 37. TEM micrographs of papaya meal fraction. **A** Lipid moieties. **B** Cellular material. Carotenoid crystal (Cr), lipid of uncertain origin (yogurt or papaya) (L), yogurt lipid (L_Y), papaya lipid (plastoglobuli) (L_P).

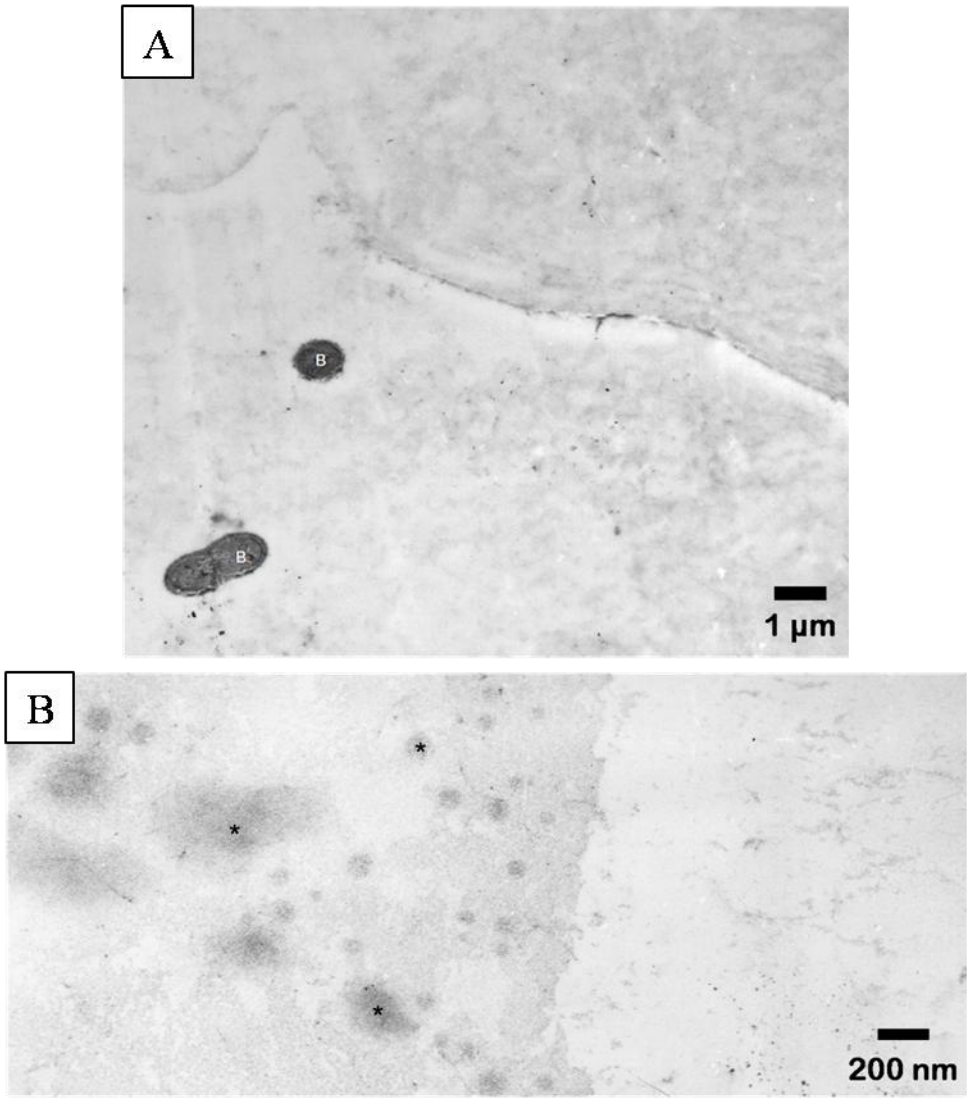

Figure 38. TEM micrographs of papaya digest fraction. **A** Digesta with yogurt bacteria (B). Upper portion of micrograph may be expanded cell wall material. **B** Shadowed areas (asterisks) may be lipid moieties.

Though conjectures were made about the composition of the digest fraction, little certain is known about what cellular materials persisted into this fraction. In general, papaya seems well digested and the high plastoglobule content imply the possibility of good carotenoid bioaccessibility.

Sweet Potato (*Ipomoea batatas* Lam.)

Whole Food

Sweet potato edible parenchyma cells were moderate to small in size (3451±2344 μm^2) (**Figure 39**). Starch grains were a prominent feature, characterized by large, crystalline structures which take the appearance of a deflated object, very light with darker "wrinkles" (*96*). These structures did stain with iodine, confirming their identity. Cell walls were 1 µm thick, dark, and very fibrous (**Figure 40**). Dramatic constrictions were present at plasodesma.

Sweet potato chromoplasts were highly varied in sub-structure. Some were very simple and only contained only a few plastoglobuli (**Figure 41A**). Others have internal and multiple membrane-bound structures which may be carotenoid-containing (**Figure 41B**). Though they are not concentric and contiguous with the outer envelope of the chromoplast as described in the literature, the membranes are very electron dense, indicative of high lipid content. It is important to note the difference between structures like these for which the "internal" material matches that of the background in the rest of the chromoplast versus a vaculate-type structure which would be three-dimensionally bound and therefore its contents would be unique from the background material (see **Figure 41C**). **Figure 41C** also displays another variation of chromoplast seen in sweet potato, containing a true concentric membranous structure, plastoglobuli, carotenoid crystals, and a granular material in the background.

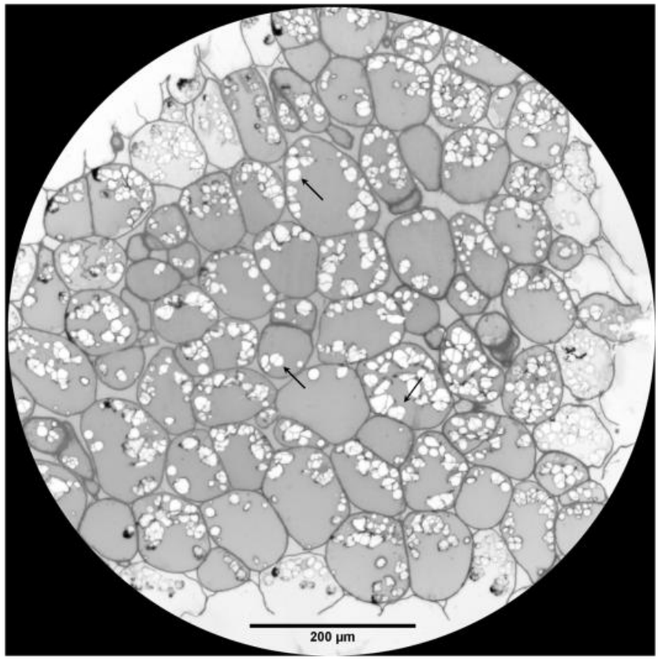

Figure 39. Light micrograph of sweet potato (*Ipomoea batatas* Lam.) parenchyma cells . Starch grains indicated by arrows.

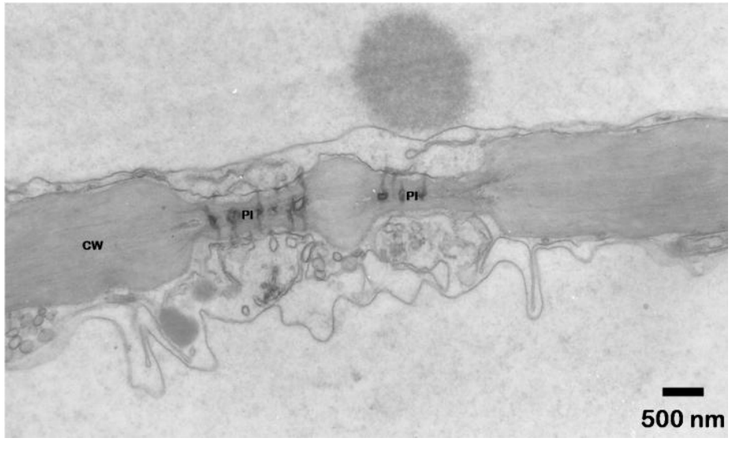

Figure 40. TEM micrograph of sweet potato cell wall with plasmodesmata. Cell wall (CW), plasmodesmata (Pl).

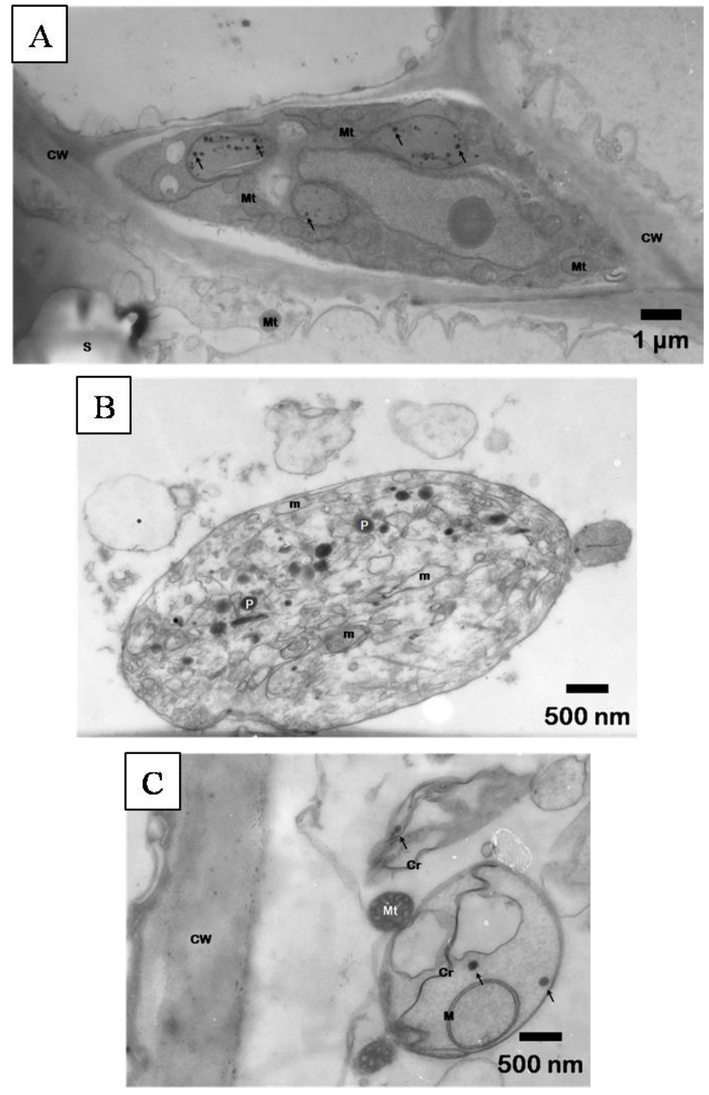

Figure 41. TEM micrographs of sweet potato chromoplasts. **A** Three globular chromoplasts. **B** "Membranous" chromoplasts. **C** True membranous chromoplast with carotenoid crystal. Cell wall (CW), carotenoid crystal (Cr), carotenoid membrane (M), complex, unorganized membranes (m), mitochondrion (Mt), plastoglobule (arrows, P), starch grain (S).

Meal

Mostly dark lipid moieties which may be sweet potato lipid (plastoglobuli) were mingled with fewer, faint moieties which may represent the yogurt lipid (**Figure 42**). The background of the meal fraction consisted of abundant fibrous, granular material with islands of electron-neutral material. The electron transparent material may be an artifact of the agarose embedding material (ie. the agarose is "floating" in a sea of granular material from the meal).

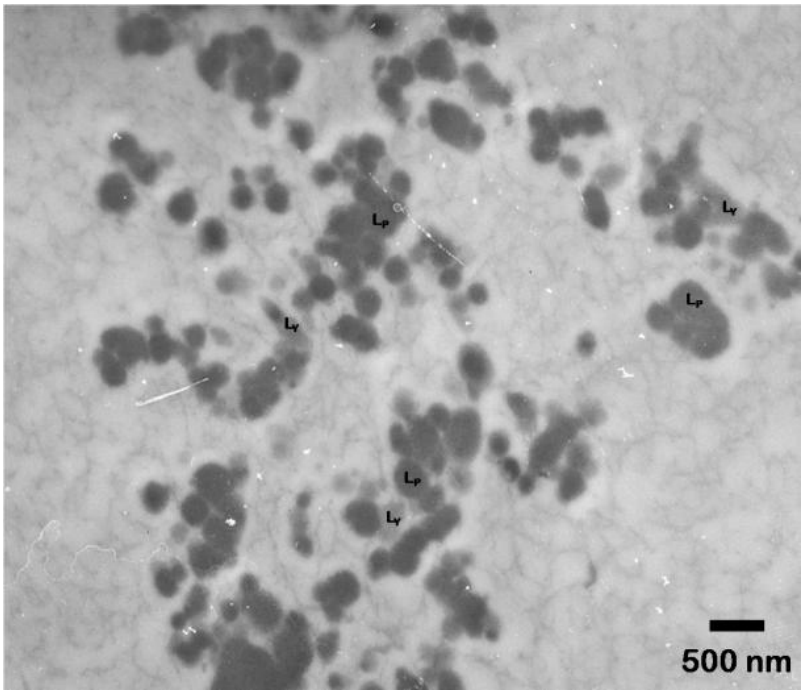

Figure 42. TEM micrograph of sweet potato meal fraction lipids. Yogurt lipid (L_Y), sweet potato lipid (plastoglobuli) (L_P). Background may consist of agarose pieces surrounded by ground cellular material.

Digest

The digest fraction was very similar to the background found in the meal sample without the lipid moieties (**Figure 43**), though the granular material was more concentrated.

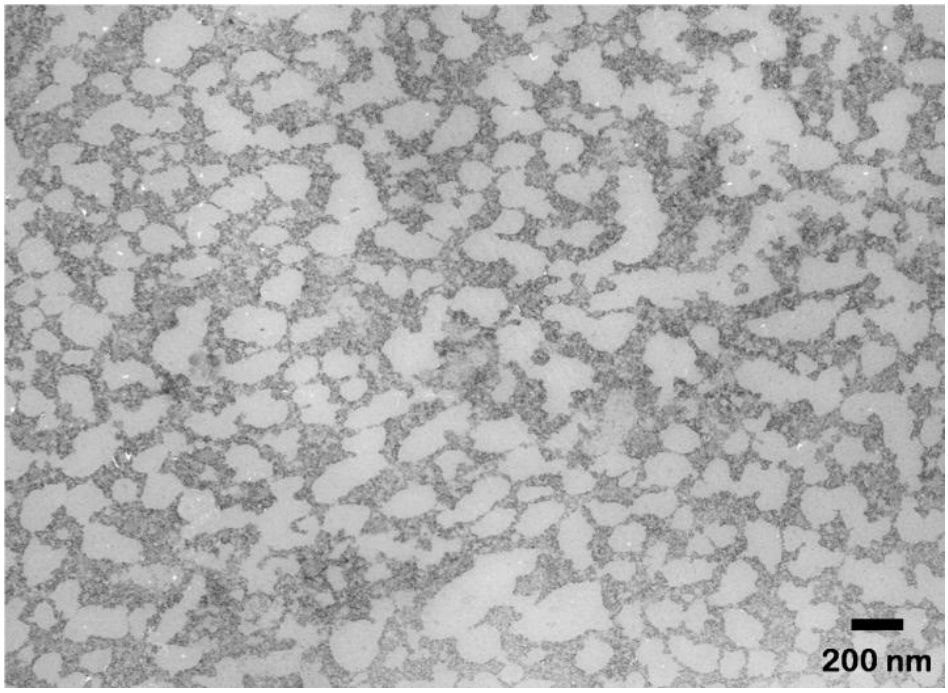

Figure 43. TEM micrograph of sweet potato digest fraction . May consist of agarose pieces surrounded by digested cellular material.

Membranes appear to be the major carotenoid storage organs in sweet potato. Membranous carotenoids are also bound by proteins and thought to be less accessible (*26*). Considering the considerable proportion of plastoglobuli also present, however, a hypothesis concerning the overall accessibility of the food's carotenoids is less certain.

Tomato (*Lycopersicon esculentum* L.)

Whole Food

Tomato pericarp parenchyma cells were very large (13627±9188 μm^2, n=33), irregularly shaped, and often angular (**Figure 44**). Extensive cell wall loosening and loss of cell-to-cell adhesion was apparent. Cell walls were thin (250-400 nm), fibrous, and compact (**Figure 45A**).

Tomato chromoplasts have been described in multiple studies (*66*, *97*). Harris and Spurr's (*66*) account describes well the chromoplasts observed here. There was a large range of chromoplast maturities, some still containing starch grains and a few grana stacks (**Figure 45B**). In these chromoplasts, the plastoglobuli initiate within the degrading thylakoid stacks and appear membrane-bound. Other chromoplasts resemble what Harris and Spurr described as an "ovid" shaped chromoplast containing a thylakoid plexus with emerging thylakoid membranes (**Figure 45C**). An "elongate" type was also observed with a large central lycopene crystal surrounded by multiple, long layers of membranes from which the large crystal originated (**Figure 45A**). All types contained plastoglobuli, often still membrane-bound in groups. Many simple chromoplasts were present which contained only plastoglobuli, often divided by a central region of moderately electron dense material (**Figure 45D)** which may be preliminary to chromoplast division as seen in **Figure 45E**. There was a relatively high chromoplast to cell volume ratio.

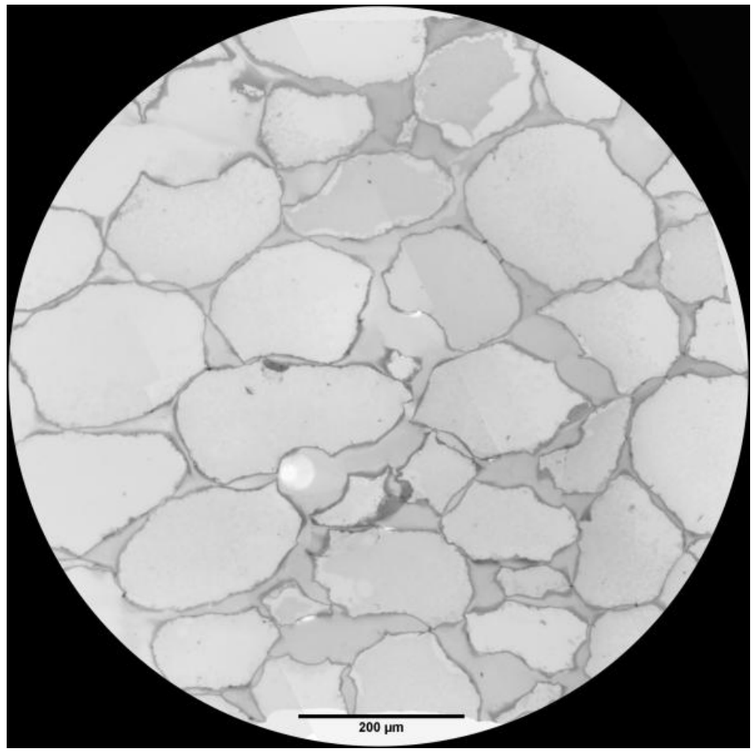

Figure 44. Light micrograph of tomato (*Lycopersicon esculentum* L.) pericarp. Cell wall loosening and loss of cell-to-cell adhesion is apparent.

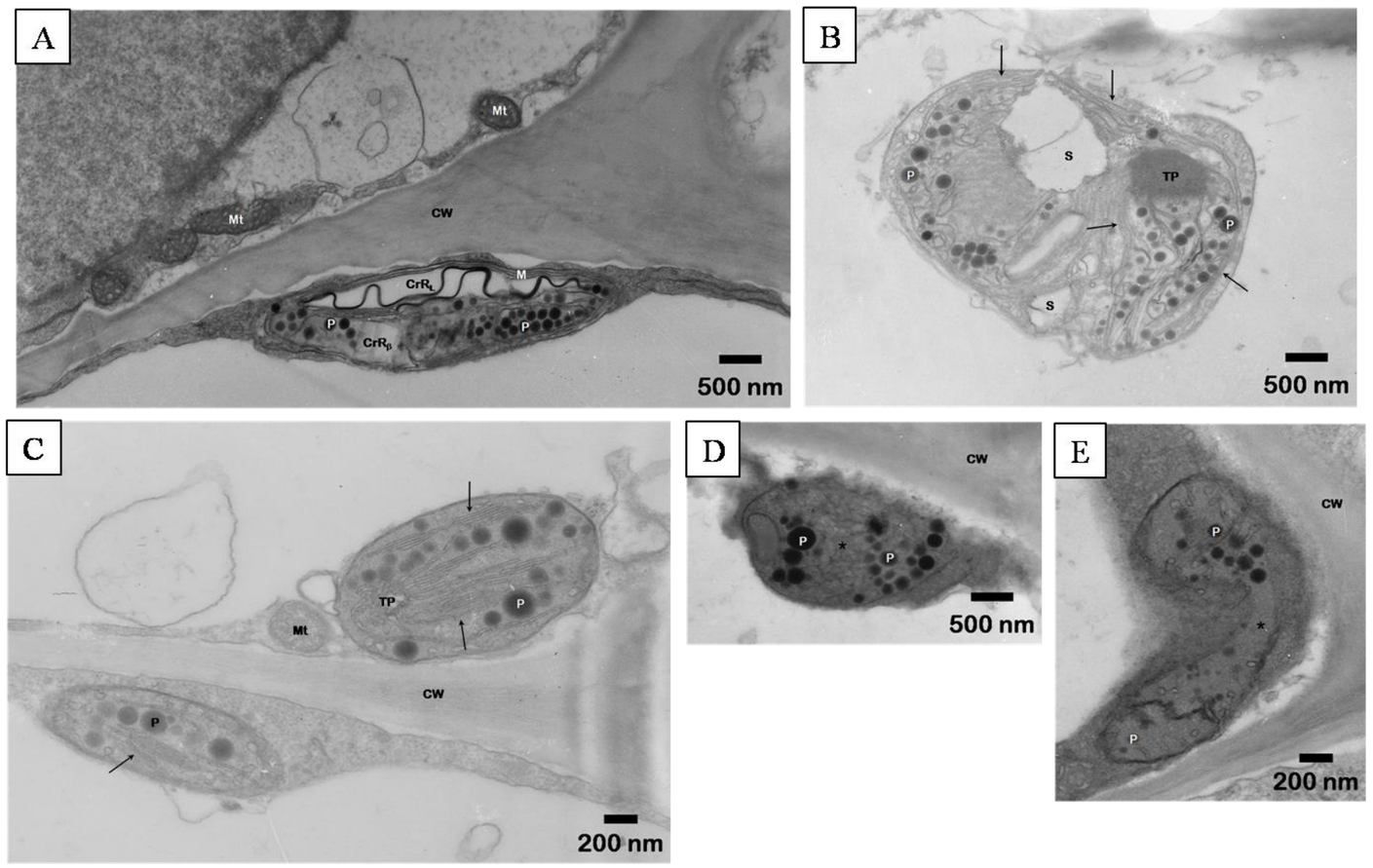

Figure 45. TEM micrographs of tomato chromoplasts and cell walls. **A** Globular/crystalline/membranous chromoplasts. **B** Young tomato chromoplast. **C** "Ovid" tomato chromoplasts. **D** Globular chromoplast preliminary to division. **E** Globular chromoplast during division. Lycopene carotenoid crystal remnant (CrR_L), β-carotene carotenoid crystal remnant (CrR_β), cell wall (CW), carotenoid membranes (M), mitochondrion (Mt), plastoglobule (P), strarch grain (S), thylakoid plexus (TP), thylakoid remnants (arrows).

Meal

Uniform lipid moieties, indistinguishable between tomato and yogurt sources, were present (**Figure 46**). These moieties had unusually soft, diffuse boarders.

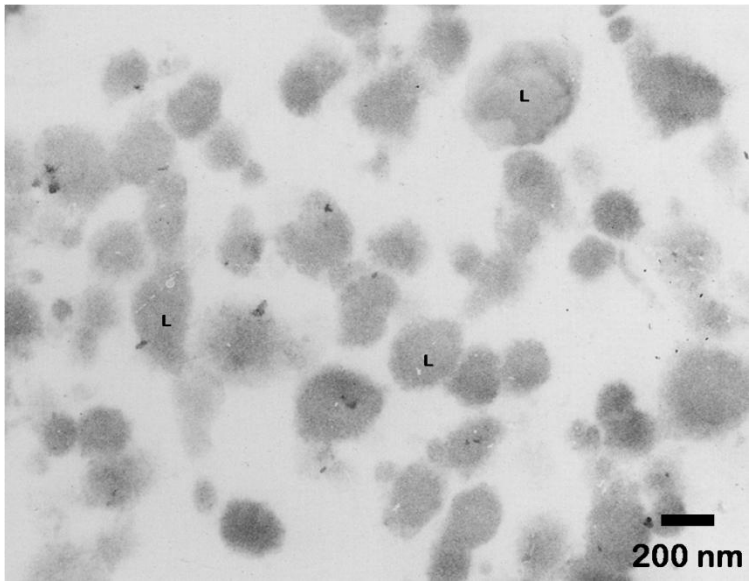

Figure 46. TEM micrograph of tomato meal fraction lipids. Lipid of uncertain source (L).

Digest

The digest fraction mainly consisted of a homogenous, granular material (**Figure 47A**). One instance of a membrane-like structure, too thin to be a cell wall, was conspicuous (**Figure 47B**). This structure may have been the remnant of a lycopene crystal or a lipid rich membrane.

Though the bioavailability of tomatoes has been investigated, the comparison was made with tomato paste, food matrices from other sources (*98*). Therefore, it is difficult to make applications to the present work. From what was seen here of

relatively equal portions of plastoglobuli, carotenoid crystals, and carotenogenic membranes, as well as the cell walls being thin, we would conjecture a moderate level of carotenoid bioaccessibility.

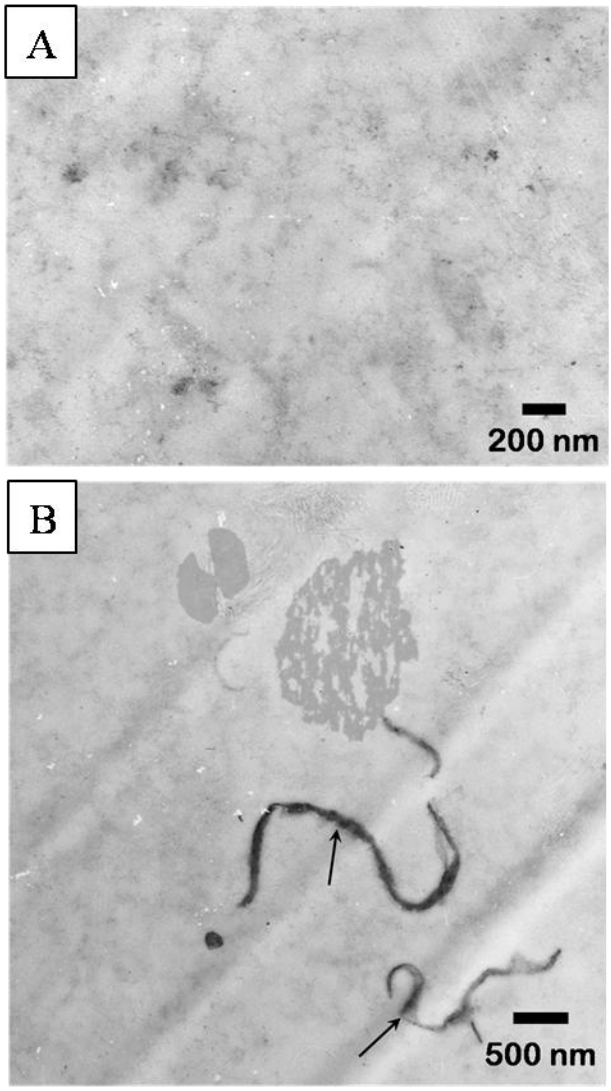

Figure 47. TEM micrographs of tomato digest fraction. **A** Granular material. **B** Fiberous structures. Fibrous structure (arrows) may have been the remnant of a lycopene crystal or a lipid rich membrane.

Watermelon (*Citrullus lanatus* (Thunb.) Matsum. & Nakai)

Whole Food

Watermelon mesocarp parenchyma cells were very large (16604±4535 μm^2, n=8), showing an open, loose intercellular connectivity (**Figure 48**). Cell walls were of moderate thickness (250-1000 nm), mildly textured but not fibrous, and relatively electron poor, indicating low density (**Figure 49A**).

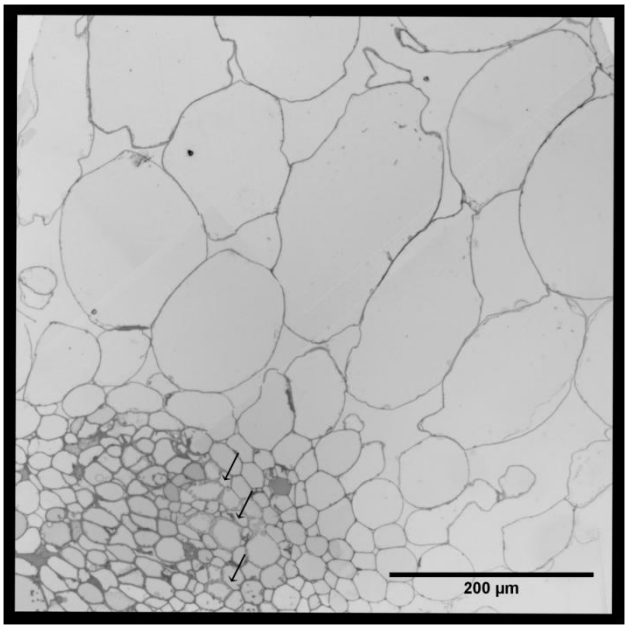

Figure 48. Light micrograph of watermelon (*Citrullus lanatus* (Thunb.) Matsum. & Nakai) mesocarp. Loss of cell-to-cell adhesion is apparent. Lower left portion of the micrograph shows vascular tissue composed of smaller cells; xylem cells indicated by arrows.

Two types of chromoplasts were found in approximately equal proportions. The first contained membranous layers for which the distance between membranes was intermittently exaggerated, being pinched together at regular intervals (**Figure 49A** and

B). Though this type usually contained a few small plastoglobuli, in one instance the chromoplast contained only several layers of membranes (**Figure 49A**). Also, in a few instances, the chromoplasts contained vesicular structures. The boarders of these structures was not unlike the membranes seen in the chromoplasts, but their interiors were electron transparent to various degrees, implying a difference in contents from the membranous inclusions seen elsewhere which contained the same electron dense material seen in the background of the chromoplasts.

The second type of chromoplast observed in watermelon had a relatively electron transparent material which filled most of the internal space (**Figure 49C** and **D**). These chromoplasts contained a few small plastoglobuli and carotenoid crystals of various lengths and characters.

It should be acknowledged that Bangalore et al (*99*) recently attempted to describe watermelon chromoplast ultrastructure. Their specimen preparation was inappropriate, however, yielding poor structural preservation and their knowledge of plant ultrastructure inadequate for describing their results.

Meal

Both watermelon and yogurt lipids were observed in the meal fraction interspersed with carotenoid crystals (**Figure 50**). There was a large range of sizes of the yogurt lipid moieties.

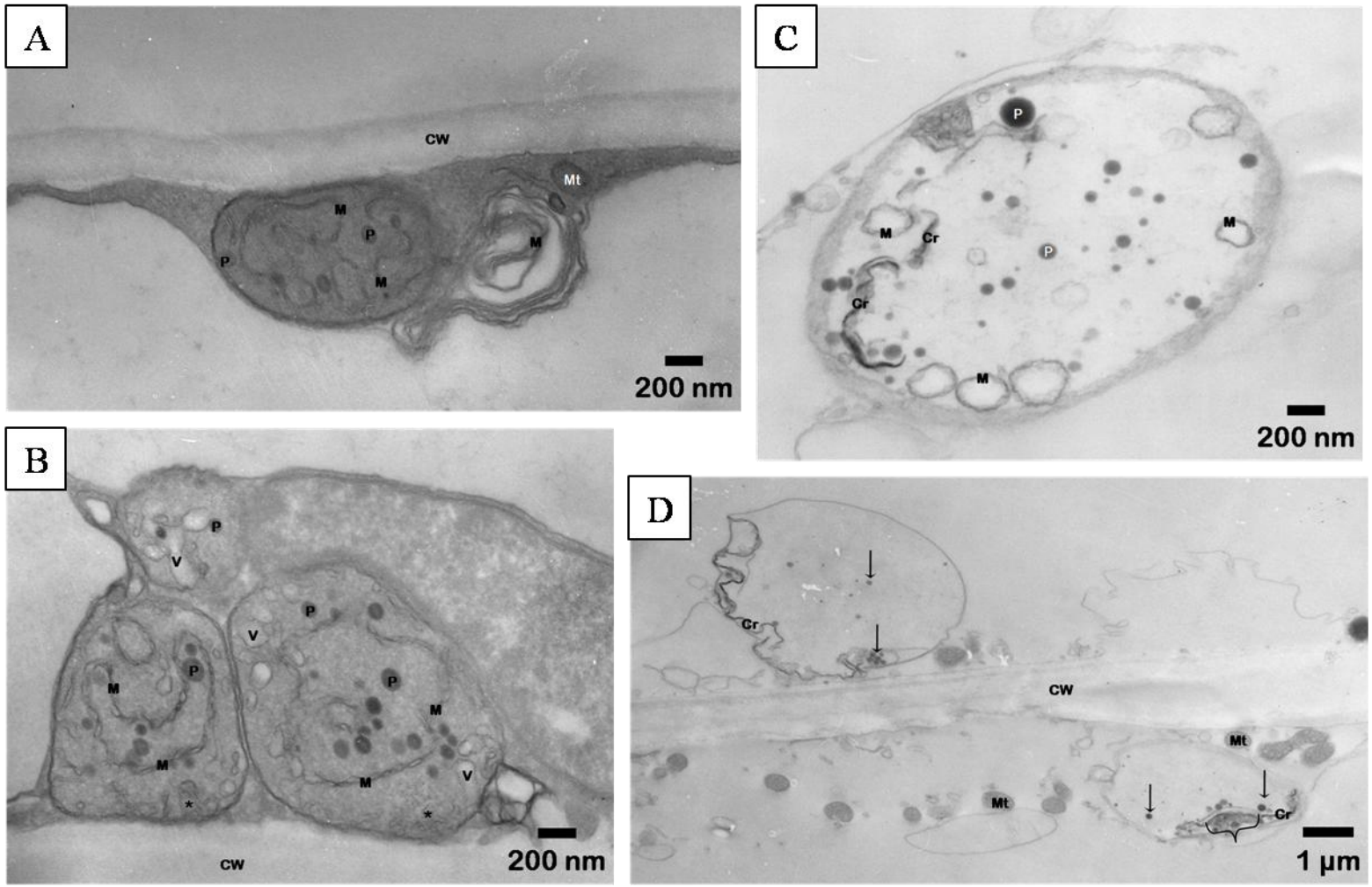

Figure 49. TEM micrographs of watermelon chromoplasts and cell walls. **A** A membranous/globular chromoplast and a highly membranous chromoplasts. **B** Three membranous/globular chromoplasts. **C** Crystalline/globular chromoplasts. **D** Two mostly vacant crystalline/globular chromoplasts. Carotenoid crystal (Cr), carotenoid crystal remnant (brace), cell wall (CW), carotenoid membranes (M), association of membranes with outer envelope of chromoplast (asterisks), mitochondrion (Mt), plastoglobule (P), vesicle (V).

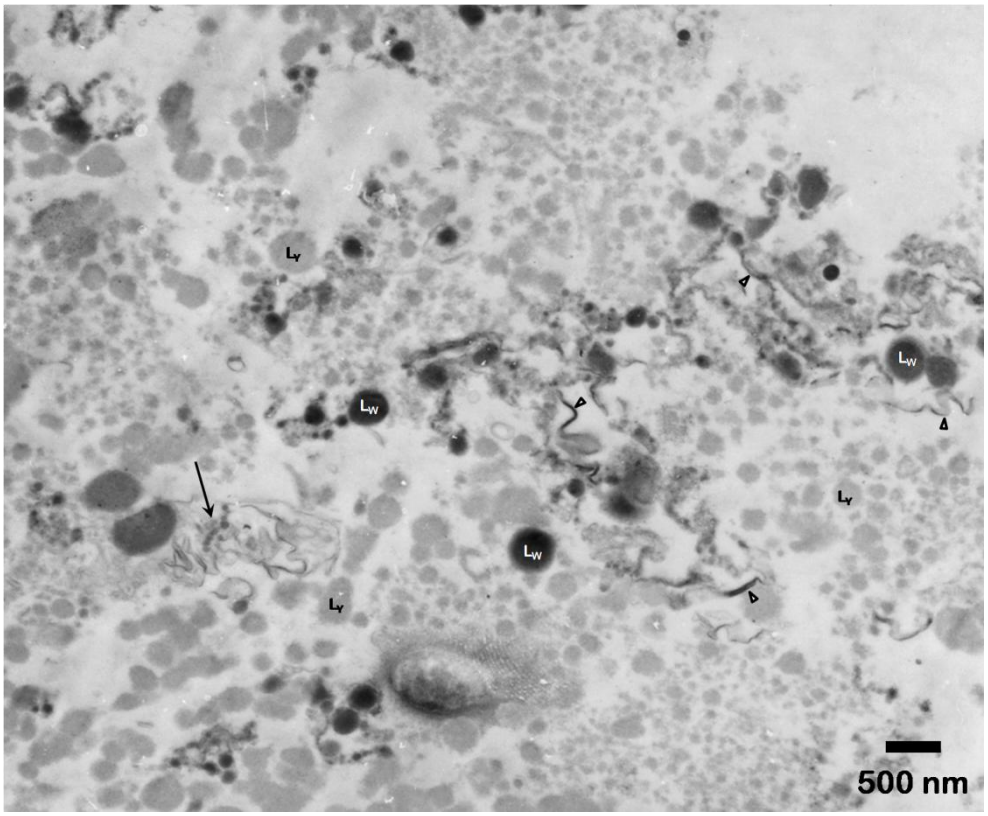

Figure 50. TEM micrograph of watermelon meal fraction lipid and cellular materials. Carotenoid crystal (empty arrowhead), watermelon lipid (plastoglobuli) (L_W), yogurt lipid (L_Y), possibly intact plastoglobuli trapped in chromoplast membranes (arrow).

Digest

Long granular, continuous structures were the only feature observed in the digest fraction (**Figure 51**). These may either be individual structures or an amorphous material in a background of agarose as seen in other samples (ex. Sweet potato digest, **Figure 43**).

Perkins-Veazie et al (*100*) showed that unheat-treated watermelon juice was as bioavailable as heat treated tomato juice. Conjectures about the differences in food matrix and ability to be mechanically disrupted may be made. It might be reasonable to

hypothesize that the watermelon matrix allows easier release of carotenoids since heat treatment was not needed in addition to the mechanical disruption to reach the same level of bioavailability. This difference may be attributable to lower carotenoid crystal content of watermelon, solubilization of which may require the heat in tomato.

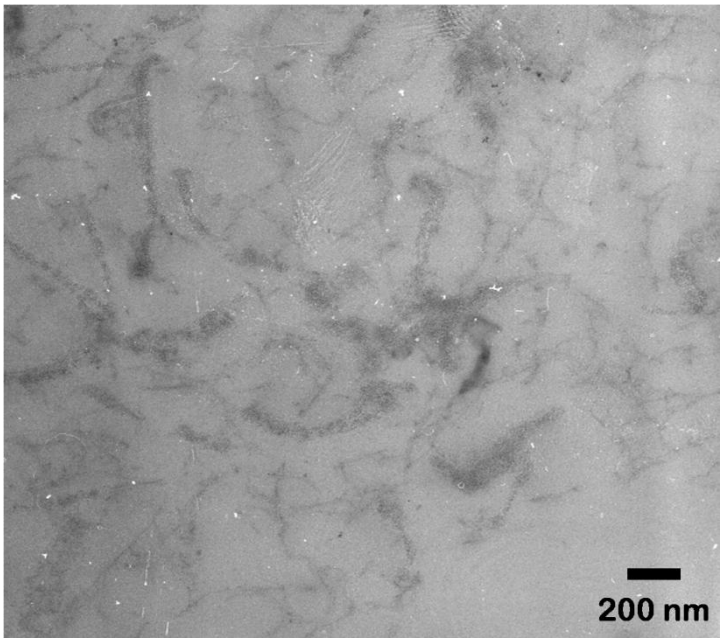

Figure 51. TEM micrograph of watermelon digest fraction.

Data Analysis

Cell sizes varied greatly between species observed and significant differences were noted. **Figure 52** reports all cell sizes with least significant differences.

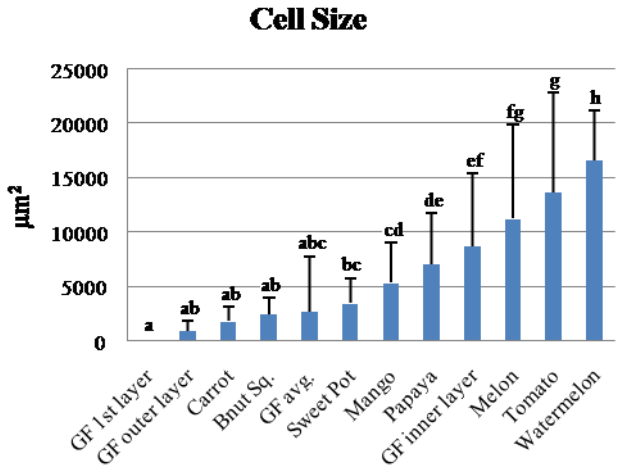

Figure 52. Cell size. Data represent mean±SD of cell size observed. Letters above SD bar represent least significant differences. Grapefruit cell sizes reported for each individual layer (see *Results* for *Grapefruit*) and as an average.

Cell and cell wall characteristics correlated on many occasions with reported fiber content. Cell size was negatively correlated with all soluble and most insoluble (except pectin and lignin) fiber contents. This is understandable since the fiber content is on a fresh weight basis, ie. as cells are larger, the proportional fiber composition will be less, especially since no relationship was found between cell size and cell wall thickness which could offset this relationship. An additional explanation for this observation is presented by the negative correlation found between cell size and the cell wall description. Cell walls were scored on a scale of 1 to 4 (no detail, textured but not

fibrous, fibrous, or very fibrous). This inverse correlation suggests that cell wall structure and composition is inherently responsible for the correlations observed with fiber content, not simply proportional volume.

The cell wall description was also positively correlated in all cases to soluble fiber content but no correlation was found with insoluble fiber content. Contrary to what might be supposed, this suggests that fibrous cell walls contain more soluble fibers while insoluble fibers have no bearing on the appearance of the cell wall. Conversely, cell wall minimal thickness was positively correlated with all insoluble fibers except lignin content. (Minimal and maximal thickness values were evaluated separately. In cases where they were the same, this measurement was used for both variables.) Together these data suggest that while soluble fiber plays a role in cell wall appearance, and possibly fibrosity, insoluble fibers may dictate the minimal cell wall thickness possible to maintain cellular integrity. Indeed, this hypothesis is supported by the evidence of cell wall degradation seen in melon (**Figure 31**) concomitant with low total insoluble fibers and relatively thin cell walls. Loss of cellular integrity was also seen in mango (**Figure 27**), but no fiber data was available.

Most of the correlations seen between whole food structures and materials seen in the meal and digest fractions were based on unique observations for limited foods. The following hypotheses derived from these correlations, therefore, are rather straight forward. The homogenous granular material as well as what was interpreted as tubular material seen in the butternut squash meal and digest fractions, respectively, may derive from its chromoplasts' high native tubule content. A similar correlation was found

between the short fibers found in the grapefruit meal and the fibrous, stippled background of the digest.

A general negative correlation found between the observation of vesicles and plastoglobuli in the whole foods. The physiological basis for a trade-off between vesicular and plastoglobule chromoplasts content is unknown. A related correlation (also negative) was found between vesicular content in the meal fraction and the ability to distinguish yogurt and plant-based lipid in the same fraction. This strongly suggests a relation to the above observation, but lacks the support of a positive correlation between plastoglobule content and the ability to distinguish the lipids. It is somewhat unlikely that an alternative hypothesis, that vesicles aid in lipid emulsification during mastication, is responsible.

FUTURE WORK

The conspicuous lack of general correlative data between whole food structures and materials found in the meal and digest fractions suggests possibilities for future work. It is possible that components of the meal and digest fractions were lost during removal of the supernantant for those samples centrifuged at 4000 rpm and or not observed in those samples for which strata formed during ultra centrifugation (efforts at rehomogenization may not have been sufficient) (see MATERIALS AND METHODS subheading Ground “meal” and Digested Samples). In defense of the methodologies used, however, it should be noted that no notable difference between quantities of

materials found in the meal and digest fractions was found between these two treatments.

Alternatives to this methodology obviously exist, but may be equally problematic. Following ultracentrifugation of samples, mechanical homogenization with buffer would ensure equal sampling. This is somewhat impractical since it would necessitate mechanical intervention which may disrupt the sample past homogenization, thus adding other artifacts. It may also require larger sample volumes which would be beyond the abilities of the current digestion protocol.

Another alternative for definitively describing all components of the meal and digest fraction would be to take sequential TEM sections through the ultracentrifuged pellet. This is an intensive process by which observations are made at consistent intervals through the layers of the pellet (ex. Take sections every 10 µm through a 1 cm pellet for 100 observations per sample). The combined information from all sections would yield the total contents of each fraction.

CONCLUSION

While generalizations about the bioaccessibility of carotenoids have been made in other studies about a few of the food sources investigated here, only a small set of fruits and vegetables have been observed for chromoplast or cell wall morphology. The current study, although being far from exhaustive, does add generously to the descriptive knowledge about commercially available carotenoid-containing fruits and vegetables.

Quantification of cell size and qualitative measurements of cell wall and chromoplast characteristics may aid in the explaination of nutrient accessibility in these foods. Detailed knowledge about food sources can aid consumers in making informed and confident nutritional decisions. It is hoped that studies like the one presented here will further our understanding of factors related to and aid in the making of these decisions.

CHAPTER VI

CAROTENOID BIOACCESSIBILITY FROM NINE CAROTENOID-CONTAINING FRUITS AND VEGETABLES USING AN *IN VITRO* MODEL

INTRODUCTION

Though there are many plant sources available for incorporating significant levels of carotenoids into the diet, the role the source plays in carotenoid bioavailability is not well understood. Most bioavailability studies conducted thus far have focused on assessing the effects of processing and cooking, co-consumption with fat, and competition of carotenoids for absorption. In general, most studies showed cooking (or other heat treatments associated with processing), mechanical disruption of the food, and the presence of lipids in the meal increase bioavailability. This trend is consistent throughout the most often investigated foods: tomatoes, carrots, and spinach (representative studies: *98*, *74*, *31*, respectively).

While these studies assessed the influence of processing the food matrix on carotenoid bioavailability, the current study observed bioaccessibility as a function of plant source. The objective of this research was to determine relative rates of bioaccessibility in an array of commercially-available carotenoid-containing raw fruits and vegetables. Very few studies compare raw foods themselves, a notable exception being van het Hof et al (*30*) which compared the influence of several green vegetables

on plasma β-carotene levels in humans. The comparison of raw food sources is important since carotenoids are unique in their thermostability in the native food matrix, while many of the other important nutrients are often degraded or lost during the same processing believed to aid carotenoid bioaccessibility (*101*). This work is important in understanding the effects of carotenoid source on bioaccessibility since no broad survey of whole, raw foods is in the literature.

Bioavailability studies often use full human trials to assess the full scope of nutrient absorption. Conversely, an *in vitro* method can be used to assess bioaccessibility while eliminating complicating factors such as genetics, diet, and environment (*24*) which may mask the underlying principles of nutrient extraction from our foods. An *in vitro* method which mimics the digestive processes of the stomach and small intestine to measure carotenoid bioaccessibility was developed by Failla and Chitchumroonchokchai (*102*) and used in the current study. At the end of this digestive process, the bioaccessible carotenoids are housed in lipid-based carriers called micelles. Failla and Chitchumroonchokchai showed that *in vitro* intestinal cell carotenoid uptake is directly proportional to micellular content over time, regardless of carotenoid source. Therefore, it was considered unnecessary in the current work to carry the bioaccessibility study through an *in vitro* cell model (thereby partially extending it to bioavailability) since the variability imparted by the food source is the point of interest and will be manifest in the earlier phase.

Carotenoids as Sunscreen

An additional benefit of a broad carotenoid bioaccessibility survey like that presented here is the identification of good sources of individual carotenoids. Of particular interest are good phytoene sources since carotenoids, notably phytoene, have been found to be good ultra-violet (UV) radiation blockers when consumed and consequently deposited in the skin. Early studies showed that mega-doses of phytoene (17 mg/g body weight) significantly reduced erythema (reddening) of the skin in guinea pigs when exposed to radiation (*103*). A novel approach to chemoprevention using phytoene was implemented by Nishino et al (*104*) using biotechnology to integrate phytoene synthase activity into mammalian cells. Endogenous production of phytoene in these cells resulted in dramatic chemoprevention. A more recent study evaluated the affects of three lycopene sources: synthetic lycopene, tomato extract, and solubilized tomato extract, on radiation-induced erythema (*105*). The tomato-based treatments were found to significantly reduce erythema while the synthetic lycopene did not have the same effect. The presence of phytoene and phytofluene were suspected to be the source of the effect. Phytoene becomes unstable upon purification (*104*), thus increasing the importance and novelty of whole food sources. The effective absorption range of phytoene is 300-250nm. Phytoene may act more powerfully than other carotenoids in reducing cancer risk since it absorbs UVC radiation, the most damaging form of solar radiation, where this is outside the capabilities of other common dietary carotenoids.

MATERIALS AND METHODS

Nine fruits and vegetables (butternut squash, carrot, red grapefruit, mango, melon, papaya, sweet potato, tomato, and watermelon) were analyzed for carotenoid bioaccessibility according to modification of the methods described in Chitchumroonchokchai et al (*83*) and as previously outlined in Chapter V. After digestion, the method was completed by filling polyallomer tubes (Beckman Coulter) with the digesta and ultracentrifuging at 308,444*g* (40,000 rpm) for 35 min (Beckman Coulter 90Ti rotor) to separate any particulate matter and residual oils. The aqueous supernatant was drawn off with an 18 gauge syringe, filtered (Milipore, 0.22 µm polypropylene filter) to remove unmicellularized carotenoids, and labeled "Aqueous".

"Meal", "digesta", and "aqueous" fractions were all kept on ice until carotenoid extraction was performed at the end of each day. A sample amount inversely proportional to the total amount of carotenoids present was extracted using a modification of Garrett (*106*). A hexane (JT Baker) volume equal to the sample volume was shaken with the sample for 1 min. Volumes equal to half the sample amount were added of ethanol (EMD Biosciences Inc.) and acetone (EMD) and shaken for 30 sec. Samples were centrifuged for 5 min to aid phase separation. The hexane layer was removed to a glass vial and extraction was repeated until all color was removed, usually 2-3 times. Hexanes were pooled and dried under nitrogen gas. The vials were then tightly capped and stored at -80°C.

High Performance Liquid Chromatography (HPLC) analysis was performed as described in Chapter II, except data was analyzed using Chromeleon software (Dionex Corp., Sunnyvale, CA) and β-carotene standard calibration was also used to quantify α-carotene.

Percent bioaccessibility was calculated as the fraction of carotenoids in the digesta which remained in the micellular aqueous fraction after centrifugation. Digestive stability, or recovery, was calculated as the percentage of carotenoids detected in the digesta originally present in the meal fraction.

A pilot study was conducted to determine the appropriate food load on the *in vitro* system. Four food amounts were tested in the system. The test amounts were determined by approximating and equalizing total carotenoid load on the system using published carotenoid data (*89*). Test load amounts were also modified by the volume limits of the system and previous data. The titration samples were extracted as outlined above but total carotenoid content was measured using a spectrophotometer (445 nm) to estimate total carotenoid bioaccessibility. The point of maximal linear micellularization along with preliminary data were used to determine the load for all further experiments. The food load used was the only difference in treatment between samples.

Data were analyzed using a univariate general linear model (GLM). Post hoc tests, Tukey's Honestly Significant Difference (HSD), were conducted to establish statistical differences. With the aid of these indicators of significant difference, data were sorted by carotenoid then food according to level of bioaccessibility. A trend in bioaccessibility across foods and carotenoinds was noted and then tested using linear

regression with Pearson correlation statistics. Spearman's rho correlation statistics were used to determine effect of meal pH (experimental data) and fiber content (published data, *82*) on bioaccessibility. All statistics were run using SPSS 15.0.

RESULTS AND DISCUSSION

Bioaccessibility

Statistically significant differences in carotenoid bioaccessibility were observed among the fruits and vegetables tested (**Figure 53**). Both carotenoid type and food were found to be correlated with bioaccessibility (see **Table 7**). Though this analysis confirms a general trend, the amount of variation explained (33.8%) conveys that additional factors are likely present. According to a regression analysis, carotenoid bioaccessibility ranked by food from lowest to highest as follows: grapefruit, melon, sweet potato, butternut squash, carrot, tomato, mango, watermelon, and papaya. For carotenoids, the order is lycopene, α-carotene, β-carotene, lutein, violaxanthin, and phytoene.

Mean bioaccessibilities for each carotenoid (**Figure 54**) generally follow trends suggested throughout the literature (ie. bioaccessibility of xanthophylls > carotenes > lycopene) (reviewed in *102*). Additionally, it was noted that phytoene had a consistently high bioaccessibility. These means, however, do not fully represent the complexity seen here. Percent bioaccessibility varied widely between foods for each given carotenoid and for different carotenoids within foods. For each given food, however, this order of

bioaccessibility was consistent, despite the wide variation in bioaccessibility for each carotenoid. This relationship further emphasizes the role of carotenoid source over simple carotenoid content.

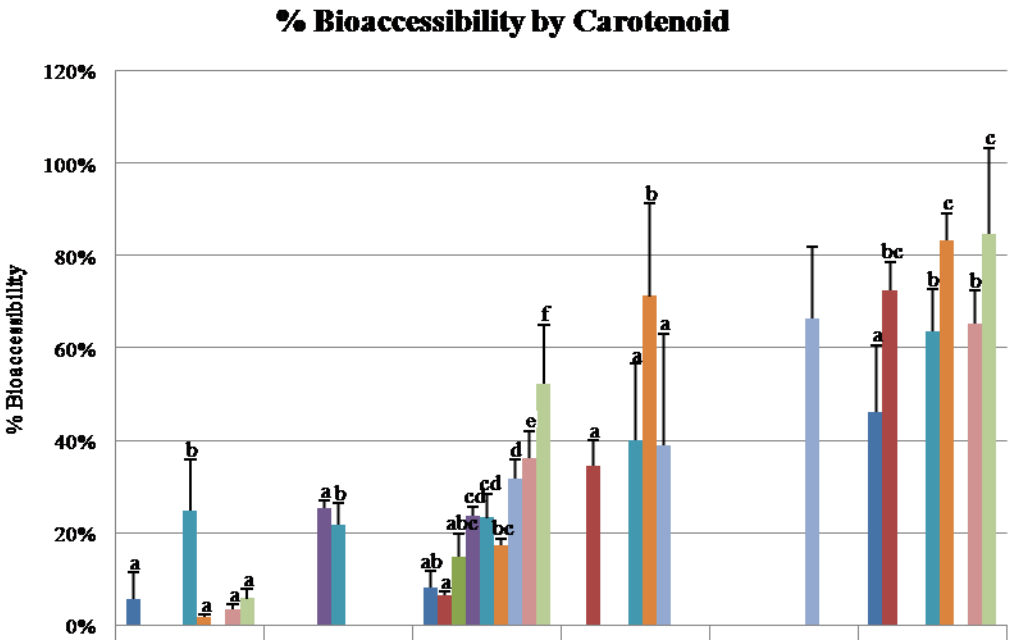

	Lycopene	α-carotene	β-carotene	Lutein	Violaxanthin	Phytoene
Gf	6±5.6%	ND	8±3.6%	ND	ND	46±14.38%
Melon	ND	ND	7±0.8%	34±5.6%	ND	72±6.2%
SP	ND	ND	15±5.0%	ND	ND	ND
Bn Sq	ND	25±1.9%	24±2.1%	ND	ND	ND
Carrot	25±11.1%	22±4.8%	23±5.1%	40±16.6%	ND	63±9.1%
Tomato	2±0.8%	ND	17±1.6%	71±20.2%	ND	83±5.9%
Mango	ND	ND	32±4.1%	39±24.2%	66±15.59%	ND
Wm	3±1.3%	ND	36±6.0%	ND	ND	65±7.3%
Papaya	6±2.0%	ND	52±12.8%	ND	ND	85±18.5%

Figure 53. Bioaccessibility of carotenoids grouped by carotenoid. Data represent means ± SD of four replicated samples. Letters above SD bar represent significant difference (α=.05) in bioaccessibility of each carotenoid between the foods (letters are not comparable between carotenoids). ND = not determinable.

Table 7. Pearson Correlation Coefficients for Carotenoid Content, Bioaccessibility, Fiber, and pH Components at α<.05 (*) and α<.01 (**). Correlations Given in Regard to Both Experimental (Determined in Current Study) and Published Carotenoid Contents (*88*).

Correlation Components		Correlation Coefficient
Carotenoid Type	Overall bioaccessibility	0.557**
Food	Overall bioaccessibility	0.167**
Lutein content	Lutein bioaccessibility	.733*
Lycopene content	Lycopene bioaccessibility	0.803**
α-carotene content	α-carotene bioaccessibility	.969**
Violaxanthin content	Violaxanthin bioaccessibility	0.750*
Soluble hemi-cellulose	Phytoene bioaccessibility	.764*
Soluble pectin	α-carotene bioaccessibility	.762*
Insoluble cellulose	α-carotene bioaccessibility	0.713*
Soluble pectin	α-carotene content (experimental)	.762*
Soluble pectin	α-carotene content (published)	0.866**
Soluble pectin	β-carotene content (experimental)	.854**
Soluble pectin	β-carotene content (published)	0.909**
Soluble hemi-cellulose	β-carotene content (published)	.830*
Soluble pectin	Lycopene content (experimental)	neg .750*
Insoluble cellulose	Lycopene content (published)	neg .708*
Meal pH	Overall bioaccessibility	.165*
Meal pH	β-carotene content (experimental)	.312**
Meal pH	Phytoene content (experimental)	.383**

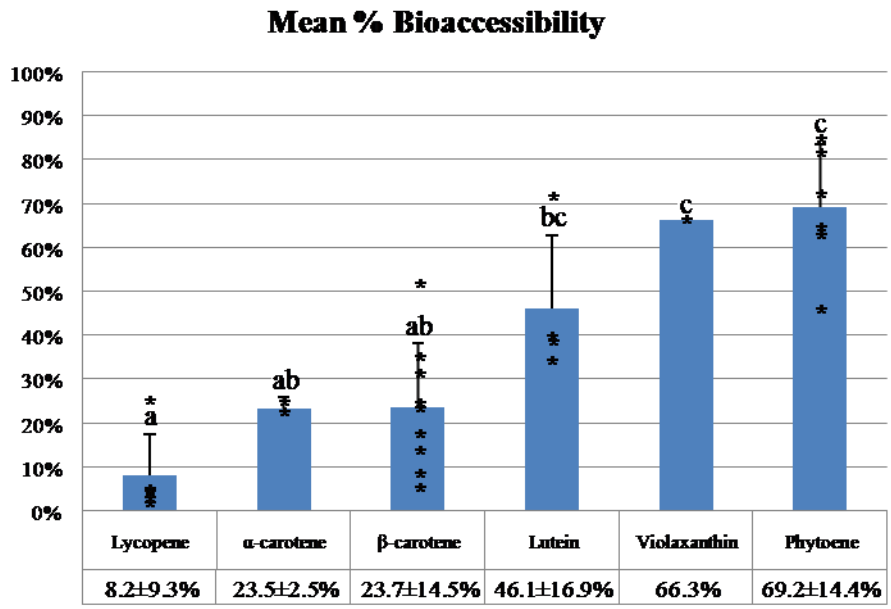

Figure 54. Mean percent bioaccessibility. Data represent means ± SD of mean carotenoid bioaccessibility. Letters above SD bar represent significant difference (α=.05) in mean percent bioaccessibility for each carotenoid type. Asterisks (*) represent the individual data points from which the means were derived (See **Figure 53**).

Amount Bioaccessible

The data of most dietary interest is the amount of carotenoids accessible from each source. Bioaccessibility is the percentage of the carotenoids found in a food that are accessible to the body and the total amount this percentage represents also varies greatly between sources due to total carotenoid content. **Figure 55** shows the amount of each carotenoid accessible from a gram of food. Per gram food, grapefruit, watermelon, and papaya yielded the most lycopene. Carrot imparted the most α- and β-carotene, lutein, and phytoene. Mango imparted the most violaxanthin. Note the dramatic influence of the high bioaccessibility of phytoene on the amounts accessible in the foods.

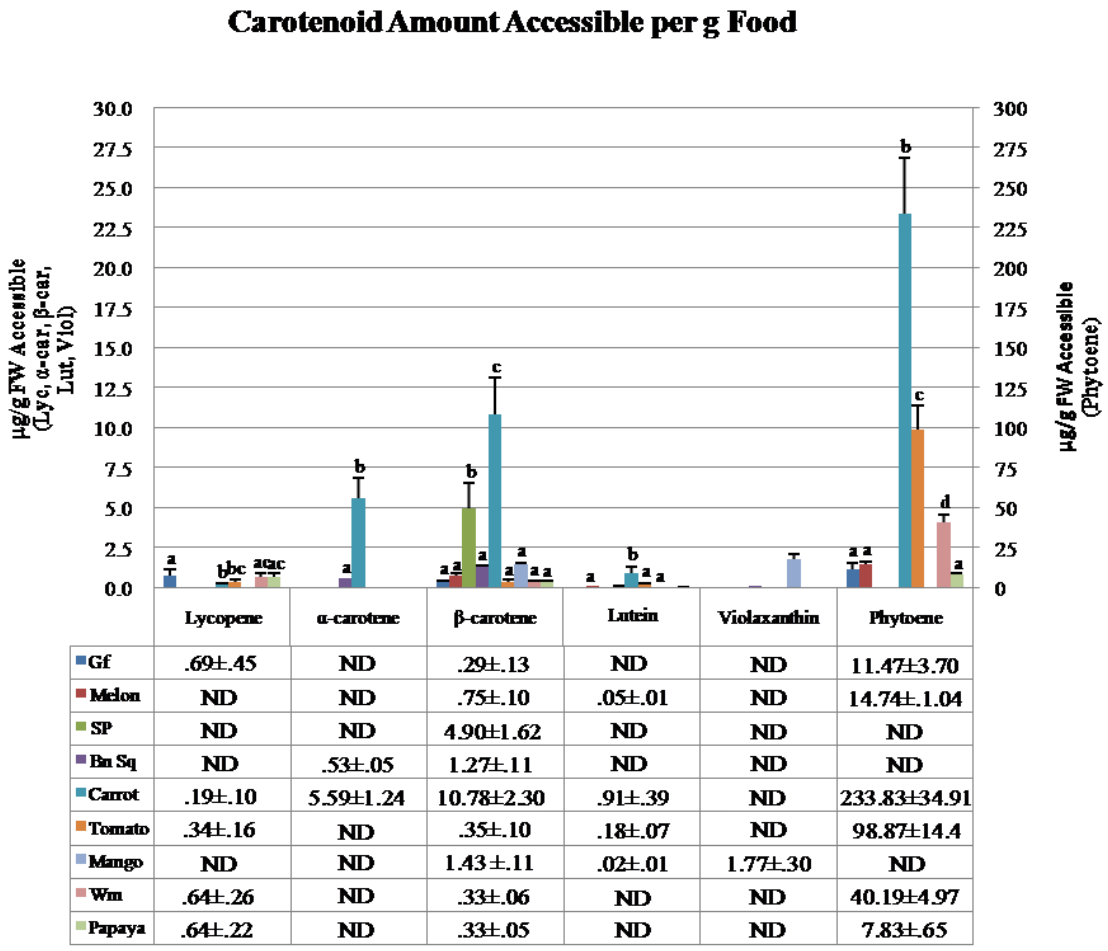

	Lycopene	α-carotene	β-carotene	Lutein	Violaxanthin	Phytoene
Gf	.69±.45	ND	.29±.13	ND	ND	11.47±3.70
Melon	ND	ND	.75±.10	.05±.01	ND	14.74±.1.04
SP	ND	ND	4.90±1.62	ND	ND	ND
Bn Sq	ND	.53±.05	1.27±.11	ND	ND	ND
Carrot	.19±.10	5.59±1.24	10.78±2.30	.91±.39	ND	233.83±34.91
Tomato	.34±.16	ND	.35±.10	.18±.07	ND	98.87±14.4
Mango	ND	ND	1.43 ±.11	.02±.01	1.77±.30	ND
Wm	.64±.26	ND	.33±.06	ND	ND	40.19±4.97
Papaya	.64±.22	ND	.33±.05	ND	ND	7.83±.65

Figure 55. Micrograms of carotenoid accessible per gram of food. Secondary axis for phytoene only. Data represent means ± SD of aqueous fraction for four replicated samples. Letters above SD bar represent significant difference (α=.05) in bioaccessibility of each carotenoid between the foods (letters are not comparable between carotenoids). ND = not determinable.

In practice, serving sizes vary greatly between foods, which are not taken into account in simple bioaccessibility or on a per gram basis. Accordingly, **Figure 56** shows the amount accessible from a typical serving of each food. Serving size impacted the perceived benefit showing grapefruit to singularly lead lycopene yield, with carrot

still yielding the most α- and β-carotene, lutein, and phytoene, and mango for violaxanthin.

	Lycopene	α-carotene	β-carotene	Lutein	Violaxanthin	Phytoene
Gf	79.78±51.26	ND	32.90±14.2	ND	ND	1.32±.43
Melon	ND	ND	65.75±8.52	4.53±.61	ND	1.30±.091
SP	ND	ND	489.6±161.9	ND	ND	ND
Bn Sq	ND	53.65±5.02	129.2±10.8	ND	ND	ND
Carrot	11.35±5.71	335.5±74.6	646.7±138.2	54.64±23.33	ND	14.03±2.04
Tomato	30.30±14.30	ND	31.60±8.72	16.10±6.59	ND	8.90±1.30
Mango	ND	ND	146.9±85.8	1.53±1.17	157.6±40.6	ND
Wm	49.07±19.76	ND	25.23±4.59	ND	ND	3.09±.38
Papaya	44.48±.15.74	ND	22.86±3.57	ND	ND	.55±.05

Figure 56. Grams of carotenoid accessible per serving of food. Secondary axis for phytoene only. Data represent means ± SD of aqueous fraction for four replicated samples multiplied by serving size. Letters above SD bar represent significant difference (α=.05) in bioaccessibility of each carotenoid between the foods (letters are not comparable between carotenoids). ND = not determinable.

Serving sizes were based on MyPyramid.gov guidelines (*107*) (1/2 cup serving each). Servings were as follows: grapefruit (115g), melon (88g), sweet potato (100g), butternut squash (102g), carrot (60g), tomato (90g), mango (83g), watermelon (77g), and papaya (70g).

Correlations

An overall strong correlation (see **Table 7**) was found between carotenoid content and bioaccessibility for most of the carotenoids observed. This correlation was found individually for lutein, lycopene, α-carotene, and violaxanthin but not for β-carotene or phytoene. No interactions were found between the presence of some carotenoids and decreased bioaccessibility of others (competition) as has been observed in other studies (reviewed in *25*). This lack of correlation under this *in vitro* model may point to competition for absorption occurring at the site of transport across the epithelium as has been suggested (*102*). Since carotenoid content and profile is an inherent characteristic of each food and is therefore a tenant of bioaccessibility, competition is as well, even though only revealed under bioavailability model systems.

Fewer correlations were found between bioaccessibility and reported fiber contents of each food (*82*, Data adapted and presented in Chapter V, Table 1) than expected which may point to additional conclusions. A negative correlation between soluble hemi-cellulose fiber content and phytoene bioaccessibility was observed. Though interference with phytoene bioaccessibility has not previously been investigated, this finding is in line with those found for other carotenoids. Positive correlations

observed between α-carotene bioaccessibility and both soluble pectin and insoluble cellulose contents stand in contrast to previous findings (*31*, *33*, *34*, *35*). These correlations are most likely artificial, however, due to the fact that only two of the sources sampled, carrot and butternut squash, even contained α-carotene. This apparent inconsistency with published ideas on the influence of fiber strongly support the idea that fiber inhibits bioaccessibility in the intestine at the absorption site (*34*, *35*). This hypothesis reveals potentially flawed assumptions of previous conclusions regarding the relevance of source once carotenoids are transferred to the micellular fraction which is used for delivery to *in vitro* cell models. The assumption is that the "waste", which is not part of this fraction and contains fiber, does not play a role in bioaccessibility. The evidence presented here demands reevaluation of this tenant.

It is interesting to note unprecedented correlations between fiber content and carotenoid content itself. These correlations were evaluated using both experimental and published carotenoid content values (*89*), with similar findings in most cases. Soluble pectin content positively correlated with both experimental and published α-carotene and β-carotene contents. Published β-carotene values were additionally correlated with soluble hemi-cellulose content. Lycopene was negatively correlated with soluble pectin content when using experimental data and insoluble cellulose with the published data. This last finding may be influenced by the considerable lycopene content of papaya found in our study versus none reported in the published data. In all, the mechanism underlying these correlations is unclear and may be more of an artifact of the foods used for the study.

Overall meal pH, an indirect measure of food pH, was positively correlated with bioaccessibility. Individual carotenoid bioaccessibility, β-carotene and phytoene, were found to be the source of the pH correlation. These observations are consistent with those of Wright et al (*108*) which assessed the influence of pH on the in vitro digestive system and showed increased β-carotene transfer to the aqueous phase under higher pH conditions. Though manipulation of the pH in these two cases are endogenous and exogenous, respectively, the basis for the effect is the same.

Digestive Stability

It should be noted that digestive stability of the carotenoids (ie. percentage of carotenoids detectable in the digest from the meal) also varied among the sampled foods. Digestive stability of each carotenoid is given in **Figure 57**. No overall correlation was found between digestive stability and either food or carotenoid. However, a significant correlation between digestive stability and carotenoid for both butternut squash and watermelon was found. In this case this meant they ranked lower across all carotenoids whereas the other foods fluctuated. Chitchumroonchokchai et al (*83*) also reported significant differences in the carotenoids recovered from different food matrices.

Another consideration is that digestive "instability" may actually represent the utility of carotenoid antioxidant power in the digestive process. While most research focuses on the action of antioxidants organs and tissues after passage out of the digestive tract, others may act to protect the digestive tract organs or act synergistically to protect other antioxidants from oxidation.

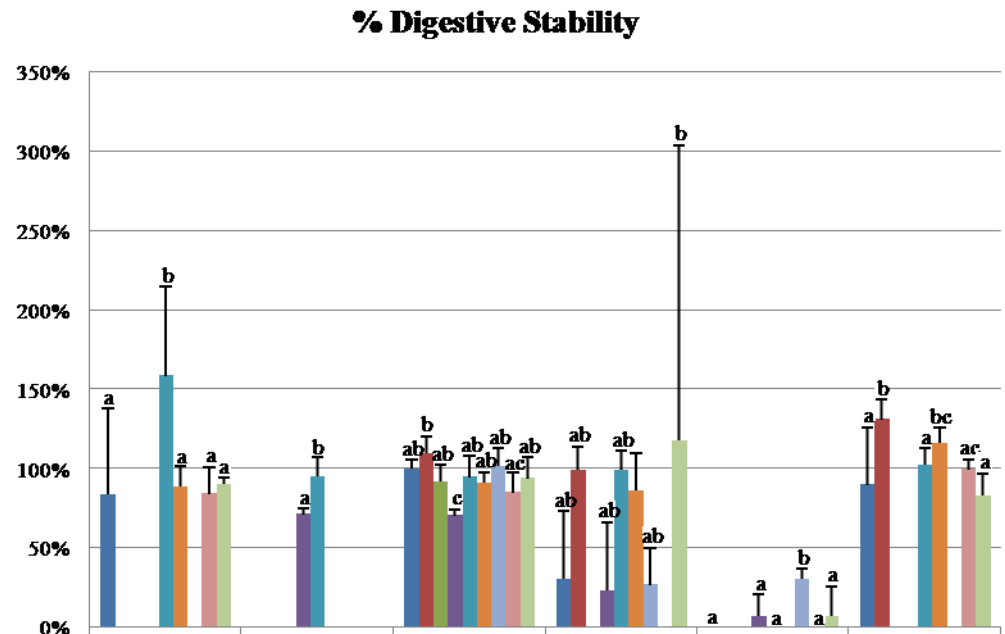

	Lycopene	α-carotene	β-carotene	Lutein	Violaxanthin	Phytoene
Gf	84±54%	ND	100±5%	30±43%	0%	89±36%
Melon	ND	ND	109±11%	99±15%	ND	131±13%
SP	ND	ND	91±10%	ND	ND	ND
Bn Sq	ND	71±4%	70±4%	23±43%	6±14%	ND
Carrot	158±56%	95±12%	94±13%	98±12%	0%	102±11%
Tomato	88±13%	ND	90±7%	86±24%	ND	116±10%
Mango	ND	ND	101±11%	26±23%	30±6%	ND
Wm	84±17%	ND	85±13%	ND	0%	99±6%
Papaya	90±4%	ND	93±13%	117±186%	7±19%	82±14%

Figure 57. Digestive stability of carotenoids (% recovery from meal fraction). Data represent means ± SD of four replicated samples. Letters above SD bar represent significant difference (α=.05) in bioaccessibility of carotenoids within each food (letters are not comparable between carotenoids). ND = not determinable.

The xanthophylls, lutein and violaxanthin, appeared to be the least digestively stable, though the trend was not statistically significant. Regardless, this instability led to several of the foods which contained these carotenoids to fall below detection limits

for the aqueous fraction and therefore did not have a final accessible content (compare **Figure 55** and **Figure 57**).

Another question raised by these data is how there could be higher than 100% digestive stability. A couple of explanations for this may apply. Other carotenoids may be converted into those under question during processing, thus leading to higher levels than seen in the less processed meal fraction. Another possibility is incomplete extraction of the carotenoids from the meal fraction. Carotenoids are tightly bound to the food matrix and, though all care was taken to obtain a complete extraction, it may have been facilitated in the digesta fraction by degradation of the matrix. The apparently random elevation of singular carotenoids within a food, however, reduces the likelihood of this possibility.

CONCLUSION

A practical ranking of foods by relative bioaccessibility gives consumers more information about their diet and a broader, more general basis for making informed decisions. For example, while tomato contains 1.5 times the β-carotene that watermelon does, watermelon's β-carotene is 19% more bioaccessible. The result is an approximately equal benefit from both per gram. While nutrient trade-offs are inevitable when evaluating all factors from shelf-life to method of consumption, this research on raw foods provides the consumer with the ability to choose carotenoid sources with

optimal bioaccessibility for most of their nutrients rather than just those optimized through selective processing.

Another application for this information may include guiding practical breeding scenarios. With new interest in phytoene's UV protective effects, breeding efforts may soon aim to increase this carotenoid in various foods. As found here, carrot is the best source of phytoene. Breeding efforts can help other fruits or vegetables to boast similar claims. The task can seem daunting when based simply on the food's content, but may be more manageable when the actual accessible amounts are considered. For example, while carrot contains over 3 times the phytoene of tomato per gram, tomato's phytoene bioaccessibility is 20% higher than carrot's. For equal benefit per serving, tomato's phytoene content must only, therefore, be increased by 56%, a much more reasonable goal.

Also, in regard to carotenoid extraction for marketing, the matrix effects investigated here may suggest improved sources for extractions, since digestive and extraction procedures act similarly on food matrices and may make them more efficient or versatile. All of these possibilities necessitate the understanding of the native food matrix and its effect on digestibility and accessibility.

On a more basic level, the potential implications of the data presented here reveal a pressing need for new *in vitro* methods which retain the strengths of measuring bioaccessibility without the confounding bioavailability factors while additionally accounting for the influences of bulk components if the food. Also, more physiological data is still needed to elucidate the underlying basis for the differences in bioaccessibility

observed. The trends and interactions of the carotenoid bioaccessibilities in these foods are complex, corroborating the complexity and diversity seen in the food matrices noted in Chapter V.

CHAPTER VII

CORRELATION OF CELLULAR AND SUBCELLULAR STRUCTURE MORPHOLOGY, FIBER CONTENT, AND CAROTENOID BIOACCESSIBILITY IN NINE CAROTENOID-CONTAINING FRUITS AND VEGETABLES

INTRODUCTION

This chapter is intended as a forum in which to view the information presented in the previous two: Chapter V - *Chromoplast and Cell wall Ultrastructure in Nine Carotenoid-Containing Fruits and Vegetables: "Whole Food", "Masticated", and "Digested" Stages* and Chapter VI - *Carotenoid Bioaccessibility of Nine Carotenoid-Containing Fruits and Vegetables.* These data are considered here as a whole in an effort to better understand the source-based mechanisms governing bioaccessibility of carotenoids from whole, raw fruits and vegetables. Correlative and observational data are presented as a means of deriving meaning from the merger of these two data sets.

METHODS

Correlation coefficients and statistics were calculated using Spearman's rho and run using SPSS 15.0 statistical software. Two sources of carotenoid content data were

considered, our experimental data and published values (*89*). Which data source was used for each correlation is noted parenthetically where applicable.

RESULTS AND DISCUSSION

Some of the correlations found between whole food structures and carotenoid content are reflections of the food sources used and are thus most likely reflected to some degree in the bioaccessibility data presented alone in Chapter VI. For example, the lycopene sources observed tended to be soft foods, having thin cell walls (watermelon, tomato, papaya) leading to a negative correlation between lycopene content (*89*) and minimal cell wall thickness (see **Table 8**). A similar phenomenon may be responsible for a correlation between α-carotene (*89*) or β-carotene (experimental) content and cell wall description for foods with more robust cell walls (carrot, butternut squash, sweet potato). Likewise, α-carotene and β-carotene (experimental) were negatively associated

Table 8. Pearson Correlation Coefficients for Carotenoid Content, Bioaccessibility, and Ultrastructure Characteristics Components at $\alpha<.05$ (*) and $\alpha<.01$ (**).

Correlation Components		Correlation Coefficient
Lycopene content (published)	Minimum cell wall thickness	neg 0.829**
α-carotene content (experimental)	Cell wall description	0.676*
β-carotene content (experimental)	Cell wall description	0.767*
α-carotene content (experimental)	Cell size	neg 0.730*
β-carotene content (experimental)	Cell size	neg 0.736*
Lutein content (published)	Carotenoid crystal content	0.752*
Lycopene bioaccessibility	Carotenoid crystal content	neg 0.789*
Granular material in meal	α-carotene bioaccessibility	0.750*
Crystals in meal	β-carotene bioaccessibility	0.725*
Tubules in digest	α-carotene bioaccessibility	0.750*

with cell size, though this is not supported by a positive statistic between cell size and cell wall thickness or description. These trends may not have held if more foods with the opposite characteristics were included (ex. lycopene carrot) and point to needed further work in this field. A perfect positive correlation was found between violaxanthin content (experimental) and tubular chromoplasts substructure, suggesting violaxanthin is preferentially stored in these structures. An unlikely correlation between lutein (*89*) and carotenoid crystal contents was observed. Lycopene and β-carotene are the only carotenoids reported to form crystalline chromoplasts structures. The correlation with lutein may have arisen coincidentally concurrent with the lack of correlation between lycopene or β-carotene and crystal content here because the carotenoid content of a crystal is ambiguous based on micrograph data except in the case of lycopene crystal remnants and were thus all considered together. Despite the lack of correlation found between lycopene and carotenoid crystal content, a positive correlation was found between lycopene bioaccessibility and crystal content. Upon closer inspection of the data relevant to this correlation, it was noted that carrot's high crystal content and lycopene bioaccessibility played a major role, despite no evidence of unique lycopene crystals or substantial lycopene content.

The appearance of a homogeneous granular background in the meal fraction seemed to correlate with a high α-carotene bioaccessibility. This data point relies on the coincident presence of α-carotene in the only sample (butternut squash) which yielded this type of material in the meal fraction. The other correlation noted for this fraction showed that the persistence of recognizable carotenoid crystals in the meal was

positively correlated with β-carotene bioaccessibility. This seems counterintuitive since bioaccessibility relies heavily on the solublization of carotenoids into the lipid fraction, though this may only happen in later stages of digestion (ie. digest fraction). Indeed, no correlation was found between carotenoid crystals in the digest fraction and bioaccessibility of any carotenoids. In fact, the only structure in the digest fraction, tubules, was correlated with α-carotene bioaccessibility. Again, the prevalence of tubules in butternut squash, combined with it being one of two food sources to contain α-carotene, make this a narrowly applicable statistic.

CONCLUSION

In all, these data did not yield the expected kind of correlations between whole food structures and the bioaccessibility of individual carotenoids. This may be due to complex factors not investigated here. These expectations may have been based on the narrow, limited data of previous studies. In other words, just as the bioaccessibility of individual carotenoids found in the present study followed the general trends in the literature but also revealed a less definite pattern when multiple sources were considered together (Chapter VI), here too, underlying inconsistencies between the effects of native food matrices may exist. This quandary points to the need for an even broader survey of foods if the influence of the food matrix is to be truly understood.

CHAPTER VIII

OXYGEN RADICAL ABSORBANCE CAPACITY: EVALUATION OF ALTERNATIVE EXTRACTION METHODOLOGIES FOR WATERMELON

INTRODUCTION

Antioxidant potential is a hot topic in nutritional circles since it is a powerful indicator of potential health benefits associated with the quenching of harmful free radicals in the body. In a review covering various aspects of an "anti-cancer" diet, antioxidants (listing carotenoids and vitamin C as the most salient) were prominent players in reducing cancer risk (*109*). Among the carotenoids and debatably among all antioxidants, lycopene has been shown to be among the most powerful singlet oxygen radical quenchers known (*110, 111*). Interestingly, the same protective effect is not always present when carotenoids are taken at hyper-physiological doses in supplement form rather than obtained from whole foods or supplemented at levels equivalent to those found in whole foods (*18, 112*). High doses of carotenoids may even have adverse effects in some cases (*113, 114*). This evidence would support the use of whole-food products rather than supplements, especially since other beneficial nutrients are found in whole foods which are not in the purified compounds.

Among the extra nutrients in a carotenoid-containing fruit or vegetable, such as watermelon, could be other antioxidants. Listed in **Table 9** are the antioxidants

commonly found in watermelon. Note that they are of two categories, amino acids and carotenoids. Each of these antioxidants contributes to the total antioxidant potential of watermelon. A quantitative measure of the total antioxidant potential in watermelon may prove a helpful measure of healthfulness rather than quantities of individual compounds.

Table 9. Antioxidants in Red Watermelon, Quantities, and Relative Polarities.

	Antioxidant	**Quantity**	**Hydro-phobicity**
Amino Acids	Alanine	0 - 2,000 ppm	1.8†
	Citrulline	0 - 1627 ppm	††
	Cysteine	0 - 236 ppm	2.5†
	Histidine	0 - 707 ppm	-3.2†
	Methionine	0 - 707 ppm	1.9†
	Tryptophan	0 - 825 ppm	-0.9†
Carotenoids	Lycopene	45 - 900 ppm	**
	β-carotene	2 - 48 ppm	**
	Lutein	0.14 - 3 ppm	**
†	Hydrophobicity index values range from -4.5 to 4.5 grading amino acids as hydrophylic to hydrophobic, respectively.		
††	Citrulline is a free amino acid and was not included in the referenced index. Other sources, however, refer to citrulline as moderately polar (hydrophilic).		
**	Carotenoids are listed in decreasing order of hydrophobicity.		
Sources: Quantities – (115) *Amino Acid Hydrophobicity Index- (122)*			

As an interesting side note, a relatively rare free amino acid with significant health benefits, citrulline, is found at its highest abundance in watermelon rind and flesh, in which it was originally identified (*115*). Watermelon boasts approximately 7 and 11

times the concentration found in the next most potent carriers, melon (cantaloupe) and cucumber, respectively (*116*).

Three lines of evidence suggest the need to investigate antioxidant activity in watermelon. First, since watermelon is shown to have a high carotenoids content, antioxidant levels should be high also. A couple of food antioxidant surveys have measured watermelon antioxidant capacity using several methods, some minimizing watermelon as a low capacity radical quencher, some as moderate to high (*117*, *118*, *119*). Further research is needed to support, negate, or explain this conflicting and seemingly counterintuitive finding. Second, although the various carotenoids which contribute to the variation in colors among watermelon varieties have been delineated along with the relative *in vitro* antioxidant capacities of their pure-compound equivalents, corresponding variation in the other antioxidant compounds is only in its preliminary stages. In support of this hypothesis (that other antioxidants vary with carotenoid composition), Rimando and Perkins-Veazie (*120*) found that the rinds of red watermelons contained less citrulline than those of the other colors. Last, one study showed that various isomers of each carotenoid had different and sometimes highly varied antioxidant capacities (*121*). An investigation of watermelon varieties which contain similar levels of total or specific carotenoids but may contain different isomer profiles may point to another cause of earlier conflicts.

The Oxygen Radical Antioxidant Capacity (ORAC) assay has recently gained popularity in antioxidant potential quantification for two reasons: 1) the reaction is driven to completion, meaning the complete depletion of activity is observed and

quantified and 2) there are two sub-assays, one hydrophilic and one lipophilic, of which either or both (for total) may be used in determining the antioxidant potential of a sample. The later of these two advantages is especially useful in the present case of an amino acid/carotenoid antioxidant mixture, each of which vary greatly in their polarities. Carotenoids in general are considered apolar, whereas carotenes (lycopene, β-carotene, etc.) are highly apolar, xanthophylls (lutein, violaxanthin, and zeaxanthin) are more polar and may be miscible under some aqueous conditions. The amino acids present in watermelon vary even more greatly in polarity as seen in **Table 9**, histidine even being very hydrophylic. The advantages of the ORAC assay seem very suitable to investigation of watermelon antioxidant capacity.

One obstacle to appropriately applying ORAC to the study of watermelon is the extraction conditions. Current protocols for compound extraction leading up to the ORAC assay most often call for freeze-drying when both the hydro- and lipophilic assays are to be performed (eg. *119*). Freeze drying is highly degrading to carotenoids, a major antioxidant in watermelon (*122*). Also, when Wu et al (*119*) ran juice samples (a close analogy to homogenized watermelon) hydrophilic ORAC was the only assay used, but this would not be an appropriate approach for watermelon samples with a high hydrophobic antioxidant content. Additionally, the traditional ORAC extraction procedures use high pressure and temperature to improve extractability of antioxidants. While elevated temperature is commonly known to be detrimental to many food nutrients, an additional factor of isomerization may be present for carotenoids during heat treatment (*97*). Since different carotenoid isomers have different antioxidant

capacities (*121*), it is important to minimize inductive conditions during sample processing.

Given the perceived benefits of this research and a need for a more appropriate protocol for applying the ORAC assay to a food high in antioxidants of various polarities, a variety of extraction and assay conditions were manipulated in hopes of finding a robust method suiting the needs of the assay. Let it first be noted that we successfully validated the ORAC method in our hands when performed on a standard (Trolox) using a previously established in-house protocol. The inconsistencies and irreproducibility later experienced should therefore be attributable to the extraction methods and modifications made to the protocol, though this was not found to be entirely true (see notes on second experiment).

EXPERIMENTS

The primary and most obvious difficulty with the protocols presented in the literature was the inapplicability of the extraction method to the needs of our subject. Each experiment included three new extraction protocols. The goal of the extraction experiments was to find an optimal extraction method (ie. yields highest ORAC values, thus signifying a complete extraction). ORAC values are calculated by measuring the area under curve (AUC) of fluorescence degradation (decay) and subtracting the AUC of the blank. Since one of the primary strengths of ORAC is its ability to run to completion, the tail of this curve must reach approximately zero by the end of the assay.

Realization of reaction completion through protocol and assay changes was our greatest hurdle, without which, attempts to quantify the ORAC values would be inaccurate.

Two goals, optimizing the extraction and driving the reaction to completion ("closing") drove our experimental design. Despite our inability to truly measure the strength of an extraction until reliable ORAC values were obtained, observations could be and were made about the qualitative strengths of the extraction, mainly that all color (ie. carotenoids) was removed from the tissue. It should be born in mind when reviewing the progression of the experiments that changes in the protocol were made based on observations of these two traits, color extraction and curve closing. Also, since these could reasonably be assessed independently, modifications to the protocol were made in regard to the extraction (for complete extraction) and assay (for closing) concurrently.

First, modifications of the published extraction protocol were attempted (*119*), eliminating freeze-drying and the high temperatures used in extraction. A second extraction was adopted from a standard carotenoid extraction which is based on the biphasic separation of hydrophilic and lypophilic compounds (*50*). The final extraction was suggested by a research scientist at the Vegetable and Fruit Improvement Center, Dr. Jayaprakasha, and involved the use of methyl ethyl ketone (MEK) as a polar, water soluble solvent in place of acetone and/or ethanol in the other extractions. None of these extractions yielded decay curves which declined appreciably from their respective original time point values (See **Figure 58**). Additionally, the first and third extractions were incomplete. We concluded that modifications to the extractions were needed and

closing may be aided by increasing dilution of the sample or extending run time of the assay.

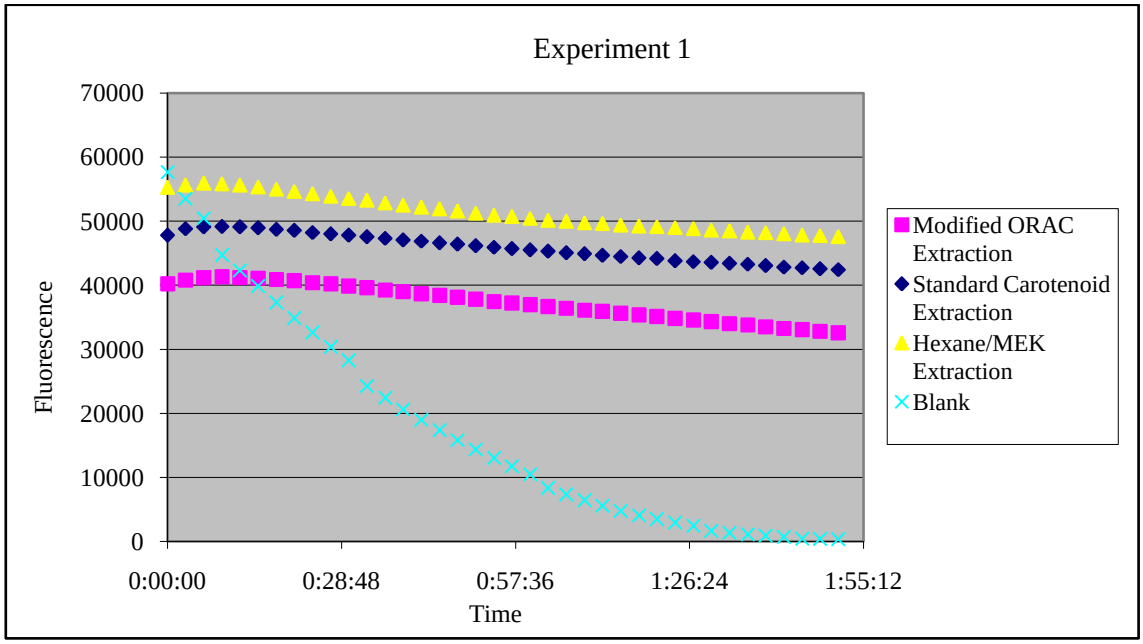

Figure 58. Typical decay curves for Experiment 1.

In an attempt to most closely adhere to published protocols, the combination of organic solvents used in the first extraction above, was applied to the other two extractions. This modification slightly changed the polarity of the organic phase (from 100% hexane to 50/50 hexane/dichloromethane). Also, the number of serial extractions was increased in the protocols which gave incomplete extractions the first time. Finally, discussion in the literature was consulted regarding methods for driving the assay to completion. During this investigation, substantial discrepancies were found between the published assay protocols and in-house protocol. Modifications were made to the assay

protocol and sample plate setup accordingly. To test whether these modifications would mitigate the problems with closing, no changes were made in sample concentrations or run time. As a side experiment, watermelon juice was attempted as a sample preparation to see if the assay could be run without extractions. Observation of results still showed little decrease in the decay curve altitude and little difference between methods (see **Figure 59**). The watermelon juice decay curve did not decrease perceptibly.

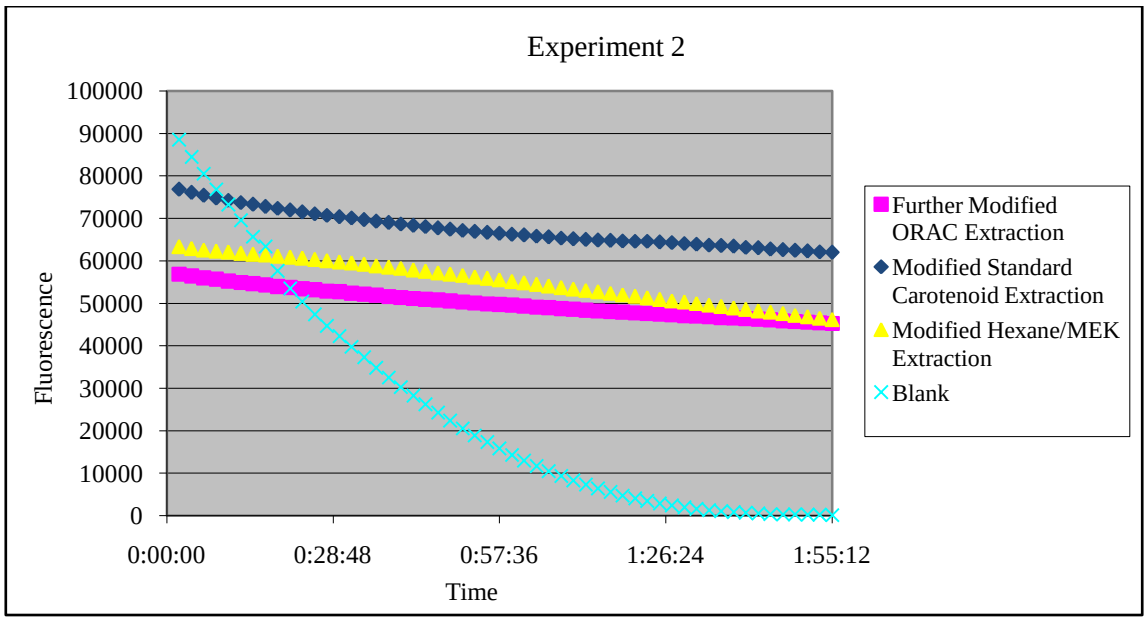

Figure 59. Typical decay curves for Experiment 2.

Modification of the organic phase's polarity for the above experiment was investigated since suspicion arose that there were antioxidants present which had borderline polarities. This suspicion was confirmed with later investigation of the hydrophobicity of the constituents. As seen in **Table 9**, the hydrophobicity index (*123*) places several of watermelon's most abundant amino acids near neutral polarity (near a

value of 0). If so, these may be partitioned into either phase and not in a consistent manner, thus leading to the observed variance in the results. This problem would be increasingly magnified for samples with more compounds that fall in this non-definitive range (ex. Colored watermelons with more xanthophylls versus red watermelon with mostly carotenes). For this reason hydrophilic and hydrophobic extractions could not feasibly be conducted separately for the same reasons that they were inconsistent together.

In the third round of experiments, the MEK method was abandoned due to consistently poor extraction qualities. This method was replaced with a second modification of the published methodology. The combination of organic solvents was maintained. Run time was extended from 2 to 3 hours. Results of the experiment showed that the samples came close to closing but their fluorescence curves were barely higher than the blank (see **Figure 60**). This was a poignant instance of getting inconsistent results, for the only appreciable change made to the protocol was extension of the run time and the changes to the extractions cannot explain this change. Since these results could not be explained, the experiment was repeated with a different additional change each time. The first follow-up experiment lowered the fluorescein to encourage closing and the second increased the dilution of the samples in pursuit of the same goal. Still inexplicably, the decay curves were close to closing but now fell below the blank's decay curve, an obvious problem insinuating that the samples had a lower antioxidant capacity than phosphate buffer alone. From these later experiments we may conclude that neither the sample nor the fluorescence concentrations affect the final

closing status. Rather, they influence the height of the curve earlier in the assay. Also, a consistently lower rate of variance for lipophilic samples than hydrophilic samples was also noted during the course of these experiments.

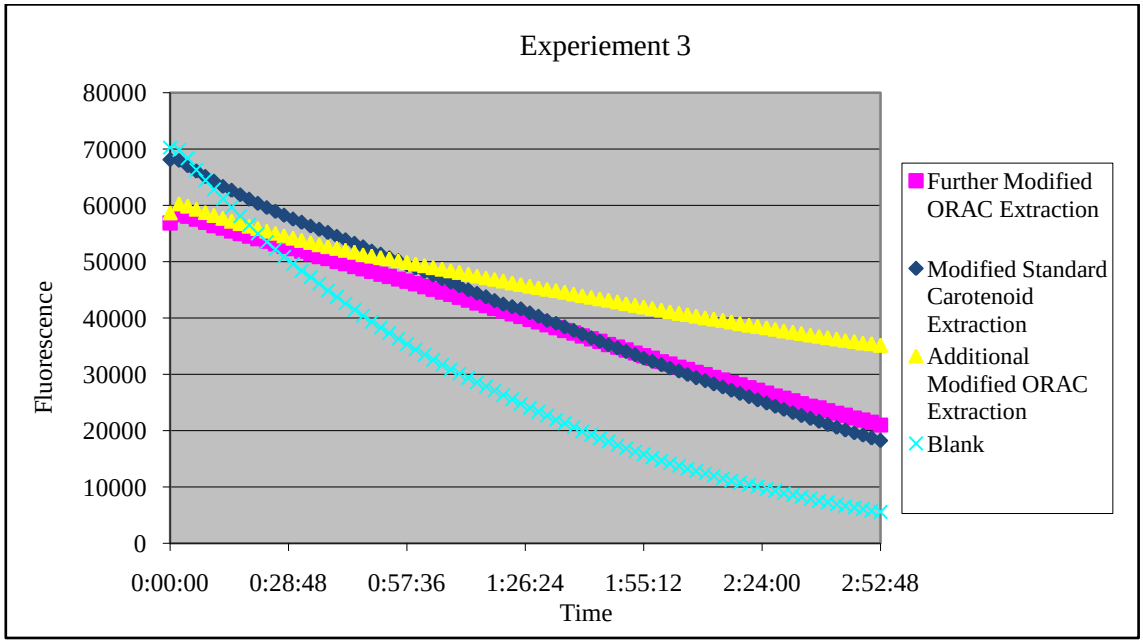

Figure 60. Typical decay curves for Experiment 3.

The use of dichloromethane in the previous two sets of experimental extractions seemed to weaken the strength of the extraction. The biphasic separation protocol therefore returned to use of only hexane as an organic solvent for further experiments. The previous experiment was repeated with this change, another biphasic separation method added which increased the amount of ethanol used to aid in greater tissue degradation. Sand was also added to one of the "published" methods (during vortexing, sand may aid in extraction) to even more closely mimic these protocols. Variance in the

hydrophilic preparations was reduced by premixing the samples with buffer, then aliquoting them, rather than adding buffer to all the samples after aljquoting as called for in the protocol. Blanks specific to each extraction method were also prepared to evaluate the influence of background solvents on closing ability. The hydrophilic solvent used in the published protocols was found to not close, thus leading to a relative closing of the sample. The lipophylic extraction of this method was still incomplete, however, while the biphasic lipophylic extraction reached 80-90% completion. Independently, these were positive outcomes to the experiments. The use of different extraction methods for the lipophilic and hydrophilic phases was not advisable for two reasons, however. First, as discussed previously, even if consistent results could be obtained for each phase, it could not be ensured that the near-neutral constituents would not be present in both phases. Second, these methods were being investigated for the express purpose of high-throughput screening and separate extractions were directly contrary to this end.

An additional difficulty arose during this set of extractions. Despite the use of the same concentration and preparation of the solubilizing agent (randomly methylated cyclodextrin, RMCD) for the lipophilic preparation, these samples became cloudy upon introduction of the RMCD. Since the measurements taken for this procedure are taken with a spectrophotometer, this precipitate could interfere with accurate readings. Again, the literature was consulted and we found an inconsistency in RMCD preparation between the published protocols and our in-house protocol. A difference in sample load volume was also noted and changes made. The prior parameter was investigated as to

various preparation methods and concentrations through a long series of experiments using carotenoid standards in hopes of stabilizing the results of the lipophilic assay. These experiments yielded neither consistent nor conclusive results. When this became apparent, it was concluded, in consultation with Dr. King, that efforts would be better focused in other directions.

CONCLUSION

Notwithstanding the apparent benefits of measuring total antioxidant capacity using the ORAC method, the various extractions, lipophilic encapsulation techniques, and modifications to the ORAC protocol attempted here were not successful in establishing a rigorous protocol for watermelon. The known deleterious effects of the parameters of the established protocols mentioned above on the major antioxidants of watermelon could not be neglected in our minds, despite these failed attempts to find a better protocol for food high in carotenoids.

Thaipong et al (*124*) reported in the same year that the present experiments were being conducted that ORAC values were not consistent between runs but ranked with the other antioxidant assays in similar ways for each experiment. This phenomenon may have played a role in the observations made in our experiments when reproducibility was tested. This variability is more problematic with our experiments, however, since a ranking of results was not the primary intent of this study. Rather, absolute values for

samples were needed for comparison. Under these conditions, only samples from the same run would be comparable.

Other antioxidant assays may have been employed to obtain the desired information, the most common of which and for which in-house capabilities were in place being FRAP, DPPH, and TEAC. However, these assays do not measure total antioxidant capacity, only hydrophilic antioxidant capacity (*125*), making the assays less useful when carotenoids, which are lipophilic, are a major antioxidant component. DPPH has also been specifically shown to be an inappropriate assay for radical scavenging ability of antioxidnats (*126*). It is our opinion that it was the abundance of antioxidants that fall near the point of neutral polarity that most greatly confounded our efforts.

CHAPTER IX

SUMMARY AND CONCLUSION

Plant natural products have been found to have profound health benefits when consumed as part of a balanced diet. In order to best utilize plant phytochemicals and nutrients, a clear and utilitarian understanding of the biosynthesis and storage within the plant as well as of the mechanisms by which we digestively access these phytochemicals must be developed first. The experiments presented here addressed each of these elements of the path from plant to consumer for the phytochemicals called carotenoids.

Carotenoid accumulation was observed in maturing watermelon fruit of four colors and three ploidy levels. The observation of these patterns revealed that the putative carotenoid biosynthesis regulation hypotheses for red tomato fruit have general applicability across all flesh colors when applied to each respective major carotenoid. By observation of both genotype and ploidy effects independently in red watermelon, it was noted that genotype may have a greater effect on carotenoid accumulation than does ploidy. A substantial environmental effect on carotenoid accumulation was also observed. By gaining a better understanding of biosynthetic pathway regulation of these phytochemicals, plant breeders will be more enabled to adjust content levels toward optimal consumer benefit.

Cellular and subcellular ultrastructure was observed in nine ripe, raw fruits and vegetables. Great variety was found in cell size, cell wall characteristics, and chromoplasts morphology. A coordinated investigation of carotenoid bioaccessibility

also revealed substantial differences between these foods. Microscopic analysis of the degree of degradation imparted by the artificial digestion was also used to assess sources of possible resistance to phytochemical bioaccessibility. Total bioaccessible carotenoids is a more accurate measure of benefit received than is simple total carotenoids. The data presented here will aid consumers in making dietary decisions based on this useful parameter.

The study of carotenoid development, storage, and bioaccessibility can serve as a model for the study of other important dietary plant phytochemical and nutritional products. This broadened approach encourages the appreciation of details of each step than may otherwise be overlooked under a narrower focus.

LITERATURE CITED

(1) Geyid, A.; Abebe, D.; Debella, A.; Makonnen, Z.; Aberra, F.; Teka, F.; Kebede, T.; Urga, K.; Yersaw, K.; Biza, T.; Mariam, B.; Guta, M. Screening of some medicinal plants of Ethiopia for their anti-microbial properties and chemical profiles. *J. Ethnopharmacology* **2005**, *97*, 421-427.

(2) Demmig-Adams, B.; Adams III, W. Food and photosynthesis: Antioxidants in photosynthesis and human nutrition. *Science* **2002**, *298*, 2149-2153.

(3) Miller, N.J.; Sampson, J.; Candeias, L.P.; Bramley, P.M.; Rice-Evans, C.A. Antioxidant activities of carotenes and xanthophylls. *Federation Eur. Biochem. Soc.* **1996**, *384*, 240-242.

(4) Giovannucci, E. Tomatoes, tomato-based products, lycopene, and cancer: Review of the epidemiologic literature. *J. Natl. Cancer Inst.* **1999**, *91*, 317-331.

(5) Agarwat, A.; Shen, H.; Agarwal, S.; Rao, A. Lycopene content of tomato products: Its stability, bioavailability and *in vivo* antioxidant properties. *J. Med. Food* **2001**, *4*, 9-15.

(6) Van Poppel, G. Epidemiological evidence for β-carotene in prevention of cancer and cardiovascular disease. *Eur. J. Clin. Nutr.* **1996**, *50*, S57-S61.

(7) Chew, B.; Park, J. Carotenoid action on the immune response. *J. Nutr.* **2004**, *134*, 257S-261S.

(8) Hammond, Jr., B.; Wooten, B.; Curran-Celentano, J. Carotenoids in the retina and lens: Possible acute and chronic effects on the human visual performance. *Arch. Biochem. Biophys.* **2001**, *385*, 41-46.

(9) Landrum, J.; Bone, R. Lutein, zeaxanthin, and the macular pigment. *Arch. Biochem. Biophys.* **2001**, *385*, 28-40.

(10) Nkondjock, A.; Ghadirian, P. Dietary carotenoids and risk of colon cancer: Case-control study. *Int. J. Cancer* **2004**, *110*, 110-116.

(11) Goodman, A.; Pardee, A. Evidence for defective retinoid transport and function in late onset Alzheimer's disease. *Proc. Nat. Acad. Sci.* **2003**, *100*, 2901-2905.

(12) Ikezoe, T.; Daar, E.; Hisatake, J.; Taguchi, H.; Koeffler, H. HIV-1 protease inhibitors decrease proliferation and induce differentiation of human mycelocytic leukemia cells. *Blood* **2000**, *96*, 3553-3559.

(13) Keaney, Jr., J.; Gaziano, J.; Xu, A.; Frei, B.; Curran-Celentano, J.; Shwaery, G.; Loscalzo, J.; Vita, J. Dietary antioxidants preserve endothelium-dependent vessel relaxation in cholesterol-fed rabbits. *Proc. Nat. Acad. Sci.* **1993**, *90*, 11880-11884.

(14) Prakash, P.; Russell, R.; Krinsky, N. *In vitro* inhibition of proliferation of estrogen-dependent and estrogen independent human breast cancer cells treated with carotenoids or retinoids. *J. Nutr.* **2001**, *131*, 1574-1580.

(15) Van Hooser, J.; Aleman, T.; He, Y.; Cideciyan, A.; Kuksa, V.; Pittler, S.; Stone, E.; Jacobson, S.; Palczewski, K. Rapid restoration of visual pigment and function with oral retinoid (B-carotene product) in a mouse model of childhood blindness. *Proc. Nat. Acad. Sci.* **2000**, *97*, 8623-8628

(16) Yang, Y.; Bailey, J.; Vacchio, M.; Yarchoan, R.; Ashwell, J. Retinoic acid inhibition of *ex vivo* human immunodeficiency virus-associated apoptosis of peripheral blood cells. *Proc. Nat. Acad. Sci.* **1995**, *92*, 3051-3055.

(17) Kim, Y.; DiSilvestro, R.; Clinton, S. Effects of lycopene-beadlet or tomato-powder feeding on carbon tetrachloride-induced hepatotoxicty in rats. *Phytomedicine* **2004**, *11*, 152-156.

(18) Boileau, T.; Liao, Z.; Kim, S.; Lemeshow, S.; Erdman, Jr., J.; Clinton, S. Prostate carcinogenesis in N-methyl-N-nitrosourea (NMU)-testosterone-treated rats fed tomato powder, lycopene, or energy-restricted diets. *J Natl Cancer Inst* **2003**, *95*, 1578–86.

(19) Limpens, J.; van Weerden, W.; Klaus, K.; Pallapies, D.; Obermu Ller-Jevic, U.; Schroder, F. Re: Prostate carcinogenesis in *N*-methyl-*N*-nitrosourea (NMU)-testosterone-treated rats fed tomato powder, lycopene, or energy-restricted diets. *J. Nat. Cancer Inst.* **2004**, *96*, 554.

(20) Shi,J.;Kakuda, Y.; Yeung, D. Antioxidative properties of lycopene and other carotenoids from tomatoes: Synergistic effects. *BioFactors* **2004**, *21*, 203–210.

(21) van Weerden, W.; de Ridder, C.; Bolder, C.; Wildhagen, M.; Kraemer, K.; Schroeder, F. Oral supplementation of vitamin E and lycopene reduces orthotopic growth of PC-346C prostate tumors. *J. Urol.* **2003**, *169*, 218.

(22) Redgwell, R.; Fischer, M. Fruit texture, cell wall metabolism and consumer perceptions. In *Fruit quality and its biological basis*, 1st ed.; Knee, M., Eds.; CRC Press: Boca Raton, FL, 2002; pp. 46-48.

(23) van het Hof, K.; West, C.; Weststrate, J.; Hautvast, J. Dietary factors that affect the bioavailability of carotenoids. *J. Nutr.* **2000**, *130*, 503–506.

(24) Faulks, R.; Southon, S. Challenges to understanding and measuring carotenoid bioavailability. *Biochimica et Biophysica Acta* **2005**, *1740*, 95– 100.

(25) West, C.; Castenmiller, J. Quantification of the "SLAMENGHI" factors for carotenoid bioavailability and bioconversion. *Int. J. Vit. Nutr.* **1998**, *68*, 371-377.

(26) van het Hof, K.; Brouwer, I.; West, C.; Haddeman, E.; Steegers-Theunissen, R.; van Dusseldorp, M.; Weststrate, J.; Eskes, T.; Hautvast, J. Bioavailability of lutein from vegetables 5 times higher than that of β-carotene. *Amer. J. Clin. Nutr.* **1999**, *70*, 261-268.

(27) de Pee, S.; West, C.; Permaesih, D.; Martuti, S.; Muhilal, J.; Hautvast, A. Orange fruit is more effective than are dark-green, leafy vegetables in increasing serum concentrations of retinol and β-carotene in schoolchildren in Indonesia. *Am. J. Clin. Nutr.* **1998**, *68*, 1058–67.

(28) Tyssandier, V.; Lyan, B.; Borel, P. Main factors governing the transfer of carotenoids from emulsion lipid droplets to micelles. *Biochimica et Biophysica Acta* **2001**, *1533*, 285-292.

(29) Yeum, K.; Russell, R. Carotenoid bioavailability and bioconversion. *Ann. Rev. Nutr.* **2002**, *22*, 483-504.

(30) van het Hof, K.; Brouwer, I.; West, C.; Haddeman, E.; Steegers-Theunissen, R.; van Dusseldorp, M.; Weststrate, J.; Eskes, T.; Hautvast, J. Bioavailability of lutein from vegetables 5 times higher than that of β-carotene. *Amer. J. Clin. Nutr.* **1999**, *70*, 261-268.

(31) Hoffmann, J.; Linseisen, J.; Riedl, J.; Wolfram, G. Dietary fiber reduces the antioxidative effect of a carotenoid and a-tocopherol mixture on LDL oxidation *ex vivo* in humans. *Eur. J. Nutr.* **1999**, *38*, 278–285.

(32) Castenmiller, J.; West, C.; Linssen, J.; van het Hof, K.; Voragen, A. The food matrix of spinach is a limiting factor in determining the bioavailability of β-carotene and to a lesser extent of lutein in humans. *J. Nutr.* **1999**, *129*, 349–355.

(33) Riedl, J.; Linseisen, J.; Hoffmann, J.; Wolfram, J. Some dietary fibers reduce the absorption of carotenoids in women. *J. Nutr.* **1999**, *129*, 2170–2176.

(34) Schneeman, B. Macronutrient absorption. In *Dietary fiber. Chemistry, physiology, and health effects*, 1st ed.; Kritchevsky, D.; Bobfield, C.; Anderson, J., Eds.; Plenum Press: New York, 1990, pp. 157–166.

(35) Phillips, D. The effect of guar gum in solution on diffusion of cholesterol mixed micelles. *J. Sci. Food Agr.* **1986**, *37*, 548–552.

(36) Strzaka, K.; Kostecka-Guga, A.; Latowski, D. Carotenoids and environmental stress in plants: significance of carotenoid-mediated modulation of membrane physical properties. *Russian J. Plant Physiol.* **2003**, *50*, 168–172.

(37) Chen, H.; Klein, A.; Xiang, M.; Backhaus, R.; Kuntz, M. Drought- and wound-induced expression in leaves of a gene encoding a chromoplast carotenoid-associated protein. *Plant J.* **1998**, *14*, 317-326.

(38) Corona, V.; Aracci, B.; Kosturkova, G.; Bartley, G.; Pitto, L.; Giorgetti, L.; Scolnik, P.; Giuliano, G. Regulation of a carotenoid biosynthesis gene promoter during plant development. *Plant J.* **1996**, *9*, 505-512.

(39) Ronen, G.; Cohen, M.; Zamir, D.; Hirschberg, J. Regulation of carotenoid biosynthesis during tomato fruit development: expression of the gene for lycopene epsilon cyclase is down regulated during ripening and is elevated in the mutant delta. *Plant J.* **1999**, *17*, 341-351.

(40) Deruere, J.; Romer, S.; d'Harlingue, A.; Backhaus, R.; Kuntz, M., Camara, B. Fibril assembly and carotenoid over-accumulation in chromoplasts: A model for supramolecular lipoprotein structures. *Plant Cell* **1994**, *6*, 119-133.

(41) Al-Babili, S.; von Lintig, J.; Haubruck, H.; Beyer, P. A novel, soluble form of phytoene desaturase in *Narcissus pseudonarcissus* chromoplasts is Hsp 70-complexed and competent for flavinylation, membrane association and enzymatic activation. *Plant J.* **1996**, *9*, 601-612.

(42) Bramley, P. Inhibition of carotenoid biosynthesis. In *Carotenoids in photosynthesis*, 1st ed.; Young, A.; Britton, G., Eds.; Chapman and Hall: London, 1993; pp. 127-159.

(43) Romer, S.; Fraser, P.; Kiano, J.; Shipton, C.; Misawa, N.; Schuch, W.; Bramley, P. Elevation of the provitamin A content of transgenic tomato plants. *Nature Biotech.* **2000**, *18*, 666-669.

(44) Giovannoni, J. Molecular biology of fruit maturation and ripening. *Annu. Rev. Plant Physiol. Plant Mol. Biol.* **2001**, *52*, 725–749.

(45) Khudairi, K. The ripening of tomatoes. *Am. Sci.* **1972**, *60*, 696-707.

(46) Poole, C. Genetics of cultivated cucurbits. *J. Hered.* **1944**, *35*, 122–128.

(47) Henderson, W. Inheritance of orange flesh color in watermelon. *Cucur. Genet. Coop. Rpt.* **1989**, *12*, 59–63.

(48) Bang, H.; Kim, S.; Leskovar, D.; King, S. Development of a codominant CAPS marker for allelic selection between canary yellow and red watermelon based on SNP in lycopene β-cyclase (*LCYB*) gene. *Molec. Breed.* **2007**, *20*, 63-72.

(49) King, S. Putative carotenoid biosynthetic pathway in higher plants. *Unpublished* **2004**, Texas A&M University, College Station.

(50) Fish, W.; Perkins-Veazie, P.; Collins, J. A quantitative assay for lycopene that utilizes reduced volumes of organic solvents. *J. Food Compos. Anal.* **2002**, *15*, 309-317.

(51) Britton, G. Worked examples of isolation and analysis. Example 1: Higher plants. In: *Carotenoids, Volume 1A: Isolation and analysis*, 1st ed.; Britton, G.; Liaaen-Jensen, S.; Pfander, H., Eds.; Birkhäuser: Basel, Switzerland, 1995; 1A, pp. 201–214.

(52) Tadmor, Y.; King, S.; Levi, A.; Davis, A.; Meir, A.; Wasserman, B.; Hirschberg, J.; Lewinsohn, E. Comparative fruit colouration in watermelon and tomato. *Food Res. Intl.* **2005**, *38*,837–41.

(53) Tadmor, Y.; Katzir, N.; King, S.; Levi, A.; Davis, A.; Hirschberg, J. Fruit coloration in watermelon: lessons from the tomato. In *Eucarpia '04, progress in cucurbit genetics and breeding*, 1st ed.; Lebeda, A.; Paris,H., Eds.; Palack´y Univ. in Olomouc: Olomouc, Czech Republic, 2004; pp. 181–185.

(54) Bang, H. Environmental and genetic strategies to improve carotenoids and quality in watermelon. Ph.D. Dissertation. 2005, Texas A&M University, College Station.

(55) Perkins-Veazie, P.; Collins, J.; Pair, S.; Roberts, W. Lycopene content differs among red-fleshed watermelon cultivars. *J. Sci. Food Agric.* **2001**, *81*, 983-987.

(56) Udall, J.; Wendel, J. Polyploidy and crop improvement. *Crop Sci.* **2006**, *46*, S3-14.

(57) Maynard, D.; Hochmuth, G. *Knott's handbook for vegetable growers*, 4th ed.; Wiley: New York, 1997.

(58) Rich, G.; Bailey, A.; Faulks, R.; Parker, M.; Wickham, M.; Fillery-Travis, A. Solubilization of carotenoids from carrot juice and spinach in lipid phases: I. Modeling the gastric lumen. *Lipids* **2003**, *38*, 933-945.

(59) Castenmiller, J.; West, C. Bioavailability and bioconversion of carotenoids. *Annu. Rev. Nutr.* **1998**, *18*, 19–38.

(60) Camara, B.; Hugueney, P.; Bouvier, F.; Kuntz, M.; Moneger, R. Biochemistry and molecular biology of chromoplast development. *Intern. Rev. Cytol.* **1995**, *163*, 175-247.

(61) Hansmann, P.; Sitte, P. Composition and molecular structure of chromoplast globules in *Viola tricolor*. *Plant Cell Rep.* **1982**, *1*, 111-114.

(62) Steffen, K.; Walter, F. Die Chromoplasten von *Solanum capsicastrum* L. und ihre Genese. *Planta* **1958**, *50*, 640-670.

(63) Simpson, D.; Lee, T. Fine structure and formation of fibrils of *Capsicum annum* L. chromoplasts. *Z Pflanzenphysiol.* **1976**, *77*, 127-138.

(64) Knoth, R.; Hansmann, P.; Sitte, P. Chromoplast of *Palisota barteri*, and the molecular structure of chromoplast tubules. *Planta* **1986**, *168*, 167-174.

(65) Walles, B. Chromoplast development in a carotenoid mutant of maize. *Protoplasma* **1971**, *73*, 159-175.

(66) Harris, W.; Spurr, A. Chromoplasts of tomato fruits. II. The red tomato. *Amer. J. Bot.* **1969**, *56*, 380-389.

(67) Harris, W.; Spurr, A. Chromoplasts of tomato fruits. I. Ultrastructure of low-pigment and high-beta mutants. Carotene analyses. *Amer. J. Bot.* **1969**, *56*, 369-379.

(68) Wrischer, M.; Ljubesic, N. Plastid differentiation in *Claceolaria* petals. *Acta. Bot. Croat.* **1984**, *43*, 19-24.

(69) Paolillo, Jr., D.; Garvin, D.; Parthasarathy, M. The chromoplasts of *Or* mutants of cauliflower (*Brassica oleracea* L. var. *botrytis*). *Protoplasma* **2004**, *224*, 245–253.

(70) Shi, J.; Maguer, M. Lycopene in tomatoes: chemical and physical properties affected by food processing. *Crit. Rev. Biotechnol.* **2000**, *42*, 293-334.

(71) Faisant, N.; Gallant, D.; Bouchet, B.; Champ, M. Banana starch breakdown in the human small-intestine studied by electron microscopy. *Eur. J. Clin. Nut.* **1995**, *49*, 98-104.

(72) Stahl, W.; Sies, H. Uptake of lycopene and its geometrical isomers is greater from heat-processed than from unprocessed tomato juice in humans. *J. Nutr.* **1992**, *122*, 2161-2166.

(73) Böhm, V.; Bitsch, R. Intestinal absorption of lycopene from different matrices and interactions to other carotenoids, the lipid status, and the antioxidant capacity of human plasma. *Eur. J. Nutr.* **1999**, *38*, 118-125.

(74) Torronen, R.; Lehmusaho, M.; Hakkinen, S.; Hanninen, O.; Mykkanen. Serum β-carotene response to supplementation with raw carrots, carrot juice of purified β-carotene in healthy non-smoking women. *Nutr. Res.* **1996**, *16*, 565-575.

(75) Pitt, R. Models for the rheology and statistical strength of uniformly stressed vegetative tissue. *Trans. ASAE* **1982**, *25*, 1776–1784.

(76) Pitt, R.; Chen, H. Time-dependent aspects of the strength and rheology of vegetative tissue. *Trans. ASAE* **1983**, *26*, 1275–1280.

(77) Lin, T.; Pitt, R. Rheology of apple and potato tissue as affected by cell turgor pressure. *J. Texture Studies* **1986**, *17*, 291–313.

(78) Hepworth, D.; Bruce, D. Measuring the deformation of cells within a piece of compressed potato tuber tissue. *Ann. Bot.* **2000**, *86*, 287– 292.

(79) Zdunek, A.; Umeda, M. Influence of cell size and cell wall volume fraction on failure properties of potato and carrot tissue. *J. Texture Studies* **2005**, *36*, 24-43.

(80) Carpita, N.; Gibeaut, D. Structural models of primary cell walls in flowering plants: Consistency of molecular structure with the physical properties of the walls during growth. *Plant J.* **1993**, *3*, 1–30.

(81) Iwai, H.; Masaoka, N.; Ishii, T.; Satoh, S. A pectin glucuronyltransferase gene is essential for intercellular attachment in the plant meristem. *Proc. Natl Acad. Sci. USA* **2002**, *99*, 16319–16324.

(82) Marlett, J. Database and quick methods of assesing typical dietary fiber intakes using data for 228 commonly consumed foods. *J. Am. Diet Assoc.* **1997**, *97*, 1148-1151.

(83) Chitchumroonchokchai,C.; Schwartz,S.; Failla, M. Assessment of lutein bioavailability from meals and a supplement using smulated digestion and caco-2 human intestinal cells. *J. Nutr.* **2004**, *134*, 2280–2286.

(84) Rich, G.; Fillery-Travis, A.; Parker, M. Low pH enhances the transfer of carotene from carrot juice to olive oil. *Lipids* **1998**, *33*, 985-992.

(85) Reynolds, E. The use of lead citrate at high pH as an electron-opaque stain in electron microscopy. *J. Cell Biol.* **1963**, *17*, 208-212.

(86) Ledingham, J.; Simpson, P. The use of *p*-phenylenediaminediamine in the block to enhance osmium staining for electron microscopy. *Stain Tech.* **1972**, *47*, 239.

(87) Caiola, M.; Canini, A. Ultrastructure of chromoplasts and other plastids in *Crocus sativus* L. (Iridaceae). *Plant Biosystems* **2004**, *138*, 43-52.

(88) Grote, M.; Fromme, H. Electron microscopic studies in cultivated plants. *Z. Lebensm. Uters.-Forsch.* **1978**, *166*, 74-79.

(89) United States Department of Agriculture national nutrient database for standard reference, Release 18 (2005) (http://www.nal.usda.gov/fnic/foodcomp/Data/)

(90) Shomer, I. Mechanism of structural freezing injury in citrus fruit segments. *Bot. Gaz.* **1986**, *147*, 55-64.

(91) Mitcham, E.; McDonald, R. Cell wall modification during ripening of 'Keitt' and 'Tommy Atkins' mango fruit. *J. Amer. Soc. Hort. Sci.* **1992**, *117*, 919-924.

(92) Va´squez-Caicedo, A.; Sruamsiri, P.; Carle, R.; Neidhart, S. Accumulation of all-*trans*-*â*-carotene and its 9-*cis* and 13-*cis* stereoisomers during postharvest ripening of nine Thai mango cultivars. *J. Agric. Food Chem.* **2005**, *53*, 4827-4835.

(93) Va´squez-Caicedo, A.; Heller, A.; Neidhart, S.; Carle, R. Chromoplast morphology and *α*-carotene accumulation during postharvest ripening of mango Cv. 'Tommy Atkins'. *J. Agric. Food Chem.* 2006, *54*, 5769-5776.

(94) Wrischer, M.; Prebeg, T.; Magnus, V.; Ljubesic, N. Crystals and fibrils in chromoplast plastoglobules of *Solanum capsicastrum* fruit. *Acta Bot. Croat.* **2007**, *66*, 81-87.

(95) Bonora, A.; Pancaldi, S.; Gualandri, R.; Fasulo, M. Carotenoid and ultrastructure variations in plastids of *Arum italicum* Miller fruit during maturation and ripening. *J. Exper. Biol.* **2000**, *51*, 873-884.

(96) Badenhuizen, N. *The biogenesis of starch granules in higher plants.* Appelton-Century-Crofts: New York, 1969.

(97) Ben-Shaul, Y.; Naftali, Y. The development and ultrasturcture of lycopene bodies in chromoplasts of *Lycopersicum esculentum*. *Protoplasma* **1969**, *67*, 333-344.

(98) Gartner, C.; Stahl, W.; Sies, H. Lycopene is more bioavailable from tomato paste than from fresh tomatoes. *Amer. J. Clin. Nutr.* **1997**, *66*, 116-122.

(99) Bangalore, D.; McGlynn, W.; Scott, D. Effects of fruit maturity on watermelon ultrastructure and intracellular lycopene distribution. *J. Food Sci.* **2008**, *73*, S222-S228.

(100) Perkins Veazie, P.; Collins, J.; Edwards, A.; Wiley, E.; Clevidence, B. Watermelon: Rich in the antioxidant lycopene. *Acta Horticulturae* **2003**, *628*, 663-668.

(101) United States Department of Agriculture table of nutrient retention factors, Release 5 (2003) (http://www.nal.usda.gov/fnic/foodcomp/Data/)

(102) Failla, M.; Chitchumroonchokchai. C. *In vitro* models as tools for screening the relative bioavailabilities of provitamin A carotenoids in foods. *Harvest Plus Technical Monograph Series*, **2005**, *3*, 1-32.

(103) Mathews-Roth, M.; Pathak, M. Phytoene as a protective agent agains sunburn (>280 nm) radiation in guinea pigs. *Photochem. Photobiol.* **1975**, *21*, 261-263.

(104) Nishino, H.; Murakoshi, M.; Takemura, T.; Kuchide, M.; Kanazawa, M.; Mou, X.; Wada, S.; Masuda, M.; Ohsaka, Y.; Yogosawa, S.; Satomi, Y.; Jinno, K. Carotenoids in cancer chemoprevention. *Cancer Metastasis Rev.* **2002**, *21*, 257-264.

(105) Aust, O.; Stahl, W.; Sies, H.; Tronnier, H.; Heinrich, U. Supplementation with tomato-based products increases lycopene, phytofluene, and phytoene levels in human serum and protects against UV-light induced erythema. *Internat. J. Vit. Nutr. Res.* **2005**, *75*, 54-60.

(106) Garrett, D.; Failla, M.; Sarama, R. Development of an *in vitro* digestion method to assess carotenoid bioavailability from meals. *J. Agric. Food Chem.* **1999**, *47*, 4301-4309.

(107) United States Department of Agriculture. MyPyramid.gov dietary guidelines (2005) (http://www.mypyramid.gov/index.html)

(108) Wright, A.; Pietrangelo, C.; MacNaughton, A. Influence of simulated upper intestinal parameters on the efficiency of beta carotene micellarisation using an *in vitro* model of digestion. *Food Chem.* **2008**, *107*, 1253–1260.

(109) Donaldson, M. Nutrition and cancer: A review of the evidence for and anti-cancer diet. *Nutr. J.* **2004**, *3*, 19-40.

(110) DiMascio, P.; Kalser, S.; Sies, H. Lycopene as the most efficient biological carotenoid singlet oxygen quencher. *Arch. Biochem. Biophys.* **1989**, *274*, 532-538.

(111) Miller, N.; Sampson, J.; Candeias, L.; Bramley, P.; Rice-Evans, C. Antioxidant activities of carotenes and xanthophylls. *FEBS Letters* **1996**, *384*, 240-242.

(112) van Weerden, W.; de Ridder, C.; Bolder, C.; Wildhagen, M.; Kraemer, K.; Schroeder, F. Oral supplementation of vitamin E and lycopene reduces orthotopic growth of PC-346C prostate tumors (abst.). *J. Urol.* **2003**, *169*, 218.

(113) Hennekens, C.; Buring, J.;Manson, J.; Stampfer, M.; Rosner, B.; Cook, N.; Belanger, C.; La Motte, F.; Gaziano, J.; Ridker, P.; Willet, W.; Peto, R. Lack of effect of long term supplementation with b-carotene on the incidence of malignant neoplasm and cardiovascular disease. *New. Engl. J. Med.* **1996**, *334*, 1145–1149.

(114) Pryor, W.; Stahl, W.; Rock, C. Beta-carotene: from biochemistry to clinical trials. *Nutr. Rev.* **2000**, *58*, 39–53.

(115) Wada, M. Uber Citrullin, eine neue AminosJure im Pressaft der Wassermelone, *Citrullus vulgaris* Schrad. *Biochem Z.* **1930**, *224*, 420-429.

(116) Duke, J. *Handbook of phytochemical constituents of GRAS herbs and other economic plants.* CRC Press: Boca Raton, FL, 1992.

(117) Murcia, M.; Jimenez, A.; Martinez-Tome, M. Evaluation of the antioxidant properties of Mediterranean and tropical fruits compared with common food additives. *J. Food Prot.* **2001**, *64*, 2037-2046.

(118) Djuric, Z.; Powell, L. Antioxidant capacity of lycopene-containing foods. *Int. J. Food. Sci. Nutr.* **2001**, *52*, 143-149.

(119) Wu, X.; Beecher, G.; Holden, J.; Haytowitz, D.; Gebhardt, S.; Prior, R. Lipophilic and hydrophilic antioxidant capacities of common foods in the United States. *J. Agric. Food Chem.* **2004**, *52*, 4026-4037.

(120) Rimando, A.; Perkins-Veazie, P. Determination of citrulline in watermelon rind. *J. Chromatogr. A.* **2005**, *1078*, 196-200.

(121) Bohm, V.; Puspitasari-Nienaber, N.; Ferruzzi, M.; Schwartz, S. Trolox equivalent antioxidant capacity of different geometrical isomers of α-carotene, *β*-carotene, lycopene, and zeaxanthin. *J. Agric. Food Chem.* **2002**, *50*, 221-226.

(122) Sharma,S.; Le Maguer, M. Kinetics of lycopene degradation in tomato pulp solids under different processing and storage conditions. *Food Research Int.* **1996**, *29*, 309-315.

(123) Kyte, J.; Doolittle, R. A simple method for displaying the hydropathic character of a protein. *J. Mol. Biol.* **1982**, *157*, 105–32.

(124) Thaipong, K.; Boonprakob, U.; Crosby, K., Cisneros-Zevallos, L.; Byrne, D. Comparison of ABTS, DPPH, FRAP, and ORAC assays for estimating antioxidant activity from guava fruit extracts. *J. Food Comp. Anal.* **2006**, *19*, 669-675.

(125) Aruoma, O. Methodological considerations for characterizing potential antioxidant actions of bioactive components in plant foods. *Mutation Res.* **2003**, *523–524*, 9–20.

(126) Huang, D.; Ou, B.; Prior, R. The chemistry behind antioxidant capacity assays. *J. Agric. Food Chem.* **2005**, *53*, 1841-1856.

APPENDIX A

STATISTICAL ANALYSES FOR CHAPTER II

Page

Page

Page

Page

APPENDIX A-1

PHYTOENE DESCRIPTIVE STATISTICS, YEAR 1. MEANS MEASURED IN AUC. LETTERS REPRESENT TUKEY'S HSD WITHIN EACH VARIETY.

† STATISTICAL SIGNIFICANCE OF CAROTENOID LEVEL DIFFERENCES BETWEEN DPP.

‡ STATISTICAL SIGNIFICANCE OF DIFFERENCE BETWEEN TRIPLOID AND DIPLOID VARIETY.

	Dixie Queen		Summer Sweet			Orange Flesh Tender Sweet		Orange Sunshine			Yellow Flesh Black Diamond		Early Moonbeam		Amarillo		
DPP	mean	SD	mean	SD	Sig.‡	mean	SD	mean	SD	Sig.‡	mean	SD	mean	SD	mean	SD	Sig.‡
10	.	.	0a	.	.	.	.	.	.	.	.	.	0a	.	0a	.	.
20	0a	.	38940a	36153	0.136	0a	.	123577a	123067	0.157	0a	.	0a	.	0a	.	.
40	362006b	43662	138993b	7615	0.001**	881650b	543375	1908531b	327773	0.049*	369265ab	105909	13678a	14234	52078a	45111	0.232
55	141615c	11797	236331c	8103	0.000**	1076186b	116998	2383121b	217758	0.001**	652993b	272380	85432a	74197	67822a	34189	0.728
Sig.†	0.000**		0.000**			.014*		0.000**			.018*		0.068		.037*		

APPENDIX A-2

ζ-CAROTENE DESCRIPTIVE STATISTICS, YEAR 1. MEANS MEASURED IN AUC. LETTERS REPRESENT TUKEY'S HSD WITHIN EACH VARIETY.

† STATISTICAL SIGNIFICANCE OF CAROTENOID LEVEL DIFFERENCES BETWEEN DPP.

‡ STATISTICAL SIGNIFICANCE OF DIFFERENCE BETWEEN TRIPLOID AND DIPLOID VARIETY.

	Dixie Queen		Summer Sweet			Orange Flesh Tender Sweet		Orange Sunshine			Yellow Flesh Black Diamond		Early Moonbeam		Amarillo		
DPP	mean	SD	mean	SD	Sig.‡	mean	SD	mean	SD	Sig.‡	mean	SD	mean	SD	mean	SD	Sig.‡
10	.	.	0a	.	.	.	.	.	.	.	.	.	0a	.	0a	.	.
20	0a	.	0a	.	.	0a	.	185441a	169464	0.131	10111a	17513	0a	.	0a	.	.
40	206972b	15432	57622b	15531	0.000**	872046b	499730	735506b	85436	0.665	439310b	164423	32923ab	30971	67006b	33115	0.263
55	104988c	30576	120634c	17942	0.487	775730b	146887	1336400c	65888	0.004*	520121b	124894	207245b	142346	86477b	27375	0.222
Sig.†	0.000**		0.000**			.023*		0.000**			.005**		.023*		.002**		

APPENDIX A-3

PRONEUROSPORENE DESCRIPTIVE STATISTICS, YEAR 1. MEANS MEASURED IN AUC. LETTERS REPRESENT TUKEY'S HSD WITHIN EACH VARIETY. † STATISTICAL SIGNIFICANCE OF CAROTENOID LEVEL DIFFERENCES BETWEEN DPP.

‡ STATISTICAL SIGNIFICANCE OF DIFFERENCE BETWEEN TRIPLOID AND DIPLOID VARIETY.

	Dixie Queen		Summer Sweet			Orange Flesh Tender Sweet		Orange Sunshine			Yellow Flesh Black Diamond		Early Moonbeam		Amarillo		
DPP	mean	SD	mean	SD	Sig.‡	mean	SD	mean	SD	Sig.‡	mean	SD	mean	SD	mean	SD	Sig.‡
10	.	.	.	.	.	.	.	.	.	.	.	.	.	.	.	.	.
20	.	.	.	.	.	0a	.	71555a	72234	0.161	0a	.	.	.	.	.	.
40	.	.	.	.	.	141084b	51736	174796a	18489	0.348	154767b	41841	.	.	.	.	.
55	.	.	.	.	.	130494b	9611	307564b	33743	0.001**	110571b	46226	.	.	.	.	.
Sig.†	.		.			.002**		.003**			.009**		.		.		

APPENDIX A-4

PROLYCOPENE DESCRIPTIVE STATISTICS, YEAR 1. MEANS MEASURED IN AUC. LETTERS REPRESENT TUKEY'S HSD WITHIN EACH VARIETY.

† STATISTICAL SIGNIFICANCE OF CAROTENOID LEVEL DIFFERENCES BETWEEN DPP.

‡ STATISTICAL SIGNIFICANCE OF DIFFERENCE BETWEEN TRIPLOID AND DIPLOID VARIETY.

	Dixie Queen		Summer Sweet			Orange Flesh Tender Sweet		Orange Sunshine			Yellow Flesh Black Diamond		Early Moonbeam		Amarillo		
DPP	mean	SD	mean	SD	Sig.‡	mean	SD	mean	SD	Sig.‡	mean	SD	mean	SD	mean	SD	Sig.‡
10	.	.	.	.	.	.	.	.	.	.	.	.	.	.	.	.	.
20	.	.	.	.	.	0a	.	585003a	817436	0.283	0a	.	.	.	.	.	.
40	.	.	.	.	.	1009399a	744729	2439736b	485204	0.049*	1028031b	250511	.	.	.	.	.
55	.	.	.	.	.	297395a	116352	3056251b	51559	0.000**	402373c	115753	.	.	.	.	.
Sig.†	.		.			0.071		.004**			.001**		.		.		

APPENDIX A-5

LYCOPENE DESCRIPTIVE STATISTICS, YEAR 1. MEANS MEASURED IN AUC. LETTERS REPRESENT TUKEY'S HSD WITHIN EACH VARIETY.

† STATISTICAL SIGNIFICANCE OF CAROTENOID LEVEL DIFFERENCES BETWEEN DPP.

‡ STATISTICAL SIGNIFICANCE OF DIFFERENCE BETWEEN TRIPLOID AND DIPLOID VARIETY.

	Dixie Queen		Summer Sweet			Orange Flesh Tender Sweet		Orange Sunshine			Yellow Flesh Black Diamond		Early Moonbeam		Amarillo		
DPP	mean	SD	mean	SD	Sig.‡	mean	SD	mean	SD	Sig.‡	mean	SD	mean	SD	mean	SD	Sig.‡
10	.	.	0a	.	.	.	.	.	.	.	.	.	0a	.	0a	.	.
20	118646a	112640	1143070a	284070	0.004**	0a	.	174092a	139974	0.098	0a	.	0a	.	0a	.	.
40	6702163b	3204232	4379475b	906026	0.294	811979b	158247	583580a	117557	0.115	747719a	171693	0a	.	0a	.	.
55	2559133ab	1570981	3600104b	588340	0.343	1559618c	216797	1738835b	433117	0.556	780915a	483188	41976a	72705	7492a	12977	0.464
Sig.†	0.210		.000**			.000**		.001**			0.053		0.441		0.441		

APPENDIX A-6

β-CAROTENE DESCRIPTIVE STATISTICS, YEAR 1. MEANS MEASURED IN AUC. LETTERS REPRESENT TUKEY'S HSD WITHIN EACH VARIETY.

† STATISTICAL SIGNIFICANCE OF CAROTENOID LEVEL DIFFERENCES BETWEEN DPP.

‡ STATISTICAL SIGNIFICANCE OF DIFFERENCE BETWEEN TRIPLOID AND DIPLOID VARIETY.

	Dixie Queen		Summer Sweet			Orange Flesh Tender Sweet		Orange Sunshine			Yellow Flesh Black Diamond		Early Moonbeam		Amarillo		
DPP	mean	SD	mean	SD	Sig.‡	mean	SD	mean	SD	Sig.‡	mean	SD	mean	SD	mean	SD	Sig.‡
10	.	.	0a	.	.	.	.	.	.	.	.	.	0a	.	0a	.	.
20	0a	.	0a	.	.	0a	.	48464a	45547	0.139	0a	.	0a	.	0a	.	.
40	438378b	78665	190594b	6658	0.006**	451921b	97442	415975a	239230	0.821	190024ab	70916	49943ab	6002	105474ab	45938	0.106
55	506379b	62103	549408c	47879	0.396	846083c	127963	923184b	183635	0.583	517049b	216776	49943b	51998	183058b	83603	0.258
Sig.†	0.000**		0.000**			0.000**		.003**			.017*		.003**		.004**		

APPENDIX A-7

LUTEIN DESCRIPTIVE STATISTICS, YEAR 1. MEANS MEASURED IN AUC. LETTERS REPRESENT TUKEY'S HSD WITHIN EACH VARIETY.

† STATISTICAL SIGNIFICANCE OF CAROTENOID LEVEL DIFFERENCES BETWEEN DPP.

‡ STATISTICAL SIGNIFICANCE OF DIFFERENCE BETWEEN TRIPLOID AND DIPLOID VARIETY.

	Dixie Queen		Summer Sweet			Orange Flesh Tender Sweet		Orange Sunshine			Yellow Flesh Black Diamond		Early Moonbeam		Amarillo		
DPP	mean	SD	mean	SD	Sig.‡	mean	SD	mean	SD	Sig.‡	mean	SD	mean	SD	mean	SD	Sig.‡
10	.	.	58274a	33688	.	.	.	.	.	.	.	.	23330a	6742	32070a	8248	0.228
20	29797a	7213	28035ab	17307	0.879	40372a	14924	15291a	20822	0.165	41954a	22285	19043a	10026	22280a	5058	0.644
40	0b	.	0b	.	.	0b	.	0a	.	.	15950a	22557	15164a	13436	19339a	17259	0.758
55	0b	.	0b	.	.	0b	.	0a	.	.	0a	.	50254a	23943	16311a	16623	0.114
Sig.†	0.000**		0.160			.002**		0.274			0.077		0.075		0.510		

APPENDIX A-8

VIOLAXANTHIN DESCRIPTIVE STATISTICS, YEAR 1. MEANS MEASURED IN AUC. LETTERS REPRESENT TUKEY'S HSD WITHIN EACH VARIETY.

† STATISTICAL SIGNIFICANCE OF CAROTENOID LEVEL DIFFERENCES BETWEEN DPP.

‡ STATISTICAL SIGNIFICANCE OF DIFFERENCE BETWEEN TRIPLOID AND DIPLOID VARIETY.

	Dixie Queen		Summer Sweet			Orange Flesh Tender Sweet		Orange Sunshine			Yellow Flesh Black Diamond		Early Moonbeam		Amarillo		
DPP	mean	SD	mean	SD	Sig.‡	mean	SD	mean	SD	Sig.‡	mean	SD	mean	SD	mean	SD	Sig.‡
10	.	.	17802a	5390	.	.	.	.	.	.	.	.	33736a	11127	27540a	2673	0.401
20	43124a	4172	62929b	8863	0.025*	45682a	15106	24696a	27636	0.313	40378a	10180	134196ab	23199	235391b	25288	0.007**
40	0b	.	0c	.	.	11995b	11530	23185a	4289	0.190	13359b	2271	243619b	98861	260462b	114784	0.857
55	0b	.	0c	.	.	6477b	11218	40059a	8841	0.015*	0b	.	70882a	55526	201364b	49179	0.038*
Sig.†	0.000**		0.000**			0.019*		0.451			0.002**		0.010**		0.008**		

APPENDIX A-9

PHYTOENE DESCRIPTIVE STATISTICS, YEAR 2. MEANS MEASURED IN µg/g. LETTERS REPRESENT TUKEY'S HSD WITHIN EACH VARIETY.

† STATISTICAL SIGNIFICANCE OF CAROTENOID LEVEL DIFFERENCES BETWEEN DPP.

‡ STATISTICAL SIGNIFICANCE OF DIFFERENCE BETWEEN TRIPLOID AND DIPLOID VARIETY.

	Dixie Queen		Summer Sweet			Orange Flesh Tender Sweet		Orange Sunshine			Yellow Flesh Black Diamond		Early Moonbeam		Amarillo		
DPP	mean	SD	mean	SD	Sig.‡	mean	SD	mean	SD	Sig.‡	mean	SD	mean	SD	mean	SD	Sig.‡
10	0a	.	0a	.	.	0a	.	0a	.	.	0a	.	.	.	.	.	.
20	0.95a	1.109	2.27a	1.040	0.109	1.51a	0.708	7.123a	3.704	0.012*	1.494a	0.944	.	.	.	.	.
30	.	.	10.54b	1.457	.	19.68b	.	30.45ab	.	0.115	11.354b	3.757	.	.	.	.	.
40	12.648a	16.386	8.746b	1.869	0.608	8.948c	2.188	53.12b	20.040	0.005**	6.564b	2.179	.	.	.	.	.
50	7.135a	3.656	8.345b	1.453	0.563	15.044c	1.855	52.885b	13.657	0.000**	8.142b	3.459	.	.	.	.	.
Sig.†	0.306		.000**			.000**		.001**			.000**		.		.		

APPENDIX A-10

ζ-CAROTENE DESCRIPTIVE STATISTICS, YEAR 2. MEANS MEASURED IN µg/g. LETTERS REPRESENT TUKEY'S HSD WITHIN EACH VARIETY.

† STATISTICAL SIGNIFICANCE OF CAROTENOID LEVEL DIFFERENCES BETWEEN DPP.

‡ STATISTICAL SIGNIFICANCE OF DIFFERENCE BETWEEN TRIPLOID AND DIPLOID VARIETY.

	Dixie Queen		Summer Sweet			Orange Flesh Tender Sweet		Orange Sunshine			Yellow Flesh Black Diamond		Early Moonbeam		Amarillo		
DPP	mean	SD	mean	SD	Sig.‡	mean	SD	mean	SD	Sig.‡	mean	SD	mean	SD	mean	SD	Sig.‡
10	0a	.	0a	.	.	0a	.	0a	.	.	0a	.	.	.	.	.	.
20	0.16a	0.185	0.524a	0.214	0.031*	0.33a	0.171	1.557ab	0.860	0.035*	0.428a	0.253	.	.	.	.	.
30	.	.	3.735c	0.078	.	3.78b	.	3.08abc	.	0.865	3.236b	1.532	.	.	.	.	.
40	1.023b	0.395	2.176b	0.507	0.007**	1.485c	0.191	5.865bc	2.989	0.026*	2.166ab	2.315	.	.	.	.	.
50	1.405b	0.559	1.993b	0.702	0.368	2.606c	0.473	6.643c	1.708	0.001**	1.336ab	0.361	.	.	.	.	.
Sig.†	.001**		.000**			.000**		.005**			.001**		.		.		

APPENDIX A-11

PRONEUROSPORENE DESCRIPTIVE STATISTICS, YEAR 2. MEANS MEASURED IN µg/g. LETTERS REPRESENT TUKEY'S HSD WITHIN EACH VARIETY. † STATISTICAL SIGNIFICANCE OF CAROTENOID LEVEL DIFFERENCES BETWEEN DPP.

‡ STATISTICAL SIGNIFICANCE OF DIFFERENCE BETWEEN TRIPLOID AND DIPLOID VARIETY.

	Dixie Queen		Summer Sweet			Orange Flesh Tender Sweet		Orange Sunshine			Yellow Flesh Black Diamond		Early Moonbeam		Amarillo		
DPP	mean	SD	mean	SD	Sig.‡	mean	SD	mean	SD	Sig.‡	mean	SD	mean	SD	mean	SD	Sig.‡
10	0a	.	0a	.	.	0a	.	0.055a	0.007	0.000**	0a	.	.	.	.	.	.
20	0a	.	0a	.	.	0.178a	0.089	1.507ab	0.822	0.009**	0.216ab	0.116	.	.	.	.	.
30	.	.	0a	.	.	1.7b	.	2.04ab	.	0.403	1.026c	0.419	.	.	.	.	.
40	0a	.	0a	.	.	0.835bc	0.251	2.898b	1.396	0.027*	0.534b	0.144	.	.	.	.	.
50	0a	.	0a	.	.	1.344c	0.370	2.55b	0.409	0.002**	0.516b	0.117	.	.	.	.	.
Sig.†		.		.		.000**		.047*			.000**			.		.	

APPENDIX A-12

PROLYCOPENE DESCRIPTIVE STATISTICS, YEAR 2. MEANS MEASURED IN µg/g. LETTERS REPRESENT TUKEY'S HSD WITHIN EACH VARIETY.

† STATISTICAL SIGNIFICANCE OF CAROTENOID LEVEL DIFFERENCES BETWEEN DPP.

‡ STATISTICAL SIGNIFICANCE OF DIFFERENCE BETWEEN TRIPLOID AND DIPLOID VARIETY.

	Dixie Queen		Summer Sweet			Orange Flesh Tender Sweet		Orange Sunshine			Yellow Flesh Black Diamond		Early Moonbeam		Amarillo		
DPP	mean	SD	mean	SD	Sig.‡	mean	SD	mean	SD	Sig.‡	mean	SD	mean	SD	mean	SD	Sig.‡
10	0a	.	0a	.	.	0a	.	0.315a	0.035	0.000**	0a	.	.	.	.	.	.
20	0a	.	0a	.	.	0.96a	0.457	12.89ab	7.213	0.008**	1.51ab	1.007	.	.	.	.	.
30	.	.	0a	.	.	13.3b	.	18.35b	.	0.326	3.146b	1.415	.	.	.	.	.
40	0a	.	0a	.	.	5.355b	1.921	20.5b	3.413	0.000**	2.528b	0.512	.	.	.	.	.
50	0a	.	0a	.	.	5.092c	0.980	18.133b	4.542	0.000**	2.096b	1.200	.	.	.	.	.
Sig.†		.		.		.000**		.008**			.000**			.		.	

APPENDIX A-13

LYCOPENE DESCRIPTIVE STATISTICS, YEAR 2. MEANS MEASURED IN µg/g. LETTERS REPRESENT TUKEY'S HSD WITHIN EACH VARIETY.

† STATISTICAL SIGNIFICANCE OF CAROTENOID LEVEL DIFFERENCES BETWEEN DPP.

‡ STATISTICAL SIGNIFICANCE OF DIFFERENCE BETWEEN TRIPLOID AND DIPLOID VARIETY.

	Dixie Queen		Summer Sweet			Orange Flesh Tender Sweet		Orange Sunshine			Yellow Flesh Black Diamond		Early Moonbeam		Amarillo		
DPP	mean	SD	mean	SD	Sig.‡	mean	SD	mean	SD	Sig.‡	mean	SD	mean	SD	mean	SD	Sig.‡
10	0.083a	0.040	1.446a	1.466	0.170	0a	.	0.09a	0.042	0.008**	0a	.	.	.	.	.	.
20	9.503a	9.628	29.384b	11.947	0.031*	0.178a	0.060	1.283a	0.814	0.002**	0.206a	0.057	.	.	.	.	.
30	.	.	112.375c	21.079	0.084	1.75ab	.	1.33a	.	0.879	1.05b	0.417	.	.	.	.	.
40	82.543b	15.162	121.462c	14.853	0.006**	1.87b	0.794	2.685a	0.993	0.247	1.346b	0.501	.	.	.	.	.
50	77.84b	39.089	105.995c	8.795	0.196	3.604c	1.210	4.75a	3.251	0.485	3.834c	0.391	.	.	.	.	.
Sig.†	.000**		.000**			.000**		0.131			.000**		.		.		

APPENDIX A-14

β-CAROTENE DESCRIPTIVE STATISTICS, YEAR 2. MEANS MEASURED IN µg/g. LETTERS REPRESENT TUKEY'S HSD WITHIN EACH VARIETY.

† STATISTICAL SIGNIFICANCE OF CAROTENOID LEVEL DIFFERENCES BETWEEN DPP.

‡ STATISTICAL SIGNIFICANCE OF DIFFERENCE BETWEEN TRIPLOID AND DIPLOID VARIETY.

	Dixie Queen		Summer Sweet			Orange Flesh Tender Sweet		Orange Sunshine			Yellow Flesh Black Diamond		Early Moonbeam		Amarillo		
DPP	mean	SD	mean	SD	Sig.‡	mean	SD	mean	SD	Sig.‡	mean	SD	mean	SD	mean	SD	Sig.‡
10	0a	.	0a	.	.	0a	.	0a	.	.	0a	.	.	.	.	.	.
20	0.113a	0.130	0.112a	0.076	0.994	0a	.	0.367a	0.251	0.001**	0a	.	.	.	.	.	.
30	.	.	2.095ab	0.050	.	0.93a	.	0.79a	.	0.664	0.408b	0.293	.	.	.	.	.
40	1.875b	0.621	2.79b	1.226	0.220	1.378a	0.444	1.703ab	0.538	0.387	1.004c	0.259	.	.	.	.	.
50	2.795b	0.375	4.35b	2.200	0.401	6.138a	8.878	3.793b	1.604	0.623	1.778d	0.269	.	.	.	.	.
Sig.†	.000**		.000**			0.150		0.002			.000**		.		.		

APPENDIX A-15

LUTEIN DESCRIPTIVE STATISTICS, YEAR 2. MEANS MEASURED IN µg/g. LETTERS REPRESENT TUKEY'S HSD WITHIN EACH VARIETY.

† STATISTICAL SIGNIFICANCE OF CAROTENOID LEVEL DIFFERENCES BETWEEN DPP.

‡ STATISTICAL SIGNIFICANCE OF DIFFERENCE BETWEEN TRIPLOID AND DIPLOID VARIETY.

	Dixie Queen		Summer Sweet			Orange Flesh Tender Sweet		Orange Sunshine			Yellow Flesh Black Diamond		Early Moonbeam		Amarillo		
DPP	mean	SD	mean	SD	Sig.‡	mean	SD	mean	SD	Sig.‡	mean	SD	mean	SD	mean	SD	Sig.‡
10	0.063a	0.071	0.196a	0.097	0.088	0.058a	0.072	0.075a	0.106	0.373	0.06a	0.064	0.056a	0.038	0.027a	0.046	0.363
20	0a	.	0b	.	.	0.038ab	0.043	0.337a	0.194	0.006**	0.022a	0.032	0a	.	0.105ab	0.033	0.001**
30	.	.	0b	.	.	0a	.	0.57ab	.	0.000**	0.058a	0.163	.	.	0.213ab	0.112	.
40	0a	.	0b	.	.	0.328b	0.088	0.618ab	0.354	0.163	0a	.	0a	.	0.288ab	0.147	0.003**
50	0a	.	0b	.	.	0.722c	0.223	1.045b	0.257	0.083	0a	.	0.29b	0.152	0.488b	0.323	0.250
Sig.†	0.104		.000**			.000**		.009**			0.698		.000**		.033*		

APPENDIX A-16

VIOLAXANTHIN DESCRIPTIVE STATISTICS, YEAR 2. MEANS MEASURED IN µg/g. LETTERS REPRESENT TUKEY'S HSD WITHIN EACH VARIETY.

† STATISTICAL SIGNIFICANCE OF CAROTENOID LEVEL DIFFERENCES BETWEEN DPP.

‡ STATISTICAL SIGNIFICANCE OF DIFFERENCE BETWEEN TRIPLOID AND DIPLOID VARIETY.

	Dixie Queen		Summer Sweet			Orange Flesh Tender Sweet		Orange Sunshine			Yellow Flesh Black Diamond		Early Moonbeam		Amarillo		
DPP	mean	SD	mean	SD	Sig.‡	mean	SD	mean	SD	Sig.‡	mean	SD	mean	SD	mean	SD	Sig.‡
10	0.027a	0.023	0.05a	0.028	0.276	0.025a	0.017	0.105a	0.021	0.001**	0.02a	0.014	0.1ab	0.092	0.103a	0.080	0.960
20	0.013a	0.025	0b	.	0.292	0.018ab	0.013	0.12a	0.066	0.010**	0.014ab	0.019	0.138b	0.054	0.43a	0.271	0.079
30	.	.	0b	.	.	0b	.	0b	.	.	0b	.	.	.	0.313a	0.114	.
40	0a	.	0b	.	.	0b	.	0b	.	.	0b	.	0a	.	0.305a	0.149	0.002**
50	0a	.	0b	.	.	0b	.	0b	.	.	0b	.	0.108b	0.022	0.22a	0.125	0.083
Sig.†	0.283		.000**			.012*		.001**			.006**		.008**		0.172		

APPENDIX A-17

3-WAY (COLOR X DAY X PLOIDY) MULTIVARIATE ANALYSIS OF VARIANCE (MANOVA) FOR CAROTENOID DEVELOPMENT STUDY, YEAR 1.

Source	Dependent Variable	Type III Sum of Squares	df	Mean Square	F	Sig.
Corrected Model	viol	485286771619.894(a)	23	21099424853.039	15.822	.000
	lut	21481406547.596(b)	23	933974197.722	4.920	.000
	lyc	199867105542875.300(c)	23	8689874154038.060	14.043	.000
	prolyc	43721265703812.640(d)	23	1900924595817.941	29.404	.000
	zcar	8759306849888.660(e)	23	380839428256.029	24.460	.000
	bcar	5474298889180.610(f)	23	238012995181.766	29.037	.000
	phyto	27133538576384.210(g)	23	1179719068538.444	48.541	.000
	proneuro	449288208166.216(h)	23	19534269920.270	36.785	.000
Intercept	viol	169140014554.778	1	169140014554.778	126.837	.000
	lut	21492355785.523	1	21492355785.523	113.212	.000
	lyc	48841201227965.800	1	48841201227965.800	78.927	.000
	prolyc	11379753991529.170	1	11379753991529.170	176.027	.000
	zcar	3890995892902.957	1	3890995892902.957	249.906	.000
	bcar	3074279208999.766	1	3074279208999.766	375.060	.000
	phyto	8979721898901.770	1	8979721898901.770	369.484	.000
	proneuro	169227747571.874	1	169227747571.874	318.673	.000
color	viol	274666547675.840	3	91555515891.947	68.657	.000
	lut	1180163186.079	3	393387728.693	2.072	.117
	lyc	73033773011124.100	3	24344591003708.040	39.341	.000
	prolyc	18852874101364.820	3	6284291367121.610	97.208	.000
	zcar	4037117857768.464	3	1345705952589.488	86.430	.000
	bcar	1189151238837.082	3	396383746279.027	48.359	.000
	phyto	11344800228362.410	3	3781600076120.804	155.599	.000
	proneuro	247519684758.985	3	82506561586.328	155.368	.000
day	viol	64101317257.390	3	21367105752.463	16.023	.000
	lut	7993894419.260	3	2664631473.087	14.036	.000
	lyc	35374297773622.750	3	11791432591207.580	19.055	.000
	prolyc	4072010679758.595	3	1357336893252.865	20.996	.000
	zcar	2034665222272.867	3	678221740757.622	43.560	.000
	bcar	2803433170607.804	3	934477723535.935	114.006	.000
	phyto	4971679219115.890	3	1657226406371.966	68.189	.000
	proneuro	61498708712.057	3	20499569570.686	38.603	.000
ploidy	viol	5199029225.173	1	5199029225.173	3.899	.054
	lut	128862749.347	1	128862749.347	.679	.414
	lyc	3646016252.421	1	3646016252.421	.006	.939
	prolyc	3546620453280.564	1	3546620453280.564	54.861	.000
	zcar	27954587079.347	1	27954587079.347	1.795	.187
	bcar	211473931.021	1	211473931.021	.026	.873
	phyto	881767623002.309	1	881767623002.309	36.282	.000
	proneuro	12403717534.042	1	12403717534.042	23.357	.000
color * day	viol	84108933363.117	7	12015561909.017	9.010	.000
	lut	6040428912.098	7	862918416.014	4.545	.001
	lyc	60331502140524.000	7	8618786020074.850	13.928	.000

APPENDIX A-17 CONTINUED

Source	Dependent Variable	Type III Sum of Squares	df	Mean Square	F	Sig.
	prolyc	5745878839732.180	7	820839834247.455	12.697	.000
	zcar	1545810429365.013	7	220830061337.859	14.183	.000
	bcar	827536605986.103	7	118219515140.872	14.423	.000
	phyto	5417417865097.180	7	773916837871.026	31.844	.000
	proneuro	81317208458.189	7	11616744065.456	21.876	.000
color * ploidy	viol	17138676120.037	2	8569338060.019	6.426	.003
	lut	193219101.037	2	96609550.519	.509	.604
	lyc	36855032555.441	2	18427516277.721	.030	.971
	prolyc	7597649148805.190	2	3798824574402.596	58.762	.000
	zcar	173240082782.923	2	86620041391.461	5.563	.007
	bcar	33448229145.333	2	16724114572.667	2.040	.141
	phyto	2072517497561.327	2	1036258748780.663	42.638	.000
	proneuro	26571519339.592	2	13285759669.796	25.018	.000
day * ploidy	viol	13549575014.940	3	4516525004.980	3.387	.026
	lut	736391796.482	3	245463932.161	1.293	.288
	lyc	4670696364330.980	3	1556898788110.328	2.516	.070
	prolyc	1200864579976.416	3	400288193325.472	6.192	.001
	zcar	128355018059.715	3	42785006019.905	2.748	.053
	bcar	48322825121.832	3	16107608373.944	1.965	.132
	phyto	374670299663.264	3	124890099887.755	5.139	.004
	proneuro	5519524139.815	3	1839841379.938	3.465	.023
color * day * ploidy	viol	8461434885.407	4	2115358721.352	1.586	.194
	lut	1661616530.296	4	415404132.574	2.188	.085
	lyc	6753544468667.100	4	1688386117166.775	2.728	.040
	prolyc	2401729159952.893	4	600432289988.223	9.288	.000
	zcar	282619299272.964	4	70654824818.241	4.538	.004
	bcar	42613680418.667	4	10653420104.667	1.300	.284
	phyto	861546768982.297	4	215386692245.574	8.862	.000
	proneuro	11039048279.630	4	2759762069.907	5.197	.002
Error	viol	62675559250.500	47	1333522537.245		
	lut	8922566503.333	47	189841840.496		
	lyc	29084417496236.670	47	618817393536.951		
	prolyc	3038438487659.334	47	64647627397.007		
	zcar	731781029517.167	47	15569809138.663		
	bcar	385247613203.333	47	8196757727.730		
	phyto	1142261851103.334	47	24303443640.496		
	proneuro	24958808843.333	47	531038486.028		
Total	viol	845636340374.000	71			
	lut	52993837912.000	71			
	lyc	306284115734150.000	71			
	prolyc	55865458128754.000	71			
	zcar	13483489657910.000	71			
	bcar	9639489035419.000	71			
	phyto	37239477966960.000	71			
	proneuro	611151722889.000	71			
Corrected Total	viol	547962330870.394	70			
	lut	30403973050.930	70			
	lyc	228951523039112.000	70			

APPENDIX A-17 CONTINUED

Source	Dependent Variable	Type III Sum of Squares	df	Mean Square	F	Sig.
	prolyc	46759704191471.900	70			
	zcar	9491087879405.830	70			
	bcar	5859546502383.940	70			
	phyto	28275800427487.550	70			
	proneuro	474247017009.549	70			

a R Squared = .886 (Adjusted R Squared = .830)
b R Squared = .707 (Adjusted R Squared = .563)
c R Squared = .873 (Adjusted R Squared = .811)
d R Squared = .935 (Adjusted R Squared = .903)
e R Squared = .923 (Adjusted R Squared = .885)
f R Squared = .934 (Adjusted R Squared = .902)
g R Squared = .960 (Adjusted R Squared = .940)
h R Squared = .947 (Adjusted R Squared = .922)

APPENDIX A-18

2-WAY (COLOR X DAY) MANOVA (SEPARATED BY PLOIDY) FOR DIPLOID CAROTENOID DEVELOPMENT, YEAR 1. NULL HYPOTHESIS: CAROTENOID DEVELOPMENT PATTERN IS THE SAME AMONG DIPLOIDS FOR ALL COLORS.

Source	Dependent Variable	Type III Sum of Squares	df	Mean Square	F	Sig.
Corrected Model	viol	171502157055.175(a)	12	14291846421.265	12.644	.000
	lut	11740807080.912(b)	12	978400590.076	6.352	.000
	lyc	126198232645601.500(c)	12	10516519387133.460	10.055	.000
	prolyc	4563409280655.010(d)	12	380284106721.251	7.755	.000
	zcar	3413816167005.431(e)	12	284484680583.786	11.005	.000
	bcar	2827467796963.430(f)	12	235622316413.619	33.408	.000
	phyto	4999182797075.570(g)	12	416598566422.965	13.134	.000
	proneuro	139597351520.482(h)	12	11633112626.707	25.153	.000
Intercept	viol	43170238222.316	1	43170238222.316	38.192	.000
	lut	9910184693.895	1	9910184693.895	64.334	.000
	lyc	37246508417676.790	1	37246508417676.790	35.613	.000
	prolyc	1577316398148.214	1	1577316398148.214	32.167	.000
	zcar	1957600956048.094	1	1957600956048.094	75.730	.000
	bcar	1931384993158.042	1	1931384993158.042	273.845	.000
	phyto	2628209624240.708	1	2628209624240.708	82.857	.000
	proneuro	60690271801.263	1	60690271801.263	131.223	.000
color	viol	115811655981.015	3	38603885327.005	34.153	.000
	lut	1708236748.626	3	569412249.542	3.696	.025
	lyc	51095344486691.800	3	17031781495563.950	16.285	.000

APPENDIX A-18 CONTINUED

Source	Dependent Variable	Type III Sum of Squares	df	Mean Square	F	Sig.
	zcar	1294179981801.904	3	431393327267.301	16.688	.000
	bcar	686819173478.667	3	228939724492.889	32.461	.000
	phyto	1930060072298.994	3	643353357432.998	20.282	.000
	proneuro	69542580727.909	3	23180860242.636	50.121	.000
day	viol	47651000711.768	3	15883666903.923	14.052	.000
	lut	4146624184.185	3	1382208061.395	8.973	.000
	lyc	23886153856825.860	3	7962051285608.620	7.613	.001
	prolyc	1498002759622.154	3	499334253207.385	10.183	.000
	zcar	1226200248058.977	3	408733416019.659	15.812	.000
	bcar	1482137679745.390	3	494045893248.463	70.049	.000
	phyto	1631605743878.363	3	543868581292.788	17.146	.000
	proneuro	35978258188.628	3	11992752729.543	25.930	.000
color * day	viol	36414256470.288	6	6069042745.048	5.369	.001
	lut	5663838004.232	6	943973000.705	6.128	.000
	lyc	45521211511775.300	6	7586868585295.890	7.254	.000
	prolyc	1529483895655.496	6	254913982609.249	5.199	.001
	zcar	728000359908.208	6	121333393318.035	4.694	.003
	bcar	474227948429.825	6	79037991404.971	11.207	.000
	phyto	1175973518503.833	6	195995586417.306	6.179	.000
	proneuro	36365394080.485	6	6060899013.414	13.105	.000
Error	viol	28258438827.167	25	1130337553.087		
	lut	3851048646.667	25	154041945.867		
	lyc	26146626454931.990	25	1045865058197.280		
	prolyc	1225872783675.333	25	49034911347.013		
	zcar	646245710607.833	25	25849828424.313		
	bcar	176320724753.333	25	7052828990.133		
	phyto	792994792840.000	25	31719791713.600		
	proneuro	11562432421.333	25	462497296.853		
Total	viol	296466284155.000	38			
	lut	28180504574.000	38			
	lyc	192821410144950.000	38			
	prolyc	7147270942619.000	38			
	zcar	6224462735210.000	38			
	bcar	5199176671749.000	38			
	phyto	8627124964234.000	38			
	proneuro	206946117425.000	38			
Corrected Total	viol	199760595882.342	37			
	lut	15591855727.579	37			
	lyc	152344859100533.500	37			
	prolyc	5789282064330.340	37			

APPENDIX A-18 CONTINUED

Source	Dependent Variable	Type III Sum of Squares	df	Mean Square	F	Sig.
	bcar	3003788521716.763	37			
	phyto	5792177589915.570	37			
	proneuro	151159783941.816	37			

a R Squared = .859 (Adjusted R Squared = .791)
b R Squared = .753 (Adjusted R Squared = .634)
c R Squared = .828 (Adjusted R Squared = .746)
d R Squared = .788 (Adjusted R Squared = .687)
e R Squared = .841 (Adjusted R Squared = .764)
f R Squared = .941 (Adjusted R Squared = .913)
g R Squared = .863 (Adjusted R Squared = .797)
h R Squared = .924 (Adjusted R Squared = .887)
i ploidy = 2n

APPENDIX A-19

2-WAY (COLOR X DAY) MANOVA (SEPARATED BY PLOIDY) FOR TRIPLOID CAROTENOID DEVELOPMENT, YEAR 1. NULL HYPOTHESIS: CAROTENOID DEVELOPMENT PATTERN IS THE SAME AMONG TRIPLOIDS FOR ALL COLORS.

Source	Dependent Variable	Type III Sum of Squares	df	Mean Square	F	Sig.
Corrected Model	viol	297058157576.727(a)	10	29705815757.673	18.988	.000
	lut	9729774899.394(b)	10	972977489.939	4.221	.002
	lyc	73657925670231.200(c)	10	7365792567023.120	55.160	.000
	prolyc	36820593665940.060(d)	10	3682059366594.007	44.691	.000
	zcar	5345299849014.910(e)	10	534529984901.491	137.483	.000
	bcar	2639255525310.182(f)	10	263925552531.018	27.791	.000
	phyto	21582225643866.180(e)	10	2158222564386.619	135.944	.000
	proneuro	307130246754.000(g)	10	30713024675.400	50.438	.000
Intercept	viol	169820154051.664	1	169820154051.664	108.552	.000
	lut	10768909819.250	1	10768909819.250	46.715	.000
	lyc	29812855854974.750	1	29812855854974.750	223.257	.000
	prolyc	13047801278161.080	1	13047801278161.080	158.368	.000
	zcar	2206404789260.989	1	2206404789260.989	567.495	.000
	bcar	1618748034944.139	1	1618748034944.139	170.454	.000
	phyto	8153195720168.300	1	8153195720168.300	513.562	.000
	proneuro	108262143838.369	1	108262143838.369	177.792	.000
color	viol	212432857039.708	2	106216428519.854	67.895	.000
	lut	516333894.282	2	258166947.141	1.120	.344

APPENDIX A-19 CONTINUED

Source	Dependent Variable	Type III Sum of Squares	df	Mean Square	F	Sig.
	prolyc	24652290217404.470	2	12326145108702.230	149.608	.000
	zcar	2916416018657.123	2	1458208009328.561	375.056	.000
	bcar	584934903828.166	2	292467451914.083	30.797	.000
	phyto	11503916027023.700	2	5751958013511.850	362.310	.000
	proneuro	204548623370.666	2	102274311685.333	167.958	.000
day	viol	52020687494.347	3	17340229164.782	11.084	.000
	lut	5807772596.755	3	1935924198.918	8.398	.001
	lyc	20311443240305.420	3	6770481080101.810	50.702	.000
	prolyc	3309062052014.727	3	1103020684004.909	13.388	.000
	zcar	935946000393.461	3	311982000131.154	80.243	.000
	bcar	1436826730193.777	3	478942243397.926	50.433	.000
	phyto	3526349142733.189	3	1175449714244.396	74.040	.000
	proneuro	27995431328.667	3	9331810442.889	15.325	.000
color * day	viol	56156111778.236	5	11231222355.647	7.179	.000
	lut	2038207438.162	5	407641487.632	1.768	.161
	lyc	21563835097415.710	5	4312767019483.142	32.297	.000
	prolyc	6618124104029.480	5	1323624820805.897	16.065	.000
	zcar	1100429368729.760	5	220085873745.952	56.607	.000
	bcar	395922337974.944	5	79184467594.989	8.338	.000
	phyto	5102991115575.610	5	1020598223115.122	64.287	.000
	proneuro	55990862657.333	5	11198172531.467	18.390	.000
Error	viol	34417120423.333	22	1564414564.697		
	lut	5071517856.667	22	230523538.939		
	lyc	2937791041304.667	22	133535956422.939		
	prolyc	1812565703984.000	22	82389350181.091		
	zcar	85535318909.333	22	3887969041.333		
	bcar	208926888450.000	22	9496676747.727		
	phyto	349267058263.333	22	15875775375.606		
	proneuro	13396376422.000	22	608926201.000		
Total	viol	549170056219.000	33			
	lut	24813333338.000	33			
	lyc	113462705589200.000	33			
	prolyc	48718187186135.000	33			
	zcar	7259026922700.000	33			
	bcar	4440312363670.000	33			
	phyto	28612353002726.000	33			
	proneuro	404205605464.000	33			
Corrected Total	viol	331475278000.061	32			
	lut	14801292756.061	32			
	lyc	76595716711535.800	32			

APPENDIX A-19 CONTINUED

Source	Dependent Variable	Type III Sum of Squares	df	Mean Square	F	Sig.
	zcar	5430835167924.240	32			
	bcar	2848182413760.182	32			
	phyto	21931492702129.510	32			
	proneuro	320526623176.000	32			

a R Squared = .896 (Adjusted R Squared = .849)
b R Squared = .657 (Adjusted R Squared = .502)
c R Squared = .962 (Adjusted R Squared = .944)
d R Squared = .953 (Adjusted R Squared = .932)
e R Squared = .984 (Adjusted R Squared = .977)
f R Squared = .927 (Adjusted R Squared = .893)
g R Squared = .958 (Adjusted R Squared = .939)
h ploidy = 3n

APPENDIX A-20

2-WAY (PLOIDY X DAY) MANOVA (SEPARATED BY COLOR) FOR CAROTENOID DEVELOPMENT IN CANARY YELLOW WATERMELON, YEAR 1. NULL HYPOTHESIS: CAROTENOID DEVELOPMENT PATTERN IS THE SAME AMONG PLOIDIES FOR CANARY YELLOW FLESH WATERMELONS.

Source	Dependent Variable	Type III Sum of Squares	df	Mean Square	F	Sig.
Corrected Model	viol	197738750034.292(a)	7	28248392862.042	7.594	.000
	lut	2811219294.500(b)	7	401602756.357	2.050	.111
	lyc	4536759371.292(c)	7	648108481.613	.951	.497
	prolyc	.000(d)	7	.000	.	.
	zcar	109896771904.292(e)	7	15699538843.470	5.445	.002
	bcar	101669544092.000(f)	7	14524220584.571	9.814	.000
	phyto	26405792999.958(g)	7	3772256142.851	3.386	.021
	proneuro	.000(d)	7	.000	.	.
Intercept	viol	546489480645.375	1	546489480645.375	146.910	.000
	lut	14670529328.167	1	14670529328.167	74.870	.000
	lyc	917668501.042	1	917668501.042	1.346	.263
	prolyc	.000	1	.000	.	.
	zcar	58110416175.375	1	58110416175.375	20.153	.000
	bcar	74797461232.667	1	74797461232.667	50.540	.000
	phyto	17986962785.042	1	17986962785.042	16.147	.001
	proneuro	.000	1	.000	.	.
day	viol	156356630174.125	3	52118876724.708	14.011	.000

APPENDIX A-20 CONTINUED

Source	Dependent Variable	Type III Sum of Squares	df	Mean Square	F	Sig.
	lyc	2753005503.125	3	917668501.042	1.346	.295
	prolyc	.000	3	.000	.	.
	zcar	86277017519.458	3	28759005839.819	9.974	.001
	bcar	88623802864.667	3	29541267621.556	19.961	.000
	phyto	23728844039.125	3	7909614679.708	7.100	.003
	proneuro	.000	3	.000	.	.
ploidy	viol	22020527109.375	1	22020527109.375	5.920	.027
	lut	118690432.667	1	118690432.667	.606	.448
	lyc	445938467.042	1	445938467.042	.654	.431
	prolyc	.000	1	.000	.	.
	zcar	2817815117.042	1	2817815117.042	.977	.338
	bcar	6381842293.500	1	6381842293.500	4.312	.054
	phyto	162068445.375	1	162068445.375	.145	.708
	proneuro	.000	1	.000	.	.
day * ploidy	viol	19361592750.792	3	6453864250.264	1.735	.200
	lut	1765863842.333	3	588621280.778	3.004	.061
	lyc	1337815401.125	3	445938467.042	.654	.592
	prolyc	.000	3	.000	.	.
	zcar	20801939267.792	3	6933979755.931	2.405	.105
	bcar	6663898933.833	3	2221299644.611	1.501	.252
	phyto	2514880515.458	3	838293505.153	.753	.537
	proneuro	.000	3	.000	.	.
Error	viol	59518446133.333	16	3719902883.333		
	lut	3135135377.333	16	195945961.083		
	lyc	10908855744.667	16	681803484.042		
	prolyc	.000	16	.000		
	zcar	46135197661.333	16	2883449853.833		
	bcar	23679308311.333	16	1479956769.458		
	phyto	17823467588.000	16	1113966724.250		
	proneuro	.000	16	.000		
Total	viol	803746676813.000	24			
	lut	20616884000.000	24			
	lyc	16363283617.000	24			
	prolyc	.000	24			
	zcar	214142385741.000	24			
	bcar	200146313636.000	24			
	phyto	62216223373.000	24			
	proneuro	.000	24			
Corrected Total	viol	257257196167.625	23			
	lut	5946354671.833	23			

APPENDIX A-20 CONTINUED

Source	Dependent Variable	Type III Sum of Squares	df	Mean Square	F	Sig.
	prolyc	.000	23			
	zcar	156031969565.625	23			
	bcar	125348852403.333	23			
	phyto	44229260587.958	23			
	proneuro	.000	23			

a R Squared = .769 (Adjusted R Squared = .667)
b R Squared = .473 (Adjusted R Squared = .242)
c R Squared = .294 (Adjusted R Squared = -.015)
d R Squared = . (Adjusted R Squared = .)
e R Squared = .704 (Adjusted R Squared = .575)
f R Squared = .811 (Adjusted R Squared = .728)
g R Squared = .597 (Adjusted R Squared = .421)
h color = CY

APPENDIX A-21

2-WAY (PLOIDY X DAY) MANOVA (SEPARATED BY COLOR) FOR CAROTENOID DEVELOPMENT IN ORANGE WATERMELON, YEAR 1. NULL HYPOTHESIS: CAROTENOID DEVELOPMENT PATTERN IS THE SAME AMONG PLOIDIES FOR ORANGE FLESH WATERMELONS.

Source	Dependent Variable	Type III Sum of Squares	df	Mean Square	F	Sig.
Corrected Model	viol	3508201215.111(a)	5	701640243.022	3.125	.049
	lut	4041892221.111(b)	5	808378444.222	7.391	.002
	lyc	7609198491687.110(c)	5	1521839698337.422	31.159	.000
	prolyc	22937939978900.440(d)	5	4587587995780.090	18.668	.000
	zcar	3545638517971.779(e)	5	709127703594.356	13.652	.000
	bcar	2236928735588.445(f)	5	447385747117.689	22.577	.000
	phyto	13509553432416.940(g)	5	2701910686483.389	33.848	.000
	proneuro	160889201303.611(h)	5	32177840260.722	20.393	.000
Intercept	viol	11566393814.222	1	11566393814.222	51.508	.000
	lut	1549166230.222	1	1549166230.222	14.163	.003
	lyc	11849224768214.220	1	11849224768214.220	242.608	.000
	prolyc	27289671290138.950	1	27289671290138.950	111.051	.000
	zcar	7624994124272.230	1	7624994124272.230	146.793	.000
	bcar	3606297086773.556	1	3606297086773.556	181.989	.000
	phyto	20307987244533.400	1	20307987244533.400	254.410	.000
	proneuro	340720447182.723	1	340720447182.723	215.938	.000

APPENDIX A-21 CONTINUED

Source	Dependent Variable	Type III Sum of Squares	df	Mean Square	F	Sig.
	lut	3098332460.444	2	1549166230.222	14.163	.001
	lyc	7437309205680.770	2	3718654602840.389	76.138	.000
	prolyc	7938872515763.110	2	3969436257881.558	16.153	.000
	zcar	2994564379830.112	2	1497282189915.056	28.825	.000
	bcar	2222550696224.111	2	1111275348112.056	56.080	.000
	phyto	9342801899748.110	2	4671400949874.050	58.521	.000
	proneuro	104473349874.778	2	52236674937.389	33.106	.000
ploidy	viol	282871040.889	1	282871040.889	1.260	.284
	lut	314519920.222	1	314519920.222	2.875	.116
	lyc	7801254050.000	1	7801254050.000	.160	.696
	prolyc	11396473723208.000	1	11396473723208.000	46.376	.000
	zcar	185788605210.889	1	185788605210.889	3.577	.083
	bcar	4015692962.000	1	4015692962.000	.203	.661
	phyto	3019390178224.496	1	3019390178224.496	37.826	.000
	proneuro	39857279009.389	1	39857279009.389	25.260	.000
day * ploidy	viol	2257152717.444	2	1128576358.722	5.026	.026
	lut	629039840.444	2	314519920.222	2.875	.095
	lyc	164088031956.333	2	82044015978.167	1.680	.227
	prolyc	3602593739929.330	2	1801296869964.665	7.330	.008
	zcar	365285532930.777	2	182642766465.389	3.516	.063
	bcar	10362346402.333	2	5181173201.167	.261	.774
	phyto	1147361354444.332	2	573680677222.166	7.187	.009
	proneuro	16558572419.444	2	8279286209.722	5.247	.023
Error	viol	2694653024.667	12	224554418.722		
	lut	1312566578.667	12	109380548.222		
	lyc	586092475718.667	12	48841039643.222		
	prolyc	2948885317266.666	12	245740443105.556		
	zcar	623328159070.000	12	51944013255.833		
	bcar	237792598282.000	12	19816049856.833		
	phyto	957887502970.667	12	79823958580.889		
	proneuro	18934383558.667	12	1577865296.556		
Total	viol	17769248054.000	18			
	lut	6903625030.000	18			
	lyc	20044515735620.000	18			
	prolyc	53176496586306.000	18			
	zcar	11793960801314.000	18			
	bcar	6081018420644.000	18			
	phyto	34775428179921.000	18			
	proneuro	520544032045.000	18			
Corrected Total	viol	6202854239.778	17			

APPENDIX A-21 CONTINUED

Source	Dependent Variable	Type III Sum of Squares	df	Mean Square	F	Sig.
	lyc	8195290967405.770	17			
	prolyc	25886825296167.110	17			
	zcar	4168966677041.779	17			
	bcar	2474721333870.445	17			
	phyto	14467440935387.610	17			
	proneuro	179823584862.278	17			

a R Squared = .566 (Adjusted R Squared = .385)
b R Squared = .755 (Adjusted R Squared = .653)
c R Squared = .928 (Adjusted R Squared = .899)
d R Squared = .886 (Adjusted R Squared = .839)
e R Squared = .850 (Adjusted R Squared = .788)
f R Squared = .904 (Adjusted R Squared = .864)
g R Squared = .934 (Adjusted R Squared = .906)
h R Squared = .895 (Adjusted R Squared = .851)
i color = O

APPENDIX A-22

2-WAY (PLOIDY X DAY) MANOVA (SEPARATED BY COLOR) FOR CAROTENOID DEVELOPMENT IN RED WATERMELON, YEAR 1. NULL HYPOTHESIS: CAROTENOID DEVELOPMENT PATTERN IS THE SAME AMONG PLOIDIES FOR RED FLESH WATERMELONS.

Source	Dependent Variable	Type III Sum of Squares	df	Mean Square	F	Sig.
Corrected Model	viol	11835676605.810(a)	6	1972612767.635	110.456	.000
	lut	9431726518.286(b)	6	1571954419.714	7.403	.001
	lyc	108068499258628.200(c)	6	18011416543104.710	9.009	.000
	prolyc	.000(d)	6	.000	.	.
	zcar	112207223426.571(e)	6	18701203904.429	75.403	.000
	bcar	1143848200493.810(a)	6	190641366748.968	107.780	.000
	phyto	322294975600.286(a)	6	53715829266.714	108.165	.000
	proneuro	.000(d)	6	.000	.	.
Intercept	viol	5979793674.904	1	5979793674.904	334.838	.000
	lut	7230756137.305	1	7230756137.305	34.052	.000
	lyc	126172768524952.300	1	126172768524952.300	63.107	.000
	prolyc	.000	1	.000	.	.
	zcar	96822760232.124	1	96822760232.124	390.387	.000
	bcar	1086123555581.063	1	1086123555581.063	614.042	.000
	phyto	319699866651.782	1	319699866651.782	643.766	.000

APPENDIX A-22 CONTINUED

Source	Dependent Variable	Type III Sum of Squares	df	Mean Square	F	Sig.
	proneuro	.000	1	.000	.	.
day	viol	11269912278.444	3	3756637426.148	210.353	.000
	lut	8731219460.000	3	2910406486.667	13.706	.000
	lyc	93128986995877.000	3	31042995665292.350	15.526	.000
	prolyc	.000	3	.000	.	.
	zcar	69160743447.444	3	23053581149.148	92.951	.000
	bcar	983132189242.139	3	327710729747.380	185.272	.000
	phyto	214686071537.361	3	71562023845.787	144.101	.000
	proneuro	.000	3	.000	.	.
ploidy	viol	196132216.056	1	196132216.056	10.982	.005
	lut	1552322.000	1	1552322.000	.007	.933
	lyc	33100015453.389	1	33100015453.389	.017	.899
	prolyc	.000	1	.000	.	.
	zcar	8938335240.056	1	8938335240.056	36.039	.000
	bcar	20962509768.000	1	20962509768.000	11.851	.004
	phyto	3992306938.889	1	3992306938.889	8.039	.013
	proneuro	.000	1	.000	.	.
day * ploidy	viol	392264432.111	2	196132216.056	10.982	.001
	lut	3104644.000	2	1552322.000	.007	.993
	lyc	11258814985640.770	2	5629407492820.380	2.816	.094
	prolyc	.000	2	.000	.	.
	zcar	24886845134.111	2	12443422567.056	50.172	.000
	bcar	73910260204.333	2	36955130102.167	20.893	.000
	phyto	86340833685.778	2	43170416842.889	86.930	.000
	proneuro	.000	2	.000	.	.
Error	viol	250022477.333	14	17858748.381		
	lut	2972836930.667	14	212345495.048		
	lyc	27990995950374.660	14	1999356853598.190		
	prolyc	.000	14	.000		
	zcar	3472246128.667	14	248017580.619		
	bcar	24763326568.000	14	1768809040.571		
	phyto	6952518930.000	14	496608495.000		
	proneuro	.000	14	.000		
Total	viol	18660010951.000	21			
	lut	18181998009.000	21			
	lyc	282779165944747.000	21			
	prolyc	.000	21			
	zcar	218670069489.000	21			
	bcar	2385074674742.000	21			
	phyto	690323653440.000	21			

APPENDIX A-22 CONTINUED

Source	Dependent Variable	Type III Sum of Squares	df	Mean Square	F	Sig.
	proneuro	.000	21			
Corrected Total	viol	12085699083.143	20			
	lut	12404563448.952	20			
	lyc	136059495209002.900	20			
	prolyc	.000	20			
	zcar	115679469555.238	20			
	bcar	1168611527061.810	20			
	phyto	329247494530.286	20			
	proneuro	.000	20			

a R Squared = .979 (Adjusted R Squared = .970)
b R Squared = .760 (Adjusted R Squared = .658)
c R Squared = .794 (Adjusted R Squared = .706)
d R Squared = . (Adjusted R Squared = .)
e R Squared = .970 (Adjusted R Squared = .957)
f color = R

APPENDIX A-23

3-WAY (COLOR X DAY X PLOIDY) ANALYSIS OF VARIANCE (ANOVA) FOR PHYTOENE DEVELOPMENT, YEAR 2.

Source	Type III Sum of Squares	df	Mean Square	F	Sig.
Corrected Model	19030.275 (a)	23	827.403	21.238	.000
Intercept	10400.083	1	10400.083	266.949	.000
color	2187.312	2	1093.656	28.072	.000
DPP	6510.244	4	1627.561	41.776	.000
ploidy	1112.415	1	1112.415	28.553	.000
color * DPP	2004.464	8	250.558	6.431	.000
color * ploidy	1872.500	1	1872.500	48.063	.000
DPP * ploidy	1320.425	4	330.106	8.473	.000
color * DPP * ploidy	1637.568	3	545.856	14.011	.000
Error	2844.008	73	38.959		
Total	31779.356	97			
Corrected Total	21874.284	96			

a R Squared = .870 (Adjusted R Squared = .829)

APPENDIX A-24

3-WAY (COLOR X DAY X PLOIDY) ANOVA FOR ζ-CAROTENE DEVELOPMENT, YEAR 2.

Source	Type III Sum of Squares	df	Mean Square	F	Sig.
Corrected Model	300.360(a)	23	13.059	11.625	.000
Intercept	288.121	1	288.121	256.484	.000
color	12.767	2	6.384	5.683	.005
DPP	148.640	4	37.160	33.080	.000
ploidy	14.483	1	14.483	12.892	.001
color * DPP	30.647	8	3.831	3.410	.002
color * ploidy	13.215	1	13.215	11.764	.001
DPP * ploidy	23.410	4	5.853	5.210	.001
color * DPP * ploidy	8.126	3	2.709	2.411	.074
Error	80.881	72	1.123		
Total	670.465	96			
Corrected Total	381.241	95			

a R Squared = .788 (Adjusted R Squared = .720)

APPENDIX A-25

3-WAY (COLOR X DAY X PLOIDY) ANOVA FOR PRONEUROSPORENE DEVELOPMENT, YEAR 2.

Source	Type III Sum of Squares	df	Mean Square	F	Sig.
Corrected Model	64.546(a)	23	2.806	20.197	.000
Intercept	32.244	1	32.244	232.051	.000
color	19.314	2	9.657	69.501	.000
DPP	11.464	4	2.866	20.626	.000
ploidy	3.100	1	3.100	22.309	.000
color * DPP	9.046	8	1.131	8.137	.000
color * ploidy	4.921	1	4.921	35.418	.000
DPP * ploidy	2.061	4	.515	3.709	.008
color * DPP * ploidy	1.817	3	.606	4.359	.007
Error	10.004	72	.139		
Total	108.157	96			
Corrected Total	74.550	95			

a R Squared = .866 (Adjusted R Squared = .823)

APPENDIX A-26

3-WAY (COLOR X DAY X PLOIDY) ANOVA FOR PROLYCOPENE DEVELOPMENT, YEAR 2.

Source	Type III Sum of Squares	df	Mean Square	F	Sig.
Corrected Model	3249.763(a)	23	141.294	40.163	.000
Intercept	1450.570	1	1450.570	412.331	.000
color	1078.425	2	539.213	153.274	.000
DPP	455.582	4	113.896	32.375	.000
ploidy	273.115	1	273.115	77.634	.000
color * DPP	420.218	8	52.527	14.931	.000
color * ploidy	371.974	1	371.974	105.735	.000
DPP * ploidy	117.362	4	29.341	8.340	.000
color * DPP * ploidy	111.202	3	37.067	10.537	.000
Error	253.294	72	3.518		
Total	4713.892	96			
Corrected Total	3503.058	95			

a R Squared = .928 (Adjusted R Squared = .905)

APPENDIX A-27

3-WAY (COLOR X DAY X PLOIDY) ANOVA FOR LYCOPENE DEVELOPMENT, YEAR 2 .

Source	Type III Sum of Squares	df	Mean Square	F	Sig.
Corrected Model	146539.947(a)	23	6371.302	102.087	.000
Intercept	45959.489	1	45959.489	736.407	.000
color	44777.342	2	22388.671	358.733	.000
DPP	24877.129	4	6219.282	99.651	.000
ploidy	1430.424	1	1430.424	22.920	.000
color * DPP	30740.837	8	3842.605	61.570	.000
color * ploidy	1666.970	1	1666.970	26.710	.000
DPP * ploidy	692.110	4	173.028	2.772	.033
color * DPP * ploidy	640.300	3	213.433	3.420	.022
Error	4680.786	75	62.410		
Total	193002.381	99			
Corrected Total	151220.733	98			

a R Squared = .969 (Adjusted R Squared = .960)

APPENDIX A-28

3-WAY (COLOR X DAY X PLOIDY) ANOVA FOR β-CAROTENE DEVELOPMENT, YEAR 2 .

Source	Type III Sum of Squares	df	Mean Square	F	Sig.
Corrected Model	277.582(a)	23	12.069	2.638	.001
Intercept	132.766	1	132.766	29.022	.000
color	7.826	2	3.913	.855	.429
DPP	163.401	4	40.850	8.930	.000
ploidy	.231	1	.231	.050	.823
color * DPP	27.821	8	3.478	.760	.639
color * ploidy	4.072	1	4.072	.890	.348
DPP * ploidy	2.078	4	.519	.114	.977
color * DPP * ploidy	10.097	3	3.366	.736	.534
Error	347.668	76	4.575		
Total	790.630	100			
Corrected Total	625.250	99			

a R Squared = .444 (Adjusted R Squared = .276)

APPENDIX A-29

3-WAY (COLOR X DAY X PLOIDY) ANOVA FOR LUTEIN DEVELOPMENT, YEAR 2 .

Source	Type III Sum of Squares	df	Mean Square	F	Sig.
Corrected Model	8.286(a)	32	.259	14.846	.000
Intercept	2.835	1	2.835	162.553	.000
color	2.061	3	.687	39.394	.000
DPP	1.393	4	.348	19.970	.000
ploidy	.493	1	.493	28.294	.000
color * DPP	2.195	12	.183	10.487	.000
color * ploidy	.160	2	.080	4.586	.012
DPP * ploidy	.114	4	.028	1.630	.172
color * DPP * ploidy	.143	6	.024	1.367	.235
Error	1.814	104	.017		
Total	13.898	137			
Corrected Total	10.100	136			

a R Squared = .820 (Adjusted R Squared = .765)

APPENDIX A-30

3-WAY (COLOR X DAY X PLOIDY) ANOVA FOR VIOLAXANTHIN DEVELOPMENT, YEAR 2.

Source	Type III Sum of Squares	df	Mean Square	F	Sig.
Corrected Model	1.456(a)	32	.046	10.255	.000
Intercept	.491	1	.491	110.598	.000
color	.598	3	.199	44.908	.000
ploidy	.079	1	.079	17.831	.000
DPP	.070	4	.017	3.925	.005
color * ploidy	.134	2	.067	15.070	.000
color * DPP	.124	12	.010	2.335	.011
ploidy * DPP	.039	4	.010	2.193	.075
color * ploidy * DPP	.107	6	.018	4.033	.001
Error	.453	102	.004		
Total	2.418	135			
Corrected Total	1.909	134			

a R Squared = .763 (Adjusted R Squared = .688)

APPENDIX A-31

2-WAY (COLOR X DAY) ANOVA (SEPARATED BY PLOIDY) FOR DIPLOID PHYTOENE DEVELOPMENT, YEAR 2. NULL HYPOTHESIS: PHYTOENE DEVELOPMENT PATTERN IS THE SAME AMONG DIPLOIDS FOR ALL COLORS.

Source	Type III Sum of Squares	df	Mean Square	F	Sig.
Corrected Model	1917.267(a)	13	147.482	6.759	.000
Intercept	2364.517	1	2364.517	108.368	.000
color	112.214	2	56.107	2.571	.087
DPP	1504.588	4	376.147	17.239	.000
color * DPP	207.773	7	29.682	1.360	.244
Error	1025.504	47	21.819		
Total	5498.227	61			
Corrected Total	2942.771	60			

a R Squared = .652 (Adjusted R Squared = .555)
b ploidy = 2n

APPENDIX A-32

2-WAY (COLOR X DAY) ANOVA (SEPARATED BY PLOIDY) FOR TRIPLOID PHYTOENE DEVELOPMENT, YEAR 2. NULL HYPOTHESIS: PHYTOENE DEVELOPMENT PATTERN IS THE SAME AMONG TRIPLOIDS FOR ALL COLORS.

Source	Type III Sum of Squares	df	Mean Square	F	Sig.
Corrected Model	14944.021(a)	9	1660.447	23.740	.000
Intercept	8557.842	1	8557.842	122.355	.000
color	3674.655	1	3674.655	52.538	.000
DPP	6529.487	4	1632.372	23.339	.000
color * DPP	3543.883	4	885.971	12.667	.000
Error	1818.504	26	69.942		
Total	26281.129	36			
Corrected Total	16762.525	35			

a R Squared = .892 (Adjusted R Squared = .854)
b ploidy = 3n

APPENDIX A-33

2-WAY (COLOR X DAY) ANOVA (SEPARATED BY PLOIDY) FOR DIPLOID ζ-CAROTENE DEVELOPMENT, YEAR 2. NULL HYPOTHESIS: ζ-CAROTENE DEVELOPMENT PATTERN IS THE SAME AMONG DIPLOIDS FOR ALL COLORS.

Source	Type III Sum of Squares	df	Mean Square	F	Sig.
Corrected Model	83.489(a)	13	6.422	7.179	.000
Intercept	84.107	1	84.107	94.015	.000
color	1.512	2	.756	.845	.436
DPP	53.323	4	13.331	14.901	.000
color * DPP	5.902	7	.843	.942	.484
Error	41.152	46	.895		
Total	231.067	60			
Corrected Total	124.641	59			

a R Squared = .670 (Adjusted R Squared = .577)
b ploidy = 2n

APPENDIX A-34

2-WAY (COLOR X DAY) ANOVA (SEPARATED BY PLOIDY) FOR TRIPLOID ζ-CAROTENE DEVELOPMENT, YEAR 2. NULL HYPOTHESIS: ζ-CAROTENE DEVELOPMENT PATTERN IS THE SAME AMONG TRIPLOIDS FOR ALL COLORS.

Source	Type III Sum of Squares	df	Mean Square	F	Sig.
Corrected Model	190.770(a)	9	21.197	13.872	.000
Intercept	185.946	1	185.946	121.689	.000
color	21.606	1	21.606	14.139	.001
DPP	112.010	4	28.003	18.326	.000
color * DPP	33.996	4	8.499	5.562	.002
Error	39.729	26	1.528		
Total	439.398	36			
Corrected Total	230.499	35			

a R Squared = .828 (Adjusted R Squared = .768)
b ploidy = 3n

APPENDIX A-35

2-WAY (COLOR X DAY) ANOVA (SEPARATED BY PLOIDY) FOR DIPLOID PRONEUROSPORENE DEVELOPMENT, YEAR 2. NULL HYPOTHESIS: PRONEUROSPORENE DEVELOPMENT PATTERN IS THE SAME AMONG DIPLOIDS FOR ALL COLORS.

Source	Type III Sum of Squares	df	Mean Square	F	Sig.
Corrected Model	14.416(a)	13	1.109	22.617	.000
Intercept	9.871	1	9.871	201.330	.000
color	2.765	2	1.383	28.197	.000
DPP	6.138	4	1.535	31.299	.000
color * DPP	2.366	7	.338	6.893	.000
Error	2.304	47	.049		
Total	29.887	61			
Corrected Total	16.721	60			

a R Squared = .862 (Adjusted R Squared = .824)
b ploidy = 2n

APPENDIX A-36

2-WAY (COLOR X DAY) ANOVA (SEPARATED BY PLOIDY) FOR TRIPLOID PRONEUROSPORENE DEVELOPMENT, YEAR 2. NULL HYPOTHESIS: PRONEUROSPORENE DEVELOPMENT PATTERN IS THE SAME AMONG TRIPLOIDS FOR ALL COLORS.

Source	Type III Sum of Squares	df	Mean Square	F	Sig.
Corrected Model	47.428(a)	9	5.270	17.110	.000
Intercept	22.232	1	22.232	72.182	.000
color	22.232	1	22.232	72.182	.000
DPP	8.215	4	2.054	6.668	.001
color * DPP	8.215	4	2.054	6.668	.001
Error	7.700	25	.308		
Total	78.270	35			
Corrected Total	55.128	34			

a R Squared = .860 (Adjusted R Squared = .810)
b ploidy = 3n

APPENDIX A-37

2-WAY (COLOR X DAY) ANOVA (SEPARATED BY PLOIDY) FOR DIPLOID PROLYCOPENE DEVELOPMENT, YEAR 2. NULL HYPOTHESIS: PROLYCOPENE DEVELOPMENT PATTERN IS THE SAME AMONG DIPLOIDS FOR ALL COLORS.

Source	Type III Sum of Squares	df	Mean Square	F	Sig.
Corrected Model	357.281(a)	13	27.483	24.660	.000
Intercept	271.055	1	271.055	243.210	.000
color	112.128	2	56.064	50.305	.000
DPP	184.538	4	46.134	41.395	.000
color * DPP	106.390	7	15.199	13.637	.000
Error	52.381	47	1.114		
Total	681.451	61			
Corrected Total	409.662	60			

a R Squared = .872 (Adjusted R Squared = .837)
b ploidy = 2n

APPENDIX A-38

2-WAY (COLOR X DAY) ANOVA (SEPARATED BY PLOIDY) FOR TRIPLOID PROLYCOPENE DEVELOPMENT, YEAR 2. NULL HYPOTHESIS: PROLYCOPENE DEVELOPMENT PATTERN IS THE SAME AMONG TRIPLOIDS FOR ALL COLORS.

Source	Type III Sum of Squares	df	Mean Square	F	Sig.
Corrected Model	2545.232(a)	9	282.804	35.190	.000
Intercept	1337.453	1	1337.453	166.422	.000
color	1337.453	1	1337.453	166.422	.000
DPP	408.579	4	102.145	12.710	.000
color * DPP	408.579	4	102.145	12.710	.000
Error	200.913	25	8.037		
Total	4032.441	35			
Corrected Total	2746.145	34			

a R Squared = .927 (Adjusted R Squared = .900)
b ploidy = 3n

APPENDIX A-39

2-WAY (COLOR X DAY) ANOVA (SEPARATED BY PLOIDY) FOR DIPLOID LYCOPENE DEVELOPMENT, YEAR 2. NULL HYPOTHESIS: LYCOPENE DEVELOPMENT PATTERN IS THE SAME AMONG DIPLOIDS FOR ALL COLORS.

Source	Type III Sum of Squares	df	Mean Square	F	Sig.
Corrected Model	34495.292(a)	13	2653.484	52.931	.000
Intercept	10638.016	1	10638.016	212.204	.000
color	15555.802	2	7777.901	155.151	.000
DPP	8863.959	4	2215.990	44.204	.000
color * DPP	13011.223	7	1858.746	37.078	.000
Error	2506.555	50	50.131		
Total	42413.656	64			
Corrected Total	37001.847	63			

a R Squared = .932 (Adjusted R Squared = .915)
b ploidy = 2n

APPENDIX A-40

2-WAY (COLOR X DAY) ANOVA (SEPARATED BY PLOIDY) FOR TRIPLOID LYCOPENE DEVELOPMENT, YEAR 2. NULL HYPOTHESIS: LYCOPENE DEVELOPMENT PATTERN IS THE SAME AMONG TRIPLOIDS FOR ALL COLORS.

Source	Type III Sum of Squares	df	Mean Square	F	Sig.
Corrected Model	88732.688(a)	9	9859.188	113.364	.000
Intercept	39368.930	1	39368.930	452.676	.000
color	35287.959	1	35287.959	405.752	.000
DPP	20275.294	4	5068.824	58.283	.000
color * DPP	18328.752	4	4582.188	52.687	.000
Error	2174.232	25	86.969		
Total	150588.725	35			
Corrected Total	90906.920	34			

a R Squared = .976 (Adjusted R Squared = .967)
b ploidy = 3n

APPENDIX A-41

2-WAY (COLOR X DAY) ANOVA (SEPARATED BY PLOIDY) FOR DIPLOID β-CAROTENE DEVELOPMENT, YEAR 2. NULL HYPOTHESIS: β-CAROTENE DEVELOPMENT PATTERN IS THE SAME AMONG DIPLOIDS FOR ALL COLORS.

Source	Type III Sum of Squares	df	Mean Square	F	Sig.
Corrected Model	175.762(a)	13	13.520	2.123	.029
Intercept	65.299	1	65.299	10.255	.002
color	12.019	2	6.009	.944	.396
DPP	96.014	4	24.004	3.770	.009
color * DPP	38.382	7	5.483	.861	.543
Error	318.389	50	6.368		
Total	567.746	64			
Corrected Total	494.151	63			

a R Squared = .356 (Adjusted R Squared = .188)
b ploidy = 2n

APPENDIX A-42

2-WAY (COLOR X DAY) ANOVA (SEPARATED BY PLOIDY) FOR TRIPLOID β-CAROTENE DEVELOPMENT, YEAR 2. NULL HYPOTHESIS: β-CAROTENE DEVELOPMENT PATTERN IS THE SAME AMONG TRIPLOIDS FOR ALL COLORS.

Source	Type III Sum of Squares	df	Mean Square	F	Sig.
Corrected Model	93.705(a)	9	10.412	9.246	.000
Intercept	72.784	1	72.784	64.633	.000
color	2.066	1	2.066	1.834	.187
DPP	85.479	4	21.370	18.977	.000
color * DPP	2.724	4	.681	.605	.663
Error	29.279	26	1.126		
Total	222.884	36			
Corrected Total	122.984	35			

a R Squared = .762 (Adjusted R Squared = .680)
b ploidy = 3n

APPENDIX A-43

2-WAY (COLOR X DAY) ANOVA (SEPARATED BY PLOIDY) FOR DIPLOID LUTEIN DEVELOPMENT, YEAR 2. NULL HYPOTHESIS: LUTEIN DEVELOPMENT PATTERN IS THE SAME AMONG DIPLOIDS FOR ALL COLORS.

Source	Type III Sum of Squares	df	Mean Square	F	Sig.
Corrected Model	2.702(a)	17	.159	17.435	.000
Intercept	.376	1	.376	41.193	.000
color	.590	3	.197	21.573	.000
DPP	.540	4	.135	14.819	.000
color * DPP	1.110	10	.111	12.172	.000
Error	.584	64	.009		
Total	4.165	82			
Corrected Total	3.286	81			

a R Squared = .822 (Adjusted R Squared = .775)
b ploidy = 2n

APPENDIX A-44

2-WAY (COLOR X DAY) ANOVA (SEPARATED BY PLOIDY) FOR TRIPLOID LUTEIN DEVELOPMENT, YEAR 2. NULL HYPOTHESIS: LUTEIN DEVELOPMENT PATTERN IS THE SAME AMONG TRIPLOIDS FOR ALL COLORS.

Source	Type III Sum of Squares	df	Mean Square	F	Sig.
Corrected Model	4.774(a)	14	.341	11.086	.000
Intercept	3.297	1	3.297	107.173	.000
color	1.778	2	.889	28.894	.000
DPP	1.174	4	.294	9.542	.000
color * DPP	1.339	8	.167	5.440	.000
Error	1.230	40	.031		
Total	9.733	55			
Corrected Total	6.005	54			

a R Squared = .795 (Adjusted R Squared = .723)
b ploidy = 3n

APPENDIX A-45

2-WAY (COLOR X DAY) ANOVA (SEPARATED BY PLOIDY) FOR DIPLOID VIOLAXANTHIN DEVELOPMENT, YEAR 2. NULL HYPOTHESIS: VIOLAXANTHIN DEVELOPMENT PATTERN IS THE SAME AMONG DIPLOIDS FOR ALL COLORS.

Source	Type III Sum of Squares	df	Mean Square	F	Sig.
Corrected Model	.140(a)	17	.008	9.935	.000
Intercept	.045	1	.045	53.932	.000
color	.081	3	.027	32.630	.000
DPP	.023	4	.006	6.901	.000
color * DPP	.032	10	.003	3.815	.000
Error	.051	62	.001		
Total	.245	80			
Corrected Total	.192	79			

a R Squared = .731 (Adjusted R Squared = .658)
b ploidy = 2n

APPENDIX A-46

2-WAY (COLOR X DAY) ANOVA (SEPARATED BY PLOIDY) FOR TRIPLOID VIOLAXANTHIN DEVELOPMENT, YEAR 2. NULL HYPOTHESIS: VIOLAXANTHIN DEVELOPMENT PATTERN IS THE SAME AMONG TRIPLOIDS FOR ALL COLORS.

Source	Type III Sum of Squares	df	Mean Square	F	Sig.
Corrected Model	1.067(a)	14	.076	7.595	.000
Intercept	.559	1	.559	55.692	.000
color	.723	2	.361	36.033	.000
DPP	.085	4	.021	2.125	.096
color * DPP	.191	8	.024	2.375	.034
Error	.401	40	.010		
Total	2.173	55			
Corrected Total	1.468	54			

a R Squared = .727 (Adjusted R Squared = .631)
b ploidy = 3n

APPENDIX A-47

2-WAY (PLOIDY X DAY) ANOVA (SEPARATED BY COLOR) FOR PHYTOENE DEVELOPMENT IN ORANGE WATERMELON, YEAR 2. NULL HYPOTHESIS: PHYTOENE DEVELOPMENT PATTERN IS THE SAME AMONG PLOIDIES FOR ORANGE FLESH WATERMELONS.

Source	Type III Sum of Squares	df	Mean Square	F	Sig.
Corrected Model	14345.685(a)	9	1593.965	21.829	.000
Intercept	9833.758	1	9833.758	134.673	.000
DPP	7343.105	4	1835.776	25.141	.000
ploidy	2796.836	1	2796.836	38.303	.000
DPP * ploidy	2924.597	4	731.149	10.013	.000
Error	1825.490	25	73.020		
Total	27517.296	35			
Corrected Total	16171.175	34			

a R Squared = .887 (Adjusted R Squared = .846)
b color = O

APPENDIX A-48

2-WAY (PLOIDY X DAY) ANOVA (SEPARATED BY COLOR) FOR PHYTOENE DEVELOPMENT IN RED WATERMELON, YEAR 2. NULL HYPOTHESIS: PHYTOENE DEVELOPMENT PATTERN IS THE SAME AMONG PLOIDIES FOR RED FLESH WATERMELONS.

Source	Type III Sum of Squares	df	Mean Square	F	Sig.
Corrected Model	720.252(a)	8	90.032	2.650	.030
Intercept	904.574	1	904.574	26.627	.000
DPP	678.682	4	169.671	4.994	.004
ploidy	.862	1	.862	.025	.875
DPP * ploidy	37.428	3	12.476	.367	.777
Error	849.307	25	33.972		
Total	2503.537	34			
Corrected Total	1569.559	33			

a R Squared = .459 (Adjusted R Squared = .286)
b color = R

APPENDIX A-49

2-WAY (PLOIDY X DAY) ANOVA (SEPARATED BY COLOR) FOR ζ-CAROTENE DEVELOPMENT IN ORANGE WATERMELON, YEAR 2. NULL HYPOTHESIS: ζ-CAROTENE DEVELOPMENT PATTERN IS THE SAME AMONG PLOIDIES FOR ORANGE FLESH WATERMELONS.

Source	Type III Sum of Squares	df	Mean Square	F	Sig.
Corrected Model	184.884(a)	9	20.543	12.757	.000
Intercept	170.540	1	170.540	105.905	.000
DPP	111.690	4	27.922	17.340	.000
ploidy	24.708	1	24.708	15.344	.001
DPP * ploidy	30.491	4	7.623	4.734	.006
Error	38.647	24	1.610		
Total	434.086	34			
Corrected Total	223.531	33			

a R Squared = .827 (Adjusted R Squared = .762)
b color = O

APPENDIX A-50

2-WAY (PLOIDY X DAY) ANOVA (SEPARATED BY COLOR) FOR ζ-CAROTENE DEVELOPMENT IN RED WATERMELON, YEAR 2. NULL HYPOTHESIS: ζ-CAROTENE DEVELOPMENT PATTERN IS THE SAME AMONG PLOIDIES FOR RED FLESH WATERMELONS.

Source	Type III Sum of Squares	df	Mean Square	F	Sig.
Corrected Model	37.920(a)	8	4.740	33.111	.000
Intercept	44.785	1	44.785	312.840	.000
DPP	28.672	4	7.168	50.071	.000
ploidy	2.029	1	2.029	14.177	.001
DPP * ploidy	1.455	3	.485	3.388	.034
Error	3.579	25	.143		
Total	80.640	34			
Corrected Total	41.499	33			

a R Squared = .914 (Adjusted R Squared = .886)
b color = R

APPENDIX A-51

2-WAY (PLOIDY X DAY) ANOVA (SEPARATED BY COLOR) FOR PRONEUROSPORENE DEVELOPMENT IN ORANGE WATERMELON, YEAR 2. NULL HYPOTHESIS: PRONEUROSPORENE DEVELOPMENT PATTERN IS THE SAME AMONG PLOIDIES FOR ORANGE FLESH WATERMELONS.

Source	Type III Sum of Squares	df	Mean Square	F	Sig.
Corrected Model	34.210(a)	9	3.801	10.626	.000
Intercept	44.203	1	44.203	123.565	.000
DPP	17.010	4	4.253	11.888	.000
ploidy	7.389	1	7.389	20.655	.000
DPP * ploidy	3.520	4	.880	2.460	.073
Error	8.585	24	.358		
Total	95.322	34			
Corrected Total	42.795	33			

a R Squared = .799 (Adjusted R Squared = .724) b color = O

APPENDIX A-52

2-WAY (PLOIDY X DAY) ANOVA (SEPARATED BY COLOR) FOR PROLYCOPENE DEVELOPMENT IN ORANGE WATERMELON, YEAR 2. NULL HYPOTHESIS: PROLYCOPENE DEVELOPMENT PATTERN IS THE SAME AMONG PLOIDIES FOR ORANGE FLESH WATERMELONS.

Source	Type III Sum of Squares	df	Mean Square	F	Sig.
Corrected Model	1925.439(a)	9	213.938	22.478	.000
Intercept	2285.292	1	2285.292	240.112	.000
DPP	717.665	4	179.416	18.851	.000
ploidy	617.336	1	617.336	64.863	.000
DPP * ploidy	205.704	4	51.426	5.403	.003
Error	228.422	24	9.518		
Total	4544.508	34			
Corrected Total	2153.861	33			

a R Squared = .894 (Adjusted R Squared = .854)
b color = O

APPENDIX A-53

2-WAY (PLOIDY X DAY) ANOVA (SEPARATED BY COLOR) FOR LYCOPENE DEVELOPMENT IN ORANGE WATERMELON, YEAR 2. NULL HYPOTHESIS: LYCOPENE DEVELOPMENT PATTERN IS THE SAME AMONG PLOIDIES FOR ORANGE FLESH WATERMELONS.

Source	Type III Sum of Squares	df	Mean Square	F	Sig.
Corrected Model	97.600(a)	9	10.844	6.654	.000
Intercept	80.268	1	80.268	49.252	.000
DPP	79.096	4	19.774	12.133	.000
ploidy	2.696	1	2.696	1.654	.209
DPP * ploidy	1.823	4	.456	.280	.889
Error	44.003	27	1.630		
Total	252.929	37			
Corrected Total	141.602	36			

a R Squared = .689 (Adjusted R Squared = .586)
b color = O

APPENDIX A-54

2-WAY (PLOIDY X DAY) ANOVA (SEPARATED BY COLOR) FOR LYCOPENE DEVELOPMENT IN RED WATERMELON, YEAR 2. NULL HYPOTHESIS: LYCOPENE DEVELOPMENT PATTERN IS THE SAME AMONG PLOIDIES FOR RED FLESH WATERMELONS.

Source	Type III Sum of Squares	df	Mean Square	F	Sig.
Corrected Model	77976.477(a)	8	9747.060	52.585	.000
Intercept	98032.460	1	98032.460	528.883	.000
DPP	64192.412	4	16048.103	86.579	.000
ploidy	3572.605	1	3572.605	19.274	.000
DPP * ploidy	1494.447	3	498.149	2.688	.068
Error	4633.940	25	185.358		
Total	192655.020	34			
Corrected Total	82610.417	33			

a R Squared = .944 (Adjusted R Squared = .926)
b color = R

APPENDIX A-55

2-WAY (PLOIDY X DAY) ANOVA (SEPARATED BY COLOR) FOR β-CAROTENE DEVELOPMENT IN ORANGE WATERMELON, YEAR 2. NULL HYPOTHESIS: β-CAROTENE DEVELOPMENT PATTERN IS THE SAME AMONG PLOIDIES FOR ORANGE FLESH WATERMELONS.

Source	Type III Sum of Squares	df	Mean Square	F	Sig.
Corrected Model	167.124(a)	9	18.569	1.602	.163
Intercept	64.673	1	64.673	5.579	.025
DPP	136.903	4	34.226	2.952	.037
ploidy	.851	1	.851	.073	.788
DPP * ploidy	11.082	4	2.770	.239	.914
Error	324.600	28	11.593		
Total	592.199	38			
Corrected Total	491.725	37			

a R Squared = .340 (Adjusted R Squared = .128)
b color = O

APPENDIX A-56

2-WAY (PLOIDY X DAY) ANOVA (SEPARATED BY COLOR) FOR β-CAROTENE DEVELOPMENT IN RED WATERMELON, YEAR 2. NULL HYPOTHESIS: β-CAROTENE DEVELOPMENT PATTERN IS THE SAME AMONG PLOIDIES FOR RED FLESH WATERMELONS.

Source	Type III Sum of Squares	df	Mean Square	F	Sig.
Corrected Model	80.714(a)	8	10.089	11.512	.000
Intercept	63.591	1	63.591	72.557	.000
DPP	62.432	4	15.608	17.809	.000
ploidy	2.793	1	2.793	3.187	.086
DPP * ploidy	2.882	3	.961	1.096	.369
Error	21.911	25	.876		
Total	175.099	34			
Corrected Total	102.625	33			

a R Squared = .786 (Adjusted R Squared = .718)
b color = R

APPENDIX A-57

2-WAY (PLOIDY X DAY) ANOVA (SEPARATED BY COLOR) FOR LUTEIN DEVELOPMENT IN CANARY YELLOW WATERMELON, YEAR 2. NULL HYPOTHESIS: LUTEIN DEVELOPMENT PATTERN IS THE SAME AMONG PLOIDIES FOR CANARY YELLOW FLESH WATERMELONS.

Source	Type III Sum of Squares	df	Mean Square	F	Sig.
Corrected Model	1.042(a)	8	.130	6.155	.000
Intercept	.856	1	.856	40.473	.000
DPP	.724	4	.181	8.550	.000
ploidy	.167	1	.167	7.901	.009
DPP * ploidy	.112	3	.037	1.766	.176
Error	.614	29	.021		
Total	2.754	38			
Corrected Total	1.656	37			

a R Squared = .629 (Adjusted R Squared = .527) b color = CY

APPENDIX A-58

2-WAY (PLOIDY X DAY) ANOVA (SEPARATED BY COLOR) FOR LUTEIN DEVELOPMENT IN ORANGE WATERMELON, YEAR 2. NULL HYPOTHESIS: LUTEIN DEVELOPMENT PATTERN IS THE SAME AMONG PLOIDIES FOR ORANGE FLESH WATERMELONS.

Source	Type III Sum of Squares	df	Mean Square	F	Sig.
Corrected Model	4.158(a)	9	.462	13.177	.000
Intercept	3.755	1	3.755	107.112	.000
DPP	3.117	4	.779	22.225	.000
ploidy	.579	1	.579	16.508	.000
DPP * ploidy	.121	4	.030	.863	.499
Error	.947	27	.035		
Total	10.640	37			
Corrected Total	5.104	36			

a R Squared = .815 (Adjusted R Squared = .753)
b color = O

APPENDIX A-59

2-WAY (PLOIDY X DAY) ANOVA (SEPARATED BY COLOR) FOR LUTEIN DEVELOPMENT IN RED WATERMELON, YEAR 2. NULL HYPOTHESIS: LUTEIN DEVELOPMENT PATTERN IS THE SAME AMONG PLOIDIES FOR RED FLESH WATERMELONS.

Source	Type III Sum of Squares	df	Mean Square	F	Sig.
Corrected Model	.164(a)	8	.020	10.715	.000
Intercept	.017	1	.017	8.927	.006
DPP	.100	4	.025	13.045	.000
ploidy	.008	1	.008	4.217	.051
DPP * ploidy	.025	3	.008	4.345	.014
Error	.048	25	.002		
Total	.252	34			
Corrected Total	.212	33			

a R Squared = .774 (Adjusted R Squared = .702)
b color = R

APPENDIX A-60

2-WAY (PLOIDY X DAY) ANOVA (SEPARATED BY COLOR) FOR VIOLAXANTHIN DEVELOPMENT IN CANARY YELLOW WATERMELON, YEAR 2. NULL HYPOTHESIS: VIOLAXANTHIN DEVELOPMENT PATTERN IS THE SAME AMONG PLOIDIES FOR CANARY YELLOW FLESH WATERMELONS.

Source	Type III Sum of Squares	df	Mean Square	F	Sig.
Corrected Model	.619(a)	8	.077	5.174	.000
Intercept	1.201	1	1.201	80.339	.000
DPP	.145	4	.036	2.433	.070
ploidy	.270	1	.270	18.054	.000
DPP * ploidy	.130	3	.043	2.902	.052
Error	.433	29	.015		
Total	2.298	38			
Corrected Total	1.052	37			

a R Squared = .588 (Adjusted R Squared = .474)
b color = CY

APPENDIX A-61

2-WAY (PLOIDY X DAY) ANOVA (SEPARATED BY COLOR) FOR VIOLAXANTHIN DEVELOPMENT IN ORANGE WATERMELON, YEAR 2. NULL HYPOTHESIS: VIOLAXANTHIN DEVELOPMENT PATTERN IS THE SAME AMONG PLOIDIES FOR ORANGE FLESH WATERMELONS.

Source	Type III Sum of Squares	df	Mean Square	F	Sig.
Corrected Model	.062(a)	9	.007	15.878	.000
Intercept	.020	1	.020	46.876	.000
DPP	.037	4	.009	21.621	.000
ploidy	.010	1	.010	23.633	.000
DPP * ploidy	.019	4	.005	11.239	.000
Error	.011	25	.000		
Total	.094	35			
Corrected Total	.073	34			

a R Squared = .851 (Adjusted R Squared = .798)
b color = O

APPENDIX A-62

2-WAY (PLOIDY X DAY) ANOVA (SEPARATED BY COLOR) FOR VIOLAXANTHIN DEVELOPMENT IN RED WATERMELON, YEAR 2. NULL HYPOTHESIS: VIOLAXANTHIN DEVELOPMENT PATTERN IS THE SAME AMONG PLOIDIES FOR RED FLESH WATERMELONS.

Source	Type III Sum of Squares	df	Mean Square	F	Sig.
Corrected Model	.011(a)	8	.001	5.603	.000
Intercept	.002	1	.002	9.228	.006
DPP	.008	4	.002	7.961	.000
ploidy	5.38E-005	1	5.38E-005	.219	.644
DPP * ploidy	.001	3	.000	1.811	.171
Error	.006	25	.000		
Total	.021	34			
Corrected Total	.017	33			

a R Squared = .642 (Adjusted R Squared = .527)
b color = R

APPENDIX B

STATISTICAL ANALYSES FOR CHAPTER IV

Page

APPENDIX B-1

2-WAY (PLOIDY X DAY) ANOVA FOR PHYTOENE DEVELOPMENT IN DIXIE QUEEN AND SUMMER SWEET 5244 RED WATERMELONS. NULL HYPOTHESIS: PHYTOENE DEVELOPMENT PATTERN IS THE SAME IN DIXIE QUEEN AND SUMMER SWEET 5244 RED WATERMELONS.

Source	Type III Sum of Squares	df	Mean Square	F	Sig.
Corrected Model	720.252(a)	8	90.032	2.650	.030
Intercept	904.574	1	904.574	26.627	.000
DPP	678.682	4	169.671	4.994	.004
ploidy	.862	1	.862	.025	.875
DPP * ploidy	37.428	3	12.476	.367	.777
Error	849.307	25	33.972		
Total	2503.537	34			
Corrected Total	1569.559	33			

a R Squared = .459 (Adjusted R Squared = .286)
b R2color = R

APPENDIX B-2

2-WAY (PLOIDY X DAY) ANOVA FOR PHYTOENE DEVELOPMENT IN HNP19-2N AND HNP19-3N RED WATERMELONS. NULL HYPOTHESIS: PHYTOENE DEVELOPMENT PATTERN IS THE SAME IN HNP19-2N AND HNP19-3N RED WATERMELONS.

Source	Type III Sum of Squares	df	Mean Square	F	Sig.
Corrected Model	2900.447(a)	14	207.175	8.458	.000
Intercept	4725.533	1	4725.533	192.912	.000
DPP	1933.382	4	483.346	19.732	.000
ploidy	317.254	2	158.627	6.476	.003
DPP * ploidy	346.506	8	43.313	1.768	.103
Error	1371.763	56	24.496		
Total	9854.900	71			
Corrected Total	4272.210	70			

a R Squared = .679 (Adjusted R Squared = .599)
b R2color = R2

APPENDIX B-3

2-WAY (PLOIDY X DAY) ANOVA FOR ζ-CAROTENE DEVELOPMENT IN DIXIE QUEEN AND SUMMER SWEET 5244 RED WATERMELONS. NULL HYPOTHESIS: ζ-CAROTENE DEVELOPMENT PATTERN IS THE SAME IN DIXIE QUEEN AND SUMMER SWEET 5244 RED WATERMELONS.

Source	Type III Sum of Squares	df	Mean Square	F	Sig.
Corrected Model	37.920(a)	8	4.740	33.111	.000
Intercept	44.785	1	44.785	312.840	.000
DPP	28.672	4	7.168	50.071	.000
ploidy	2.029	1	2.029	14.177	.001
DPP * ploidy	1.455	3	.485	3.388	.034
Error	3.579	25	.143		
Total	80.640	34			
Corrected Total	41.499	33			

a R Squared = .914 (Adjusted R Squared = .886)
b R2color = R

APPENDIX B-4

2-WAY (PLOIDY X DAY) ANOVA FOR ζ-CAROTENE DEVELOPMENT IN HNP19-2N AND HNP19-3N RED WATERMELONS. NULL HYPOTHESIS: ζ-CAROTENE DEVELOPMENT PATTERN IS THE SAME IN HNP19-2N AND HNP19-3N RED WATERMELONS.

Source	Type III Sum of Squares	df	Mean Square	F	Sig.
Corrected Model	50.983(a)	14	3.642	3.702	.000
Intercept	77.123	1	77.123	78.407	.000
DPP	31.401	4	7.850	7.981	.000
ploidy	2.433	2	1.217	1.237	.298
DPP * ploidy	9.057	8	1.132	1.151	.345
Error	55.083	56	.984		
Total	204.737	71			
Corrected Total	106.066	70			

a R Squared = .481 (Adjusted R Squared = .351)
b R2color = R2

APPENDIX B-5

2-WAY (PLOIDY X DAY) ANOVA FOR LYCOPENE DEVELOPMENT IN DIXIE QUEEN AND SUMMER SWEET 5244 RED WATERMELONS. NULL HYPOTHESIS: LYCOPENE DEVELOPMENT PATTERN IS THE SAME IN DIXIE QUEEN AND SUMMER SWEET 5244 RED WATERMELONS.

Source	Type III Sum of Squares	df	Mean Square	F	Sig.
Corrected Model	77976.477(a)	8	9747.060	52.585	.000
Intercept	98032.460	1	98032.460	528.883	.000
DPP	64192.412	4	16048.103	86.579	.000
ploidy	3572.605	1	3572.605	19.274	.000
DPP * ploidy	1494.447	3	498.149	2.688	.068
Error	4633.940	25	185.358		
Total	192655.020	34			
Corrected Total	82610.417	33			

a R Squared = .944 (Adjusted R Squared = .926)
b R2color = R

APPENDIX B-6

2-WAY (PLOIDY X DAY) ANOVA FOR LYCOPENE DEVELOPMENT IN HNP19-2N AND HNP19-3N RED WATERMELONS. NULL HYPOTHESIS: LYCOPENE DEVELOPMENT PATTERN IS THE SAME IN HNP19-2N AND HNP19-3N RED WATERMELONS.

Source	Type III Sum of Squares	df	Mean Square	F	Sig.
Corrected Model	168857.518(a)	14	12061.251	12.999	.000
Intercept	273298.844	1	273298.844	294.540	.000
DPP	113176.153	4	28294.038	30.493	.000
ploidy	5765.022	2	2882.511	3.107	.053
DPP * ploidy	12093.806	8	1511.726	1.629	.137
Error	51961.553	56	927.885		
Total	576508.389	71			
Corrected Total	220819.071	70			

a R Squared = .765 (Adjusted R Squared = .706)
b R2color = R2

APPENDIX B-7

2-WAY (PLOIDY X DAY) ANOVA FOR β-CAROTENE DEVELOPMENT IN DIXIE QUEEN AND SUMMER SWEET 5244 RED WATERMELONS. NULL HYPOTHESIS: β-CAROTENE DEVELOPMENT PATTERN IS THE SAME IN DIXIE QUEEN AND SUMMER SWEET 5244 RED WATERMELONS.

Source	Type III Sum of Squares	df	Mean Square	F	Sig.
Corrected Model	80.714(a)	8	10.089	11.512	.000
Intercept	63.591	1	63.591	72.557	.000
DPP	62.432	4	15.608	17.809	.000
ploidy	2.793	1	2.793	3.187	.086
DPP * ploidy	2.882	3	.961	1.096	.369
Error	21.911	25	.876		
Total	175.099	34			
Corrected Total	102.625	33			

a R Squared = .786 (Adjusted R Squared = .718)
b R2color = R

APPENDIX B-8

2-WAY (PLOIDY X DAY) ANOVA FOR β-CAROTENE DEVELOPMENT IN HNP19-2N AND HNP19-3N RED WATERMELONS. NULL HYPOTHESIS: β-CAROTENE DEVELOPMENT PATTERN IS THE SAME IN HNP19-2N AND HNP19-3N RED WATERMELONS.

Source	Type III Sum of Squares	df	Mean Square	F	Sig.
Corrected Model	760.388(a)	14	54.313	16.978	.000
Intercept	574.039	1	574.039	179.443	.000
DPP	685.922	4	171.480	53.604	.000
ploidy	10.522	2	5.261	1.645	.202
DPP * ploidy	30.301	8	3.788	1.184	.325
Error	179.144	56	3.199		
Total	1607.411	71			
Corrected Total	939.532	70			

a R Squared = .809 (Adjusted R Squared = .762)
b R2color = R2

APPENDIX B-9

2-WAY (PLOIDY X DAY) ANOVA FOR LUTEIN DEVELOPMENT IN DIXIE QUEEN AND SUMMER SWEET 5244 RED WATERMELONS. NULL HYPOTHESIS: LUTEIN DEVELOPMENT PATTERN IS THE SAME IN DIXIE QUEEN AND SUMMER SWEET 5244 RED WATERMELONS.

Source	Type III Sum of Squares	df	Mean Square	F	Sig.
Corrected Model	.164(a)	8	.020	10.715	.000
Intercept	.017	1	.017	8.927	.006
DPP	.100	4	.025	13.045	.000
ploidy	.008	1	.008	4.217	.051
DPP * ploidy	.025	3	.008	4.345	.014
Error	.048	25	.002		
Total	.252	34			
Corrected Total	.212	33			

a R Squared = .774 (Adjusted R Squared = .702)
b R2color = R

APPENDIX B-10

2-WAY (PLOIDY X DAY) ANOVA FOR LUTEIN DEVELOPMENT IN HNP19-2N AND HNP19-3N RED WATERMELONS. NULL HYPOTHESIS: LUTEIN DEVELOPMENT PATTERN IS THE SAME IN HNP19-2N AND HNP19-3N RED WATERMELONS.

Source	Type III Sum of Squares	df	Mean Square	F	Sig.
Corrected Model	.417(a)	14	.030	33.753	.000
Intercept	.057	1	.057	64.741	.000
DPP	.253	4	.063	71.821	.000
ploidy	.016	2	.008	9.345	.000
DPP * ploidy	.092	8	.011	13.001	.000
Error	.049	56	.001		
Total	.533	71			
Corrected Total	.466	70			

a R Squared = .894 (Adjusted R Squared = .868)
b R2color = R2

APPENDIX B-11

2-WAY (PLOIDY X DAY) ANOVA FOR VIOLAXANTHIN DEVELOPMENT IN DIXIE QUEEN AND SUMMER SWEET 5244 RED WATERMELONS. NULL HYPOTHESIS: VIOLAXANTHIN DEVELOPMENT PATTERN IS THE SAME IN DIXIE QUEEN AND SUMMER SWEET 5244 RED WATERMELONS.

Source	Type III Sum of Squares	df	Mean Square	F	Sig.
Corrected Model	.011(a)	8	.001	5.603	.000
Intercept	.002	1	.002	9.228	.006
DPP	.008	4	.002	7.961	.000
ploidy	5.38E-005	1	5.38E-005	.219	.644
DPP * ploidy	.001	3	.000	1.811	.171
Error	.006	25	.000		
Total	.021	34			
Corrected Total	.017	33			

a R Squared = .642 (Adjusted R Squared = .527)
b R2color = R

APPENDIX B-12

2-WAY (PLOIDY X DAY) ANOVA FOR VIOLAXANTHIN DEVELOPMENT IN HNP19-2N AND HNP19-3N RED WATERMELONS (CHAPTER IV). NULL HYPOTHESIS: VIOLAXANTHIN DEVELOPMENT PATTERN IS THE SAME IN HNP19-2N AND HNP19-3N RED WATERMELONS.

Source	Type III Sum of Squares	df	Mean Square	F	Sig.
Corrected Model	.171(a)	14	.012	1.660	.091
Intercept	.038	1	.038	5.181	.027
DPP	.073	4	.018	2.465	.055
ploidy	.018	2	.009	1.230	.300
DPP * ploidy	.045	8	.006	.773	.628
Error	.412	56	.007		
Total	.636	71			
Corrected Total	.583	70			

a R Squared = .293 (Adjusted R Squared = .117)
b R2color = R2

APPENDIX B-13

2-WAY (PLOIDY X DAY) ANOVA FOR PHYTOENE DEVELOPMENT IN DIPLOID AND TRIPLOID VARIETIES OF RED WATERMELON. NULL HYPOTHESIS: PHYTOENE DEVELOPMENT PATTERN IS THE SAME IN DIPLOID AND TRIPLOID RED WATERMELONS, REGARDLESS OF GENOTYPE.

Source	Type III Sum of Squares	df	Mean Square	F	Sig.
Corrected Model	.034(a)	9	.004	8.770	.000
Intercept	.010	1	.010	22.749	.000
DPP	.034	4	.008	19.630	.000
ploidy	.000	1	.000	.460	.500
DPP * ploidy	.000	4	8.67E-005	.203	.936
Error	.032	74	.000		
Total	.074	84			
Corrected Total	.065	83			

a R Squared = .516 (Adjusted R Squared = .457)

APPENDIX B-14

2-WAY (PLOIDY X DAY) ANOVA FOR ζ-CAROTENE DEVELOPMENT IN DIPLOID AND TRIPLOID VARIETIES OF RED WATERMELON. NULL HYPOTHESIS: ζ-CAROTENE DEVELOPMENT PATTERN IS THE SAME IN DIPLOID AND TRIPLOID RED WATERMELONS, REGARDLESS OF GENOTYPE.

Source	Type III Sum of Squares	df	Mean Square	F	Sig.
Corrected Model	67.276(a)	9	7.475	17.384	.000
Intercept	108.376	1	108.376	252.033	.000
DPP	51.820	4	12.955	30.127	.000
ploidy	5.957	1	5.957	13.853	.000
DPP * ploidy	5.645	4	1.411	3.282	.016
Error	31.821	74	.430		
Total	208.834	84			
Corrected Total	99.096	83			

a R Squared = .679 (Adjusted R Squared = .640)

APPENDIX B-15

2-WAY (PLOIDY X DAY) ANOVA FOR LYCOPENE DEVELOPMENT IN DIPLOID AND TRIPLOID VARIETIES OF RED WATERMELON. NULL HYPOTHESIS: LYCOPENE DEVELOPMENT PATTERN IS THE SAME IN DIPLOID AND TRIPLOID RED WATERMELONS, REGARDLESS OF GENOTYPE.

Source	Type III Sum of Squares	df	Mean Square	F	Sig.
Corrected Model	213711.533(a)	9	23745.726	39.492	.000
Intercept	381613.653	1	381613.653	634.676	.000
DPP	185177.181	4	46294.295	76.994	.000
ploidy	11461.734	1	11461.734	19.062	.000
DPP * ploidy	5548.522	4	1387.131	2.307	.066
Error	44494.186	74	601.273		
Total	644798.744	84			
Corrected Total	258205.720	83			

a R Squared = .828 (Adjusted R Squared = .807)

APPENDIX B-16

2-WAY (PLOIDY X DAY) ANOVA FOR β-CAROTENE DEVELOPMENT IN DIPLOID AND TRIPLOID VARIETIES OF RED WATERMELON. NULL HYPOTHESIS: β-CAROTENE DEVELOPMENT PATTERN IS THE SAME IN DIPLOID AND TRIPLOID RED WATERMELONS, REGARDLESS OF GENOTYPE.

Source	Type III Sum of Squares	df	Mean Square	F	Sig.
Corrected Model	507.400(a)	9	56.378	15.444	.000
Intercept	496.931	1	496.931	136.130	.000
DPP	439.140	4	109.785	30.075	.000
ploidy	7.651	1	7.651	2.096	.152
DPP * ploidy	17.926	4	4.482	1.228	.306
Error	270.131	74	3.650		
Total	1261.466	84			
Corrected Total	777.530	83			

a R Squared = .653 (Adjusted R Squared = .610)

APPENDIX B-17

2-WAY (PLOIDY X DAY) ANOVA FOR LUTEIN DEVELOPMENT IN DIPLOID AND TRIPLOID VARIETIES OF RED WATERMELON. NULL HYPOTHESIS: LUTEIN DEVELOPMENT PATTERN IS THE SAME IN DIPLOID AND TRIPLOID RED WATERMELONS, REGARDLESS OF GENOTYPE.

Source	Type III Sum of Squares	df	Mean Square	F	Sig.
Corrected Model	.208(a)	9	.023	22.022	.000
Intercept	.043	1	.043	40.949	.000
DPP	.167	4	.042	39.797	.000
ploidy	.005	1	.005	4.702	.033
DPP * ploidy	.019	4	.005	4.570	.002
Error	.078	74	.001		
Total	.330	84			
Corrected Total	.286	83			

a R Squared = .728 (Adjusted R Squared = .695)

APPENDIX B-18

2-WAY (PLOIDY X DAY) ANOVA FOR VIOLAXANTHIN DEVELOPMENT IN DIPLOID AND TRIPLOID VARIETIES OF RED WATERMELON. NULL HYPOTHESIS: VIOLAXANTHIN DEVELOPMENT PATTERN IS THE SAME IN DIPLOID AND TRIPLOID RED WATERMELONS, REGARDLESS OF GENOTYPE.

Source	Type III Sum of Squares	df	Mean Square	F	Sig.
Corrected Model	.034(a)	9	.004	8.770	.000
Intercept	.010	1	.010	22.749	.000
DPP	.034	4	.008	19.630	.000
ploidy	.000	1	.000	.460	.500
DPP * ploidy	.000	4	8.67E-005	.203	.936
Error	.032	74	.000		
Total	.074	84			
Corrected Total	.065	83			

a R Squared = .516 (Adjusted R Squared = .457)

APPENDIX B-19

2-WAY (PLOIDY X DAY) ANOVA FOR PHYTOENE DEVELOPMENT IN RED WATERMELON OF ONE GENOTYPE (HNP19). NULL HYPOTHESIS: PHYTOENE DEVELOPMENT PATTERN IS THE SAME AT ALL PLOIDY LEVELS FOR HNP19.

Source	Type III Sum of Squares	df	Mean Square	F	Sig.
Corrected Model	2900.447(a)	14	207.175	8.458	.000
Intercept	4725.533	1	4725.533	192.912	.000
DPP	1933.382	4	483.346	19.732	.000
ploidy	317.254	2	158.627	6.476	.003
DPP * ploidy	346.506	8	43.313	1.768	.103
Error	1371.763	56	24.496		
Total	9854.900	71			
Corrected Total	4272.210	70			

a R Squared = .679 (Adjusted R Squared = .599)
b R2color = R2

APPENDIX B-20

2-WAY (PLOIDY X DAY) ANOVA FOR ζ-CAROTENE DEVELOPMENT IN RED WATERMELON OF ONE GENOTYPE (HNP19). NULL HYPOTHESIS: ζ-CAROTENE DEVELOPMENT PATTERN IS THE SAME AT ALL PLOIDY LEVELS FOR HNP19.

Source	Type III Sum of Squares	df	Mean Square	F	Sig.
Corrected Model	50.983(a)	14	3.642	3.702	.000
Intercept	77.123	1	77.123	78.407	.000
DPP	31.401	4	7.850	7.981	.000
ploidy	2.433	2	1.217	1.237	.298
DPP * ploidy	9.057	8	1.132	1.151	.345
Error	55.083	56	.984		
Total	204.737	71			
Corrected Total	106.066	70			

a R Squared = .481 (Adjusted R Squared = .351)
b R2color = R2

APPENDIX B-21

2-WAY (PLOIDY X DAY) ANOVA FOR LYCOPENE DEVELOPMENT IN RED WATERMELON OF ONE GENOTYPE (HNP19). NULL HYPOTHESIS: LYCOPENE DEVELOPMENT PATTERN IS THE SAME AT ALL PLOIDY LEVELS FOR HNP19.

Source	Type III Sum of Squares	df	Mean Square	F	Sig.
Corrected Model	168857.518(a)	14	12061.251	12.999	.000
Intercept	273298.844	1	273298.844	294.540	.000
DPP	113176.153	4	28294.038	30.493	.000
ploidy	5765.022	2	2882.511	3.107	.053
DPP * ploidy	12093.806	8	1511.726	1.629	.137
Error	51961.553	56	927.885		
Total	576508.389	71			
Corrected Total	220819.071	70			

a R Squared = .765 (Adjusted R Squared = .706)
b R2color = R2

APPENDIX B-22

2-WAY (PLOIDY X DAY) ANOVA FOR β-CAROTENE DEVELOPMENT IN RED WATERMELON OF ONE GENOTYPE (HNP19). NULL HYPOTHESIS: β-CAROTENE DEVELOPMENT PATTERN IS THE SAME AT ALL PLOIDY LEVELS FOR HNP19.

Source	Type III Sum of Squares	df	Mean Square	F	Sig.
Corrected Model	760.388(a)	14	54.313	16.978	.000
Intercept	574.039	1	574.039	179.443	.000
DPP	685.922	4	171.480	53.604	.000
ploidy	10.522	2	5.261	1.645	.202
DPP * ploidy	30.301	8	3.788	1.184	.325
Error	179.144	56	3.199		
Total	1607.411	71			
Corrected Total	939.532	70			

a R Squared = .809 (Adjusted R Squared = .762)
b R2color = R2

APPENDIX B-23

2-WAY (PLOIDY X DAY) ANOVA FOR LUTEIN DEVELOPMENT IN RED WATERMELON OF ONE GENOTYPE (HNP19). NULL HYPOTHESIS: LUTEIN DEVELOPMENT PATTERN IS THE SAME AT ALL PLOIDY LEVELS FOR HNP19.

Source	Type III Sum of Squares	df	Mean Square	F	Sig.
Corrected Model	.417(a)	14	.030	33.753	.000
Intercept	.057	1	.057	64.741	.000
DPP	.253	4	.063	71.821	.000
ploidy	.016	2	.008	9.345	.000
DPP * ploidy	.092	8	.011	13.001	.000
Error	.049	56	.001		
Total	.533	71			
Corrected Total	.466	70			

a R Squared = .894 (Adjusted R Squared = .868)
b R2color = R2

APPENDIX B-24

2-WAY (PLOIDY X DAY) ANOVA FOR VIOLAXANTHIN DEVELOPMENT IN RED WATERMELON OF ONE GENOTYPE (HNP19). NULL HYPOTHESIS: VIOLAXANTHIN DEVELOPMENT PATTERN IS THE SAME AT ALL PLOIDY LEVELS FOR HNP19.

Source	Type III Sum of Squares	df	Mean Square	F	Sig.
Corrected Model	.171(a)	14	.012	1.660	.091
Intercept	.038	1	.038	5.181	.027
DPP	.073	4	.018	2.465	.055
ploidy	.018	2	.009	1.230	.300
DPP * ploidy	.045	8	.006	.773	.628
Error	.412	56	.007		
Total	.636	71			
Corrected Total	.583	70			

a R Squared = .293 (Adjusted R Squared = .117)
b R2color = R2

APPENDIX C

STATISTICAL ANALYSES FOR CHAPTER V

CORRELATION STATISTICS FOR FIBER, CELL WALL, WHOLE FOOD, MEAL, AND DIGEST CHARACTERISTICS.

Correlation Components		Correlation Coefficient	Sig.
S. Hemi-cellulose	Cell Wall Description	0.782	0.022*
S. Pectin	Cell Wall Description	0.749	0.033*
S. Total	Cell Wall Description	0.914	0.001**
I. Cellulose	Minimal Cell Wall Thickness	0.818	0.013*
I. Hemi-cellulose	Minimal Cell Wall Thickness	0.774	0.024*
I. Pectin	Minimal Cell Wall Thickness	0.835	0.010**
I. Total	Minimal Cell Wall Thickness	0.783	0.022*
S. Hemi-cellulose	Cell Size	neg. 0.817	0.013*
S. Pectin	Cell Size	neg. 0.764	0.027*
S. Total	Cell Size	neg. 0.810	0.015*
I. Cellulose	Cell Size	neg. 0.778	0.023*
I. Hemi-cellulose	Cell Size	neg. 0.747	0.033*
I. Total	Cell Size	neg. 0.786	0.021*
Total Fiber	Cell Size	neg. 0.833	0.010*
Cell Wall Description	Cell Size	neg. 0.834	0.005**
Tubules (F)	Homogenous Granular (M)	0.750	0.020*
Tubules (F)	Tubules (D)	0.750	0.020*
Globules (F)	Vaculate/Empty/Vesicles	neg. 0.682	0.043*
Distinguish Lipids (M)	Vesicles (M)	neg. 0.756	0.018*
Homogenous Granular (M)	Tubules (D)	1.000	.
Short Fibers (M)	Fibrous, Stippled Background	1.000	.

Key

S = Soluble Fiber
I = Insoluble Fiber
(F) = In Whole Food
(M) = In Meal Fraction
(D) = In Digest Fraction
* Correlation is significant at the 0.05 level (2-tailed).
** Correlation is significant at the 0.01 level (2-tailed).

APPENDIX D

TITRATION EXPERIMENT FOR CHAPTER VI

APPENDIX D-1

TREATMENT LEVELS TESTED FOR TITRATION TO DETERMINE

APPROPRIATE LOAD FOR EACH FOOD.

	Treatment levels (g food/rxn)			
Butternut	0.6	1.2	2.4	4.8
Carrot	0.4	0.8	1.6	3.2
Grapefruit	1.2	2.4	4.8	9.6
Mango	5.0	10.0	15.0	20.0
Melon	3.2	4.8	7.2	10.8
Papaya	2.3	4.5	9.0	18.0
Sweet Potato	0.3	0.6	1.2	2.4
Tomato	0.8	1.5	3.0	4.5
Watermelon	1.0	2.0	4.0	8.0

APPENDIX D-2

FOOD LOAD USED IN BIOACCESSIBILITY EXPERIMENTS.

	Amount used in Experiments
Butternut	2.4 g
Carrot	1.2 g
Grapefruit	10.0 g
Mango	8.0 g
Melon	6.0 g
Papaya	7.0 g
Sweet Potato	1.0 g
Tomato	3.0 g
Watermelon	7.0 g

APPENDIX D-3

PERCENT TOTAL CAROTENOIDS MICELLULARIZED AT EACH TREATMENT LEVEL (TITRATION) IN NINE FRUITS AND VEGETABLES (FIGURES 3.1-3.9).

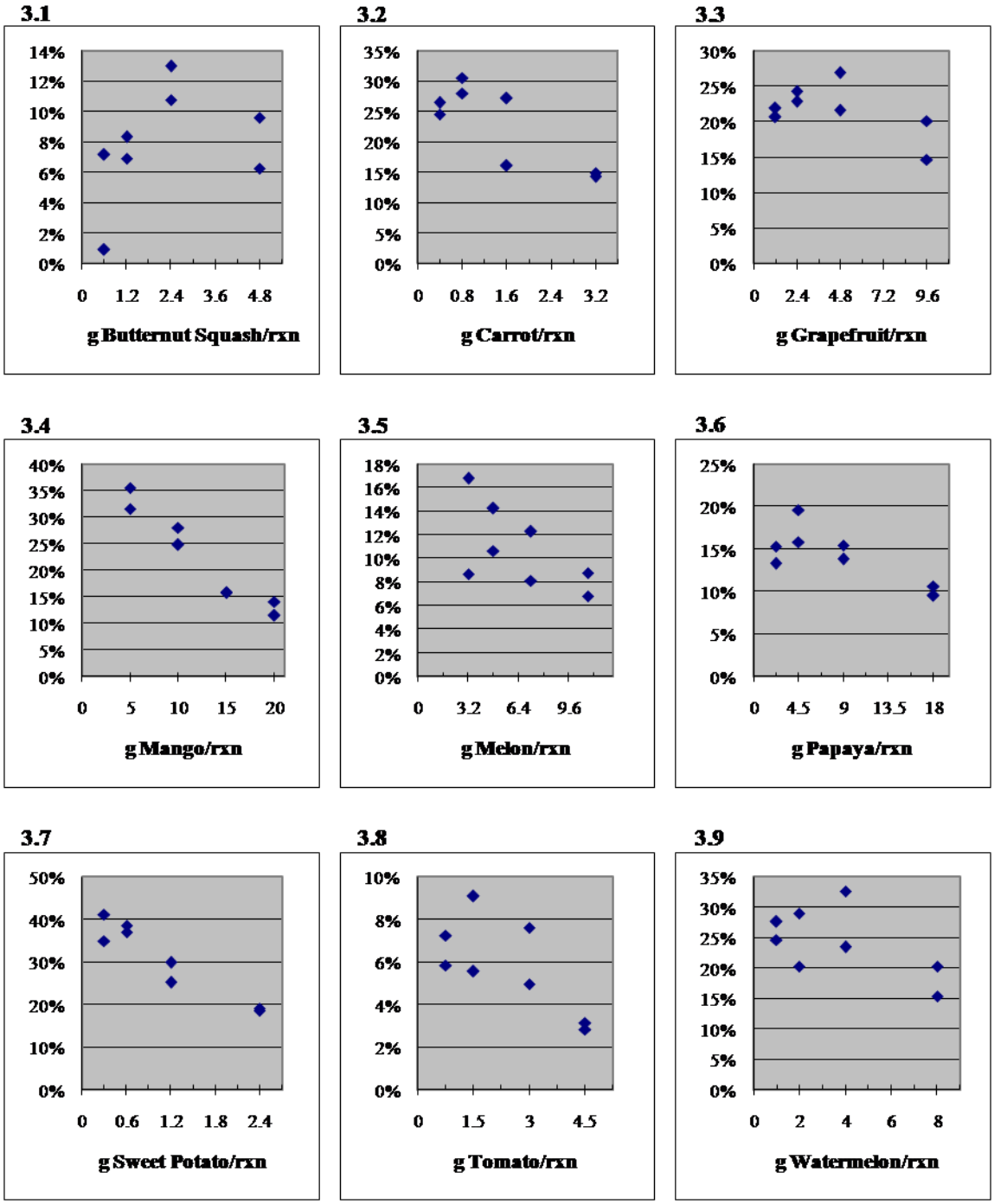

APPENDIX E

LABORATORY JOURNAL FOR CHAPTER VIII

LABORATORY JOURNAL FOR OXYGEN RADICAL ABSORBANCE CAPACITY (ORAC)

EXPERIMENTS.

*Asterisks denote note on or results of experiments.

10/26/05

1 – Biphasic carotenoid extraction: 10ml hexane, 5ml acetone, 5ml ethanol, shake, 5ml water (separate into lipo/hydro)
2 – Dr. Jay suggestion: 2ml hexane x3 rep (lipo), 2ml MEK x3 rep ("M" lipo), aqueous (hyrdo)
3 – "ORAC" extraction: 2ml hex/dichloromethane x3 reps, aqueous mix w/ 15ml AWA (acetone, water, acetic acid)

Hydrophylic and lipophylic assays run on all samples (ex. Lipo assay on lipo and hyrdo extracts and vice versa*). Did this mainly to determine the appropriate assay for the MEK fraction if that were to be used.

Lipo/MEK resuspended in 500ul, diluted 10ul:30ul buffer
Hydro 40ul straight (except #2 diluted 10:30 too)

* Hydrohylic extract curves hardly dropped under either assay (though more under lipophylic assay for extraction #3). Slope was similar for all methods, just slightly different starting points. Lipo extract very high and did not close under lipo assay. No conclusive evidence toward which assay is appropriate for MEK (lipo and hydro not sig different between assays). Conclusion: need to reduce concentration and/or run longer to close. Later found that reducing conc does not inc slope and could not reasonably run assay long enough (tried 3 hrs, vs normal 2) to close. Started manipulating assay in order to close curve.

11/9/05*

1 – 10ml hex/dichl, 5 ml ethanol, 5ml acetone, shake, 3 ml water
2 – 2 ml hex/dichl x4 rep, 2 ml MEK x2 rep
3 – 2 ml hex/dichl x4 rep; 8ml AWA

Also tried putting in straight watermelon juice.
Lipo resuspended in 1ml, MEK in 500ul, diluted 10ul:30ul buffer
Hydro (#1&3) 40ul straight**

* Found that there was supposed to be a delay between adding reagents and first readings. Added delay. Also found that others don't use exterior wells to prevent gradients, excluded these wells. Increased reps on ORAC method to improve extraction. Tried adding dichl to StdExt to modify polarity of lipophylic phase (to pull a more consistent amount of the boarderline antioxidants. Tried using MEK as hydrophilic extractor rather than AWA (MEK is more polar).
** Can only find hydro assay for this day. Very little reduction in absorbance or difference between methods. Straight watermelon will not reduce at all.

1/12/06

1 – 10ml hex/dichl, 5 ml ethanol, 5ml acetone, shake, 3 ml water
2 – 3 ml hex/dichlo x4 rep, 10 drops acetone x2 rep
3 – 3 ml hex/dichlo x4 rep, 10 drops acetone x2 rep; 8ml AWA

3hr run time
.14g AAPH (normal)
All dilutions 10:30*
Note from results: Lower fluoroscene for closing**

* Very close to closing but samples (including stds) not much higher than blank.
**1/14/06 ran exp with lower fluoroscence to encourage closing. Proximity to closing same as before, curves just lower and now all much lower than blank. Alternatively, on 1/15/06 tried increasing dilution to promote closing, but with much the same result (samples lower than blank). Conclusion: CV% was calculated as a measure of repeatability.

2/6/06

1 – 10ml hex, 5ml acetone, 5ml ethanol, shake, 3ml water
2 – 10ml hex, 5ml acetone, 10ml ethanol, shake, 3ml water
~~3 – 10ml hex/dichl, 5ml acetone, 10ml ethanol, shake, 3 ml water~~
4 – 3ml hex/dichl x3 rep; 8ml AWA*
5 – 1.5g sand, 3ml hex.dichl x3 rep; 8ml AWA

Lipo (1:1, acetone resusp:7% RMCD) cloudy – may be ok at full dilution 5:35
Hydro pre-mixed 5:35 buffer - CV% better
Blanks for ethanol/acetone/water tested to see if these were why curves not completing

* Exts with AWA came closest to closing for hydro. Lipo stds would not close; quant impossible.
Conclusions: methodology close, need to perfect extraction.

2/7/06

1 – 5ml acetone, 5ml ethanol, 10ml hex, shake, 3ml water
2 – 5ml acetone, 10ml ethanol, 10ml hex, shake, 3ml water
3 – 5ml acetone, 5ml ethanol, 10ml hex/dichl, shake, 3ml water
4 – 4ml hex/dichl; 8 ml AWA
5 – 4ml hex/dichl, 4g sand; 8ml AWA

Hydro on #3 – 6ml hydro – insoluble layer formed during drying of lipo – solubulized & removed aqueous layer as "3?" in lipo assay
Lipo dilution 2000:3 (??)
Hydro diluted 1:200*

* Ext 4&5 closest to closing because AWA blank doesn't close either. Others and lipo are 80-90% complete.

2/20/06

Found in papers that RMCD should be in 1:1 acetone:water, not phosphate buffer as in our protocol. Also found that volumes should be 40ul, not 20ul. Tested both.*

Both diluted 3:37 then either 40ul or 20ul loaded.
"Why are they the same? It should be half."

* Both leads slightly improved closing, though still not achieved.

2/21/06

1 – 5ml acetone, 5ml ethanol, 10ml hex, shake, 3ml water
2 – 5ml acetone, 10ml ethanol, 10ml hex, shake, 3ml water
3 – 5ml acetone, 5ml ethanol, 10ml hex/dichl, shake, 3ml water
4 – 4ml hex/dichl x2 rep; 10 ml AWA
5 – 4ml hex/dichl, 4g sand x2 rep; 10ml AWA

Hydro diluted 2:18
Lipo diluted 1:24

3/06

Switched gears to seeing if spec readings could be measured on carotenoids prepared in RMCD (lipophylic prep) so concentration could me measured from same prep as ORAC would be run on. *By this time I was probably convinced that I could get lipophylic consistent with better solubilization in RMCD (reduce cloudiness) and so refocused here with the intent of going back to hydrophilic at a later time.* A high concentration standard dilution curve of lycopene and B-carotene standards solubilized in 7% RMCD. Four wavelengths (505nm, 474nm, 452nm, 429nm) measured. Correlation best for lycopene and B-carotene best at 474nm (R^2 = 0.9998 and 0.975, respectively). These concentrations, however, are much higher than are reasonable with the dilutions needed for ORAC. So lower concentrations run next →

3/06

Lower concentration standard curve run. Levels overlapped with previous curve, but spec and ORAC values did not fall in line where they should (not reproducible).

4/19/06

So tried to run a large-range standard curve that would cover both.

5/3/06 ← starting

RMCD concentrations – Matrix combinations of carotenoid (2.5, 5, 10 ug/ml) and RMCD (3.7, 7, 14, 28%) concentrations. *I had found a paper that used RMCD concentrations up to 28% to get better solubilization.*

This scheme applied over several rxn conditions:*

#1 20ul sample
20ul AAPH (.166g/5ml)
160ul Fluoro (3.54x10-6ug/rxn, prep by 526ul→50ml)

#2 20ul sample
20ul AAPH (.166g/5ml)
200ul Fluoro (4.208x10-5ug/rxn, prep by 526ul→50ml)

#3 20ul sample
20ul AAPH (.166g/5ml)
240 Fluoro (5.76x10-5ug/rxn = 600ul→50ml)

#4 20ul sample
20ul AAPH (.180g/5ml)
240 Fluoro (8.64x10-5ug/rxn = 900ul→50ml)

* See stat pages for results.

5/06

Lipo dilutions: 2x RMCD in water only, add acetone, add carotenoids. *There was some suspicion here that the RMCD was not going into solution with the acetone changing the polarity. So sequential addition was attempted.*

VITA

Name: Jennifer Leanne Jeffery

Address: Horticulture Building, 2133 TAMU, College Station, TX 77843

Email Address: jennwaters@tamu.edu

Education: Ph.D., Molecular and Environmental Plant Sciences, Texas A&M University 2008
B.S., Plant Genetics and Breeding, Brigham Young University 2003

Teaching: Teaching Assistant for Labs: Floral Design (Hort 203), Vegetable Crop Production (Hort 325), Hort Science & Practices (Hort 201)

Publications: Meyer SE, Nelson DL, Waters J, Clement S, Stevens M, Fairbanks D. Genetic variation in *Ustilago bullata*: Molecular genetic markers and virulence on *Bromus tectorum* host lines. Int J Plant Sci 166: 105-115

Ramakrishnan AP, Meyer SE, Waters J, Stevens MR, Coleman CE, Fairbanks DJ. Correlation between molecular markers and adaptively significant genetic variation in *Bromus tectorum* Poacea, an inbreeding annual grass. Amer J Bot 91:797-803

Poster Papers: Jennifer L Jeffery and Stephen R King. A New Approach to Nutrative Analysis Using Watermelon as a Case Study. FAV Health Conference, Houston, TX. October 2007

Jennifer L Waters, Dr. Mark Failla, Dr. Ann Ellis, Dr. Stephen King. Correlation of Bioaccessibility and Cellular Structure in Carotenoid-Containing Fruits and Vegetables. MSIRP, Edinberg, TX. February 2006

Presentations: Jennifer Waters, Haejeen Bang, Angela Davis, Daniel Leskovar, Stephen King. Semi-Quantitative Measurement of Carotenoid Development in Four Watermelon Colors: A Discussion of the Impact of Ploidy and Other Genetic Factors. SRASHS Annual Meeting, Mobile, AL. February 2007

Awards: Tom Slick Fellowship 2007-2008
2nd place: SRASHS 2007 Warren S. Barham Competition.
1st place: MSIRP 2006 Conference Poster Competition, Science Division